

# **Geochemical and hydrodynamic phosphorus retention mechanisms in lowland catchments**

**Bas van der Grift**

Geochemical and hydrodynamic phosphorus retention mechanisms in lowland catchments

ISBN/EAN: 978-94-028-0641-0

Cover photographs: Anke van den Broek (front), Joachim Rozemeijer (back)

Cover design: Roel Savert

Lay-out: Legatron Electronic Publishing

Printing: IPSKAMP Printing

Copyright © 2017 Bas van der Grift

All rights reserved. No part of the material protected by this copyright notice may be reproduced or utilized in any form or by any other means, electronic or mechanical, including photocopying, recording or by any other information storage and retrieval system, without the prior permission of the author.

# **Geochemical and hydrodynamic phosphorus retention mechanisms in lowland catchments**

Geochemische en hydrodynamische fosforretentie mechanismes  
in laagland stroomgebieden

(met een samenvatting in het Nederlands)

## **Proefschrift**

ter verkrijging van de graad van doctor aan de Universiteit Utrecht op  
gezag van de rector magnificus, prof.dr G.J. van der Zwaan, ingevolge  
het besluit van het college voor promoties in het openbaar te  
verdedigen op vrijdag 9 juni 2017 des middags te 4.15 uur

door

**Bas van der Grift**

geboren op 16 juni 1972 te Benthuizen

Promotoren: Prof.dr. J. Griffioen  
Prof.dr. M.J. Wassen

Copromotoren: Dr. P.P. Schot  
Dr. L.A. Osté

The research in this thesis was funded by Deltares.

## Table of contents

CHAPTER 1	Introduction	7
CHAPTER 2	Iron oxidation kinetics and phosphate immobilisation along the flow-path from groundwater into surface water	25
CHAPTER 3	Fe hydroxyphosphate precipitation and Fe(II) oxidation kinetics upon aeration of Fe(II) and phosphate-containing synthetic and natural solutions	51
CHAPTER 4	Particulate phosphorus speciation in ditches, channels and streams of agriculture-dominated lowland catchments: iron as phosphorus carrier	91
CHAPTER 5	High-frequency monitoring reveals nutrient sources and transport processes in an agriculture-dominated lowland water system	131
CHAPTER 6	Erodibility of soft sediments from drainage ditches and channels in lowland catchments and associated phosphorus release	165
CHAPTER 7	Synthesis	187
	References	209
	Summary	229
	Samenvatting	233
	List of Publications	237
	Dankwoord	239
	Curriculum Vitae	243



# CHAPTER

# 1

## Introduction

Bas van der Grift

## 1.1 Eutrophication of surface water

A large number of surface water bodies in Europe have poor ecological status and are affected by pollution pressure, particularly in central and north-western Europe (Figure 1.1). Nutrient enrichment is the main cause of this poor ecological status (EEA, 2015). Major contributing nutrient sources that cause eutrophication are point sources, such as wastewater discharge from urban areas and industries, and diffuse emissions from agricultural activities, related to excess manure and fertiliser application (EEA, 2005). Nutrient loadings may cause eutrophication of surface waters, which involves a number of undesired effects such as an increase of the turbidity of the water, increase in biomass of phytoplankton and rampant growth of macrophytes, decreased oxygen levels especially in bottom water layers, toxin production by algae and bacteria, and increase of fish kills (e.g. Bouwman et al., 2013a; Correll, 1998). All these effects directly endanger the biodiversity of aquatic ecosystems, disrupt trophic chains and result in the loss of habitats (Grizzetti et al., 2012). Eutrophication also impairs the suitability of water for drinking, industry, agriculture, recreation and other purposes (Boesch, 2002).

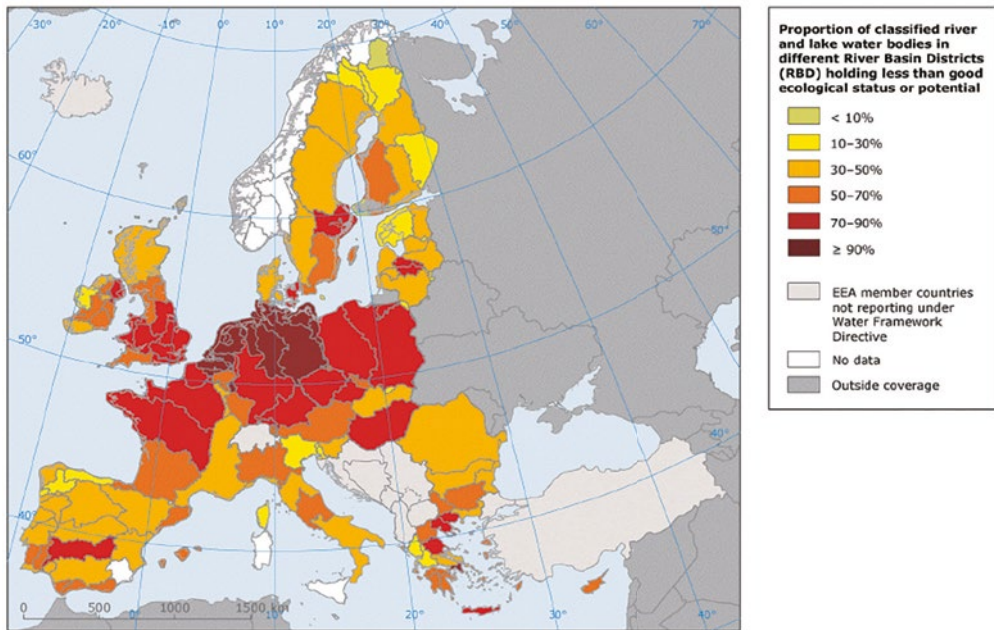


**Figure 1.1.** Proportion of river and lake water bodies in different River Basin Districts classified as having less than good ecological status or potential according to the methodology of the European Water Framework Directive in 2009 (EEA, 2015).

Whereas plant growth can be limited by a series of site-specific factors, the primary production of most aquatic ecosystems is strongly controlled by the concentration of the macronutrients N and



P (e.g. Elser et al., 2007; Hecky and Kilham, 1988). Freshwater aquatic systems such as lakes, rivers, streams and channels, have traditionally been considered phosphorus (P) limited, whereas oceans have been considered primarily nitrogen (N) limited and estuaries and continental shelf waters were considered as transition zones with both N and P co-limitation (Correll, 1998). Although a series of studies have shown that reality is more complex than this traditional view (Burson et al., 2016 and references therein), managing the P (or both P and N) supply can be an effective measure for reducing adverse impacts in freshwater systems and coastal waters (e.g. Bowes et al., 2007; Elser et al., 2007; Withers and Jarvie, 2008).

Since the early 1990s, the European Union has set various directives to control and reduce nutrient loads into receiving waters. These are surface waters, including estuarine and coastal waters, as well as groundwater (Bouraoui and Grizzetti, 2011). Controlling eutrophication and nutrient loads in receiving waters is embedded in several pieces of legislation at European level, including the Nitrate Directive (EC, 1991b), the Urban Waste Water Treatment Directive (EC, 1991a) and the Water Framework Directive (EC, 2000). Reducing P concentration in freshwater has, likewise, been a priority of the Dutch government, to improve water quality (Van Gaalen et al., 2016). This started relatively early with the implementation of the Act on Pollution of Surface Water in 1970 to reduce point sources (Act on Pollution of Surface Water, 1970) and was followed by the Dutch Manure Act in 1986 to reduce diffuse agricultural sources (Dutch Manure Act, 1986).

As a result of the de-eutrophication efforts made in northwest Europe during recent decades, a decline in total P (TP) concentration has been observed in the river Rhine (e.g. Hardenbicker et al., 2014) and large inland lakes in the Netherlands (Noordhuis et al., 2015). Recently, Burson et al. (2016) reported a strong decline of dissolved P concentrations in coastal water in the North Sea, which resulted in significant change in the N:P ratio. Since primary producers need both N and P to produce biomass, the shortage of P relative to the availability of N in the North Sea has major consequences for the growth, species composition and nutritional quality of marine phytoplankton communities.

Time series of P concentrations in the river Rhine water from 1980 to the present reveal a sharp decline of total P from the mid-1980s to the mid-1990s (Figure 1.2). This decline correlates strongly with the decline of dissolved P concentrations (measured as Dissolved Reactive P (DRP), see section 1.5.1). Point sources, such as effluent loads from wastewater treatment plants (WWTP) are typically dominated by dissolved P (e.g. Scherrenberg, 2011). Hence the observation of declining dissolved P concentrations and, consequently, declining total P concentrations in major rivers, inland freshwater lakes and coastal areas in northwest Europe suggests that policies aimed at the reduction of point sources have been more effective or have been more effectively implemented than those controlling pollution from diffuse sources (Grizzetti et al., 2012). As a result, the relative contribution from diffuse agricultural sources has risen in recent years in northwest Europe, making commercial fertilisers and animal manure the typical primary sources of nutrient enrichment in freshwater systems (EEA, 2005).

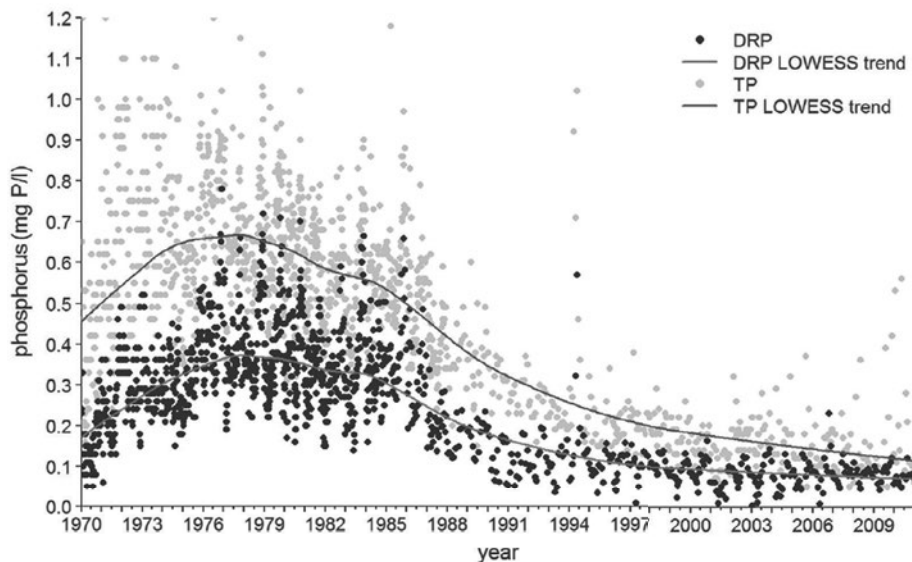


**Figure 1.2.** Time series of total P and dissolved reactive P concentrations over the period 1970-2014 in the river IJssel near Kampen, which is fed by water from the river Rhine. (Source: Rijkswaterstaat monitoring programme).

## 1.2 History of P surpluses in the Netherlands

To understand P input from agriculture to surface waters in the Netherlands, insight is needed into P application in agriculture. In the decades following World War II, the agricultural P application rates in the Netherlands grew to levels that greatly exceeded crop demand. Fertiliser application to agricultural land was virtually unrestricted. From 1960-1985, livestock numbers in the Netherlands grew, leading to increasing N and P surpluses. For example, in this period, the number of pigs grew from 2 to 14 million (Oenema et al., 2007), almost outnumbering the human population. The introduction of maize in 1970, on which a virtually unlimited amount of manure and fertiliser can be applied, allowed for greater livestock densities and a further increase in surpluses until 1986 (Visser et al., 2007). Since the mid-1980s, measures have been implemented to mitigate agricultural pollution, the ultimate goal being to achieve P application rates on agricultural land that are balanced by crop removal in the near future. Despite the environmental legislation to decrease P application rates that has been introduced since the mid-1980s, recent national P budgets in the Netherlands are still characterised by relatively large net import of P, with feed, minimal recycling of P in waste flows and a large national surplus (Table 1.1) (Smit et al., 2015). Due to high quantities of feed imports for the agricultural sector, the national P surplus amounted to almost 60 Mkg P in 2005, decreasing to 42 Mkg in the year 2011.

**Table 1.1.** National P balances of the Netherlands in 2005, 2008 and 2011 (Mkg P yr<sup>-1</sup>) (from Smit et al., 2015).

	2005	2008	2011
Imports	108.2	114.8	110.5
Food	28	31.1	32.9
Feed	50.4	60.1	58.6
Non-food	1.4	3.3	3.4
Feed additives	7.2	8.1	8.5
Mineral fertilisers	21	12	7
Livestock	0.2	0.2	0.2
Exports	48.5	63.6	69.0
Surplus	59.7	51.2	41.6
To waste	21.4	25.3	23.2
Wastewater treatment plant effluent	3.5	3.5	3.3
Leaching and runoff	3.3	3.3	3.3
Accumulation in soil	31.3	19.2	11.8

The decline of the national P surplus that took place from 2005 to 2011 can be attributed to an increase in P exports (mainly as manure) and a reduction of P fertiliser use. During this period the direct loads to surface water from WWTP effluents and indirect load from leaching and runoff remained almost equal. The figures given by Smit et al. (2015) show that the soil surplus fell from 31 Mkg P yr<sup>-1</sup> in 2005 to 12 Mkg P yr<sup>-1</sup> in 2011, indicating that although current rates of P application are somewhat better balanced with crop removal, P continues to accumulate in the soil. Because P has a strong tendency to bind to soil particles, a large part of the excess P has accumulated in the soil. Hence due to the excess fertilisation in recent decades, in the Netherlands there is a large area of P-saturated agricultural soils (Schoumans and Chardon, 2015). This enormous pool of 'legacy P' is slowly leaking P, delivering a continuous supply of P to surface water. Consequently, a large area of agricultural land is contributing to P loading of surface water and is expected to continue to do so in the near future (Schoumans and Chardon, 2015).

### 1.3 Phosphorus status of surface water bodies in the Netherlands

The Netherlands has a statutory obligation to implement the European Water Framework Directive (WFD), as do all other European Member States. The primary target of the WFD is to achieve chemically clean and ecologically healthy surface water (EC, 2000). The WFD requires all surface waters in Member States to have achieved 'good' ecological status by 2015, but two six-year extensions are permitted, making the final deadline 2027. In 2015, 45 percent of the regional freshwater bodies in the Netherlands met the P standards for 'good' ecological status (Figure 1.3). Based on model calculations, it is estimated that in 2027 only 50% of Dutch surface waters will meet this standard (Van Gaalen et al., 2016). The WFD surface water bodies are generally regional water bodies and are

influenced by municipal WWTP point sources, diffuse agricultural sources and 'natural' P sources. The improvement of P status between 2015 and 2027 is mainly due to additional measures to reduce emissions from urban WWTPs (Van Gaalen et al., 2016). Natural sources of P include the exfiltration of nutrient-rich groundwater in west Netherlands (Griffioen et al., 2013), wildlife droppings (e.g. from water fowl, especially overwintering ones) and, although largely induced by artificial drainage of the soil, mineralisation of peat.

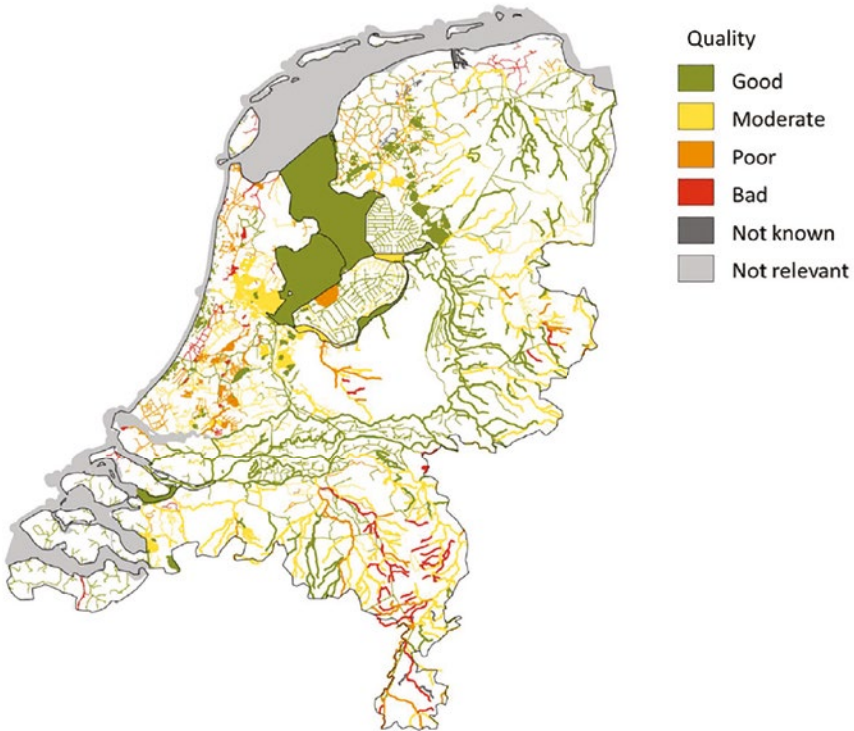


**Figure 1.3.** Phosphorus status of WFD surface water bodies in the Netherlands in 2015, according to the classification of the European Water Framework Directive (from Van Gaalen et al., 2016).

The existing national P surplus that is related to feed imports for livestock farming (Table 1.1) in combination with the enormous pool of 'legacy P' in soils may limit the improvement of water quality of regional surface water systems in the Netherlands. Here, it must be taken into account that only a small fraction of the P pool in the soil or the P load applied annually to the soil leaches to surface water each year (Table 1.1). Overland flow and soil erosion are commonly considered to be the principal pathway of P loads to surface water (Heathwaite and Dils, 2000; Kronvang et al., 2007). Such losses are related to the erosion of P-bearing soil particles during rainstorm events. Conversely, in flat low-lying well-drained lowland catchments with shallow groundwater tables, as present in large parts of the Netherlands, P loads to surface water predominantly occur via subsurface flow, i.e. interflow, tube drain discharge or groundwater discharge, whether or not through macropore

flow (Chardon and Schoumans, 2007; Reid et al., 2012; Schoumans and Groenendijk, 2000). After erosion via soil surface runoff or leaching via subsurface flow routes, P loadings from the soil have to be transported through a series of drainage ditches and channels or headwater streams before the water quality of the WFD surface water systems located further downstream is impacted. This means that there is a need to assess the P status and trends in P concentration of agriculture-dominated headwaters to manage the water quality of regional surface water systems and coastal zones. Hence, detailed insight into the mechanisms controlling P transport through field ditches, headwater streams and channels that drain agricultural lowlands is essential.

## 1.4 Phosphorus status of agriculture-dominated headwaters in the Netherlands

The water quality status and trends in local surface waters that are dominantly affected by agriculture was assessed by Rozemeijer et al. (2014), who developed a national-scale monitoring network for agriculture-dominated headwaters. The objective of their study was to evaluate the effectiveness of national and European manure legislation in the Netherlands. In the most recent update on this monitoring network, Klein and Rozemeijer (2015) used data from 172 existing monitoring locations in agricultural headwaters to test these waters for compliance with the local water quality standards for the period 2011–2014 and to ascertain the trends for the period 1990–2014. The assessment was done for the three major soil type regions in the Netherlands, i.e. sand, clay and peat and for both the summer (April–September) and winter (October–March) half-year. Trend analysis showed that water quality in agriculture-dominated headwaters in the Netherlands improved over the period 1990–2014 (Figure 1.4). Total P concentrations in agricultural headwaters decreased, with the median slope of the decline being 0.015 mg/l per decade. The LOWESS trend line, which gives a smoothed curve through the concentration time series, does not reveal many changes in the aggregated trend slopes over the years. The decrease in TP concentrations seems to accelerate slightly around 2002. The 25-percentile LOWESS gives the trends for the lower concentration range and the 75-percentile for the higher concentration range. This 75-percentile LOWESS shows a remarkable shift in trend, with concentrations falling sharply over the period 1980–1995 and rising slightly after 1995.

Despite the improvement in water quality in many agriculture-dominated headwaters in the Netherlands, the TP concentrations are still too high. The current status of TP in agricultural headwaters is therefore described in more detail in the following paragraphs.

Figure 1.5 summarises all TP concentration data and ratios of DRP over TP for the 172 agriculture-dominated monitoring locations selected for the period 2011–2014. The data for the clay, sand and peat regions are shown as separate lines. In addition, summer and winter half-year concentrations are displayed separately. For TP, highest concentrations were measured in the agricultural headwaters in the peat area and the lowest in the sand area. Although TP concentrations above 0.3 mg/l were quite common in the clay region (45% of measurements) and in the peat region (56% of measurements), only 16% of the measurements in the sand region exceeded this value. In the peat and clay regions, summer TP concentrations were higher than winter TP concentrations. For the sand region, no clear distinction between summer and winter concentrations appears from Figure 1.5a.

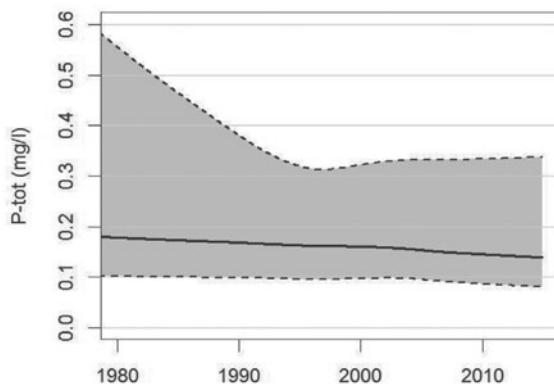


**Figure 1.4.** Trends in total phosphorus concentrations in agriculture-dominated headwaters in the Netherlands over the period 1980–2014: aggregated median LOWESS trendline (black) with uncertainty band (25- and 75-percentiles) around the median obtained using LOWESS smooths (grey) (from Klein and Rozemeijer, 2015).

The sand region showed the lowest DRP/TP ratios; this ratio was higher in the winter (median = 0.26; range of P15–P85 = 0.1–0.55) than in the summer (median = 0.20; range of P15–P85 = 0.068–0.54) (Figure 1.5b). These low DRP/TP ratios testify to the largely particulate nature of P in agriculture-dominated headwaters in the sand region. The DRP/TP ratios were higher in the clay and peat regions and were higher for the summer period than for the winter period. The peat region showed the highest DRP/TP ratios and the largest difference between winter and summer (winter median value 0.43; summer median value 0.6), showing that in these waters DRP can be the dominant P fraction.

Klein and Rozemeijer (2015) tested compliance by applying environmental quality standards (EQSs) based on summer-averaged concentrations, in accordance with the procedure decided on in the Netherlands for implementing the WFD (e.g. Heinis and Evers, 2007b). The EQSs are set by the Dutch Water Boards based on a national assessment of ecosystem vulnerability (Heinis and Evers, 2007b) and depend on water type and location. For TP, the most common EQSs are 0.15 for most ditches and channels in the clay and peat regions and 0.22 mg/l for the streams in the sandy region. The compliance percentage for TP ranged between 46% in 2012 and 2014 and 59% in 2013. Figure 1.6 is a map showing the results of the compliance test for TP for 2011–2014. The non-compliant locations were most abundant in the west of the Netherlands. In the peat region, between 8% and 42% of the locations complied with the TP EQS. This large range is the result of the relatively few locations in the peat region (between 12 and 15 for the years 2011–2014). Compared with 2012, in 2013 there were four more locations at which the TP concentrations were below the EQS. The compliance percentages ranged between 52% and 63% for the clay region and between the 48% and 62% for the sand region. Trend analysis showed that water quality in agricultural headwaters has improved in recent decades. The results show a relatively quick response to the introduction of manure legislation in 1986, but that in 2010–2014 up to 55% of the agriculture-dominated water quality monitoring locations in the Netherlands still did not comply with the EQS for TP.

The data from the national monitoring network for agriculture-dominated headwaters also revealed, however, that the effects of manure legislation on P concentration in surface water are not obvious. Firstly, the clay and peat regions in the west of the Netherlands have higher TP concentrations and a larger percentage of non-compliant concentrations than the sand region in the east and south of the Netherlands. This is remarkable, as intensive livestock farming and the highest manure surpluses are concentrated in the east and south of the Netherlands. Secondly, the compliance testing results varied considerably over 2011–2014, even though during this period there were no major changes in legislation, land use, or nutrient surpluses. Thirdly, the TP concentration had already decreased in the early 1980s, yet manure legislation only began to be implemented in 1986; prior to that, manure and fertiliser applications did not decrease. Hence, other factors such as loads from sources other than agricultural emissions, and dynamics in transport and transformation processes also control TP concentration in agriculture-dominated headwater.

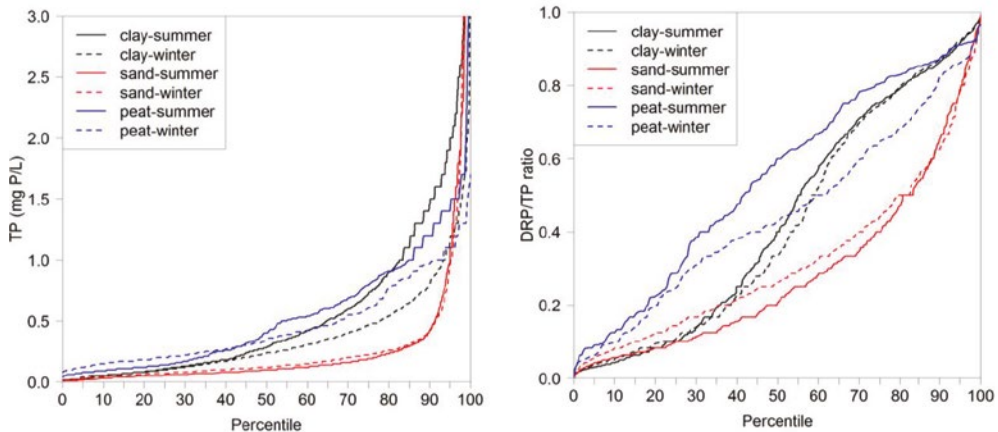


**Figure 1.5.** Cumulative frequency diagrams showing the observed TP concentrations (left) (from Klein and Rozemeijer, 2015) and DRP/TP ratios (right) in peat, sand and clay regions in winter and summer for the period 2011–2015.

## 1.5 Phosphorus behaviour in agriculture-dominated headwaters

The previous section shows that water quality in agricultural headwaters has been improved in recent decades and that effects of manure legislation on P concentration in surface water are difficult to see, which implies that P is difficult to trace to one specific source. This complexity is a result of the variety of chemical forms in which P can exist. In nature, phosphorus usually occurs as part of a phosphate molecule ( $\text{PO}_4$ ; orthophosphate). Phosphorus in aquatic systems occurs as organic and inorganic phosphate and it undergoes many transformations due to a range of dynamic biotic and abiotic processes: biological uptake/release, chemical adsorption/desorption and precipitation/

dissolution, and physical advection and diffusion (see also section 1.5.2). The environmental behaviour of P is likewise critically dependent on its physico-chemical form (Kronvang et al., 2005; Worsfold et al., 2005), and therefore relationships between P emissions to surface water, ambient P concentration in the water column and P loads to downstream water bodies are complex. For example: in contrast to dissolved P, the transport of particulate P from source areas to coastal zones is subject to sedimentation and resuspension in water courses and is therefore more strongly retarded than that of dissolved P. Whereas a decrease of riverine dissolved P concentrations and loads to coastal water can be directly linked to decreases in P emissions within catchments, the situation is much more complicated for particulate P. It may even mean that ‘downstream’ P concentrations may decrease whereas the total P emissions to surface water in the catchment or river basin do not decrease when there is simultaneously a shift from dominance of dissolved P to dominance of particulate P emissions. This may be the case in situations of declining emissions from point sources and increasing emissions from agricultural sources. Hence, a proper environmental management of water systems including the design of emission reduction measures and evaluation of the effectiveness requires knowledge of the fate of P species and of the mechanisms controlling the fate of these P species in the aquatic environment.

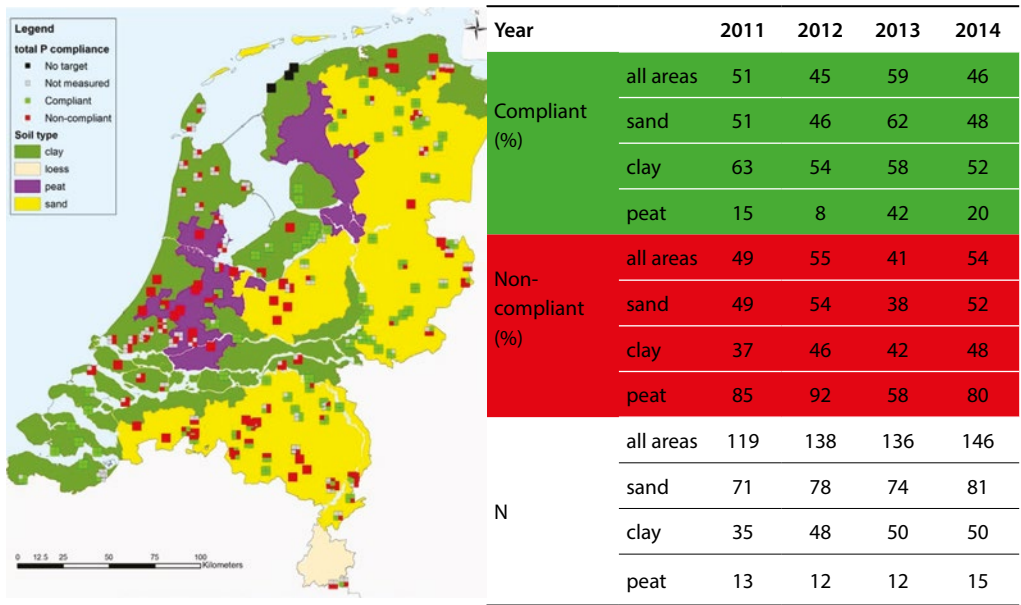


**Figure 1.6.** Compliance with regional environmental quality standards, based on average summer concentrations for four different years. At each monitoring location, four squares are shown with the compliance in 2011 (upper left), 2012 (upper right), 2013 (lower left) and 2014 (lower right) (from Klein and Rozemeijer, 2015).



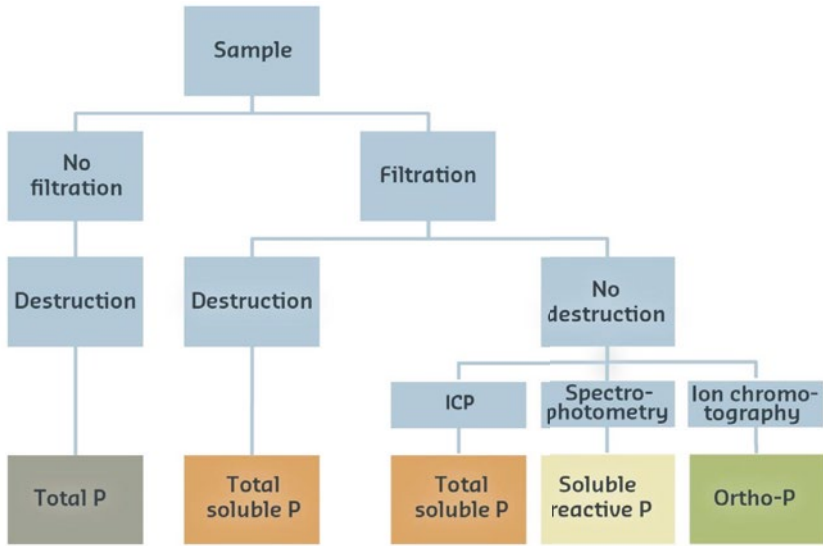
### 1.5.1 Phosphorus speciation

To trace the transport and transformations of P, it is convenient to classify forms of P in aquatic systems as inorganic and organic compounds appearing in 'dissolved', 'colloidal' and 'particulate' fractions (Robards et al., 1994; Worsfold et al., 2005). Separation of 'dissolved' from 'particulate' P phases is based mainly on filtration using 0.45  $\mu\text{m}$  or 0.7  $\mu\text{m}$  membrane filters. The filtered fraction of natural waters includes orthophosphate ( $\text{H}_2\text{PO}_4^-$ ,  $\text{HPO}_4^{2-}$ ,  $\text{PO}_4^{3-}$ ), i.e. phosphate in its simplest, free ionic form, inorganic condensed phosphates or polyphosphates (pyro-, meta- and polyphosphates), dissolved organic P and colloidal P. The colloidal fraction commonly refers to both inorganic and organic components in the size range 1–1000 nm (Worsfold et al., 2016). Organic P compounds are highly diverse; examples of simple organic P compounds include phytic acid, adenosine triphosphate (ATP) and ribonucleic acid (RNA) (Turner, 2004). The particulate fraction includes inorganic P sorbed onto the surfaces of particles (e.g. metal oxides, hydroxides, edges of clay minerals,  $\text{CaCO}_3$  particles, Al- and Fe-organic complexes) or phosphate minerals, mainly with Ca, Al or Fe (House, 2003; Withers and Jarvie, 2008) and organic P compounds.

The speciation of P in aquatic samples is usually operationally defined (as shown in Figure 1.7), since it depends on the filtration and digestion procedures (Van Moorlegheem et al., 2011; Worsfold et al., 2005) and the analytical procedure. The following determinations are made routinely and are followed in water quality monitoring programmes worldwide (Jarvie et al., 2002):

- *Soluble Reactive Phosphorus* (SRP). Other terms commonly used in the literature to describe this fraction include *Dissolved Reactive Phosphorus* (DRP), *Dissolved Inorganic Phosphorus* (DIP), *Filterable Reactive Phosphorus* (FRP) and *orthophosphate*. The term *orthophosphate* is a chemistry-based term that refers to the phosphate ion all by itself and, strictly speaking, this is not the same as DRP, as other P forms are measured as well during DRP analyses.
- *Total Dissolved Phosphorus* (TDP). This is also commonly termed *Total Filterable Phosphorus* (TFP), and is a combination of DRP and *Dissolved Hydrolysable Phosphorus* (polymeric and organic) (DHP).
- *Total Phosphorus* (TP): the TDP plus *particulate phosphorus* (PP) in a water sample.

Analytical determination of the P concentration after filtration, after filtration plus digestion, or after digestion only (without filtration) is commonly based on the colorimetric molybdenum blue method (Murphy and Riley, 1962). The colorimetric analysis generally excludes most organic P compounds, with the exception of some acid-labile organic P species, but includes the P bound to colloidal oxyhydroxides of Fe and Al (Sinaj et al., 1998; Van Moorlegheem et al., 2011). The concentration of the dissolved P fraction after filtration (DRP) as measured by the molybdenum blue method is considered equivalent to bioavailable P (Nürnberg and Peters, 1984). Inductively-coupled plasma-optical emission spectrometry (ICP-OES) or mass spectrometry (ICP-MS) is also used for determination of the TDP and TP concentrations.



	DOP	DIP	COP	CIP	POP	PIP
Total P						
Total soluble P						
Soluble reactive P						
Orthophosphate						

DOP: dissolved organic phosphorus, DIP: dissolved inorganic phosphorus (ortho-phosphate), COP: colloidal organic phosphorus, CIP: colloidal inorganic phosphorus, POP: particulate organic phosphorus, PIP: particulate inorganic phosphorus

**Figure 1.7.** Operationally defined P fractions in water samples, based on filtration, digestion and analytical methods.

### 1.5.2 Mechanism of phosphorus uptake and release

Numerous studies have shown that the sum of the P emissions to surface water in lowland catchments can deviate strongly from the flux at the outlet of the catchments (e.g. De Klein, 2008; Kronvang et al., 2009; Roelsma et al., 2011a). As mentioned before, this is because the transport of dissolved and particulate P species in surface water is controlled by a sequence of immobilisation and mobilisation processes that may occur during flow in watercourses (Figure 1.8). Reddy et al. (1999) defined retention as the capacity of a water body to remove water column phosphorus through physical, chemical and biological processes and retain it in a form not readily released under normal conditions. This implies that both biotic and abiotic processes must be considered when evaluating P retention in surface waters (Figure 1.8). Biotic processes include assimilation of dissolved P into particulate organic P by vegetation, macrofauna, algae and microorganisms. Abiotic processes include adsorption of dissolved P by sediments (whether deposited or in suspension), immobilisation of dissolved P by mineral precipitation, sedimentation and erosion/resuspension of particulate P and biochemical remobilisation of particulate P in bed sediment followed by exchange

of dissolved P between sediment and the overlying water column through diffusion or advection (Reddy et al., 1999).

The importance of biotic versus abiotic processes on the P retention is typically site-specific and varies with discharge, biological and chemical characteristics of the water column and the underlying sediments (Withers and Jarvie, 2008). The relative contribution of various in-stream processes to the overall P retention is thus dependent on the size of the water course, the catchment geology, the channel hydrology, the trophic status and the speciation of the P loads to the surface water. For example, there is a difference in retention mechanisms between water courses with typical high and low flow velocities. Higher water velocities promote particle resuspension and transport and reduce water residence times for uptake of P by bed sediments and biota. Reduced flow velocities favour enhanced nutrient retention, as a result of longer water retention times, longer contact times between water and (suspended) sediments, higher rates of algae growth and therefore biological uptake and sedimentation of particulates (Withers and Jarvie, 2008).

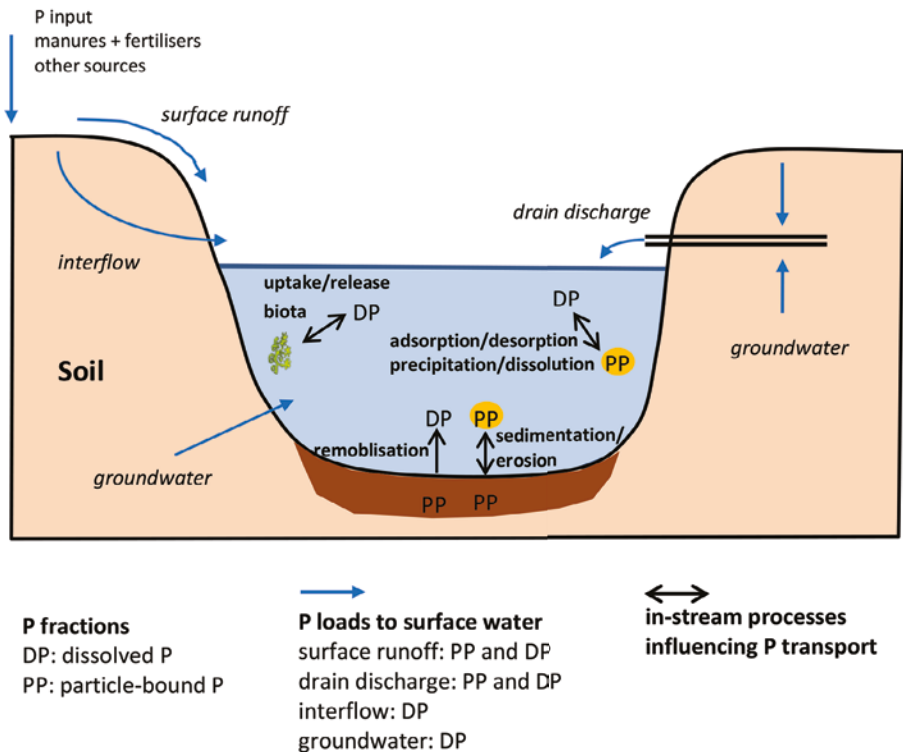


**Figure 1.8.** Main transport pathways of P loads from diffuse sources to surface water and in-stream processes controlling P transport in flowing surface waters.

### 1.5.3 Controls on phosphorus retention in lowland catchments in the Netherlands

The Netherlands is a low-lying country on the Rhine/Meuse/Scheldt delta. Surface elevations vary from a few metres below mean sea level (MSL) in the west and north to around 20–80 m above MSL

in the east and south outside southern Limburg (Figure 1.9b). The Netherlands is almost completely covered with Pleistocene and Holocene deposits. Pleistocene sandy deposits (aeolian cover sands and fluvial or glacial deposits) lie on the surface in the south and east of the country (Figure 1.9c). The surface deposits in the west and north are Holocene fluvial and marine clay sediments and peat. Many surface water bodies in the Netherlands are artificial. An extensive network of ditches (approximately 300,000 km) and canals has been created to control water levels. The lowland areas were reclaimed and drained by hydrotechnical constructions such as dikes, sluices and pumps and have drastically altered the hydromorphology and hydrodynamics of water courses (Ligtvoet et al., 2008). Such an embanked plot of land with a human-controlled water regime is called a *polder*. In the Netherlands, these regulated polder catchments cover 60% of the land surface (Van de Ven, 2004) (Figure 1.9d). Polders are found in all delta areas worldwide and are important urban and agricultural areas.

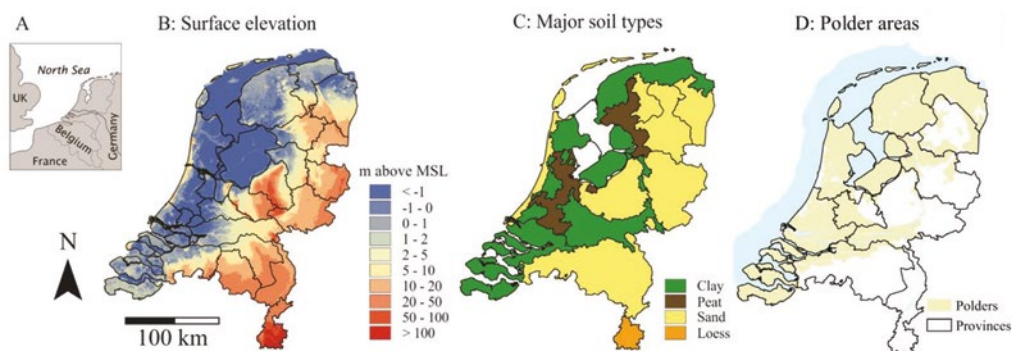


**Figure 1.9.** Study area; (A) location of the Netherlands in Europe, (B) elevation map, (C) major soil types, (D) polder areas.

The importance of the various in-stream processes in controlling P retention in headwater ditches, channels and streams as present in the agriculture-dominated settings of a Holocene polder landscape or a Pleistocene landscape in the Netherlands is unclear. De Klein (2008) found that in a Dutch brook P retention was mainly determined by sedimentation of particulate P. It was, however, not clear if this particulate P consisted mainly of organic P or inorganic P. The processes controlling the formation of particulate P (adsorption, precipitation or biological uptake) were not investigated. Finally, it was not clear whether the sedimentation of particulate P was permanent, i.e., whether stored P may be rereleased into the water column by physical resuspension or biochemical remobilisation.

A typical characteristic of the water bodies that drain agriculture-dominated areas in the Netherlands is that they are fed by groundwater from a reactive subsurface with high contents of organic matter and reactive minerals such as sulphides and carbonates (Griffioen et al., 2016). Due to the reactivity of the subsurface in delta areas, the groundwater has a chemical composition that differs from surface water in terms of redox status, pH and  $\text{CO}_2$  pressure. In the Pleistocene landscape,

the groundwater is typically fresh, pH-neutral to slightly acid (pH 5–7), anoxic (Fe reducing) and Fe-rich. At some locations it can also have relatively high phosphate concentrations, presumably due to degradation of subterranean organic matter (Griffioen et al., 2013). In the Holocene polder landscape, the groundwater is typically fresh to saline, deep anoxic (methanogenic), carbonate saturated and pH near-neutral. Furthermore, this groundwater commonly has high phosphate and ammonium concentrations, generally associated with high CO<sub>2</sub> pressures. Major changes in the redox and pH conditions take place when such water exfiltrates to surface water. These changes possibly impose important controls on immobilisation of dissolved phosphate. Two types of reactions are likely: binding by Fe hydroxides which precipitate after oxidation of dissolved Fe(II) and uptake by Ca phosphates upon degassing and rise in pH. The presence of authigenic Fe hydroxides is often witnessed at the bottom of drainage ditches or small channels or streams in the Netherlands (Figure 1.10) and in Belgium (Baken et al., 2013). From this one may hypothesise that phosphate has a tendency to transform from dissolved P to particulate P during or after discharge to the surface water. Phosphate may thus be attached to authigenic bed or suspended sediments that are precipitated during exfiltration of groundwater (Figure 1.11). Next, sedimentation and resuspension processes determine the particulate P transport and, with that, the P export from a lowland catchment or polder. Due to the presence of a dense surface water system, in a Dutch lowland catchment the water storage capacity and the residence time of the surface water is relatively long. This likely promotes sedimentation of particulate P and limits the physical resuspension. Hence, a central hypothesis in this thesis is that in the Netherlands, discharge of groundwater into surface water strongly determines the fate and transport of phosphate in surface water.

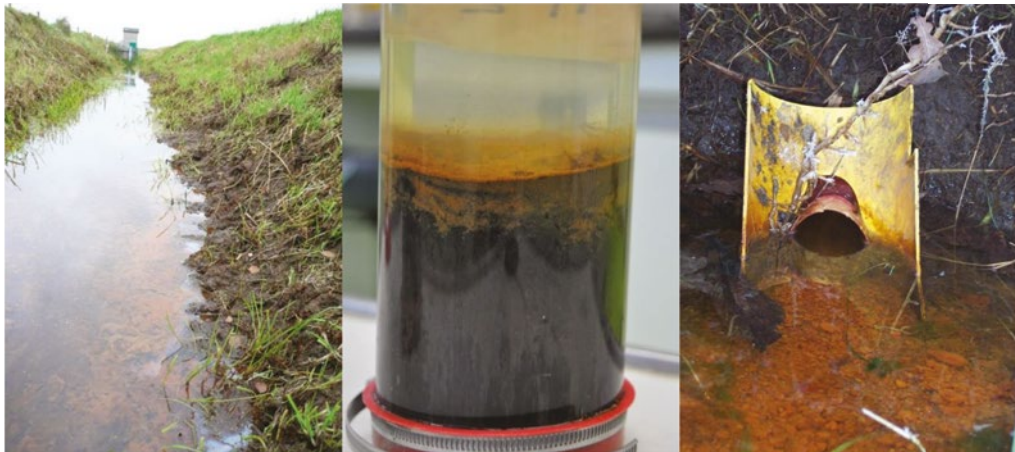


**Figure 1.10.** Orange-brown iron oxide precipitates deposited at the bottom of a drainage ditch in the east of the Netherlands (left), at the top of a ditch sediment core sampled in the western part of the Netherlands (middle) and from a drain tube (right).

## 1.6 Thesis scope, research objectives and outline

The scope of this research project is summarised as follows. Although water quality in the Netherlands has improved thanks to policies to reduce nutrient losses, the P concentrations in many soils and surface waters remain high and are adversely affecting the water quality status. This is especially true for regions with intensive agricultural production, where diffuse emissions from P-saturated soils may result in continued eutrophication problems. Before they can affect the surface water quality of regional surface water bodies, P loads from agricultural sources have to be transported through a series of headwater ditches, channels and/or streams. However, we lack deep understanding of the processes involved in P speciation in such agriculture-dominated headwaters. Furthermore, there is insufficient knowledge of the mechanisms that control P transport in streams and ditches in lowland catchments. This seriously hampers the possibility of linking agricultural practice to P concentration in surface water and, moreover, it hinders the implementation and assessment of measures to control or reduce P loads from agriculture.

The general objective of my thesis is to gain mechanistic understanding of the geochemical and hydrodynamic controls on P speciation and transport in streams, canals and ditches of agriculture-dominated lowland catchments in the Netherlands (Figure 1.11). My hope is that this contributes to the improvement of our understanding of P retention in watercourses.

Specific objectives are to determine:

- How transformation processes during exfiltration of Fe(II)-bearing anoxic groundwater affect the immobilisation of dissolved P (chapters 2 and 3).
- The chemical speciation of particulate P in surface water of groundwater-fed lowland catchments (chapter 4).
- The P sources and transport processes in an agriculture-dominated lowland water system (chapter 5).
- The erodibility of soft sediments present in ditches and channels in lowland catchments and how this affects associated P resuspension (chapter 6).

The above mentioned objectives were addressed by a combination of laboratory and field experiments, field monitoring studies, and surveys in catchments. Chapters 2 and 3 focus on the turnover process of dissolved P to particulate P during exfiltration of Fe-rich groundwater. Chapter 2 describes the results of a field experiment in which Fe and P concentrations along a flow path from groundwater into surface water were measured weekly for over 1.5 years. We studied the oxidation rates of naturally occurring dissolved Fe(II) and associated removal of P from drainage water that flows into a field ditch. Chapter 3 focuses in detail on the formation of P-rich Fe(III) precipitates during oxidation of dissolved Fe(II), based on laboratory experiments. In a series of aeration experiments with anoxic synthetic water and natural groundwater we explored the relationship between solution composition, reaction kinetics and the characteristics of the Fe hydroxyphosphate precipitates produced. Chapter 4 focuses on the chemical speciation of P apparent in groundwater-fed headwaters in the Netherlands. For this, a sequential chemical extraction method was applied

on suspended particulate matter (SPM) samples to quantify different forms of PP under various conditions in six agriculture-dominated lowland catchments in the Netherlands. Chapter 5 focusses on the hydrodynamic controls on P transport processes in a polder area. This chapter is based on one year of high-frequency water quality and turbidity measurements near a pumping station. Finally, in chapter 6 the potential for hydrodynamic resuspension of P from bed sediments induced by increases of water flow in drainage ditches and small channels is assessed, based on erosion experiments with undisturbed sediment cores in the laboratory.

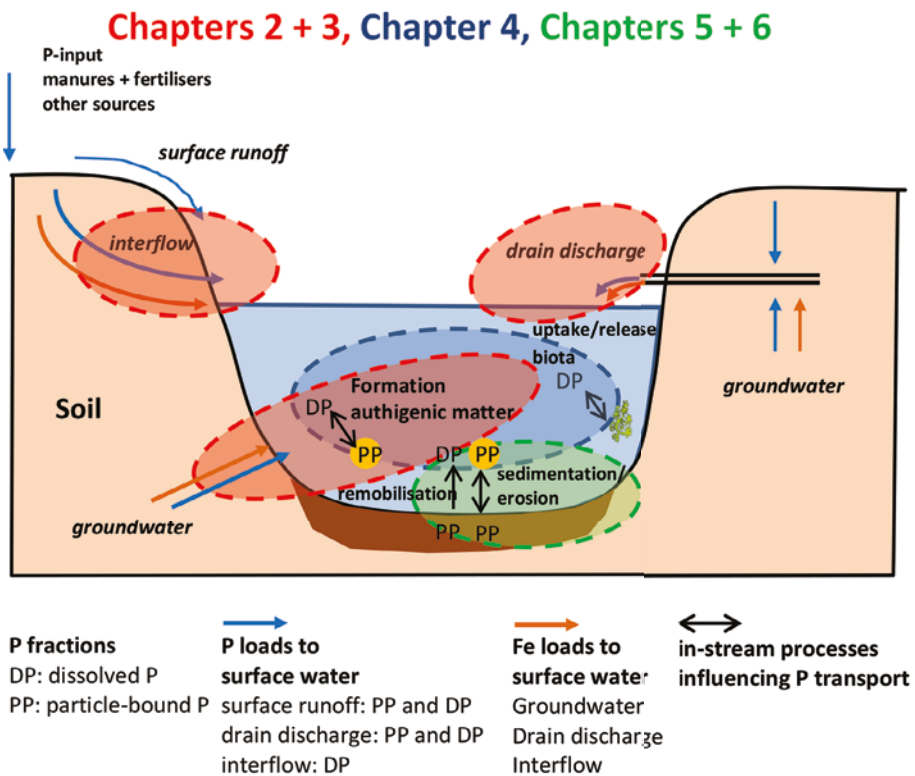


**Figure 1.11.** Main processes controlling P retention in ditches and streams in groundwater-fed lowland catchments. Coloured oblongs refer to the chapters in this thesis in which these processes are analysed: (red) chapters 2 and 3 about formation of Fe(III) precipitates and immobilisation of phosphate during exfiltration of groundwater, (blue) chapter 4 about chemical speciation of P in lowland catchments, (green) chapters 5 and 6 about hydrodynamic controls on P transport in lowland catchments.





# CHAPTER 2

## **Iron oxidation kinetics and phosphate immobilisation along the flow-path from groundwater into surface water**

Bas van der Grift, Joachim Rozemeijer, Jasper Griffioen and Ype van der Velde

*Hydrology and Earth System Sciences 18, 4687-4702.*

## 2.1 Abstract

The retention of phosphorus in surface waters through co-precipitation of phosphate with Fe-oxyhydroxides during exfiltration of anaerobic Fe(II) rich groundwater is not well understood. We developed an experimental field set-up to study Fe(II) oxidation and P immobilisation along the flow-path from groundwater into surface water in an agricultural experimental catchment of a small lowland river. We physically separated tube drain effluent from groundwater discharge before it entered a ditch in an agricultural field. Through continuous discharge measurements and weekly water quality sampling of groundwater, tube drain water, exfiltrated groundwater, and surface water, we investigated Fe(II) oxidation kinetics and P immobilisation processes. The oxidation rate inferred from our field measurements closely agreed with the general rate law for abiotic oxidation of Fe(II) by  $O_2$ . Seasonal changes in climatic conditions affected the Fe(II) oxidation process. Lower pH and lower temperatures in winter (compared to summer) resulted in low Fe oxidation rates. After exfiltration to the surface water, it took a couple of days to more than a week before complete oxidation of Fe(II) is reached. In summer time, Fe oxidation rates were much higher. The Fe concentrations in the exfiltrated groundwater were low, indicating that dissolved Fe(II) is completely oxidised prior to inflow into a ditch. While the Fe oxidation rates reduce drastically from summer to winter, P concentrations remained high in the groundwater and an order of magnitude lower in the surface water throughout the year. This study shows very fast immobilisation of dissolved P during the initial stage of the Fe(II) oxidation process which results in P-depleted water before Fe(II) is completely depleted. This cannot be explained by surface complexation of phosphate to freshly formed Fe-oxyhydroxides but indicates the formation of Fe(III)-phosphate precipitates. The formation of Fe(III)-phosphates at redox gradients seems an important geochemical mechanism in the transformation of dissolved phosphate to structural phosphate and, therefore, a major control on the P retention in natural waters that drain anaerobic aquifers.

## 2.2 Introduction

Eutrophication of freshwater ecosystems following high nutrient loads is a widely recognised water quality problem in agricultural catchments. Phosphorus (P) is often a limiting nutrient in wetlands or fresh aquatic ecosystems (Elser et al., 2007; Wassen et al., 2005) and therefore a key parameter in controlling eutrophication. P enters surface waters through point-sources such as waste water treatment plants and non-point sources via surface runoff and exfiltration of soil water and groundwater. Especially, the fate of P in surface waters originating from non-point sources is controlled strongly by biogeochemical nutrient cycling processes at the soil-water interface (Dahm et al., 1998; Dunne et al., 2006; Reddy et al., 1999).

To date, research and policy on P pollution from non-point sources have focused almost entirely on transfer of particulate phosphate from agricultural land to surface waters via overland flow or other fast flow paths during storm flow events (Jordan et al., 2012; Sharpley et al., 2008; Withers and Haygarth, 2007). However, several studies in fresh water systems suggested that substantial dissolved-phosphate loads in surface waters may originate from exfiltration of shallow or deep groundwater (Dahlke et al., 2012; Holman et al., 2008; Scanlon et al., 2005). This is especially likely to occur in delta areas (Griffioen, 2006; Hayashi and Yanagi, 2009), where the soil water and shallow groundwater is typically pH-neutral to slightly acid, anoxic, and iron-rich. The anoxic conditions are very suitable to dissolve phosphate in groundwater, which may result in relative high concentrations of dissolved phosphate from natural origin (Griffioen et al., 2013) or from leached manure or fertilizers (Chardon et al., 2007). In contrast, the chemical composition of surface waters in delta areas is normally pH-neutral to slightly alkaline and oxic with low dissolved iron and phosphate concentrations. This difference in chemical composition between groundwater and surface water creates strong redox and pH gradients at the groundwater-surface water interface (Carlyle and Hill, 2001; Frei et al., 2012). At this interface, the oxidation of iron(II) followed by iron(III) hydrolysis and precipitation of iron oxyhydroxides is the dominant chemical reaction (Baken et al., 2013; Griffioen, 2006; Gunnars et al., 2002; Kaegi et al., 2010; von Gunten and Schneider, 1991), that determines the fate of many biochemically important solutes that co-precipitate with the iron oxyhydroxides such as  $\text{PO}_4$  (Châtellier et al., 2004; Deppe and Benndorf, 2002; Fox, 1989; Lienemann et al., 1999; Mayer and Jarrell, 2000; Voegelin et al., 2013) and  $\text{AsO}_4$  (Hug and Leupin, 2003; Meng et al., 2002; Roberts et al., 2004).

The majority of studies on redox processes and P dynamics at the groundwater-surface water interface focus on mobilisation of phosphate by reductive dissolution of Fe oxyhydroxides in riparian zones or wetlands in response to rewetting (Maassen and Balla, 2010; Macrae et al., 2011; Shenker et al., 2005). In contrast, relatively little is known about the oxidation of Fe(II) in the transition zone from groundwater into surface water in lowland delta areas with (periodic) exfiltration of anaerobic groundwater in relation to P retention in surface water. The rate of Fe(II) oxidation strongly depends on pH. At neutral pH, it is a fast reaction that is expected to occur within hours when molecular oxygen is not limited (Stumm and Lee, 1961). At pH values around 6, it may take a couple of days before complete abiotic oxidation of Fe(II) occurs. The reaction rate also depends on oxygen concentration and temperature. Spiteri et al. (2006) investigated the effect of  $\text{O}_2$  and pH gradients

on oxidative precipitation of Fe(II) and subsequent phosphate sorption along a flow-line in a subterranean estuary where groundwater discharges to the sea. Their results showed that the pH is a more controlling factor than the  $O_2$  concentration.

To our knowledge, there are no field studies on the mechanisms and rates of iron oxidation with associated binding of phosphate in lowland catchments that drain anaerobic groundwater while these processes may have an important control on mobility of P in surface water (Baken et al., 2013; Fox, 1989; Griffioen, 2006). Moreover, as most of the work on Fe(II) oxidation and incorporation of phosphate into Fe(III) precipitates is performed on synthetic media, the kinetics of these processes in the natural environment are poorly known. A better understanding of these processes will improve our knowledge of P retention mechanisms in surface waters with exfiltration of anaerobic groundwater as driving force.

To study the dynamics in Fe(II) oxidation and P immobilisation along the flow-path from groundwater into surface water, we developed an experimental field set-up in an agricultural catchment of a small lowland river (the Hupsel Brook). Previous studies in the Hupsel Brook catchment have demonstrated that the groundwater in the catchment is predominantly anoxic and contains relatively high dissolved P concentrations in a range of 0.3 to 1.0 mg/l (Rozemeijer et al., 2010a). At the catchment outlet particulate P is, however, the major contributor to the total P concentrations in the surface water (Rozemeijer et al., 2010b). This indicates that transformation from dissolved P in the groundwater to particulate P in the surface water must have occurred.

In this study we aim (1) to measure the dynamics of Fe(II) and phosphate concentrations along the flow-path from groundwater into surface water in a typical lowland catchment in the Netherlands (2) to infer reaction rates and mechanisms that influence the iron oxidation process by a combination of data analysis and chemical modelling and (3) to explore the phosphate immobilisation process during the flow of anaerobic iron-rich groundwater towards surface water.

## 2.3 Methods

### 2.3.1 Study area

An experimental set-up was installed in the Hupsel Brook agricultural lowland catchment, The Netherlands (Figure 2.1) (52°03' N; 6°38' E). The size of this catchment is 6.64 km<sup>2</sup>, with altitudes ranging from 22 to 36 m +MSL (above mean sea level). A weather station of the Royal Dutch Meteorological Institute (KNMI, De Bilt, The Netherlands) is located within the catchment. The Hupsel Brook catchment has a moderate maritime climate with an average annual temperature of 9.5°C and average annual precipitation of 770 mm. Our field-scale experiment location in the Hupsel catchment is a 9000 m<sup>2</sup> tube drained meadow dominated by the grass *Lolium perenne*; surface elevation ranges from 28 to 31 m +MSL and a ditch (average depth of 1.2 m below soil surface) borders the field at the eastern side. This ditch drains a sub-catchment of the Hupsel Brook as indicated in Figure 2.1. The direction of the groundwater flow in the field is from northwest to southeast. The groundwater drains towards the eastern ditch or flows into the adjacent field south of the experimental field (Rozemeijer et al., 2010c). The drainage tubes are separated 14.5 m from

each other and discharge into the eastern ditch at 90 cm depth. To separate the water fluxes of different flow routes towards the eastern ditch, three adjacent sheet pile reservoirs were built in the ditch (Figure S2.1). These in-stream reservoirs were constructed around single drainage outlets and stretched along 43.5 m of the field. The wooden sheet piles were driven into an impermeable 30m thick Miocene clay layer starting at a depth of 3 to 5 m to capture all groundwater flow from the field into the ditch. The in-stream reservoirs captured overland flow, interflow, direct precipitation and groundwater flow from the thin, phreatic aquifer above the Miocene clay layer. The water levels in the reservoirs were measured continuously with pressure sensors from November 2007 to October 2008. The water levels inside the in-stream reservoirs were maintained at the ditch water level by pumps. Excess water was pumped from the in-stream reservoirs into the ditch, and the pumped volumes were recorded with digital flux meters (Van der Velde et al., 2010). The water flow from the individual tube drains was separated from the other flow routes by connecting each drain to a 500 L vessel. Water from these vessels was pumped into the ditch and volumes were measured with water flux meters (Van der Velde et al., 2010). The water temperature was measured continuously direct downstream the reservoirs.

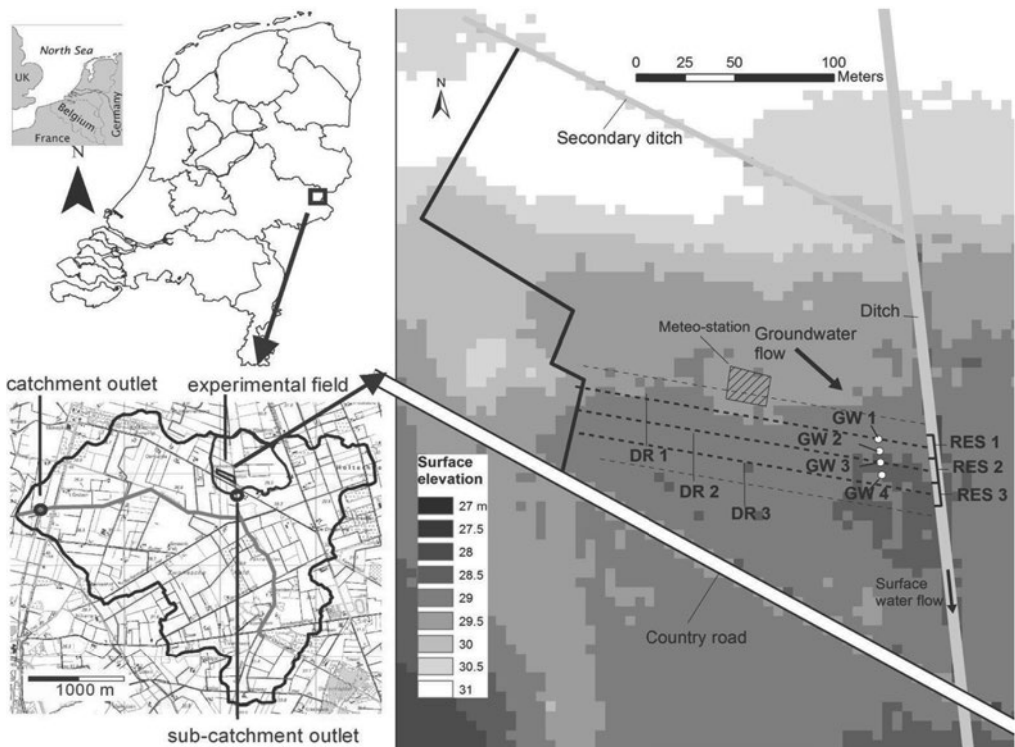


**Figure 2.1.** Location of the Hupsel catchment and the experimental field. The catchment map shows the sub-catchment outlet and catchment outlet. The field map shows the three measured tube drains (DR), the four groundwater wells (GW) and the location of the in-stream reservoirs (RES). The direction of the groundwater flow is taken from Rozemeijer et al. (2010c).

Four groundwater wells were installed for sampling of groundwater in a transect across the experimental field parallel to the ditch at a distance of 20 m from the ditch. The filters of the wells were installed 2–3 meters below the surface. More detailed information about the Hupsel catchment and all installations and measurements is found in Van der Velde et al. (2010).

### 2.3.2 Water quality measurements

We collected water samples from the four groundwater wells, the three tube drains and the three in-stream reservoirs from May 2007 until December 2008. In addition surface water samples were taken from the sub-catchment outlet and the catchment outlet. All samples were taken weekly using a peristaltic pump. During the dry summer period (July to October), the tube drains and in-stream reservoirs occasionally ran dry and sampling was sometimes not possible. We reduced the sampling to a biweekly scheme during this period. The samples were filtered in situ (0.45  $\mu\text{m}$ ) and subsamples for ICP analysis were directly acidified with  $\text{HNO}_3$ . The electrical conductivity and pH were measured immediately in the field using a flow-through cell. The samples were analysed for metals, nutrients and anions within 48 h using Ion Chromatography ( $\text{NO}_3^-$ ,  $\text{SO}_4^{2-}$ ,  $\text{Cl}^-$ ), ICP-AES (Na, K, Ca, Fe, Mg, Si), ICP-MS (P, Al) and AA3 (Automated Segmented Flow Analyzer) ( $\text{NH}_4^+$ ). Alkalinity was measured by titration. We used a variable span smoother based on local linear fits (Friedman, 1984) to aggregate trends through the concentration measurements.

### 2.3.3 Modelling reaction kinetics

To test the validity of existing chemical models developed under laboratory condition for the oxidation of Fe and co-precipitation of  $\text{PO}_4$  for our field situation, we modelled the Fe and  $\text{PO}_4$  concentrations in the reservoirs with PHREEQC (Parkhurst and Appelo, 1999) with the WATEQ4F database (Ball and Nordstrom, 1991) using the representative aqueous composition of the groundwater (Table S2.1). We compared the range and yearly average trend of measured Fe concentrations with increasing transit time of the water within the reservoirs with model scenarios. Therefore, we performed model scenarios representing a typical summer situation, a typical winter situation and a yearly average situation with their accompanying rate controlling parameters, as discussed later. First, the Fe oxidation kinetics in the reservoirs were described as a first-order reaction process following the general rate law for chemical oxidation of Fe(II) by  $\text{O}_2$ :

$$-\frac{d\text{Fe(II)}}{dt} = k[\text{Fe(II)}][\text{OH}^-]^2 P_{\text{O}_2} \quad (2.1)$$

with a value for the abiotic rate constant  $k$  at 20°C of  $7.9 (\pm 2.47) \cdot 10^{13} \text{ M}^{-2} \text{ atm}^{-1} \text{ min}^{-1}$  (Stumm and Lee, 1961). Now by assuming a continuous stirred tank reactor (CSTR) with perfect mixing and steady-state concentrations, we can describe Fe(II) concentrations in the reservoir as function of mean transit times of water through the reservoirs. (Perry et al., 1997):

$$Fe_r = \frac{Fe_i}{1 + (k \cdot T)} \quad (2.2)$$

where  $Fe_r$  is the Fe(II) concentration of the water in the reservoir,  $Fe_g$  is the Fe(II) concentration of the groundwater that flows into the reservoir,  $k'$  is the pseudo first-order reaction rate constant according Eq. 2.1 ( $k[OH]P_{O_2}$ ) and  $\bar{T}$  is the mean transit time.

The mean transit time  $\bar{T}$  of the water leaving the reservoirs at time  $t$  can be approximated through the assumption of fully mixed reservoirs with a variable flow ( $q(t)$ ) and volume ( $V(t)$ ), following (Botter et al., 2011):

$$\bar{T}(t) = \int_0^{\infty} \frac{q(t-T)}{V(t-T)} e^{-\int_0^T \frac{q(t-T+\tau)}{V(t-T+\tau)} d\tau} \cdot T dT \quad (2.3)$$

where  $q(t-T)$  is the reservoir discharge and  $V(t-T)$  is the reservoir volume at time  $t$  that has been inside the reservoir (i.e. the transit time) for a period  $T$ .

In a second step, the uptake of phosphate to Fe precipitates was modelled with two models using different concepts. First, surface complexation to ferrihydrite was considered using the Dzombak and Morel (1990) model. Surface complexation of carbonate and silicate to ferrihydrite was included, using the stability constants of Van Geen et al. (1994) and Bonte (2013). Second, precipitation of an ideal solid-solution with two endmembers, amorphous Fe hydroxide ( $Fe(OH)_3$ ) and strengite ( $FePO_4 \cdot 2H_2O$ ), was considered (Fox, 1989; Griffioen, 2006). The formation of the solid-solutions during the oxidation of Fe(II) was modelled using the solubility products of amorphous Fe hydroxide and strengite from the WATEQ4F database. Surface complexation was not included in the solid-solution model.

## 2.4 Results

### 2.4.1 Fe concentrations

The groundwater samples (Figure 2.2A) had Fe concentrations ranging between 0.2 and 45.5 mg/l with an average of 15.9 mg/l and a median value of 14.5 mg/l. The groundwater showed a temporal and spatial variation in Fe concentrations, but they were generally higher than in the other water types. The  $NO_3$ -N concentrations of the groundwater were commonly low with an average of 0.20 mg/l and a median value of 0.045 mg/l. The redox status of the groundwater can, therefore, be assessed as anaerobic and the measured Fe concentration can be attributed to Fe(II). The measured groundwater concentrations are common values for anaerobic groundwater in the eastern part of the Netherlands (Griffioen et al., 2013). The measured Fe concentration at sampling locations other than the groundwater may partly be attributed to dissolved Fe(III) colloids or complexed Fe(II) that penetrates through the 0.45  $\mu m$  filters and dissolve in the acidic media, this is discussed in the next section.

The tube drain water samples (Figure 2.2B) had Fe concentrations ranging between 0.4 and 18.9 mg/l with an average of 4.5 mg/l and a median value of 1.9 mg/l. The Fe concentrations of tube drains 1 and 2 were for the majority of samples lower than 2 mg/l. At some moments in the winter months of 2007–2008 tube drain 2 had Fe concentrations around 5 mg/l. Tube drain 3 showed a

large change in Fe concentration: the Fe concentrations increased from values around 2 mg/l to values between 10 and 15 mg/l during the period September 2007–November 2007 and exceeded 15 mg/l in November and December 2008. This water approached the Fe concentrations of the groundwater. A change in concentration of redox-sensitive components like  $\text{NO}_3^-$ ,  $\text{NH}_4^+$ , Mn, As,  $\text{HCO}_3^-$  was also observed in the drain 3 water (not shown).

The reservoir water samples (Figure 2.2C) had Fe concentrations ranging between 0.1 and 34.6 mg/l with an average of 3.9 mg/l and a median value of 2.0 mg/l. There was a winter peak in the Fe concentration of the in-stream reservoirs. During the winter (November–February), the Fe concentration reached the level of the Fe concentrations of the groundwater (5–35 mg/l), while in summer season (April–September) a majority of samples had Fe concentrations lower than 5 mg/l with an average of 1.76 mg/l. The range and average of the Fe concentrations differed between the three reservoirs during the winter period (Table 2.1). Reservoir 2 showed the highest concentrations followed by reservoir 3 and subsequently reservoir 1. Likely, this was the result of spatial variation of Fe concentrations in the groundwater, where reservoirs 2 and 3 drained groundwater with higher Fe concentrations than reservoir 1. On average, groundwater wells 1 and 2 had the highest Fe concentrations (Figure 2.2A). The groundwater flow in the field is approximately from northwest to southeast (Rozemeijer et al., 2010c). Therefore, it is conceivable that this Fe-rich groundwater flows into reservoirs 2 and 3 (Figure 2.1).

The surface water samples (Figure 2.2D) had Fe concentrations ranging between 0.15 and 2.21 mg/l with an average of 0.68 mg/l and a median value of 0.60 mg/l. There was no seasonal variation and no difference between the sub-catchment outlet and catchment outlet.

#### 2.4.2 P concentrations

The dissolved P concentrations of the groundwater were an order of magnitude higher than those of the tube drain water, reservoir water and surface water (Figure 2.3). Where the median P concentration equalled 0.33 mg/l in the groundwater, it was around 0.02 mg/l for all other water types. Despite some short-scale temporal variation in the P concentration at individual groundwater wells, the data showed increased P concentrations during summer (Figure 2.3A) (we did not investigate this further).

There was an increase in P concentration at tube drain 3 starting in November 2007 (Figure 2.3B). This was 2 months after the increase of Fe (Figure 2.3B). However, the P concentration at tube drain 3 after the redox transition did not reach the level of the P concentration of anaerobic groundwater (Figure S2.3).

There was no clear seasonal trend in P concentrations in the reservoirs and surface water (Figure 2.3C and D). Note that the Fe concentrations of the reservoir water in winter time almost matched that of the anaerobic groundwater but the P concentrations were an order of magnitude lower.

#### 2.4.3 Supporting variables

Following Eq. 2.1 and Eq. 2.2, Fe concentrations can be explained from, pH, temperature, oxygen pressure of the water and the transit time of water inside the reservoirs. These variables have been measured directly or approximated. There was a seasonal variation in the pH of the water in the



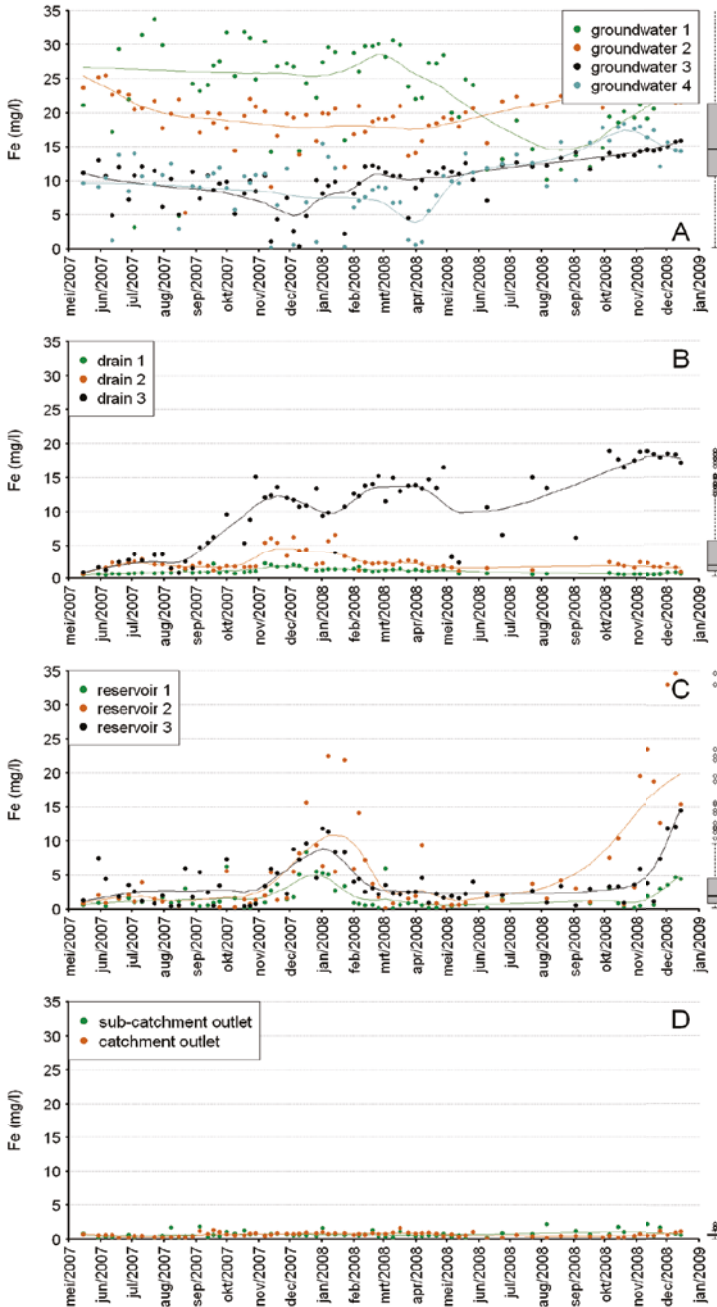


**Figure 2.2.** Time series and boxplots of Fe concentration of groundwater (A), tube drain water (B), in-stream reservoir water (C) and surface water (D). The smoothing line through the measured data points is calculated with the method of Friedman (1984). The bold solid line within each box plot is the median concentration. The lower and upper side of the box represents the 0.25 and the 0.75 quantile. Whiskers extend to the maximum and minimum value unless the values are larger than 1.5 times the box length. Open circles are extreme values.

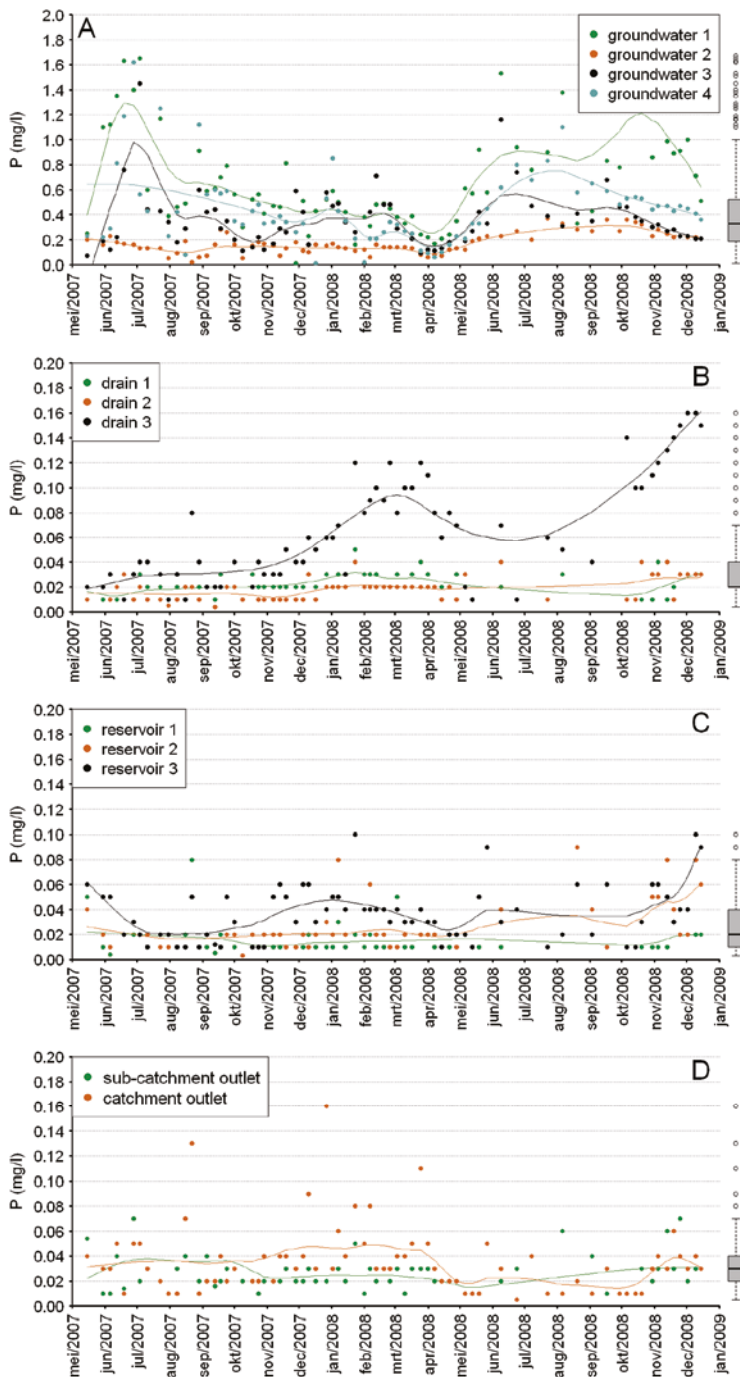


**Figure 2.3.** Time series and boxplots of dissolved total P concentrations of groundwater (A), tube drain water (B), in-stream reservoir water (C) and surface water (D). B, C and D share the same y-axis. Remarks as for Figure 2.2.

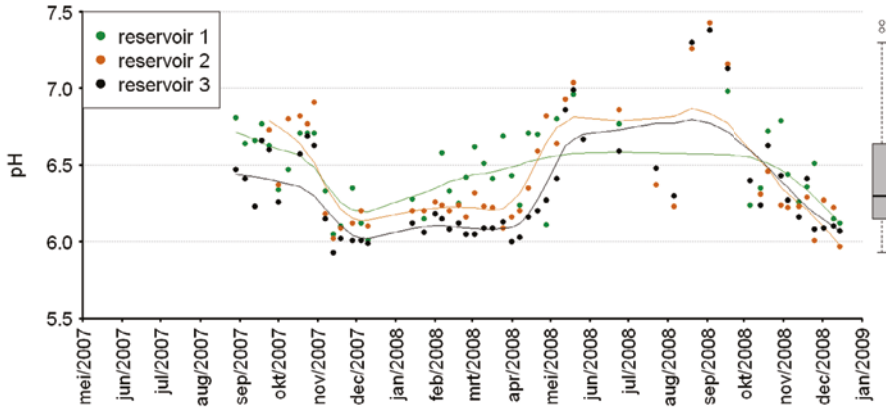


Figure 2.4. Time series and boxplot of pH of reservoir water. Remarks as for Figure 2.2.

2

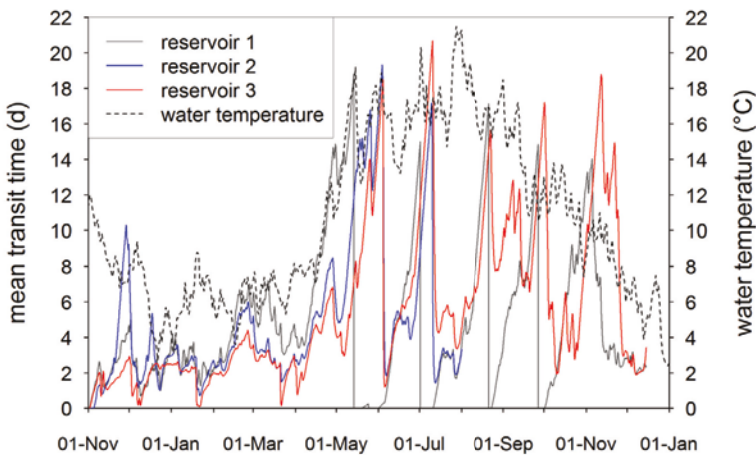


Figure 2.5. Mean transit time of the water inside the in-stream reservoirs and the temperature of the ditch water directly downstream the reservoirs.

reservoirs (Figure 2.4). The pH varied between 6 and 6.5 with an average of 6.16 during the cold November to March. Although the sampling frequency was lower during the warmer April to October, the majority of samples had pH values above 6.5 with an average of 6.6. The temperature of the ditch water varied between 2.7°C and 21.5°C (Figure 2.5).

To explore Fe oxidation kinetics and P immobilisation during exfiltration on anaerobic groundwater into surface water we calculated the mean transit time of the exfiltrated groundwater in the reservoirs from the reservoir discharge and the reservoir volume according Eq. 2.3. The

reservoir discharge and, therefore, the groundwater inflow into the reservoirs showed an decrease from winter to summer (Van der Velde et al., 2010). The reservoir volumes decreased as well but to a lesser extent than the reservoir discharge (supplement S.1). This resulted in an increase of the mean transit time of the water in the reservoirs. The mean transit time varied between 2 and 6 days during the period November 2007–March 2008 (Figure 2.5) with longer mean transit times during relatively short, drier periods and mean transit times shorter than 2 days during the intensive discharge peaks. From April 2008 to December 2008 the variation in mean transit time was larger than during the period November 2007–March 2008. Mean transit times longer than 8 days were common in the period from April 2008 to Dec. 2008. During dry periods the mean transit time increased gradually up to 20 days. Precipitation events following these drier periods reduced the mean transit time immediately to a few days. During five events in the summer of 2008 reservoir 1 went dry and, therefore, no transit time could be calculated.

**Table 2.1.** Averaged P and Fe concentrations and molar P/Fe ratios of the groundwater, the reservoir water during winter time and the drain 3 effluent.

	avg P μmol/l	avg Fe μmol/l	avg P/Fe ratio
groundwater 1	22.1	422	0.053
groundwater 2	5.6	353	0.016
groundwater 3	12.0	182	0.066
groundwater 4	14.6	184	0.079
drain 3 after Sept. 2007	2.6	235	0.011
Reservoir 1 Nov.-Feb.	0.5	56	0.009
Reservoir 2 Nov.-Feb.	1.0	229	0.004
Reservoir 3 Nov.-Feb.	1.6	119	0.014

## 2.5 Discussion

### 2.5.1 Behaviour of Fe

The first objective of our study was to measure the dynamics of Fe concentrations along the flow path from groundwater into surface water. We measured a clear trend in dissolved Fe concentration with concentration in the groundwater and low concentrations in the surface water. The Fe concentrations of the reservoir water and tube drain water were dynamic over the year. The higher Fe concentrations of the reservoir water during winter time suggest that only a part of the Fe(II) in the groundwater that was leached into the reservoirs was oxidised at the time of sampling. In summer time, the dissolved Fe concentrations of the water in the reservoirs are low. Not all the dissolved Fe in the tube drain water, reservoir water and surface water samples can be assumed as Fe(II). The presence of dissolved Fe after 0.45 μm filtration in oxygenated water has been variously

attributed to Fe(III) in colloidal phases (Lyvén et al., 2003) or complexed Fe(II) (Lofts et al., 2008). The particulate colloidal Fe(III) can exist as both organic complex and small hydroxide particle (Allard et al., 2004; Benedetti et al., 2003; Lyvén et al., 2003). Colloidal Fe(III) is stabilised against aggregation by binding of dissolved organic carbon (DOC) on its surface. Neal et al. (2008) found positive correlations between Fe and DOC concentrations of river water. However, dissolved Fe concentration in streams and rivers with near-neutral pH values do only seldom exceed 0.5 mg/l (Neal et al., 2008; Salminen, 2005). The Fe concentration in our drain water and reservoir water samples are commonly much higher and can, therefore, largely be attributed to Fe(II).

### 2.5.1.1 Reservoirs

The Fe concentrations of the reservoir water depend on the rate of the Fe oxidation process in combination with the flux of Fe-rich groundwater into the reservoirs and the transit time in the reservoirs. The pH, oxygen concentration and temperature are the major controls on the Fe(II) oxidation rate. The difference in maximum and minimum temperature of the ditch water is almost 20°C (Figure 2.5). A tenfold increase of the rate upon raising the temperature by 15°C is reported for abiotic oxidation of Fe(II) by oxygen (Sung and Morgan, 1980). This is mainly caused by the change in OH<sup>-</sup> activity due to the temperature dependence of the ionisation constant of water.

There was a seasonal variation in the pH of the water in the reservoirs (Figure 2.4), with lower values in winter and higher values in summer. According to the rate law for abiotic Fe(II) oxidation Eq. 2.3, a drop of half a pH unit for pH around 6–7 results theoretically in a ninefold increase in the half-life time of Fe(II). Therefore, the seasonal variation in the pH is another control on the dynamics in the Fe concentration of the reservoirs water. The smaller seasonal variation in the pH and Fe concentration in reservoir 1 compared to reservoirs 2 and 3 supports this conclusion.

Seasonal increases in pH may be induced by CO<sub>2</sub> degassing of surface water or by photosynthesis in the surface water column (House and Denison, 1997; Neal et al., 2002). The average  $P_{\text{CO}_2}$  of all groundwater samples is 0.056 atm., which is a common value for groundwater in the Netherlands (Griffioen et al., 2013). For the reservoir water during the summer months and winter months this is 0.024 and 0.048 atm. respectively. Degassing of CO<sub>2</sub> is kinetically controlled and, therefore, it may take a couple of days before equilibrium with air is reached. Obviously, photosynthesis occurs mainly during summer months. So, we assume that longer transit times and higher temperatures of the water in the reservoirs during summer months compared to the winter months resulted in more extensive CO<sub>2</sub> degassing. This resulted in higher pH values during summer. In contrast to CO<sub>2</sub> degassing, hydrolysis following oxidation of Fe(II) to Fe(III) generates acidity. This reduces the alkalinity of water and tempers the pH increase following CO<sub>2</sub> degassing. Modelling calculations with PHREEQC indicated that oxygenation and degassing of groundwater with a pH of 6.16, Fe(II) concentration of 15.9 mg/l, and  $P_{\text{CO}_2}$  of 0.056 atm. to the summer-average  $P_{\text{CO}_2}$  of the reservoir water of 0.024 atm. results in pH values of 6.54 and 6.39 without and with oxidative hydrolysis, respectively. These pH values are somewhat lower than a majority of pH measurements of the reservoir water during the summer months (Figure 2.4). So degassing of the surface water is not the only process that induces the seasonal pH increase.

The transit time of the water in the reservoirs also explains the low Fe concentrations in the summer months. Figure 2.6A shows that the measured concentrations decrease with an increase of the mean transit time, although a large variation of the Fe concentrations around the variable span smoother exists. Iron concentrations higher than 5 mg/l were only found when the residence time was less than 5 days. Samples from November to February have predominantly residence times shorter than 5 days and Fe concentrations above the smoother line. The Fe concentrations of samples from March to October were predominantly lower than the smoother line.

### 2.5.1.2 Tube drains

The increase in Fe concentration of tube drain 3 indicates a change in the redox status of the drained water. The flow data of the tube drains showed a decrease of the discharge rate of drain 3 starting in December 2007 (Figure S2.4). This indicates that the redox change was caused by clogging of the tube drain due to precipitation of Fe oxyhydroxides in combination with the growth of microbial biomass in the tube drain. Clogging results in an increase of the water saturation of the tube drain and therefore in a decrease of atmospheric oxygen penetration in the tube drain itself and the surrounding soil. The Fe oxidation, therefore, no longer occurs in the tube drain or the surrounding soil but after groundwater is discharged to the ditch. Clogging of filter material at redox boundaries is a common phenomenon for example in drilled wells for groundwater abstraction and also tube drains (Houot and Berthelin, 1992; Van Beek et al., 2009; Wolthoorn et al., 2004).

### 2.5.1.3 Surface water

Unlike the water in the reservoirs, the Fe concentrations of the surface water samples from the sub-catchment outlet and the catchment outlet ranges year-round around 1 mg/l. This is value range that is commonly found in (oxygenated) surface water in the Netherlands. For example, Fe concentration in filtered stream and ditch water samples in the FOREGS database for the Netherlands ranges between 0.014 and 0.787 mg/l (Salminen, 2005). This indicates that the Fe(II) from the groundwater is completely oxidised at these sampling locations. The absence of water with Fe concentrations in the range of the reservoir water is explained by the longer residence time of the surface water at the sub-catchment and catchment outlet and by contributions of the dominantly aerobic Fe-depleted tube drain water to the surface water discharge. Tube drain water was physically separated from the groundwater at our experimental field and, therefore, did not contribute to the inflow to the reservoirs. Van der Velde et al. (2010) concluded that during normal flow conditions, the tile drain contribution to surface water discharge is more important than the groundwater contribution.

Although ranging around 1 mg/l, the Fe concentrations of the surface water samples were higher than concentrations predicted by assuming equilibrium of Fe(III) with a Fe oxyhydroxide phase.

## 2.5.2 Fe oxidation kinetics

The second objective of our study was to infer reaction rates and mechanisms that influence the Fe oxidation process. The kinetic oxidation of dissolved Fe(II) was modelled according the general rate law as reported by Stumm and Lee (1961). The Fe oxidation rates inferred from our field measurements closely agree with the general rate law for abiotic oxidation of Fe(II) by O<sub>2</sub> ( $k = 7.9 \times 10^{13} \text{ M}^{-2} \text{ atm}^{-1} \text{ min}^{-1}$ )

(Figure 2.6A). Seasonal changes in pH and temperature of the reservoir water had a major effect on the Fe(II) oxidation rate as explained below.

**Table 2.2.** Input parameters for the CSTR model.

	Fe inflow (mg/l)	PO <sub>4</sub> inflow (mg/l)	pH	P <sub>O<sub>2</sub></sub> (atm.)	T (°C)
Year average	14.5	0.33	6.32	0.21	9.3
Summer situation	10.6	0.19	6.56	0.1	17
Winter situation	21.3	0.52	6.17	0.21	5

The grey lines in Figure 2.6A represent the steady-state Fe(II) concentration as a function of the mean transit times as calculated with the CSTR model. The model simulates the Fe(II) oxidation in the reservoirs for the yearly average conditions, a typical summer situation, and a typical winter situation. Table 2 gives the input parameters for the CSTR model. The Fe concentration of the groundwater (Figure 2.2A) was used as inflow concentration ( $Fe_i$  in Eq. 2.2) to the reservoir. This is variable in space and time between 0.2 and 40 mg/l. Because we don't know the values of  $Fe_i$  at sampling moments exactly, it was not possible to derive field-based oxidation rates for the individual measured Fe concentrations. The Fe concentration of the groundwater that flows into the reservoirs ( $Fe_i$ ) was set to 14.5 mg/l representing the median concentration of Fe in the groundwater. The median concentration was preferred above the average concentration due to the skewness of the Fe concentration distribution to high values. The thin lines in Figure 2.6A represent a typical summer and winter situation. The  $Fe_i$  for the summer and winter situations were set to the 25-percentile and 75-percentile of Fe concentration in the groundwater (10.6 and 21.3 mg/l, respectively). The input values for the rate controlling parameters were assigned as follows: (1) the pH values are calculated from the yearly averaged and seasonally averaged  $[H^+]$  measurements from the reservoirs (6.31, 6.17 and 6.53, respectively); (2) Biological, chemical and physical processes control the dissolved oxygen concentration of drainage ditches (Kersting and Kouwenhoven, 1989). Therefore the oxygen concentration of our reservoirs will be variable over the year and even over the day. However, low oxygen saturation levels or even hypoxia are not likely for the reservoir water. Hypoxia is not an uncommon phenomenon in ditches with free-floating plant mats (Kersting and Kouwenhoven, 1989; Verdonschot and Verdonschot, 2014) but this was not the situation for our reservoirs. Moreover, because of a high degree of atmosphere-water contact (the reservoirs have typically a small wetted volume as opposed to its wetted perimeter) equilibrium with atmospheric oxygen might be possible. In the winter situation we assume that the equilibrium time to reach complete saturation is less than the half-life time of Fe(II). Therefore, we used complete oxygen saturation ( $P_{O_2} = 0.21$  atm.) for the winter situation. The Fe(II) oxidation rate is clearly higher in the summer situation. The Fe(II) is presumably completely oxidised before the reservoir water is in equilibrium with atmospheric oxygen. For this reason we modelled the reaction for the summer situation with a  $P_{O_2}$  of 0.1 atm.; 3) the temperature for the yearly average model was set to the yearly averaged temperature of the ditch water (9.3°C) and to 17°C and 5°C for the summer and winter situation respectively (Figure 2.5).

Figure 2.6A shows that the variable span smoother through the observations matches with the model for the yearly average conditions. Although our modelled reaction rate might probably slightly be overestimated due to the presence of colloidal Fe(III) in the reservoir water samples we may safely conclude that the decrease of the Fe concentration with increasing mean transit time of the water in the reservoirs closely agreed with the reported rate law of abiotic Fe(II) oxidation in laboratory systems with a rate constant of  $7.9 \cdot 10^{13} \text{ M}^{-2} \text{ atm}^{-1} \text{ min}^{-1}$  (Stumm and Lee, 1961). Most measured Fe concentrations fall between the summer-type and winter-type lines. The winter-type model seems to underestimate the Fe(II) oxidation rate slightly. This is likely due to microbial Fe(II) oxidation that become increasingly important when abiotic rates are retarded by low temperatures (de Vet et al., 2011), like in our winter situation. Although microbial Fe(II) oxidation at low oxygen concentration and autocatalytic Fe(II) oxidation due to adsorption of Fe(II) onto surfaces of previously formed Fe(III) oxyhydroxides may happen in the reservoirs, enhanced reaction rates caused by these processes were not considered in our model. The effect of autocatalytic Fe(II) oxidation on the reaction rate is currently under debate. Sung and Morgan (1980) concluded that autocatalytic Fe(II) oxidation is only observed in experiments with a pH of 7 and higher. However, Pedersen et al. (2005) showed that Fe(II) can interact with Fe(III) oxyhydroxides surfaces and can be oxidised at pH 6.5. Schaefer et al. (2010) showed that the electron transfer between dissolved Fe(II) and structural Fe(III) can occur at the surface of Fe(III)-bearing clay minerals such as smectite. Moreover, Vollrath et al. (2012) argue that the rate law originally proposed by Stumm and Lee (1961) was already influenced by surface catalysis and, therefore, not strictly represents homogeneous Fe(II) oxidation.

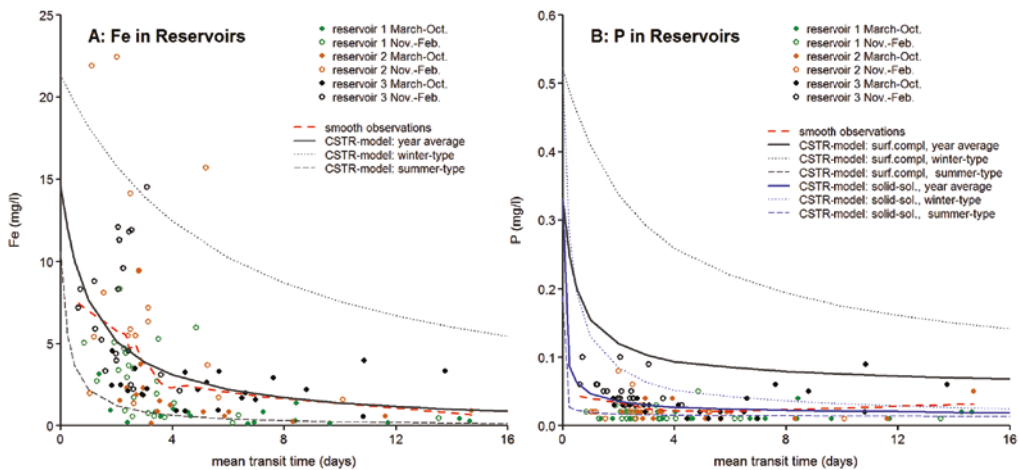


**Figure 2.6.** Measured Fe and P concentrations vs. the mean transit time of the water in the reservoirs. The blue and grey lines show the steady-state Fe and P concentrations according to the CSTR models as function of the mean transit time for the yearly average situation ( $T = 9.3^{\circ}\text{C}$ ;  $\text{pH} = 6.32$ ;  $P_{\text{O}_2} = 0.21$ ), the winter-type conditions ( $T = 5^{\circ}\text{C}$ ;  $\text{pH} = 6.17$ ;  $P_{\text{O}_2} = 0.21 \text{ atm.}$ ) and summer-type conditions ( $T = 17^{\circ}\text{C}$ ;  $\text{pH} = 6.53$ ;  $P_{\text{O}_2} = 0.1 \text{ atm.}$ ).



The large difference between the summer-type and winter-type model illustrates the effect of the temperature and pH on the abiotic Fe(II) oxidation rate. Figure 2.6A makes clear that the oxidation of Fe in anaerobic groundwater after being discharged into surface water is not instantaneous. It will take a couple of days to more than a week before complete oxidation of Fe(II) is reached, especially under winter conditions.

### 2.5.3 Behaviour of P

The third objective was to measure the dynamics in P concentrations and to explore the phosphate immobilisation process during flow of anaerobic iron-rich groundwater towards surface water. Our field data show that dissolved P preferentially precipitates from solution during the initial stage of the Fe(II) oxidation process. When high Fe concentrations happened in the reservoir water and the water from tube drain 3, substantially lower P concentrations were found in these waters compared to the groundwater. The average molar P/Fe ratios of the reservoir water and tube drain 3 varied between 0.004 and 0.014 during winter time (Table 2.1); this is distinctly lower than the P/Fe ratio in the groundwater that varied between 0.016 and 0.079. A single Fe-oxide flocs sample from a drain had a molar P/Fe ratio of 0.033. This is in the range of the groundwater P/Fe ratio. Moreover, there is no relation between the P concentration of the reservoir water and the mean transit time (Figure 2.6B) and there are no clear seasonal dynamics in P concentrations in the water other than groundwater (Figure 2.3). For tube drain 3, two mechanisms might cause these observations: (1) the average P concentration of the anaerobic groundwater that flowed into the tube drain was lower than the groundwater sampled from the four wells or (2) there was continuous immobilisation of dissolved P in tube drain 3 despite the observation that complete oxidation of Fe no longer occurred in this drain. For the reservoirs, it is not likely that the inflow of groundwater with low P concentrations determined the P concentration of this water. After all, the groundwater was sampled from four wells parallel to the reservoirs covering almost the entire stretch of the reservoirs. So the observations point to a rapid transformation of dissolved P to structural P during the initial stage of Fe(II) oxidation along the flow-path of groundwater into surface water. This resulted in nearly complete P depletion in the water before Fe(II) was depleted.

The blue and grey lines in Figure 2.6B are the steady-state P concentration according to the two CSTR models for phosphate immobilisation as a function of the mean transit time. The models simulate the binding of phosphate by surface complexation to Fe oxyhydroxide precipitates that formed during Fe(II) oxidation and precipitation of a solid-solution between amorphous Fe hydroxide ( $\text{Fe}(\text{OH})_3$ ) and strengite ( $\text{FePO}_4 \cdot 2\text{H}_2\text{O}$ ). The P concentrations of the inflow water were set to 0.33, 0.52 and 0.19 mg/l representing the median, 75-percentile and 25-percentile of P concentration in the groundwater (Table 2.2). Figure 2.6B indicates clearly that the measured P concentrations are distinctly lower than the concentrations according to the surface complexation model for the entire range of mean transit times. The immobilisation of P during aeration of groundwater could not solely be attributed to surface complexation to a Fe-oxide type of phase. The concentrations according to the model that simulate the precipitation of a solid-solution between amorphous Fe hydroxide and strengite are in the range of the measured concentrations. The variable span

smoother through the observations matches with the model for the year average conditions. The fast immobilisation of P during the short mean transit times, where Fe(II) was still present in high concentration, could satisfactorily be described by the model. This indicates the formation of Fe(III)-phosphate precipitates during the initial stage of Fe(II) oxidation until phosphate is depleted from solution. The model overestimates the lowest measured P concentration. This could be attributed to additional adsorption of phosphate to the Fe-oxides that were as well formed in the solid-solution or by uncertainty in the log K value of strengite.

Recently, Voegelin et al. (2013) studied the effect of phosphate on the formation of Fe precipitates upon oxidation of Fe(II) at near-neutral pH. Their data verify that Fe(II) oxidation initially results in the precipitation of a phosphate-rich Fe-precipitate whose P/Fe ratio reaches  $\sim 0.52$  at the time of near-complete phosphate depletion from solution. This is supported by a limited number of studies (Deng, 1997; Gunnars et al., 2002) which indicated that during Fe(II) oxidation in solutions with initial dissolved P/Fe ratio less than  $\sim 0.5$ , a phosphate-rich precipitate with molar P/Fe ratio of  $\sim 0.5$ – $0.6$  forms first. Rather than a simple formation of Fe(III)-hydroxide coupled with competitive ion adsorption, Voegelin et al. (2013) concluded that several types of Fe(III)-precipitates may form and transform over the course of Fe(II) oxidation in the presence of phosphate. Fe(III)-phosphate, phosphate-saturated hydrous ferric oxide, goethite and lepidocrocite were successively formed in their study depending on the dissolved molar P/Fe ratios. The observations from our experimental field site are thus supported by laboratory experiments on synthetic samples.

## 2.5.4 Implications

### 2.5.4.1 Dynamics in the redox gradient

The higher Fe concentration of the reservoir water during winter compared to summer are explained by a reduction of the Fe(II) oxidation rate combined with an increased inflow of groundwater into the reservoirs during winter. Based on our data, we argue that the oxidation rate of Fe(II) in combination with groundwater inflow to the ditch is such that the Fe(II) oxidation occurs at the sediment-water interface or deeper in the soil domain during summer, resulting in low Fe(II) concentrations of the reservoir water (Figure 2.2c). Fe(II) oxidation shifts to the surface water in winter evidenced by high Fe(II) concentrations. This argument is supported by visual observations of the ditch water during the field experiment. The easily resuspendable Fe-oxide flocs which have sedimented on ditch bottoms were predominantly found in winter time (Figure 2.7). So, the position of the redox gradient in the groundwater-surface water interface of our experimental field is dynamic in time as a result of dynamics in hydrological and biogeochemical conditions. Krause et al. (2009) measured highly complex temporal changes in redox status and pore water nitrate concentrations at the groundwater-surface water interface of a small river. Maassen and Balla (2010) measured the effect of these redox dynamics on phosphorus mobilisation from the sediment to the surface water. We show that dynamics in redox processes as well may impact the Fe(II) oxidation process and phosphorus immobilisation during flow from groundwater into surface water.

Due to deeper groundwater tables in summer oxygen-saturated surface water may start to infiltrate and atmospheric oxygen may penetrate the soil surrounding the tube drains. Through higher groundwater tables and more discharge this oxygen-saturated water is flushed out again

in winter time. Moreover, the abundant growth of grasses and reeds inside the ditches is likely to actively transfer oxygen through the groundwater-surface water interface during summer time. In a previous experiment at the same field site an iron-rich zone was observed directly around the drain tube, causing an orange-colored 'ring' in the soil around the tube drain (Van den Eertwegh, 2002). The P content of the solid material in this ring was three times higher than for soil samples taken just outside this iron-rich zone. Although the Fe content of the soil samples and the P concentrations of the groundwater were not measured this indicates at least a partial retardation of dissolved P in this soil domain.

#### **2.5.4.2 Suspended sediment**

The formation of Fe-oxide flocs in the surface water will contribute to the suspended sediment concentration of this surface water. The origin of suspended sediments and particulate-bound P in agricultural catchments is widely studied (Ballantine et al., 2008; Walling et al., 2008). Traditionally, two source types of suspended sediment are being distinguished: surface erosion and resuspension of streambed sediment. Rainstorm events and high discharge peaks are commonly considered as the trigger for mobilisation of these source materials (Horowitz, 2008). Little attention has been paid to the formation of authigenic sediment in the surface water systems formed by exfiltration and oxygenation of anaerobic groundwater. However, we argue that it may be an important suspended sediment source in areas draining anaerobic groundwater. The only studies, known to us, on authigenic sediments in freshwater systems formed by oxidation of iron-rich groundwater are from Baken et al. (2013) and Vanlierde et al. (2007). They reported an average annual authigenic mineral contribution to the total suspended sediment flux between 31% and 75% for a catchment in Belgium. Based on the Hupsel field experiment data, we argue that the formation of authigenic suspended sediments in the surface water domain predominantly occurs in winter time and that this attributes to an increase in the turbidity of surface water combined with a change in colour of the surface water compared to the summer situation.

#### **2.5.4.3 Remobilisation of phosphate**

Finally, the question arises: what the effect of the preferential P precipitation during oxidation of Fe(II) will be on phosphate retention. The formation of Fe(III)-phosphate precipitates during oxygenation of groundwater in the soil surrounding the ditch or tube drain may result in permanent retention of phosphate at the transition zone from groundwater into surface water. However, the structural P stored in this zone may be discharged to the surface water by erosion during high flow conditions or remobilised to dissolved P by reductive dissolution or aging of Fe(III) precipitates. Thus, the transformation of the Fe precipitates may result in the release of dissolved phosphate. A limited number of time-resolved experiments addressed the effect of transformation processes. All measured an increase in dissolved phosphate (Gerke, 1993; Mayer and Jarrell, 2000; Voegelin et al., 2013). Voegelin et al. (2013) attributed this phosphate release to ongoing Fe(III) polymerisation into (crystalline) Fe(III)-(hydr)oxides combined with no further Fe(III) supply to the solid phase that could have retained phosphate. The question remains whether this phosphate release process due to aging of minerals occurs in the natural environment as well at these reported levels. After all,

there is an ongoing Fe(II) supply in the natural environment resulting in the formation of new Fe(III) precipitates. Moreover, solutes such as silicate or humic acid interfere with Fe(III) polymerisation and may markedly slow down Fe(III) polymerisation, phase transformation and associated phosphate release (Gerke, 1993; Mayer and Jarrell, 2000).



**Figure 2.7.** Photos of the field ditch in the late summer (left) and winter (right). The red sediment indicates the presence of iron hydroxides in the winter situation. These were absent in summer.

## 2.6 Conclusions

This field study demonstrates that: (1) the Fe concentrations of water in in-stream reservoirs capturing exfiltrating anaerobic groundwater and the tube drain water were dynamic over the year. The Fe concentrations of the water in the reservoirs were high and reached the levels of the groundwater in winter time and were low in summer time. This indicates seasonal changes in the Fe(II) oxidation rate. The dissolved P concentration of the reservoir water and tube drain water were an order of magnitude lower than observed in the groundwater throughout the year. Seasonal changes in the Fe(II) oxidation rate had no impact on the P immobilisation; (2) the Fe(II) oxidation rate at our field site closely agrees with reported rate laws for abiotic oxidation of Fe(II) by  $O_2$ . Due to a lower pH and temperature the Fe(II) oxidation rates are lower in winter time compared to summer time. Combined with higher groundwater fluxes during winter this likely resulted in a shift from Fe(II) oxidation occurring in the soil or ditch sediment in summer time to the surface water in winter time; 3) Phosphorus immobilisation at our field site is much faster than the surface complexation model

proposed by Dzombak and Morel (1990). This results in nearly depletion of phosphate water before Fe(II) is depleted. The fast P immobilisation could satisfactorily be described by the precipitation of a solid-solution between amorphous Fe hydroxide and strengite (Fe(III)-phosphate). The formation of Fe(III)-phosphates at redox gradients seems to be an important biogeochemical mechanism in the transformation of dissolved phosphate to structural phosphate and, therefore, a major control on the phosphate retention in streams and ditches that drain anaerobic groundwater.

## Acknowledgements

The authors would like to thank Søren Jessen and Steeve Bonneville for their valuable comments and suggestions, which have greatly improved this paper. We would like to acknowledge Deltares for financing this study.

## 2.7 Supplement

### S.1 Meteorology and Discharge

The monthly averaged temperature during the field experiment varied between 2.2 and 17.9°C and the monthly precipitation varied between 15 and 114 mm (Table S2.2). The year 2008 was with an average temperature of 11.1°C and a total precipitation of 889 mm a normal climatological year. The in-stream reservoir discharge (resembling the combined discharges of overland flow, interflow, direct precipitation and groundwater inflow towards the ditch) varied between no flow and 0.9 l.s<sup>-1</sup> (Van der Velde et al., 2010) (Figure S2.2). The reservoir volume varied between zero and 5500 l (Figure S2.2). During several periods with high precipitation intensities, the reservoir discharges showed high peaks, especially for in-stream reservoir 3. Overland flow and interflow through macro-fauna burrows ('biopore flow') towards reservoir 3 was visually observed during the January event. Overland flow towards reservoir 2 was observed to a smaller extent. No overland flow or biopore flow was observed towards reservoir 1. Apart from the intense peaks in reservoirs 2 and 3, as indicated with arrows in Figure S2.2, all discharge to the reservoirs originated from groundwater inflow and direct precipitation (Van der Velde et al., 2011). No water quality samples were taken on days with intense discharge peaks so the effect of overland flow or biopore flow on the concentrations observed was minimal.

Monthly cumulative discharge of the reservoirs showed an increase in the groundwater inflow into the reservoirs from reservoir 1 to reservoir 3 (Table S2.2). Reservoir 3 was constructed at the lowest part of the field (Figure 2.1) which explains the higher groundwater inflow in this reservoir. Differences in groundwater inflow may also have been caused by spatial heterogeneity in the hydrologic conductivity of the thin aquifer. In the period November 2007–August 2008 the monthly averaged inflow into reservoir 2 was 1.3 to 4.5 times higher than into reservoir 1, while the monthly averaged inflow into reservoir 3 was 2.4 to 11.1 times higher than into reservoir 1. The groundwater inflow into the reservoirs was lower in summer (April–September) than in winter (October–March).

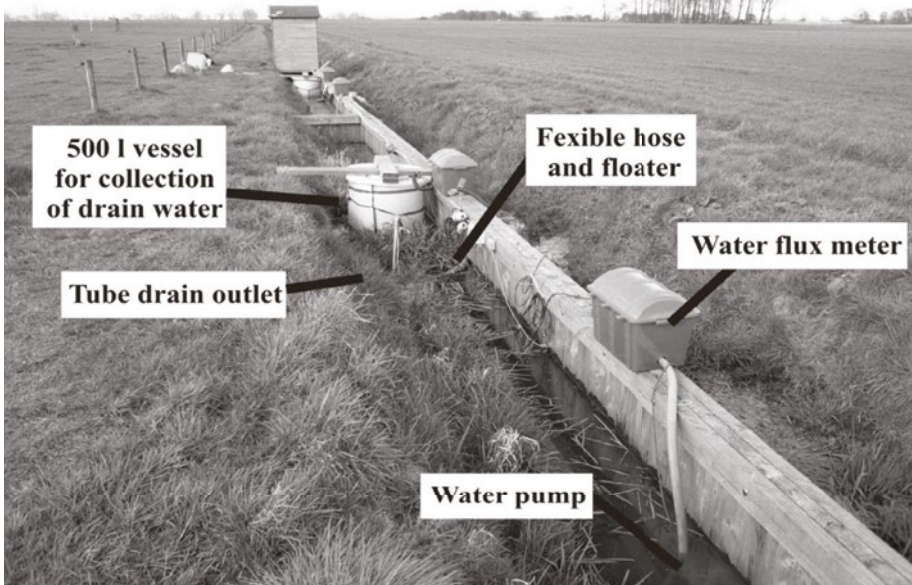


**Figure S2.1.** Measurement setup with collector vessels for drain discharge, pumps, and water flux meters. The shed in the back houses the data acquisition and control equipment (from Van der Velde et al., 2010).

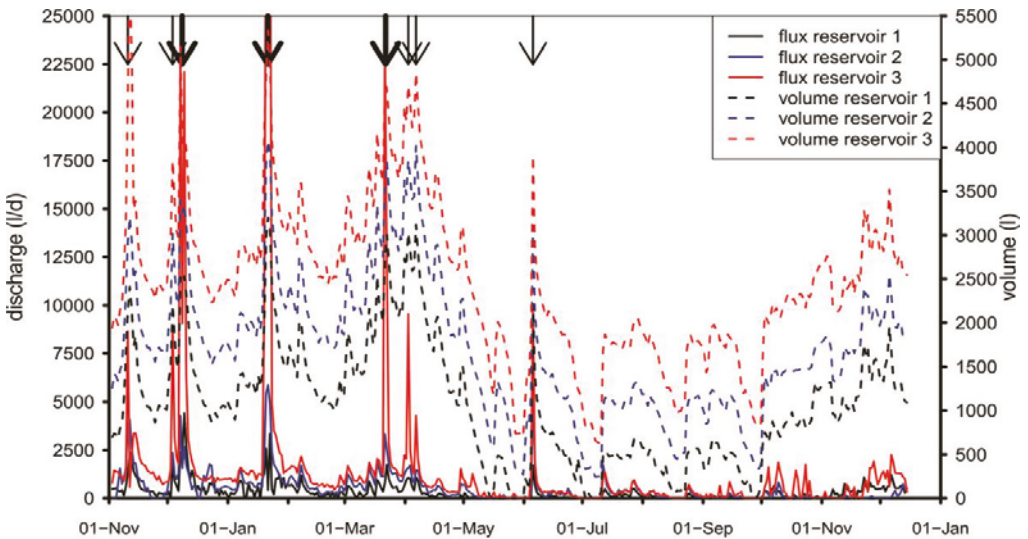


**Figure S2.2.** Daily average value of hourly measured in-stream reservoir discharge and reservoir volume. Arrows indicate discharge events on which overland flow and interflow towards the reservoirs occurred (bold arrows multiple day events, thin arrows one day events).

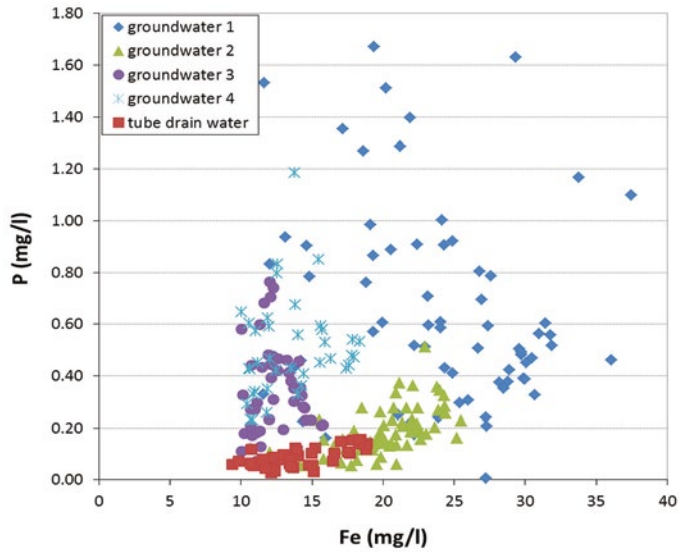


**Figure S2.3.** Measured Fe and P concentrations in groundwater and tube drain effluent samples with Fe concentration exceeding 10 mg/l.

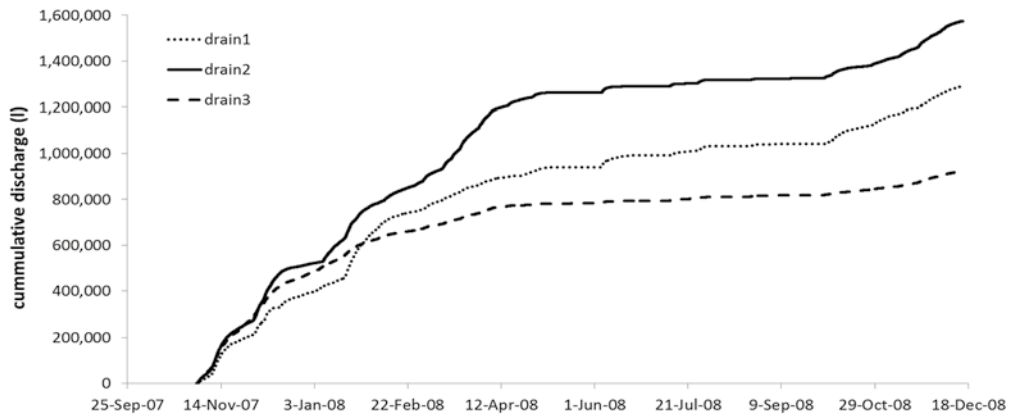


**Figure S2.4.** Measured cumulative discharge of three tube drains, until early December 2007 the discharge of tube drain 3 equals the discharge of tube drain 1. Afterwards, the discharge of tube drain 3 decreases. The increase in Fe concentration of tube drain 3 ends early December.



**Table S2.1.** Aqueous composition of a representative groundwater sample.

Compound	Unit	Value
pH		6.4
Elec. conductivity	µS/cm	363
Cl <sup>-</sup>	mg/l	19.98
NO <sub>3</sub> <sup>-</sup>	mg/l	< 0.1
SO <sub>4</sub> <sup>2-</sup>	mg/l	48.65
NH <sub>4</sub> <sup>+</sup>	mg/l	0.92
P	mg/l	0.33
Alkalinity	mg/l	107.8
Na <sup>+</sup>	mg/l	19.96
K <sup>+</sup>	mg/l	9.74
Ca <sup>2+</sup>	mg/l	27.54
Fe <sup>2+</sup>	mg/l	14.5
Mg <sup>2+</sup>	mg/l	10.94
Si <sup>4+</sup>	mg/l	5.62
Al <sup>3+</sup>	mg/l	0.5

**Table S2.2.** Monthly averaged meteorological data (derived from KNMI) and groundwater inflow to the in-stream reservoirs.

month	year	temp avg °C	precipitation sum mm	reservoir 1 m <sup>3</sup>	sum discharge reservoir 2 m <sup>3</sup>	reservoir 3 m <sup>3</sup>
11	2007	6.11	71	16.2	21.7	41.2
12	2007	3.15	74	17.3	22.9	41.8
1	2008	4.33	114	15.1	27.0	54.4
2	2008	4.67	29	9.5	17.4	30.3
3	2008	5.37	99	12.8	29.9	40.7
4	2008	8.34	49	6.8	15.8	24.7
5	2008	14.95	48	0.7	3.0	7.5
6	2008	16.48	76	2.2	7.5	9.6
7	2008	17.87	93	4.5	11.0	10.9
8	2008	17.25	61	1.8	4.0	5.6
9	2008	13.13	53	1.0	-	4.2
10	2008	9.72	52	5.0	-	16.6
11	2008	6.20	56	11.3	-	12.5
12	2008	2.16	15	8.4	-	17.4



# CHAPTER 3

## **Fe hydroxyphosphate precipitation and Fe(II) oxidation kinetics upon aeration of Fe(II) and phosphate-containing synthetic and natural solutions**

Bas van der Grift, Thilo Behrends, Leonard Osté,  
Paul Schot, Martin Wassen and Jasper Griffioen

### 3.1 Abstract

Exfiltration of anoxic Fe-rich groundwater into surface water and the concomitant oxidative precipitation of Fe are important processes controlling the transport of phosphate ( $\text{PO}_4$ ) from agricultural areas to aquatic systems. Here, we explored the relationship between solution composition, reaction kinetics, and the characteristics of the produced Fe hydroxyphosphate precipitates in a series of aeration experiments with anoxic synthetic water and natural groundwater. A pH stat device was used to maintain constant pH and to record the  $\text{H}^+$  production during Fe(II) oxidation in the aeration experiments in which the initial aqueous P/Fe ratios ( $(\text{P}/\text{Fe})_{\text{ini}}$ ), oxygen concentration and pH were varied. In general, Fe(II) oxidation proceeded slower in the presence of  $\text{PO}_4$  but the decrease of the  $\text{PO}_4$  concentration during Fe(II) oxidation due to the formation of Fe hydroxyphosphates caused additional deceleration of the reaction rate. The progress of the reaction could be described using a pseudo-second-order rate law with first-order dependencies on  $\text{PO}_4$  and Fe(II) concentrations. After  $\text{PO}_4$  depletion, the Fe(II) oxidation rates increased again and the kinetics followed a pseudo-first-order rate law. The first-order rate constants after  $\text{PO}_4$  depletion, however, were lower compared to the Fe(II) oxidation in a  $\text{PO}_4$ -free solution. Hence, the initially formed Fe hydroxyphosphates also affect the kinetics of continuing Fe(II) oxidation after  $\text{PO}_4$  depletion. Presence of aqueous  $\text{PO}_4$  during oxidation of Fe(II) led to the formation of Fe hydroxyphosphates. The P/Fe ratios of the precipitates ( $(\text{P}/\text{Fe})_{\text{ppt}}$ ) and the recorded ratio of  $\text{H}^+$  production over decrease in dissolved Fe(II) did not change detectably throughout the reaction despite a changing P/Fe ratio in the solution. When  $(\text{P}/\text{Fe})_{\text{ini}}$  was 0.9, precipitates with a  $(\text{P}/\text{Fe})_{\text{ppt}}$  ratio of about 0.6 were formed. In experiments with  $(\text{P}/\text{Fe})_{\text{ini}}$  ratios below 0.6, the  $(\text{P}/\text{Fe})_{\text{ppt}}$  decreased with decreasing  $(\text{P}/\text{Fe})_{\text{ini}}$  and pH value. Aeration experiments with natural groundwater showed no principal differences in Fe(II) oxidation kinetics and in  $\text{PO}_4$  immobilisation dynamics compared with synthetic solutions with corresponding P/Fe ratio, pH and oxygen pressure. However, aeration of groundwater with relative high DOC concentrations and a low salinity lead to P-rich Fe colloids that were colloidally stable. The formation of a Fe hydroxyphosphate phase with a molar P/Fe ratio of 0.6 can be used for predictive modelling of  $\text{PO}_4$  immobilisation upon aeration of pH-neutral natural groundwater with an  $(\text{P}/\text{Fe})_{\text{ini}}$  ratio up to 1.5. These findings provide a solid basis for further studies on transport and bioavailability of phosphorus in streams, ditches and channels that receive anoxic Fe-rich groundwater.

### 3.2 Introduction

The chemistry of phosphate in aquatic systems is often controlled through interactions with iron (Fox, 1989; Mayer and Jarrell, 2000). Under oxidising conditions, aqueous phosphate has a strong affinity to associate with Fe oxyhydroxides (Filippelli, 2008). Association with Fe oxyhydroxides may include adsorption, surface precipitation, formation of solid solutions and co-precipitation (Dzombak and Morel, 1990; Fox, 1989; Griffioen, 2006; Ler and Stanforth, 2003; van Riemsdijk et al., 1984; Voegelin et al., 2010). Iron associated  $\text{PO}_4$  can be solubilised under reducing conditions due to reductive dissolution of Fe oxyhydroxides (Mayer and Jarrell, 2000). However, under anoxic conditions, mobilisation of  $\text{PO}_4$  can be limited due to formation of Fe(II)-phosphate minerals such as vivianite (Heiberg et al., 2012; Roden and Edmonds, 1997). Redox transformations of iron in natural environments thus exert a strong influence on the mobility of  $\text{PO}_4$ .

Lowland areas, like the Netherlands, typically have redox-reactive aquifers containing anoxic Fe(II)-rich groundwater (Frapporti et al., 1993; Griffioen et al., 2013). When Fe(II)-rich groundwater enters surface water, Fe(III) precipitates are formed at the groundwater-surface water interface upon oxygenation of the anoxic groundwater (Baken et al., 2013; Baken et al., 2015b; Van der Grift et al., 2014; Vanlierde et al., 2007). The formation of Fe oxyhydroxides during groundwater exfiltration is expected to be accompanied by the immobilisation of aqueous phosphate due to its association with the Fe precipitates (Baken et al., 2015a; Griffioen, 1994). The release of  $\text{PO}_4$  to surface water following  $\text{PO}_4$  leaching from heavily fertilised agricultural fields to groundwater and the extent of  $\text{PO}_4$  retention at the redox interface are of major importance for surface water quality (Baken et al., 2015b; Schoumans and Chardon, 2014). Based on field data, Van der Grift et al. (2014) proposed that the formation of Fe(III) phosphate precipitates can be an important natural immobilisation mechanism for aqueous  $\text{PO}_4$  during flow of groundwater into surface water. This may reduce the  $\text{PO}_4$  load from agricultural land to surface water. Consequently, formation of Fe(III) phosphates at redox interfaces might be a major control on the  $\text{PO}_4$  transport in the continuum from land to sea and on the bioavailability of  $\text{PO}_4$  in natural waters that drain anoxic aquifers. Detailed insight into the chemical stoichiometry and the kinetics of formation of Fe(III) phosphate phases during oxygenation of anoxic, Fe and  $\text{PO}_4$  containing groundwater is therefore of great interest.

Precipitation of Fe(III) from  $\text{PO}_4$  containing aqueous solutions is expected to lead to the formation of Fe hydroxyphosphates (Stumm and Morgan, 1970) with variable P/Fe ratio according to the stoichiometry:



where  $1/r$  is the stoichiometric molar P/Fe ratio of the Fe hydroxyphosphate. The solubility constants for mineral phases have been reported for  $r = 1$  (strengite) by Nriagu (1972) and later by Iuliano et al. (2007), for  $1/r = 0.66$  (tinticite) by Nriagu and Dell (1974) and for  $1/r = 0.4$  by Luedecke et al. (1989). Pratesi et al. (2003) described the existence of an amorphous Fe hydroxyphosphate, santabarbarite, with a  $1/r$  value of 0.66 but no solubility data were presented. Iron(III) phases with high P/Fe ratios have been identified in natural systems such as lakes (Buffle et al., 1989; Gunnars et al., 2002;

Lienemann et al., 1999) as well as estuarine or lake sediments (Hyacinthe and Van Cappellen, 2004; Tessenow, 1974). Precipitation of these phases has also been reported as a mechanism for  $\text{PO}_4$  removal from wastewater (Fytianos et al., 1998; Luedecke et al., 1989; Stumm and Sigg, 1979).

Formation of Fe hydroxyphosphates induced by Fe(II) oxidation at near-neutral pH has been investigated in various studies (Einsele, 1934; Griffioen, 2006; Gunnars et al., 2002; Kaegi et al., 2010; Lienemann et al., 1999; Matthiesen et al., 2001; Mayer and Jarrell, 2000; Senn et al., 2015; Tessenow, 1974; Voegelin et al., 2010; Voegelin et al., 2013). Phosphate uptake per oxidised Fe was found to be limited to a P/Fe molar ratio of  $\approx 0.5$ – $0.6$  under varying experimental conditions regarding initial Fe(II) and  $\text{PO}_4$  concentrations, pH and background electrolytes, (Gunnars et al., 2002; He et al., 1996; Tessenow, 1974; Voegelin et al., 2013). This suggests the formation of a single type of Fe hydroxyphosphate phase at initial aqueous P/Fe ( $(\text{P/Fe})_{\text{ini}}$ ) ratios larger than  $\approx 0.5$ . A limited number of studies indicate that P-rich precipitates with molar P/Fe ratio of  $0.5$ – $0.6$  can form in the beginning of Fe(II) oxidation even when the  $(\text{P/Fe})_{\text{ini}}$  is less than  $0.5$  (Deng, 1997; Einsele, 1934; Gunnars et al., 2002; Tessenow, 1974; Voegelin et al., 2013). As a consequence, the P/Fe ratio in the solution progressively decreases when precipitates form which are relatively enriched in P. By using TEM and XAS, Voegelin et al. (2013) showed that, in solutions with  $(\text{P/Fe})_{\text{ini}}$  less than  $0.5$ , early formation of amorphous Fe hydroxyphosphates is followed by the formation of short-range ordered ferrihydrite-type precipitates in silicate-containing solutions or poorly-crystalline lepidocrocite in silicate-free solutions when the solution becomes depleted in  $\text{PO}_4$ . The sequential precipitation of Fe hydroxyphosphates followed by precipitation of Fe oxyhydroxides during Fe(II) oxidation indicates that formation of Fe hydroxyphosphates with a P/Fe ratio around  $0.5$ – $0.6$  is either kinetically controlled or Fe hydroxyphosphates with a P/Fe ratio around  $0.5$ – $0.6$  are the thermodynamically favoured precipitates in the initial stage of homogeneous nucleation due to low surface energies (Navrotsky et al., 2008). The molar P/Fe ratio in precipitates was also around  $0.5$ – $0.6$  in studies on As removal in presence of  $\text{PO}_4$ . This finding has been used to rationalize variations in the efficiency of As removal techniques from drinking water in areas with different groundwater chemistry (Hug et al., 2008; Roberts et al., 2004). Since the P/Fe ratios in the Fe hydroxyphosphates seem to vary to a small extent for several experimental conditions, it is likely that these precipitates can not be considered as a distinct mineral phase. Several authors observed, for instance, that Fe- $\text{PO}_4$  solids in natural systems contain other major cations like Ca (Matthiesen et al., 2001; Perret et al., 2000). Senn et al. (2015) recently published results of Fe(II) aeration experiments in  $\text{PO}_4$  and Ca containing solutions and showed that the formed precipitates are not distinct phases but mixtures of different types of polymers whose fractional contribution gradually varies with solution chemistry. In addition, Voegelin et al. (2013) measured P/Fe ratios in precipitates that formed at different time intervals during Fe(II) oxidation. The P/Fe ratios varied in a single experiment indicating that not a distinct Fe- $\text{PO}_4$  phase is formed but that the precipitates are a solid-solution whose composition depends on the  $\text{PO}_4$  activities in the solution. Fox (1989) argued that  $\text{PO}_4$  levels in rivers with low calcium concentrations are controlled by a solid-solution of Fe phosphate and Fe oxyhydroxide.

The kinetics of Fe(II) oxidation and precipitation of Fe oxyhydroxides has been investigated intensively (e.g. Davison and Seed, 1983; Millero, 1985; Stumm and Lee, 1961; Sung and Morgan, 1980), but there is a limited number of studies that addressed the kinetics of Fe(II) oxidation in

presence of  $\text{PO}_4$  (Cumplido et al., 2000; Mao et al., 2011; Mitra and Matthews, 1985; Tamura et al., 1976; Wolthoorn et al., 2004). These studies indicate that the presence of  $\text{PO}_4$  affects the kinetics of Fe(II) oxidation. Phosphate accelerates the oxidation of dissolved Fe(II) (Mao et al., 2011; Mitra and Matthews, 1985; Tamura et al., 1976). Tamura et al. (1976) found that the rate of oxidation of micromolar Fe(II) could be expressed as a function of the concentration of  $\text{H}_2\text{PO}_4^-$ . Conversely, Mitra and Matthews (1985) concluded that  $\text{HPO}_4^{2-}$  was the sole phosphate species controlling the Fe(II) oxidation rate. Mao et al. (2011) found that the aqueous phosphate complex  $\text{FePO}_4^-$  was the most important Fe(II) species contributing to the oxidation kinetics of nanomolar Fe(II) at circumneutral pH. Cumplido et al. (2000) showed that the rate of Fe(II) oxidation in presence of Fe oxyhydroxides phases accelerates with increasing  $\text{PO}_4$  concentrations. Oxidation of adsorbed Fe(II) slows down in heterogeneous systems upon addition of  $\text{PO}_4$  as shown by Wolthoorn et al. (2004). None of these studies characterised the kinetics of Fe(II) oxidation when the composition of the Fe(III)-precipitates changes during the reaction. This is usually the case when Fe(II) containing groundwater becomes exposed to atmospheric oxygen because the initial P/Fe ratio is typically below 0.5.

Most experimental work on  $\text{PO}_4$  immobilisation induced by Fe(II) oxidation have used synthetic solutions. However, the presence of other constituents in natural groundwater can additionally alter the Fe(II) oxidation kinetics and  $\text{PO}_4$  immobilisation. Studies that use natural groundwater are, to our knowledge, limited to the work of Baken et al. (2013) and Griffioen (2006) and the applicability of experimental results on  $\text{PO}_4$  immobilisation during groundwater seepage into surface water is still unclear. For example, Griffioen (2006) was not able to model the immobilisation of  $\text{PO}_4$  by Fe oxide type phases that form upon oxygenation of dissolved Fe(II) in natural groundwater using existing solid phase association concepts.

In this study we aim to: (1) determine the P/Fe ratios in Fe hydroxyphosphates that form during Fe(II) oxidation in presence of  $\text{PO}_4$  as a function of pH, the initial aqueous P/Fe ratio and the reaction progress; (2) establish the kinetics of Fe(II) oxidation upon aeration of synthetic solutions with varying P/Fe ratios; (3) assess the effectiveness of the formation of Fe- $\text{PO}_4$  phases to immobilise  $\text{PO}_4$  when natural Fe(II) and  $\text{PO}_4$ -containing groundwater is exposed to atmospheric oxygen; and (4) explore the possibility of using predictive mechanistic models for  $\text{PO}_4$  immobilisation during groundwater seepage. Oxidation of Fe(II) was studied in a series of time-resolved aeration experiments with synthetic water and natural groundwater with variable  $(\text{P/Fe})_{\text{ini}}$  while pH values and oxygen concentrations were kept constant at various levels. The combination of continuously monitoring acid production with a pH stat device and discrete sampling and analyses allowed us to follow the kinetics of the reaction and the chemical composition of the precipitates throughout the experiments.

### 3.3 Materials and Methods

#### 3.3.1 Batch experiments with synthetic solutions

Aeration experiments with synthetic aqueous solutions were carried out at Fe(II) concentrations between 0.2 and 0.27  $\text{mmol L}^{-1}$  and  $\text{PO}_4$  concentrations in the range of 0-0.18  $\text{mmol L}^{-1}$ . Hence, initial

aqueous P/Fe ratios ( $(P/Fe)_{\text{ini}}$ ) were varied between 0 and  $\approx 0.9$  (Table 3.1). The experimental setup was similar to that used by Vollrath et al. (2012). The experiments were carried out in a 1 litre glass reactor with an electrically powered stirrer (Applikon Stirrer Controller P100) and a dissolved oxygen sensor (Applisens DO2 sensor, low drift). The drift of the sensor is negligible and the response time is less than 30 seconds. The pH was kept constant during the experiment using an automated pH stat device which delivered a  $0.01 \text{ mol L}^{-1}$  NaOH solution to the reactor vessel (Metrohm unitrode PT 100 electrode coupled to titrino Metrohm 736 GP controlled by TiNET 2.4 software). The oxygen concentration was kept constant during the experiments by purging a gas with defined  $\text{O}_2$  content through the reactor. The  $\text{O}_2$  content of the gas was maintained by a mass flow control unit (Bronkhorst HI-TEC) that regulated gas mixtures of compressed air and argon. In the experiments with synthetic solutions, the gas was conveyed through two gas washing bottles, first through a bottle with soda lime pellets followed by a bottle with a  $0.05 \text{ mol L}^{-1}$  NaOH solution in order to remove  $\text{CO}_2$ . Then the gas was humidified in a third gas-washing bottle before it finally entered the reactor. The experiments with synthetic solutions were performed using  $500 \text{ ml } 4.8 \text{ mmol L}^{-1}$  KCl background electrolyte solution. The stirring rate was set to 200 rpm to minimise local pH fluctuations during NaOH addition. A solution of  $0.2 \text{ mol L}^{-1} \text{ Fe}(\text{NH}_4)_2(\text{SO}_4)_2 \cdot 6 \text{ H}_2\text{O}$  in  $0.032 \text{ mol L}^{-1}$  HCl was used as Fe(II) stock. The stock solution was kept constantly under Ar atmosphere in a glovebox to prevent iron oxidation. A solution of  $0.2 \text{ mol L}^{-1} \text{ KH}_2\text{PO}_4$  was used as  $\text{PO}_4$  stock. The KCl solution was purged with Ar prior to Fe(II) addition until the concentration of  $\text{O}_2$  in solution concentration was lower than  $0.001 \text{ mmol L}^{-1}$ . Next, the reactor was spiked with the desired amount of the  $\text{PO}_4$  stock solution and Fe(II) stock solution. The Fe(II) oxidation experiment was started by switching from Ar to pressurised air or a pressurised air/Ar mixture in the purging gas. The desired  $\text{O}_2$  level was reached in the reactor within a few minutes after changing the gas composition. The experiments were conducted in a climate controlled room at  $20^\circ\text{C}$ .

### 3.3.1.1 Monitoring reaction progress

The reaction progress was followed by continuously monitoring the supply of NaOH by the pH stat device. Before and during the experiment, samples were taken from the solution in the reactor to follow the evolution of Fe(II), Fe(III) and  $\text{PO}_4$  concentrations over time. Each sample (6 ml) was retrieved with a syringe from the reactor and was immediately filtered through  $0.45 \mu\text{m}$  nylon membranes and acidified to a  $\text{pH} = 1.5$  using a  $6 \text{ M HCl}$  solution. The Fe(II) concentrations were measured within 6 h after sampling. The concentrations were determined using spectrophotometric methods. Iron(II) and total-Fe were measured in separate sub-samples using the ferrozine method from Viollier et al. (2000). In the total-Fe subsample, Fe(III) was reduced to Fe(II) using a hydroxylamine hydrochloride solution. The Fe(II) concentrations were measured spectrophotometrically with Ferrozine at  $562 \text{ nm}$  (Shimadzu UV Spectrophotometer, UV-1800) against standard series in a range between 0 and  $100 \mu\text{mol L}^{-1}$  obtained with  $\text{Fe}(\text{NH}_4)_2(\text{SO}_4)_2 \cdot 6\text{H}_2\text{O}$  (Sigma-Aldrich) in  $0.5 \text{ mol L}^{-1}$  HCl. The Fe(III) concentrations were calculated from the differences between total-Fe and Fe(II) concentrations. The detection limit of the spectrophotometric method was  $3 \mu\text{mol L}^{-1}$ . The 95% confidence interval of the calibration line varied between  $1.2$  and  $2.3 \mu\text{mol L}^{-1}$ , leading to an uncertainty of the measured



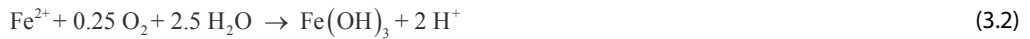
concentration that ranged between 55% at the detection limit and 1.4% in the middle of the calibration range.

Phosphate concentrations were determined according to the molybdenum blue method of Koroleff (1983). This method is based on the reaction of the  $\text{PO}_4$  ion with an acidified molybdate reagent to yield a phosphormolybdate complex, which is then reduced to the intensely coloured mixed-valence complex. The  $\text{PO}_4$  concentrations were measured at 880 nm against standard series in a range between 0 and  $25 \mu\text{mol L}^{-1}$  prepared with  $\text{KH}_2\text{PO}_4$  (Fulka-analytical). The detection limit of the spectrophotometric method was  $1 \mu\text{mol L}^{-1}$ . The 95% confidence interval of the calibration line varied between 0.14 and  $0.17 \mu\text{mol L}^{-1}$ , leading to an uncertainty of the measured concentrations that ranged between 15% at the detection limit and 0.4% for concentrations in the middle of the calibration range.

The Fe/P ratio in the precipitates ( $(\text{Fe}/\text{P})_{\text{ppt}}$ ) was calculated from the reduction of dissolved Fe(II) and  $\text{PO}_4$  concentrations over the duration of the experiment. The Fe(III) concentrations during the oxidation reaction were in a range from  $-6$  to  $9 \mu\text{mol L}^{-1}$  (details in the supplementary material, Figure S3.1) and were in the range of the uncertainties related to the different measurement. This indicated that colloidal Fe(III) was effectively retained by the filter membranes and that Fe passing the filter was mostly dissolved Fe(II).

### 3.3.1.2 Reaction stoichiometry

According to the ideal stoichiometry of Fe(II) oxidation by oxygen followed by precipitation of Fe hydroxide, 2 moles of protons are released per mole oxidised Fe(II):



Incorporation of water molecules or anions other than hydroxide in freshly formed Fe oxyhydroxides results in stoichiometric ratios between  $\text{H}^+$  production and Fe(II) oxidation lower than 2 (Bonneville et al., 2004; Fox, 1988; Vollrath et al., 2012). Hence, the stoichiometric ratio between produced  $\text{H}^+$  and oxidised Fe(II) is expected to be lower when Fe hydroxyphosphates form during Fe(II) oxidation compared to formation of pure Fe oxyhydroxides. For a Fe hydroxyphosphate with the general empirical stoichiometry  $\text{Fe}_r\text{PO}_4(\text{OH})_{3r-3(s)}$  (s) the molar P/Fe ratio of the precipitates equals  $1/r$  (Eq. 3.1). In solutions with  $\text{H}_2\text{PO}_4^-$  as the sole aqueous phosphate species,  $2-1/r$  moles of protons are released per mole  $\text{Fe}^{2+}$  oxidised:



An increase in the molar P/Fe ratio of the precipitate results in a decrease of the amount of produced protons per oxidised aqueous Fe(II) (hereinafter referred to as the molar  $\text{H}^+/\text{Fe}^{2+}$  ratio) with a lowest possible  $\text{H}^+/\text{Fe}^{2+}$  ratio of 1 for  $r = 1$ , resembling the precipitation of strengite ( $\text{FePO}_4 \cdot 2\text{H}_2\text{O}$ ). The speciation of the phosphoric acid depends on pH and changes in the phosphoric acid speciation have an impact on the  $\text{H}^+/\text{Fe}^{2+}$  ratio. Geochemical modelling was used to calculate the effect of phosphoric acid speciation on the  $\text{H}^+/\text{Fe}^{2+}$  ratio (see section 2.1.3).

For each experiment, the molar  $H^+/Fe^{2+}$  ratio was calculated from the Fe(II) concentration measured directly on the discrete samples and the continuously recorded NaOH consumption. The experimentally derived molar  $H^+/Fe^{2+}$  ratio can be used to derive the  $(P/Fe)_{ppt}$  of the Fe hydroxyphosphates by geochemical modelling based on Eq. 3.3. By this, we evaluated whether the derived  $H^+/Fe^{2+}$  ratio for one experiment with Fe hydroxyphosphate formation is consistent with the measured  $(P/Fe)_{ppt}$  ratios obtained from the loss of dissolved Fe(II) and  $PO_4$  which was measured in discrete samples.

The  $H^+/Fe^{2+}$  calculation ignores Fe(II) associated with the particulate phase. It is not unlikely that Fe(II) oxidation triggers precipitation of an initially mixed-valence Fe(II, III) hydroxyphosphate. Under corresponding conditions, initial uptake of Fe(II) by Fe hydroxyphosphates has been documented by Voegelin et al. (2013). Replacement of Fe(III) by Fe(II) does not change the number of released  $H^+$  at a given  $(P/Fe)_{ppt}$  ratio (details in the supplementary material). That is, solid phase Fe(II) oxidation without a change in the  $(P/Fe)_{ppt}$  does not result in further  $H^+$  production or consumption. Iron(II) association with the solid phase has, thus, no effect on the interpretation of  $(P/Fe)_{ppt}$  ratios based on the measured  $H^+$  production over dissolved Fe(II) decrease. Iron(II) association with the particulate phase can also be caused by surface complexation of Fe(II) on ferrihydrite. Surface complexation modelling calculations indicated that the fraction adsorbed Fe(II) is less 0.5% during the initial state of the reaction and can be, hence, neglected.

The continuous evolution of dissolved Fe(II) concentration with time was obtained from the continuously monitored NaOH addition and the molar  $H^+/Fe^{2+}$  ratio. The continuous evolution of Fe(II) concentration was used to explore the Fe(II) oxidation kinetics throughout the experiments. Since Fe(II) association with the particulate phase is ignored, the Fe(II) oxidation rates can be considered as maximum values.

### 3.3.1.3 Geochemical modelling

PHREEQC (Parkhurst and Appelo, 1999) with the WATEQ4F database (Ball and Nordstrom, 1991) was used for modelling the  $H^+/Fe^{2+}$  molar ratio according to Eq. 3.3 for the experiments with synthetic solutions and for predictive modelling for  $PO_4$  immobilisation during groundwater seepage. Therefore, data were used from groundwater aeration experiments published by Griffioen (2006). In this study, fast immobilisation of  $PO_4$  ( $< 1$  day) was investigated in aeration experiments with nutrient-rich anoxic groundwater having a wide variety in chemical composition and  $(P/Fe)_{ini}$  ratios ranging from 0.07 to 40. The synthetic solution experiments were geochemically modelled starting with the measured initial Fe(II) and  $PO_4$  concentrations, pH, temperature and the concentration of the background electrolyte. The groundwater experiments from Griffioen (2006) were modelled starting with the measured groundwater composition. Next, a constant oxygen pressure was imposed ( $P_{O_2} = 0.2$  atm) and, by this, the equilibrium Fe redox state changed and Fe(II) became oxidised to Fe(III). The activities of the various species in solution, the precipitation of the Fe hydroxyphosphate, the molar  $H^+/Fe^{2+}$  ratio (Eq. 3.3) and the residual  $PO_4$  concentrations after precipitation of Fe hydroxyphosphates were calculated with PHREEQC. For describing the precipitation of Fe hydroxyphosphates  $Fe_rPO_4(OH)_{3r-3(s)}$  we used the solubility constant of  $Fe_{2.5}PO_4(OH)_{4.5}$  (Luedecke et al., 1989) with a  $r$  value of 2.5:

$$\text{Log } K_{\text{Fe}_{2.5}\text{PO}_4(\text{OH})_{4.5}} = 2.5 \log [\text{Fe}^{3+}] + \log [\text{PO}_4^{3-}] + 4.5 \log [\text{OH}^-] = -96.7 \quad (3.4)$$

wherein [i] refers to the activity of species i. Solubility constants for Fe hydroxyphosphates with  $r$  values deviating from 2.5 were calculated from Eq. 3.4 using PHREEQC and the assumption that the solubility of the Fe hydroxyphosphates did not change significantly within the range of  $r$  values of our experiments. Therefore, we replaced the stoichiometric coefficients in Eq. 3.4 with the corresponding values and calculated the *Ion Activity Product (IAP)* for the Fe hydroxyphosphate  $\text{Fe}_r\text{PO}_4(\text{OH})_{3r-3(s)}$  in a  $\text{Fe}_{2.5}\text{PO}_4(\text{OH})_{4.5}$  saturated solution (*Saturation Index (SI)* = 0). When assuming equilibrium for the  $\text{Fe}_r\text{PO}_4(\text{OH})_{3r-3(s)}$  phase in this system as well, the  $\text{LogIAP}_{\text{Fe}_r\text{PO}_4(\text{OH})_{3r-3}}$  equals the  $\text{Log}K_{\text{Fe}_r\text{PO}_4(\text{OH})_{3r-3}}$ .

### 3.3.2 Batch experiments with natural groundwater

Aeration experiments with natural groundwater were done with groundwater collected from piezometers in an experimental field within the Hupsel brook catchment in the eastern part of the Netherlands (Van der Velde et al., 2010). The groundwater was sampled from two piezometers, gw3 and gw4, at a distance of 20 m from a drainage ditch (Van der Grift et al., 2014) during the summer of 2013. The filters of the piezometers were situated at one to three metres depth into the three metre thick sandy aquifer. The groundwater in this part of the experimental field is dominantly anoxic with Fe concentrations varying between 0.1 and 0.5 mmol L<sup>-1</sup>, PO<sub>4</sub> concentrations between 6 and 50 μmol L<sup>-1</sup> and P/Fe ratios varying between 0.01 and 0.83 (Van der Grift et al., 2014). The collected water is representative for the anoxic groundwater seepage into surface water.

The groundwater was sampled with a peristaltic pump after first discarding at least three well volumes and no entrainment of bubbles was apparent in the tubes. The aqueous oxygen concentration, temperature and pH were measured on site. The anoxic water was directed into the bottom of 2 L glass bottles under continuous purging with N<sub>2</sub>. Additionally, water samples for chemical analysis were also taken from the two piezometers. All samples were filtered through a 0.45 μm pore size cellulose nitrate filter. A sub-sample was collected in a polyethylene bottle and acidified to a pH of 1 using suprapur nitric acid (Inorganic Ventures). This sample was analysed for metals and total P by ICP-OES and Fe(II) using the ferrozine method (Viollier et al., 2000).

The anoxically sampled natural groundwater was transferred into the batch reactor by purging the bottle with N<sub>2</sub> while draining the water through a tube directly into the reactor purged with Ar. The oxidation experiment was initiated by changing the gas composition from Ar to a CO<sub>2</sub> / pressurised air mixture. In contrast to the experiments with synthetic solution, the pH-stat device could not be used to derive Fe(II) oxidation rates due to the presence of dissolved carbonate in groundwater. The pH was not controlled by a pH stat device but the pH was constrained by the equilibrium between the CO<sub>2</sub> pressure and the inorganic carbon concentration. The required CO<sub>2</sub> content of the purging gas in order to maintain the in-situ pH was calculated with PHREEQC (Parkhurst and Appelo, 1999) from the measured pH and alkalinity. The pH of the solution was continuously monitored and did not change by more than 0.05 pH-values. Regularly, aliquots from the experimental solutions were taken and analysed as described in section 3.3.1.1. Additional to the concentration measurements in the < 0.45 μm filtrate, the 'truly' dissolved Fe(II), Fe(III) and PO<sub>4</sub> concentrations were measured after ultrafiltration of the < 0.45 μm filtrates using membranes with nominal molecular weight

cutoffs (MWCO) of 50 kDa (Amicon XM Polyacrylonitrile/PVC Copolymer membranes). For this, the  $< 0.45 \mu\text{m}$  filtrates were immediately transferred into a 10 ml stirred ultrafiltration cell (Amicon 8010) and filtered with  $\text{N}_2$  overpressure. It should be noted that even a 50 kDa cutoff may not be sufficient to reliably isolate the truly dissolved fraction (50 kDa equals  $\approx 50000$  atomic units, this are polymers with up to 500  $\text{Fe}(\text{OH})_3$  units and a diameter up to a few nm). The obtained dissolved concentrations are still an upper estimate.

## 3.4 Results

The results of the experiments with synthetic solutions are presented in the next sections for the experiments without  $\text{PO}_4$ , with an excess of P ( $(\text{P}/\text{Fe})_{\text{ini}} = 0.9$ ) and with an excess of Fe ( $(\text{P}/\text{Fe})_{\text{ini}} = 0.3, 0.18$  and  $0.12$ ), respectively. In each section first the reaction stoichiometry and, second, the reaction progress is presented. Examples of the reaction progress curves at a constant pH value of 6.1 and  $\text{O}_2$  concentrations of  $10.5 \text{ mg L}^{-1}$  are shown in Figure 3.1 presenting the results from one experiment of a series of experiments with identical  $(\text{P}/\text{Fe})_{\text{ini}}$  ratios. Detailed results of all experiments are shown in the supplement (Figures S3.2–S3.6) and summarised in Table 3.1. Finally, the results of the groundwater aeration experiments are presented.

### 3.4.1 Fe(II) oxidation experiments at $(\text{P}/\text{Fe})_{\text{ini}} = 0$

#### 3.4.1.1 Reaction stoichiometry

The Fe(II) concentrations decreased over time after starting the aeration of the solution (Figure 3.1) and this decrease was accompanied by the production of protons. The time evolution of the dissolved Fe(II) concentration at different pH values and  $\text{O}_2$  concentrations are shown in Figure S3.2, Row A. For the  $\text{PO}_4$ -free experiments, the  $\text{H}^+/\text{Fe}^{2+}$  ratio equalled 1.90–1.94 and a good match was obtained between the progress of Fe(II) oxidation, calculated from the NaOH consumption, and discrete measurements of Fe(II) concentrations throughout these experiments (Table 3.1, Figure S3.2, Row A). That is, the  $\text{H}^+/\text{Fe}^{2+}$  ratio remained constant throughout the entire experiment. The experimentally derived  $\text{H}^+/\text{Fe}^{2+}$  ratio closely matched the ideal stoichiometry of Fe(II) oxidation by oxygen in combination with Fe oxyhydroxide precipitation, i.e. 2 moles of protons were released per mole  $\text{Fe}(\text{OH})_3$  being formed.

#### 3.4.1.2 Reaction progress

The experiments without  $\text{PO}_4$  had in common that the rates of Fe(II) oxidation were slow during the first tens of minutes and, subsequently, the rates went through a phase of acceleration. Afterwards, rates continuously slowed down upon consumption of reactants and finally approached completion after several hundreds of minutes (Figure 3.1 and Figure S3.2, Row B). The target  $\text{O}_2$  concentration was reached in less than ten minutes after the start of the experiment. During this period, an acceleration of the oxidation rate can be attributed to the build-up of the  $\text{O}_2$  concentration. The increase of the reaction rate continued, however, up to several tens of minutes for the experiment at pH = 6.1 and  $\text{O}_2 = 10.5 \text{ mg L}^{-1}$  to over 100 minutes for exp. pH = 6.1,  $\text{O}_2 = 8.5 \text{ mg L}^{-1}$  and exp.

pH = 6.4,  $O_2 = 3.6 \text{ mg L}^{-1}$ . This extended period of acceleration could, therefore, not be attributed to the adjustment of  $O_2$  concentrations in the reactor. The existence of distinct stages in the reaction progress is most apparent when using log-linear plots (Figure 3.1 and Figure S3.2, Row C). After the initial stage, Fe(II) oxidation followed first-order kinetics which is reflected in a linear trend in the log-linear plots. The apparent rate constant was obtained from the slope of a linear regression line and varied between  $0.0039$  and  $0.0053 \text{ min}^{-1}$  (Table 3.1, Figure S.32). The measured rate constants were a factor 1.3–1.6 higher than those derived from the rate law established by Stumm and Lee (1961).

### 3.4.2 Fe oxidation experiments at $(P/Fe)_{\text{ini}} = 0.9$

#### 3.4.2.1 Reaction stoichiometry

The  $PO_4$  and Fe(II) concentrations decreased over time after starting the aeration of the solution. The Fe(II) consumption rate was, however, higher than the  $PO_4$  consumption rate (Figure 3.1 and Figure S3.3, Row A). When the Fe(II) oxidation approached completion, the  $PO_4$  concentration remained around  $60\text{--}80 \text{ }\mu\text{mol L}^{-1}$  irrespective of the oxygen concentration. The concomitant consumption of dissolved  $PO_4$  and Fe(II) confirmed the formation of a Fe hydroxyphosphate precipitate during Fe(II) oxidation. It was possible to reproduce the time evolution of measured Fe(II) concentrations from the continuously recorded NaOH addition by optimising a constant molar  $H^+/Fe^{2+}$  ratio for the  $P/Fe = 0.9$  experiments (Figure 3.1 and Figure S3.3, Row A). The molar  $H^+/Fe^{2+}$  ratios were lower than for the  $PO_4$ -free experiments and equalled 1.33 and 1.27 for the three experiments at pH = 6.1 and pH = 6.4, respectively (Table 3.1 and Figure S3.3, Row A). In replicate experiments at pH = 6.1 and  $O_2 = 10.5 \text{ mg L}^{-1}$  identical  $H^+/Fe^{2+}$  ratios were obtained. Also the molar  $(P/Fe)_{\text{ppt}}$  ratio of the precipitates stayed relatively constant after the initial stage of the experiments. Deviation from this ratio during the initial stage of the experiment can be attributed to analytical inaccuracy as the decrease in Fe(II) and  $PO_4$  concentrations was only around  $10 \text{ }\mu\text{mol L}^{-1}$  or less. The  $(P/Fe)_{\text{ppt}}$  ratios were, with values around 0.6, similar for all experiments at pH = 6.1 and slightly lower (0.56) for the experiment at pH = 6.4 (Table 3.1). A Fe hydroxyphosphate with a molar  $P/Fe$  ratio of 0.60 has the stoichiometry  $Fe_{1.67}PO_4(OH)_{2.01}$  and one with a molar  $P/Fe$  ratio of 0.56 has the stoichiometry of  $Fe_{1.79}PO_4(OH)_{2.37}$ .

Model calculations give a molar  $H^+/Fe^{2+}$  ratio of 1.31 during precipitation of a  $Fe_{1.67}PO_4(OH)_{2.01}$  phase from an aerated solution with a  $(P/Fe)_{\text{ini}}$  ratio of 0.9 and a pH = 6.1. This calculated ratio matches the experimentally observed ratio of 1.33 almost perfectly. A similar good match was obtained for the other experiment with a  $(P/Fe)_{\text{ini}}$  ratio of 0.9 (Table 3.1). In addition, the time evolution of  $PO_4$  concentrations, as calculated from the NaOH addition, the molar  $H^+/Fe^{2+}$  ratio and the  $(P/Fe)_{\text{ppt}}$  ratio were consistent with the  $PO_4$  concentrations measurement on discrete samples, too. Hence, the alternative approaches for deriving the  $(P/Fe)_{\text{ppt}}$  ratios yielded consistent results: at high  $(P/Fe)_{\text{ini}}$  ratios the precipitating solid can be represented by an empirical stoichiometry of  $Fe_{1.67}PO_4(OH)_{2.01}$  to  $Fe_{1.79}PO_4(OH)_{2.37}$  and the stoichiometry did not seem to change throughout the reaction.

#### 3.4.2.2 Reaction progress

Similar to the  $PO_4$ -free experiments, the course of the reaction can be divided into two stages with different Fe(II) oxidation kinetics. The existence of an initial reaction stage is most apparent when

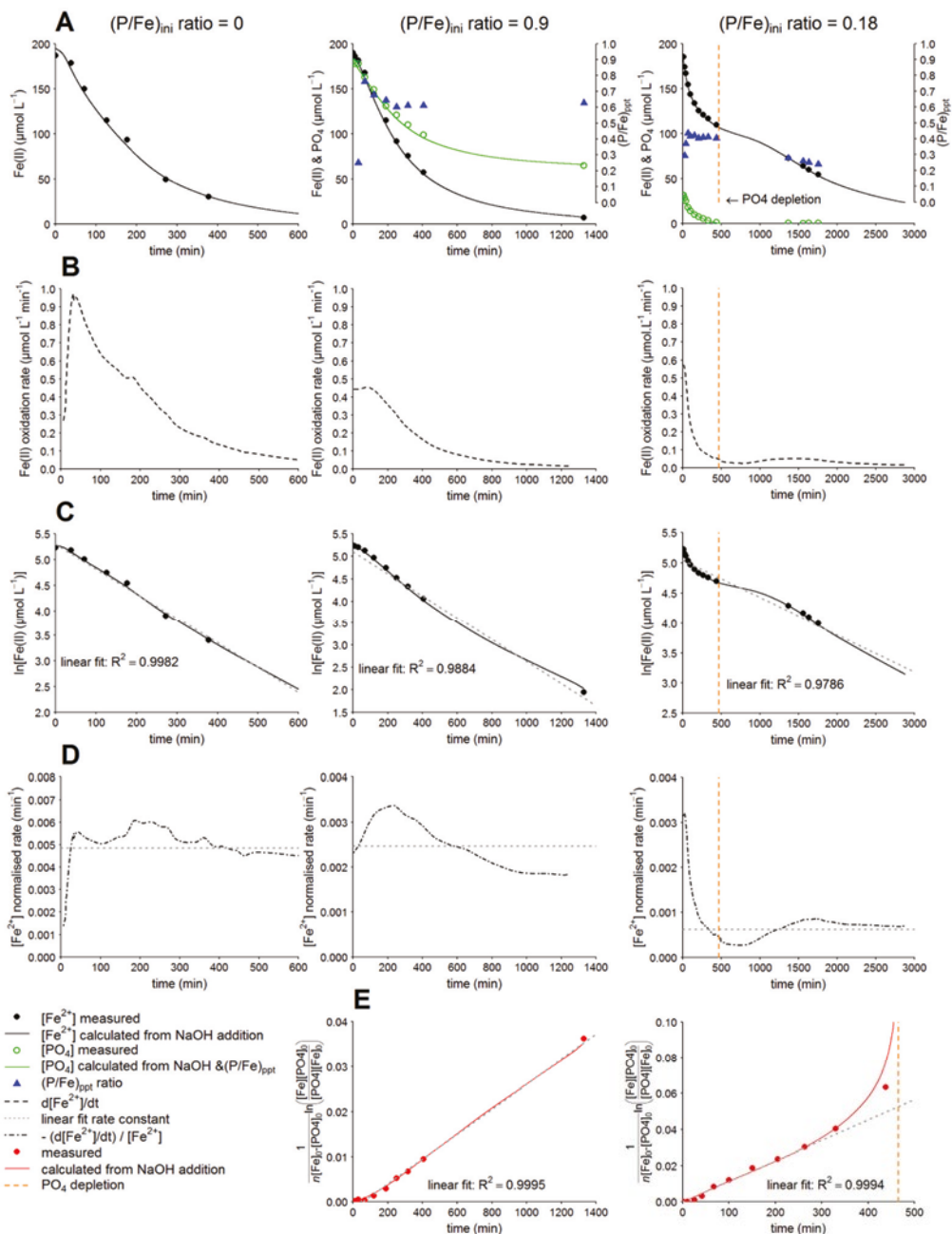


**Figure 3.1.** Examples of the time evolution of Fe(II) oxidation during aeration experiments with  $(P/Fe)_{ini}$  ratios of 0.9, 0.18 and 0 at pH = 6.1 and  $O_2 = 10.5 \text{ mg L}^{-1}$ . (Row A) Fe(II),  $PO_4$  concentration and  $(P/Fe)_{ppt}$  ratio of precipitate. (Row B) Fe(II) oxidation rate. (Row C) semi logarithmic plot of the time evolution of Fe(II) concentration. (Row D) Fe(II) normalised rates as a function of time. Row E: plot of the integrating the second-order rate law term vs. time. For the experiment at  $(P/Fe)_{ini} = 0.18$  only data before  $PO_4$  depletion are plotted. Symbols are measurements on discrete samples. Solid lines are computed from the continuously monitored NaOH addition.

**Table 3.1.** Overview of synthetic solutions aeration experiments. The experimental stages before and after near-depletion of  $\text{PO}_4$  are indicated as  $\text{PO}_4$  stage and  $\text{PO}_4$  free stage, respectively.

P/Fe ratio initial	pH	$\text{O}_2$ mg L <sup>-1</sup>	P/Fe ratio precipitates <sup>1)</sup>	stoichiometry precipitate	(H <sup>+</sup> /Fe <sup>2+</sup> ) ratio measured $\text{PO}_4$ stage	(H <sup>+</sup> /Fe <sup>2+</sup> ) ratio measured $\text{PO}_4$ free stage	(H <sup>+</sup> /Fe <sup>2+</sup> ) ratio measured $\text{PO}_4$ free stage	$t_{3/4}$ min	Fe(II) normalised oxidation rate $\text{PO}_4$ stage min <sup>-1</sup>	first-order rate constant $\text{PO}_4$ free stage min <sup>-1</sup>	second-order constant $\text{PO}_4$ stage $\mu\text{mol}^{-1}\text{L min}^{-1}$	moment depletion min	moment $\text{PO}_4$ min	moment dFe/dt minimal min
0	6.1	8.5	0	$\text{Fe}(\text{OH})_3$	-	-	1.94	390	-	0.0039	-	-	-	-
0	6.1	10.5	0	$\text{Fe}(\text{OH})_3$	-	-	1.93	290	-	0.0049	-	-	-	-
0	6.4	3.5	0	$\text{Fe}(\text{OH})_3$	-	-	1.90	300	-	0.0053	-	-	-	-
0.90	6.1	8.5	0.60 ± 0.01	$\text{Fe}_{1.67}\text{PO}_4(\text{OH})_{2.01}$	1.33	1.31	-	790	0.0022-0.0011	-	1.53x10 <sup>-5</sup>	-	-	-
0.93	6.1	10.5	0.61 ± 0.01	$\text{Fe}_{1.64}\text{PO}_4(\text{OH})_{1.92}$	1.33	1.30	-	460	0.0034-0.0018	-	2.78x10 <sup>-5</sup>	-	-	-
0.93	6.1	10.5	0.61 ± 0.01	$\text{Fe}_{1.64}\text{PO}_4(\text{OH})_{1.92}$	1.33	1.30	-	480	0.0032-0.0016	-	2.48x10 <sup>-5</sup>	-	-	-
0.96	6.4	3.6	0.56 ± 0.01	$\text{Fe}_{1.79}\text{PO}_4(\text{OH})_{2.37}$	1.27	1.29	-	750	0.0023-0.0014	-	1.79x10 <sup>-5</sup>	-	-	-
0.30	6.1	10.5	0.48 ± 0.02	$\text{Fe}_{2.08}\text{PO}_4(\text{OH})_{3.24}$	1.42	1.46	1.95	2020	0.003-0.0003	0.0007	5.25x10 <sup>-5</sup>	790	1180	-
0.28	6.4	3.6	0.44 ± 0.02	$\text{Fe}_{2.27}\text{PO}_4(\text{OH})_{3.81}$	1.47	1.47	1.85	1670	0.0013-0.0004	0.0013	3.53x10 <sup>-5</sup>	1000	1460	-
0.18	6.1	10.5	0.41 ± 0.02	$\text{Fe}_{2.44}\text{PO}_4(\text{OH})_{4.32}$	1.55	1.52	1.89	1890	0.003-0.0004	0.0008	1.13x10 <sup>-4</sup>	480	760	-
0.18	6.4	3.6	0.36 ± 0.02	$\text{Fe}_{2.78}\text{PO}_4(\text{OH})_{4.34}$	1.48	1.54	1.91	930	0.004-0.0007	0.0022	9.46x10 <sup>-5</sup>	430	490	-
0.12	6.1	10.5	0.39 ± 0.01	$\text{Fe}_{2.56}\text{PO}_4(\text{OH})_{4.68}$	1.48	1.54	1.85	1200	0.0015-0.0005	0.0014	5.72x10 <sup>-5</sup>	340	390	-
0.12	6.4	3.6	0.40 ± 0.02	$\text{Fe}_{2.5}\text{PO}_4(\text{OH})_{4.5}$	1.46	1.49	1.84	890	0.0001-0.0007	0.0023	4.08x10 <sup>-5</sup>	380	430	-

1) Average value and standard deviation of series of calculated (P/Fe)<sub>ppt</sub> ratio bases on the decrease in measured Fe(II) and  $\text{PO}_4$  concentrations.

2) Time required for 75% Fe(II) oxidation.

plotting the Fe(II) oxidation rate as function of time (Figure 3.1 and Figure S3.3, Row B). During the initial reaction stage (to  $\approx 200$  min) the Fe(II) oxidation rate increased with time. This initial acceleration of the rates was also observed in the experiments in the absence of  $\text{PO}_4$ . However, the initial stage lasted longer in the presence of excess  $\text{PO}_4$  compared with the  $\text{PO}_4$ -free experiments. During the second stage (after  $\approx 200$  min), the rate decreased with time.

The Fe(II) oxidation rates were lower in the  $\text{PO}_4$  excess experiments compared with the  $\text{PO}_4$ -free experiments (Figure 3.1, row B). For example, at a Fe(II) concentration of  $100 \mu\text{mol L}^{-1}$  in the experiment at  $\text{pH} = 6.1$  and  $\text{O}_2 = 10.5 \text{ mg L}^{-1}$ , the Fe(II) oxidation rate was  $0.54 \mu\text{mol L}^{-1} \text{ min}^{-1}$  in the absence of  $\text{PO}_4$ . In comparison, the rates were  $0.32\text{--}0.34 \mu\text{mol L}^{-1} \text{ min}^{-1}$  in the experiments with  $(\text{P}/\text{Fe})_{\text{ini}}$  ratios of 0.9 at the same Fe(II) and  $\text{O}_2$  concentration. This trend also persisted at a lower  $\text{O}_2$  concentration ( $\text{O}_2 = 3.6 \text{ mg L}^{-1}$ ): at the same Fe(II) concentration in the experiments at  $\text{pH} = 6.4$ , the rate was  $0.57 \mu\text{mol L}^{-1} \text{ min}^{-1}$  without  $\text{PO}_4$  compared with  $0.22 \mu\text{mol L}^{-1} \text{ min}^{-1}$  in presence of  $\text{PO}_4$ .

In contrast to the  $\text{PO}_4$ -free experiments, the reaction did not follow pseudo-first-order kinetics after the initial acceleration phase when  $\text{PO}_4$  was present. Although the decrease of  $\ln[\text{Fe}^{2+}]$  showed an almost linear trend with time after  $\approx 200$  min (Figure 3.1 and Figure S3.3, Row C) the overall order of the reaction is not 1. The  $[\text{Fe}^{2+}]$  normalised rates decreased after  $\approx 200$  min (Figure 3.1 and Figure S3.3, Row D) but the deviation from first-order kinetics becomes apparent when plotting the logarithmised reaction rates ( $\ln(v)$ ) as a function of the logarithmised  $\text{Fe}^{2+}$  concentrations ( $\ln[\text{Fe}^{2+}]$ ) (Figure 3.2, top row). In the absence of  $\text{PO}_4$ ,  $\ln(v)$  decreased linearly with decreasing  $\ln[\text{Fe}^{2+}]$  with a slope of about 1. When  $\text{PO}_4$  was present, the slope of the trend line was significantly steeper. That is, the apparent pseudo-first-order rate constant decreased after the initial stage (after  $\approx 200$  min) when  $\text{PO}_4$  was present while it remains unchanged in the  $\text{PO}_4$ -free experiments. Hence, the results indicate that  $\text{PO}_4$  concentrations influence Fe(II) oxidation rates in addition to temperature,  $\text{O}_2$  concentration, Fe(II) concentration and pH.

### 3.4.3 Fe oxidation experiments with $(\text{P}/\text{Fe})_{\text{ini}} = 0.3, 0.18$ and $0.12$

#### 3.4.3.1 Reaction stoichiometry

The experiments with  $(\text{P}/\text{Fe})_{\text{ini}}$  ratios of 0.3, 0.18 and 0.12 have in common that  $\text{PO}_4$  was virtually removed from solution before Fe(II) oxidation reached completion (Figure 3.1 and Figures S4-S6, Row A). In contrast to the experiments without  $\text{PO}_4$  and higher  $(\text{P}/\text{Fe})_{\text{ini}}$  ratios, an initial stage with retarded Fe(II) oxidation was not noticeable. Nevertheless, the progress of Fe(II) oxidation exhibited two major stages: stage 1 where  $\text{PO}_4$  is present in solution and the Fe(II) oxidation led to formation of Fe hydroxyphosphates and stage 2, after almost complete  $\text{PO}_4$  removal from solution, when Fe(II) oxidation resulted in precipitation of Fe oxyhydroxide. The  $(\text{P}/\text{Fe})_{\text{ppt}}$  ratio of the Fe hydroxyphosphates that were formed during reaction stage 1, as calculated from the decrease in aqueous Fe(II) and  $\text{PO}_4$  concentrations, varied only to a minor extent in the course of the reaction. When comparing experiments with different  $(\text{P}/\text{Fe})_{\text{ini}}$  ratios and pH, however, the  $(\text{P}/\text{Fe})_{\text{ppt}}$  ratios were not similar but varied between 0.38 and 0.48 (Table 3.1). A decrease of the  $(\text{P}/\text{Fe})_{\text{ini}}$  ratio from 0.3 to 0.12 resulted in a 0.06–0.09 lower  $(\text{P}/\text{Fe})_{\text{ppt}}$  ratio. In experiments conducted at pH 6.4, the  $(\text{P}/\text{Fe})_{\text{ppt}}$  ratios were similar (for  $(\text{P}/\text{Fe})_{\text{ini}} = 0.12$ ) or 0.04–0.05 units lower (for  $(\text{P}/\text{Fe})_{\text{ini}} = 0.18$  and 0.3) compared to experiments at pH 6.1. This resulted in  $r$  values between 2.08 and 2.78 for the Fe hydroxyphosphate  $\text{Fe}_r\text{PO}_4(\text{OH})_{3-3(s)}$ .



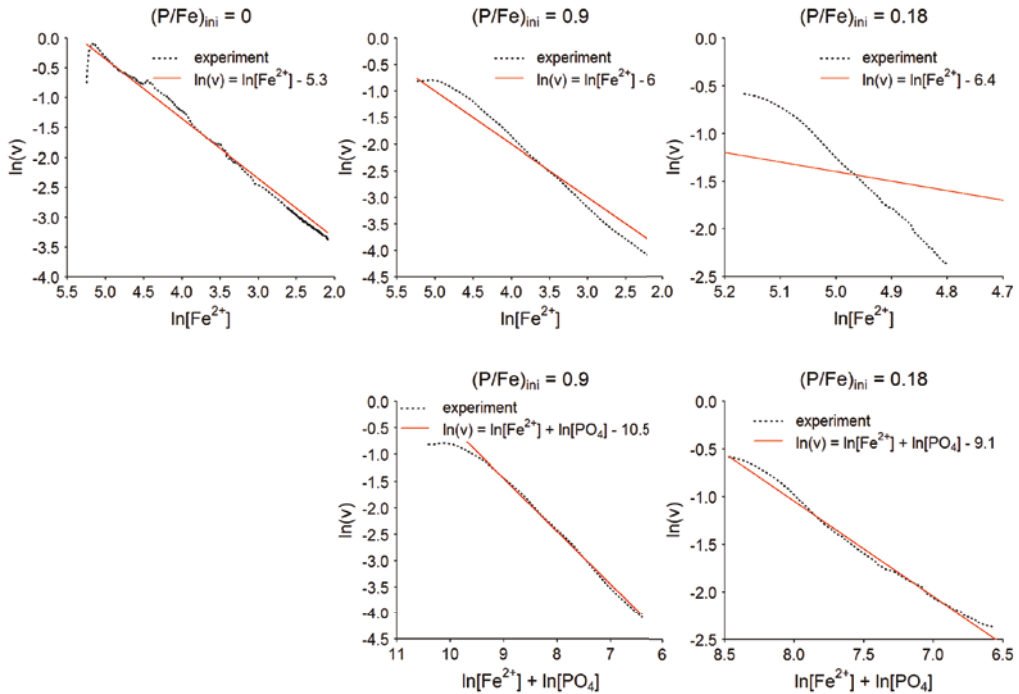


**Figure 3.2.** Logarithmised Fe(II) oxidation rates of experiments with  $(P/Fe)_{ini}$  ratio of 0, 0.9 and 0.18 at  $pH = 6.1$  and  $O_2 = 10.5 \text{ mg L}^{-1}$  against the logarithmised Fe(II) concentrations (top row) and against the sum of the logarithmised Fe(II) and  $PO_4$  concentrations (bottom row). Units in  $\mu\text{mol L}^{-1}$ . The red lines indicate a logarithmised Fe(II) oxidation rate with a slope of 1.

The molar  $H^+/Fe^{2+}$  ratio during reaction stage 1 varied between 1.42, for a precipitate with a  $(P/Fe)_{ppt}$  ratio of 0.48, and 1.55 for a precipitate with a  $(P/Fe)_{ppt}$  ratio of 0.41 (Table 3.1). The measured molar  $H^+/Fe^{2+}$  ratios for the individual experiments agreed with the molar  $H^+/Fe^{2+}$  ratios that were obtained from modelling the formation of Fe hydroxyphosphates with the experimentally derived  $(P/Fe)_{ppt}$  ratio. The continuous Fe(II) curve, calculated with the  $H^+/Fe^{2+}$  ratio from the recorded NaOH addition, traced the discretely measured Fe(II) concentrations during reaction stage 1. A similar good match was also found between the measured  $PO_4$  concentrations and the  $PO_4$  concentrations obtained from the recorded NaOH addition. This indicates that the  $(P/Fe)_{ppt}$  ratio stayed practically constant in the various experiments as long as  $PO_4$  was present in solution but varied between experiments with different initial conditions. After  $PO_4$  was virtually depleted, the molar  $H^+/Fe^{2+}$  ratios increased to values between 1.84–1.95 indicating that an Fe oxyhydroxide precipitated during the second stage of the reaction.

### 3.4.3.2 Reaction progress

Despite the absence of an initial reaction stage with retarded Fe(II) oxidation rates, the course of the reaction can be divided into different stages. During the first reaction stage with decreasing

$\text{PO}_4$  concentrations, Fe(II) oxidation rates slowed down and exhibited a period of retardation when  $\text{PO}_4$  was virtually depleted. After the Fe(II) oxidation rates had reached a minimum, they accelerated intermediately. Eventually, consumption of Fe(II) caused a decrease of the reaction rate during the experimental trajectory after  $\text{PO}_4$  depletion (Figure 3.3). Depending on the  $(\text{P}/\text{Fe})_{\text{ini}}$  ratio, a minimum in the reaction rate was reached within  $\approx 45 - \approx 460$  min after the moment of  $\text{PO}_4$  depletion (Figure 3.3, Table 3.1). The time interval between  $\text{PO}_4$  depletion and the minimum in Fe(II) oxidation rate was longest for the experiment with the  $(\text{P}/\text{Fe})_{\text{ini}}$  ratio of 0.3 and shortest for the experiment with the  $(\text{P}/\text{Fe})_{\text{ini}}$  ratio of 0.12. The intermittent increase in reaction rate was most pronounced for the experiment with  $(\text{P}/\text{Fe})_{\text{ini}} = 0.12$  and  $\text{pH} = 6.4$  (from 0.11 to 0.32  $\mu\text{mol L}^{-1} \text{min}^{-1}$ ) and smallest for the experiments with  $(\text{P}/\text{Fe})_{\text{ini}} = 0.3$  and  $\text{pH} = 6.1$  (from 0.018 to 0.030  $\mu\text{mol L}^{-1} \text{min}^{-1}$ ). At equal  $(\text{P}/\text{Fe})_{\text{ini}}$  ratios, the increase was larger for the experiments at pH values of 6.4 than at pH values of 6.1.

The shift in Fe(II) oxidation kinetics during the reaction is distinct and visible when plotting the time evolution of the rates on log-linear scale (Figure 3.1 and Figures S4-S6. Row C). During the presence of aqueous  $\text{PO}_4$ , the  $[\text{Fe}^{2+}]$  normalised rates decreased up to an order of magnitude (Figure 3.1 and Figures S4-S6. Row D). When plotting the  $\ln(v)$  as a function of the  $\ln[\text{Fe}^{2+}]$  the slope of the trend line was much steeper than 1 (Figure 3.2, top row). This indicates that the reaction kinetics are not pseudo-first-order but the decrease of  $\text{PO}_4$  affected the Fe(II) oxidation rate as well.

After  $\text{PO}_4$  depletion and acceleration of Fe(II) oxidation rate,  $[\text{Fe}^{2+}]$  normalised rates stayed virtually constant. Hence, after  $\text{PO}_4$  depletion, Fe(II) oxidation followed first-order kinetics. The related first-order rate constant ranged from 0.0007 to 0.0023  $\text{min}^{-1}$  for the reaction stage after  $\text{PO}_4$  depletion (Table 3.1). These values are lower than the first-order rate constants obtained from  $\text{PO}_4$ -free experiments (0.0049–0.0053  $\text{min}^{-1}$ ) and also lower than the rate constant derived from Stumm and Lee (1961) at the same pH and  $\text{O}_2$  conditions (0.0030–0.0040  $\text{min}^{-1}$ ).

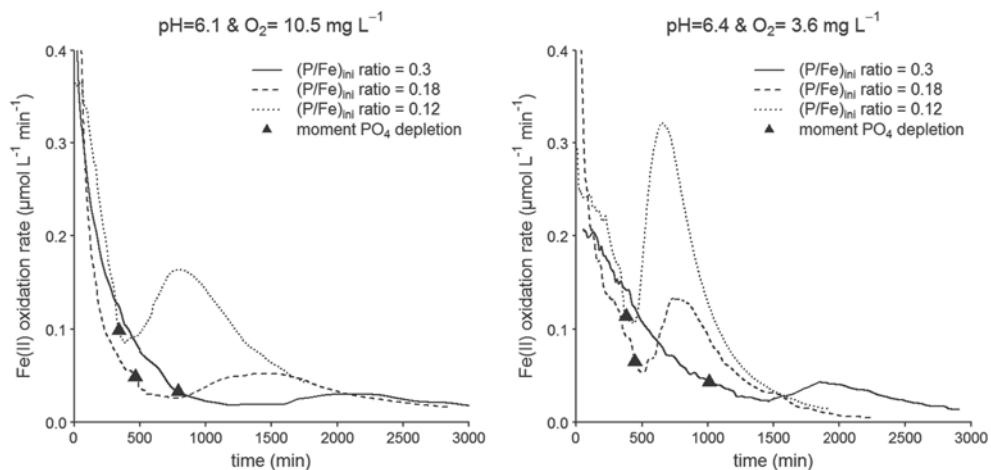


**Figure 3.3.** Fe(II) oxidation rate during aeration experiments with initial aqueous P/Fe ratios of 0.3, 0.18 and 0.12. The P/Fe 0.12 experiment started with higher initial Fe(II) concentrations than the P/Fe 0.3 and 0.18 experiments.

### 3.4.4 Groundwater aeration experiments

The aqueous composition of groundwater sampled from the Hupsel field can be characterised as anoxic fresh water with near-neutral pH (Table S3.1). Iron concentrations ranged from 175 to 188  $\mu\text{mol L}^{-1}$  and  $\text{PO}_4$  concentrations ranged from 5.8 to 11.3  $\mu\text{mol L}^{-1}$ , leading to aqueous P/Fe ratios from 0.037 to 0.073. These P/Fe ratios were in the lower range of the previously observed P/Fe ratios in the groundwater (Van der Griff et al., 2014). The DOC concentrations varied between 35 to 41.2  $\text{mg L}^{-1}$ . In order to increase the  $(\text{P/Fe})_{\text{ini}}$  ratio, two experiments were spiked with 20  $\mu\text{mol L}^{-1}$   $\text{KH}_2\text{PO}_4$  before the start of aeration (Table 3.2).

Aeration of the anoxic groundwater caused a decrease in Fe(II) concentrations, usually to values below 5  $\mu\text{mol L}^{-1}$  over the duration of the experiments (Figure 3.4). In the experiments gw3.2 and gw4.2, initial Fe(III) concentrations were 15 and 24  $\mu\text{mol L}^{-1}$ , respectively, indicating that some Fe(II) oxidation had occurred before the start of the experiment. Phosphate concentrations before spiking were 2 and 3  $\mu\text{mol L}^{-1}$  lower than the concentrations measured in the field samples, implying that some  $\text{PO}_4$  immobilisation had occurred as well.

During the first hours of the aeration experiment,  $\text{PO}_4$  concentrations decreased until they stabilised around values of 4–5  $\mu\text{mol L}^{-1}$  for experiment gw3.1 and gw4.1 and of 20–22  $\mu\text{mol L}^{-1}$  for experiment gw3.2 and gw4.2. This fast decrease in the beginning of the experiment was comparable with the decrease as observed in the experiments with synthetic solutions. A remarkable difference was, however, that in the experiments with the synthetic solution virtually all aqueous  $\text{PO}_4$  was removed from solutions while in the groundwater aeration experiments  $\text{PO}_4$  remained in solution although  $\text{PO}_4$  was not in excess. After about 24 h reaction time, the  $\text{PO}_4$  concentrations stabilised at a level that was higher for the  $\text{PO}_4$ -spiked experiment compared with that for the unspiked experiments. Another difference to the experiments with synthetic solutions was that Fe(III) was also detected in solution. Dissolved Fe(III) concentration reached levels of 40–55, 80, 70–75 and 90  $\mu\text{mol L}^{-1}$  for experiment gw3.1, gw4.1, gw3.2 and gw4.2, respectively. It is most likely that this Fe(III) is not truly dissolved but that stable  $\text{PO}_4$ -rich Fe(III) colloids were formed which were able to pass through the 0.45  $\mu\text{m}$  filter membranes.

The 'dissolved' ( $< 0.45 \mu\text{m}$ ) Fe(III) and  $\text{PO}_4$  concentrations were stable for up to 44 days with Fe(III) concentrations between 79 and 94  $\mu\text{mol L}^{-1}$  and  $\text{PO}_4$  concentrations of 3.6–4.1  $\mu\text{mol L}^{-1}$  for the non-amended experiments and 21  $\mu\text{mol L}^{-1}$  for the two spiked experiments (Table 3.2). Between 62 and 85% of the initially dissolved  $\text{PO}_4$  ended in the  $< 0.45 \mu\text{m}$  fraction. This fraction accounted for between 37 and 55% of total Fe (Figure 3.4).

The chemical compositions of the colloidal and particulate phase differed from each other. The P/Fe ratio of the  $< 0.45 \mu\text{m}$  fraction was higher than that of the particulate fraction that had not passed the 0.45  $\mu\text{m}$  filters. After all Fe(II) had been oxidised, the  $(\text{P/Fe})_{\text{ppt}}$  ratio of the particulate fraction was lower than the  $(\text{P/Fe})_{\text{ini}}$  ratio while the  $(\text{P/Fe})_{\text{ppt}}$  ratio of the  $< 0.45 \mu\text{m}$  fraction was higher than the  $(\text{P/Fe})_{\text{ini}}$  ratio (Table 3.2).

For experiment gw4.2, the 'truly' dissolved Fe(II), Fe(III) and  $\text{PO}_4$  concentrations were measured additionally after ultrafiltration with 50 kDa membranes. The 'truly' dissolved ( $< 50 \text{ kDa}$ ) Fe(II) and colloidal ( $< 0.45 \mu\text{m}$ ,  $> 50 \text{ kDa}$ ) Fe(III) concentrations during the experiment were similar to the total

dissolved Fe(II) and Fe(III) concentrations, respectively. This implies that Fe in the colloidal fraction dominated the total dissolved concentrations at the end of the experiments (Figure 3.4D).

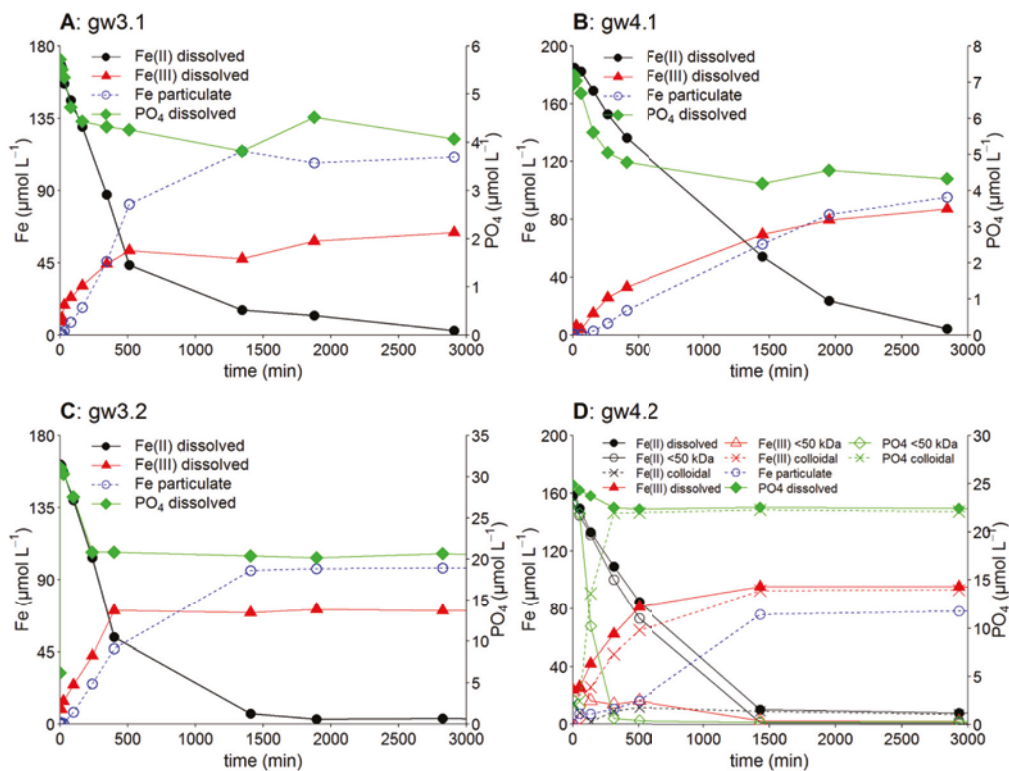


**Figure 3.4.** Measured Fe(II), Fe(III) and  $\text{PO}_4$  concentrations ( $< 0.45 \mu\text{m}$ ) and calculated particulate Fe concentrations during groundwater aeration experiments (A) gw3.1, (B) gw4.1, (C) gw3.2 and (D) gw4.2. Plot (D) gives also the measured truly dissolved concentrations ( $< 50 \text{kDa}$ ) and calculated colloidal concentrations ( $< 0.45 \mu\text{m}$  &  $> 50 \text{kDa}$ ).

During the first 5 h of experiment gw4.2, less than 30% of the initial Fe(II) was transformed into colloidal Fe(III). This transformation was accompanied by an almost complete transition of ‘truly’ dissolved  $\text{PO}_4$  into colloidal  $\text{PO}_4$  (Figure 3.4D). Quantitative fixation of  $\text{PO}_4$  in colloidal form coupled to partial oxidation of the initially present Fe(II) resulted in high  $(\text{P}/\text{Fe})_{\text{colloid}}$  ratios during this period. The  $(\text{P}/\text{Fe})_{\text{colloid}}$  ratio was about 0.45 after 5 h, which is comparable with the  $(\text{P}/\text{Fe})_{\text{ppt}}$  ratios of precipitates formed in the synthetic water experiments with excess of Fe(II). During the first 5 h of this experiment, the colour intensity of the filter residues on the 50 kDa filters increased while the appearance of the residue on the  $0.45 \mu\text{m}$  filters did not change over this period (Figure S3.7). This is another indication for the predominant formation of colloids during this experimental period. The partitioning of  $\text{PO}_4$  between particulate ( $> 0.45 \mu\text{m}$ ), colloidal and truly dissolved fractions did not

Table 3.2. Overview of groundwater aeration experiments.

Sample	PO <sub>4</sub> spiked μmol L <sup>-1</sup>	pH exp.	Fe <sup>2+</sup> initial μmol L <sup>-1</sup>	PO <sub>4</sub> initial μmol L <sup>-1</sup>	(P/Fe) <sub>ini</sub>	Fe <sup>3+</sup> diss. initial μmol L <sup>-1</sup>	Fe <sup>3+</sup> diss. final μmol L <sup>-1</sup>	PO <sub>4</sub> diss. final μmol L <sup>-1</sup>	first-order rate constant min <sup>-1</sup>	(P/Fe) ratio colloidal fraction	(P/Fe) ratio particulate fraction
gw3.1	-	6.1	169	5.7	0.033	9	84 (at 888 h.)	3.6	0.0018	0.085	0.017
gw4.1	-	5.9	185	7.0	0.038	2	79 (at 1056 h.)	4.1	0.0012	0.057	0.029
gw3.2	20	6.1	161	31	0.19	15	93 (at 576 h.)	21	0.0021	0.28	0.11
gw4.2	20	6.0	158	25	0.16	24	94 (at 146 h.)	21	0.0019	0.24	0.03

show significant shifts between 5 h and 48 h reaction time. A small increase in the particulate  $\text{PO}_4$  fraction together with a decrease in the colloidal  $\text{PO}_4$  fraction was observed after 48 h. The colloidal Fe(III) concentration continued to increase after near-depletion of truly dissolved  $\text{PO}_4$  up to 24 h and was stable afterwards up to the end of the experiment. After complete Fe(II) oxidation, about 85% of the initial aqueous  $\text{PO}_4$  ended in the colloidal fraction and this resulted in a colloidal phase with a (P/Fe) ratio almost twice the  $(\text{P/Fe})_{\text{ini}}$  ratio.

## 3.5 Discussion

### 3.5.1 P/Fe ratios of the Fe hydroxyphosphate precipitate

The first objective of our study was to determine the  $(\text{P/Fe})_{\text{ppt}}$  ratios in Fe hydroxyphosphates that form during Fe(II) oxidation in synthetic  $\text{PO}_4$  containing solutions as a function of pH, the aqueous  $(\text{P/Fe})_{\text{ini}}$  ratio and the reaction progress. The pH and the  $(\text{P/Fe})_{\text{ini}}$  ratio in solution influence the  $(\text{P/Fe})_{\text{ppt}}$  ratios of the precipitates forming from homogeneous solution: with decreasing  $(\text{P/Fe})_{\text{ini}}$  ratios and increasing pH,  $(\text{P/Fe})_{\text{ppt}}$  ratios decrease. Interestingly, measured  $\text{H}^+/\text{Fe}^{2+}$  ratios and  $(\text{P/Fe})_{\text{ppt}}$  ratios did not change detectably throughout the experiments although the P/Fe ratios of the solutions changed due to either superproportional removal of  $\text{PO}_4$  in the  $(\text{P/Fe})_{\text{ini}} = 0.3, 0.18$  and  $0.12$  experiments or superproportional removal of Fe(II) in the  $(\text{P/Fe})_{\text{ini}} = 0.9$  experiments. Hence, the chemical composition of the Fe hydroxyphosphate seems to be determined during the initial stage of Fe(II) oxidation, which may be considered as the nucleation stage of the precipitate formation sequence. This suggests that the initially formed precipitates function as a template for Fe hydroxyphosphates precipitating at the particle surfaces as a consequence of surface catalytic Fe(II) oxidation. A small but detectable decrease in  $(\text{P/Fe})_{\text{ppt}}$  ratios with decreasing  $(\text{P/Fe})_{\text{ini}}$  ratios has been observed in precipitates formed in excess of P leading to exclusive formation of Fe(III)-phosphate (Voegelin et al., 2013, Senn et al., 2015; Châtellier et al., 2013). Voegelin et al. (2013) performed a time-resolved aeration experiment with a synthetic solution with a  $(\text{P/Fe})_{\text{ini}}$  ratio of 0.29. In their experiments, the  $(\text{P/Fe})_{\text{ppt}}$  ratio of the formed precipitate decreased from  $\approx 0.6$  to  $\approx 0.52$  during Fe(II) oxidation in presence of  $\text{PO}_4$ . This ratio is higher than obtained in our experiments at a  $(\text{P/Fe})_{\text{ini}}$  ratio of 0.3 (0.48 and 0.44 at pH values of 6.1 and 6.4, respectively), and we observed no decline of the  $(\text{P/Fe})_{\text{ppt}}$  ratios to such an extent and no detectable change in the  $\text{H}^+/\text{Fe}^{2+}$  ratio during the experiment. However, the  $(\text{P/Fe})_{\text{ppt}}$  values we obtain from the loss of dissolved Fe(II) and  $\text{PO}_4$  are reflecting the average composition of the precipitates. Formation of precipitates with lower  $(\text{P/Fe})_{\text{ppt}}$  ratios, when approaching  $\text{PO}_4$  depletion in solution, might not lead to a significant shift in the average  $(\text{P/Fe})_{\text{ppt}}$  values when the difference in  $(\text{P/Fe})_{\text{ppt}}$  ratio is small and the relative contribution to the total amount of precipitate is small. Furthermore, in our experiments the pH was kept constant over time by 0.01 M NaOH titration. Although rapid stirring was used to minimize local pH maxima, it cannot be excluded that locally elevated pH may favour Fe(III) hydrolysis over  $\text{PO}_4$  complexation and may lead to lower  $(\text{P/Fe})_{\text{ppt}}$  ratios than observed in experiments performed in pH-buffered solutions. In contrast to our experiments, the pH was not maintained constant in the experiments by Voegelin et

al. (2013). Hence, the shift in  $(P/Fe)_{ppt}$  ratios during their experiments could also be attributed to the drifting pH value.

Recent studies show that electrolyte cations like  $Na^+$  and  $Ca^{2+}$  can enter amorphous Fe hydroxyphosphates and, therefore, affect the OH/Fe ratio of the precipitate (Châtellier et al., 2013; Senn et al., 2015). Châtellier et al. (2013) reported a  $(Na/Fe)_{ppt}$  ratio up to  $\approx 0.2$  at pH 6.0. In our experiments, we used  $K^+$  as background electrolyte and  $NH_4^+$  is added with the Fe(II) stock solution. Like  $Na^+$  these cations may enter the precipitate and affect P/Fe and OH/Fe ratios. Based on charge balance, uptake of  $Na^+$  in a precipitate with a  $(Na/Fe)_{ppt}$  ratio of 0.2 increases the molar  $H^+/Fe^{2+}$  ratio with 0.2. Our PHREEQC calculated molar  $H^+/Fe^{2+}$  ratios do not differ to such an extent from the measured molar  $H^+/Fe^{2+}$  ratio (Table 3.1). This indicates that incorporation of other cations into the Fe hydroxyphosphates is of minor relevance in our experiments. The experiments of Châtellier et al. (2013) were conducted at much higher initial  $Fe^{2+}$  concentrations than our experiments ( $5 \text{ mmol L}^{-1}$  compared to  $\approx 0.2 \text{ mmol L}^{-1}$ ) as well as higher background electrolyte concentration ( $133 \text{ mmol L}^{-1}$  NaCl compared to  $4.8 \text{ mmol L}^{-1}$  KCl). In particular the higher background electrolyte concentration might be the reason why incorporation of other cations is observed in the experiments by Châtellier et al. (2013).

Our experimental results with  $(P/Fe)_{ini}$  ratios of 0.9 are in line with earlier work that concluded that  $PO_4$  uptake per oxidised Fe is limited to a solid P/Fe ratio of  $\approx 0.5$ -0.6 (Gunnars et al., 2002; Roberts et al., 2004; Tessenow, 1974; Voegelin et al., 2010). Voegelin et al. (2013) reported an increase of the  $(P/Fe)_{ppt}$  ratio from 0.56 to 0.72 upon increase of the  $(P/Fe)_{ini}$  ratio from 0.55 to 1.91 and concluded that increasing  $(P/Fe)_{ini}$  ratios above 0.55 affects  $(P/Fe)_{ppt}$  ratio only to a minor extent. A similar result was reported by Châtellier et al. (2013). Although many arrangements of Fe octahedrons and  $PO_4$  tetrahedrons in primary building blocks may yield to formation of Fe hydroxyphosphates with a maximal  $(P/Fe)_{ppt}$  of  $\approx 0.5$ , the appearance of this maximum  $(P/Fe)_{ppt}$  ratio is supported by the nucleation and growth mechanism of Fe oxyhydroxides in presence of  $PO_4$  as postulated by Rose et al. (1996) based on EXAFS analyses. Rose et al. (1996) concluded that presence of chloride and  $PO_4$  as ligands in Fe(III) dimers inhibits the linkage of other Fe(III) octahedra through double corner sharing. These complexes, consisting of two Fe octahedrons and one  $PO_4$  tetrahedron, form then the building blocks in the continuation of polymerisation. Dependent on the  $(P/Fe)_{ini}$  ratio, further growth occurs through association of such small units through  $PO_4$  bridges, which results in a precipitate with a solid P/Fe ratio of  $\approx 0.5$  or by bridging the basic units through Fe single-corner sharing, which generates lower  $(P/Fe)_{ppt}$  ratios (Rose et al., 1996).

Other studies provide indications that the stoichiometry of the building blocks might be different when amorphous Fe(III) phosphates are synthesised at elevated  $(P/Fe)_{ini}$  and high total P and Fe concentrations (Voegelin et al., 2010) or at low pH (Mikutta et al., 2014). In precipitates with P/Fe ratios close to 1.0, double-corner sharing Fe(III) dimers are absent in the structure. This suggests that monomeric Fe(III) complexes serve as building blocks for the formation of Fe(III) phosphates under the corresponding conditions. Hence, the model proposed by Rose et al. (1996) might provide an explanation for the formation of precipitates with  $(P/Fe)_{ppt}$  values roughly around 0.5 for a relatively wide range of  $(P/Fe)_{ini}$  values in our experiments. However, the model is not of general validity and does not imply the formation of a distinct stoichiometric phase.

### 3.5.2 Kinetics of Fe(II) oxidation

The second objective of our study was to establish the kinetics of Fe(II) oxidation upon aeration of synthetic solutions with varying  $(P/Fe)_{ini}$  ratios. Our experiments show that presence of dissolved  $PO_4$  exerts influence on the rates of Fe(II) oxidation. In general, Fe(II) oxidation proceeds slower in the presence of dissolved  $PO_4$  but decrease of the  $PO_4$  concentration during Fe(II) oxidation due to the formation of Fe hydroxyphosphates causes additional deceleration.

#### 3.5.2.1 Kinetics of Fe(II) oxidation in phosphate free experiments

The pseudo-first-order Fe(II) oxidation rate constants in our experiments are a factor 1.3–1.6 higher than those derived for the rate law established by Stumm and Lee (1961). This may be the result of the lower initial Fe(II) concentration that were used in the experiments of Stumm and Lee (1961) ( $50 \mu\text{mol L}^{-1}$ ) which likely results in lower surface catalysis, or by the higher ionic strength in their experiments due to the use of the bicarbonate buffer to control the pH which reduces the Fe(II) oxidation rate (Sung and Morgan, 1980). In the absence of  $PO_4$ , Fe(II) oxidation rates increase during the initial stage for the experiments. Occurrence of an initial stage with retarded Fe(II) oxidation rates has been reported by Vollrath et al. (2012) and the increase in rates after the initial state has been attributed to surface catalysis by the accumulation of Fe oxyhydroxides. Vollrath et al. (2012) argued that surface catalysis might also affected the Fe(II) oxidation rates measured by Stumm and Lee (1961) and that their rate law might not represent exclusively homogeneous Fe(II) oxidation. In this case, the initial stage reflects the period of Fe oxyhydroxide nucleation until surface catalysis of Fe(II) oxidation coupled to particle growth becomes the dominant pathway. Surface catalysis is well documented for Fe(II) oxidation. Sung and Morgan (1980) concluded that surface catalytic Fe(II) oxidation is only observed in experiments with a pH of 7 and higher. However, Pedersen et al. (2005) showed that Fe(II) can interact with Fe oxyhydroxides surfaces and surface-bound Fe(II) can be oxidised at pH 6.5. When surface catalysis is affecting Fe(II) oxidation rates the structure and properties of the precipitate are expected to exert influence on the rates among other factors. The background electrolyte composition and concentration may influence the precipitate properties. Differences in pH control (pH-stat in our experiments versus bicarbonate buffer used by Stumm and Lee, 1961) may lead to different precipitates and, therefore, to differences in Fe(II) oxidation rates.

#### 3.5.2.2 Dependency of Fe(II) oxidation kinetics on phosphate

The overall dependency of Fe(II) oxidation rates on  $PO_4$  concentrations demonstrate the ambivalent effect of  $PO_4$  on Fe(II) oxidation kinetics. This effect is observed when comparing the time required to oxidise 75% of the initially added Fe(II) ( $t_{3/4}$ ). The shortest  $t_{3/4}$  values are obtained for experiments with  $PO_4$ -free solutions. In experiments with  $(P/Fe)_{ini}$  values between 0.12 and 0.3, the  $t_{3/4}$  values increase with increasing  $PO_4$  concentration but with  $(P/Fe)_{ini} = 0.9$ , the  $t_{3/4}$  is shorter than in the experiments with lower  $(P/Fe)_{ini}$  values (Table 3.1). In earlier work on Fe(II) oxidation in presence of  $PO_4$  it was reported that dissolved  $PO_4$  accelerates the oxidation of aqueous Fe(II) in homogenous systems (Mao et al., 2011; Mitra and Matthews, 1985; Tamura et al., 1976) but slows down oxidation of adsorbed Fe(II) in heterogeneous systems (Wolthoorn et al., 2004). The acceleration of homogenous Fe(II) oxidation in the presence of  $PO_4$  may be an explanation for the less pronounced or not noticeable



initial stage with retarded Fe(II) oxidation rates during our experiments with  $(P/Fe)_{ini}$  ratios greater than zero. The general trend in our experiments is, however, that Fe(II) oxidation rates are lower in the presence of  $PO_4$  than in  $PO_4$ -free solutions. Based on the consideration that heterogeneous oxidation is the dominant pathway for Fe(II) oxidation after the initial phase, our observations agree with those of Wolthoorn et al., (2004). That is,  $PO_4$  reduces the rate of surface catalysed Fe(II) oxidation which is the dominant mechanism for Fe(II) oxidation after the initial stage of experiments in the presence as well as in the absence of  $PO_4$ . Hence, the general trend that addition of  $PO_4$  slows down Fe(II) oxidation rates could be ascribed to a weaker catalytic effect of Fe hydroxyphosphates compared to Fe oxyhydroxides.

This mechanism alone, however, cannot account for the shorter  $t_{3/4}$  at  $(P/Fe)_{ini} = 0.9$  compared with  $t_{3/4}$  values of experiments with  $(P/Fe)_{ini} = 0.12, 0.18$  and  $0.3$ . In the experiments with  $(P/Fe)_{ini} = 0.3$  and lower,  $PO_4$  becomes depleted before 75% of the added Fe(II) is oxidised. Phosphate depletion is followed by a period of delayed Fe(II) oxidation rates and the length of the timeframe between the moment of  $PO_4$  depletion and minimum in Fe(II) oxidation rate increases with increasing  $(P/Fe)_{ini}$  ratios (Table 3.1). This phenomenon additionally controls the  $t_{3/4}$ . When  $(P/Fe)_{ini} = 0.9$ ,  $PO_4$  is in excess and an intermediate period of delayed Fe(II) oxidation is absent. As a consequence,  $t_{3/4}$  is shorter at  $(P/Fe)_{ini} = 0.9$ . Relating Fe(II) oxidation rates and  $PO_4$  concentration is further complicated by the observation that, against the general trend of delaying Fe(II) oxidation upon  $PO_4$  addition, removal of  $PO_4$  upon progressing reaction decelerates the reaction within one experiment. This phenomenon is addressed in more detail below.

Dissolved  $PO_4$  might affect Fe(II) oxidation by multiple mechanisms: changing the speciation of dissolved Fe(II), influencing the nucleation of iron precipitates, and interfering with surface catalysis by changing the surface speciation of the Fe hydroxyphosphates. Consequently, the dependency of the rates on  $PO_4$  concentration might vary in the different stages of the reaction. The complexity of the dependency on  $PO_4$  concentration becomes obvious when plotting  $\ln(v)$  as a function of  $(\ln[Fe^{2+}] + \ln[PO_4])$  (Figure 3.2, bottom row). At the beginning of the reaction, the curves do not follow a linear trend, but in a later phase a linear function with a slope of 1 resembles the experimentally derived results well. Hence, a pseudo-second-order rate law provides a good description of the progress of Fe(II) oxidation in the presence of  $PO_4$  when surface catalysis is the dominant pathway:

$$\frac{d[Fe^{2+}]}{dt} = -k_2[Fe^{2+}][PO_4] \quad (3.5)$$

where  $[i]$  refers to the concentration of species  $i$ ,  $k$  denotes the reaction rate constant. We may reformulate Eq. 3.5 in terms of reacted Fe(II) at time  $t$ , with a standard reaction progress parameter  $\xi$ . Then  $[Fe^{2+}] = [Fe^{2+}]_0 - \xi$  and  $[PO_4] = [PO_4]_0 - n\xi$ , where  $n$  is the stoichiometric  $(P/Fe)_{ppt}$  ratio of the Fe hydroxyphosphate. Then, the expression of the rate law becomes:

$$-\frac{d\xi}{dt} = -k_2([Fe^{2+}]_0 - \xi)([PO_4]_0 - n\xi) \quad (3.6)$$

In Eq. 3.6 we assume that the reaction rate is first-order with respect to the total  $PO_4$  concentration. Integration between  $t = 0$  (when  $\xi = 0$ ) and  $t$ , the time of interest, yields:

$$\int_0^{\xi} \frac{d\xi}{([\text{Fe}^{2+}]_0 - \xi)([\text{PO}_4]_0 - n\xi)} = k_2 \int_0^t dt \quad (3.7)$$

$$\frac{\ln(\xi - [\text{Fe}^{2+}]_0) - \ln([\text{PO}_4]_0 - n\xi) - \ln(-[\text{Fe}^{2+}]_0) + \ln([\text{PO}_4]_0)}{n[\text{Fe}^{2+}]_0 - [\text{PO}_4]_0} = k_2 t \quad (3.8)$$

Upon rearrangement of the integrated rate equation, this becomes:

$$\ln\left(\frac{[\text{Fe}^{2+}][\text{PO}_4]_0}{[\text{PO}_4][\text{Fe}^{2+}]_0}\right) = k_2 (n[\text{Fe}^{2+}]_0 - [\text{PO}_4]_0)t \quad (3.9)$$

For all four experiments with an  $(\text{P}/\text{Fe})_{\text{ini}}$  ratio of 0.9 the plot of  $\frac{1}{n[\text{Fe}^{2+}]_0 - [\text{PO}_4]_0} \ln\left(\frac{[\text{Fe}^{2+}][\text{PO}_4]_0}{[\text{PO}_4][\text{Fe}^{2+}]_0}\right)$  versus time yields a straight line after the initial stage (Figure 3.1 and Figure S3.3, Row E). Hence, progress of the reaction can be described using a pseudo-second-order rate law with first-order dependencies on  $\text{PO}_4$  and  $\text{Fe}(\text{II})$ . The pseudo-second-order rate constant for the experiments with a  $(\text{P}/\text{Fe})_{\text{ini}}$  ratio of 0.9 can be obtained from the slope of a linear regression line and varies between  $1.53 \times 10^{-5}$  and  $2.78 \times 10^{-5} \mu\text{mol}^{-1} \text{L min}^{-1}$  (Table 3.1). Pseudo-second-order kinetics can also describe the progress of  $\text{Fe}(\text{II})$  oxidation in the experiments with lower  $(\text{P}/\text{Fe})_{\text{ini}}$  ratios during the first reaction stage wherein  $\text{PO}_4$  is present. Application of Eq. 3.9 gives a satisfactory description of the reaction until the  $\text{PO}_4$  concentrations fall to a level that ranges from 7 to 18% of the initial  $\text{PO}_4$  concentration ( $2.1$  and  $9.5 \mu\text{mol IL}^{-1}$ ) (Figure 3.1 and Figure S3.4-S3.6, row E). Pseudo-second-order rate constants vary between  $5.72 \times 10^{-5}$  and  $1.13 \times 10^{-4} \mu\text{mol}^{-1} \text{L min}^{-1}$  (Table 3.1). The pseudo-second-order rate constants, obtained from the integrated rate law, match the y-intercept from the linear trend line in the  $\ln(v)$  versus  $(\ln[\text{Fe}^{2+}] + \ln[\text{PO}_4])$  plots (Figure 3.2).

Tamura et al. (1976) and Mao et al. (2011) studied  $\text{Fe}(\text{II})$  oxidation in the presence of excess  $\text{PO}_4$  and concluded that the kinetics are first order with respect to dissolved  $\text{PO}_4$  concentration. Tamura et al. (1976) proposed following rate law:

$$\frac{d[\text{Fe}]}{dt} = -k[\text{OH}^-][\text{O}_2][\text{Fe}][\text{H}_2\text{PO}_4^-]^n \quad (3.10)$$

with  $k = 5.02 \times 10^9 \text{M}^{-3} \text{s}^{-1}$ ,  $n = 1$  for  $\text{H}_2\text{PO}_4^- < 0.1 \text{mol L}^{-1}$  and  $k = 5.02 \times 10^{10} \text{M}^{-4} \text{s}^{-1}$ ,  $n = 1$  for  $\text{H}_2\text{PO}_4^- > 0.1 \text{M}$ .

For the experimental conditions  $\text{pH} = 6.1$ ,  $\text{O}_2 = 10.5 \text{mg L}^{-1}$  and  $[\text{PO}_4]_{\text{ini}} = 0.0002 \text{mol L}^{-1}$  the rate law of Tamura et al. (1976) gives pseudo-second-order rate constants of  $1.24 \times 10^{-6} \mu\text{mol}^{-1} \text{L min}^{-1}$  and for the experimental condition  $\text{pH} = 6.4$ ,  $\text{O}_2 = 3.6 \text{mg L}^{-1}$  and  $[\text{PO}_4]_{\text{ini}} = 0.0002 \text{mol L}^{-1}$ , a value of  $0.85 \times 10^{-6} \mu\text{mol}^{-1} \text{L min}^{-1}$  is obtained. These values are lower compared with our experimentally derived second-order rate constants. Mao et al. (2011) reported even lower reaction rates but they investigated systems with nanomolar  $\text{Fe}$  concentrations in which surface catalysis is less important and homogeneous oxidation dominates. They concluded that the aqueous  $\text{FePO}_4^-$  complex is the most reactive phosphate complex and due to its higher abundance than the aqueous  $\text{Fe}(\text{OH})_2$

complex the  $\text{FePO}_4^-$  complex is the most important Fe(II) species contributing to the overall rate of Fe(II) oxygenation at circumneutral pH. Although Fe(II) oxidation is most likely predominantly heterogeneous in our experiments and  $(\text{P}/\text{Fe})_{\text{ini}}$  ratios are much lower, the effect of phosphate on Fe(II) speciation and formation of reactive Fe(II)-phosphate complexes in solution or at the solid surface may also provide an explanation for the observed first-order dependency of Fe(II) oxidation rate on  $\text{PO}_4$  concentration.

### 3.5.2.3 Kinetics of Fe(II) oxidation after phosphate depletion

The Fe(II) oxidation rates increase after  $\text{PO}_4$  depletion and the Fe(II) oxidation kinetics become first-order with respect to the Fe(II) concentration at fixed pH and oxygen conditions (Table 3.1 and Figures S4-S6, Row C). Voegelin et al. (2013) reported an increase of Fe(II) oxidation rates after  $\text{PO}_4$  depletion as well. Based on data published by Wolthoorn et al. (2004), Voegelin et al. (2013) suggested that this can be ascribed to stronger catalytic properties of Fe oxyhydroxide surfaces compared with the surfaces of Fe hydroxyphosphates. Our results support this interpretation which can also explain the differences in Fe(II) oxidation rates in experiments with  $(\text{P}/\text{Fe})_{\text{ini}}$  ratios of 0.12, 0.18 and 0.3 after  $\text{PO}_4$  depletion. Even when  $\text{PO}_4$  is consumed, Fe(II) oxidation rates in experiments with  $\text{PO}_4$  are lower than those in  $\text{PO}_4$ -free experiments and, hence, depend on the history of the system. When comparing the time between the moments of  $\text{PO}_4$  depletion and minimal Fe(II) oxidation rate or when comparing the extent of intermittent increase in reaction rate after  $\text{PO}_4$  depletion, it turns out that the Fe(II) oxidation rate accelerates faster in experiments with lower  $(\text{P}/\text{Fe})_{\text{ini}}$  ratios (Table 3.1). Additionally, the first-order rate constants after  $\text{PO}_4$  depletion are generally lower than those obtained from  $\text{PO}_4$ -free experiments and decrease with increasing  $(\text{P}/\text{Fe})_{\text{ini}}$  (Table 3.1). Hence, the amount of the initially formed Fe hydroxyphosphate or its  $(\text{P}/\text{Fe})_{\text{ppt}}$  ratio affects the kinetics of continuing Fe(II) oxidation after  $\text{PO}_4$  depletion. In other words, the phases formed before and after  $\text{PO}_4$  depletion are not completely independent from each other. Voegelin et al. (2013) found that about half of newly formed Fe(III) after  $\text{PO}_4$  depletion contributes to the polymerisation of initially precipitated Fe hydroxyphosphate into  $\text{PO}_4$ -rich Fe oxyhydroxides with a maximum P/Fe ratio of 0.25. The other half of the formed Fe(III) precipitates as poorly-crystalline lepidocrocite. That is, the initially formed Fe hydroxyphosphate acts as a sink for Fe(III) which is formed after  $\text{PO}_4$  depletion. In this case, the amount of Fe hydroxyphosphate determines how much of newly formed Fe(III) becomes available for the formation of lepidocrocite. This mechanism may explain the dependency of Fe(II) oxidation rates after  $\text{PO}_4$  depletion on  $(\text{P}/\text{Fe})_{\text{ini}}$ : at low  $(\text{P}/\text{Fe})_{\text{ini}}$  only small amounts of Fe hydroxyphosphate are formed and more Fe(III) can be channelled towards lepidocrocite. At high  $(\text{P}/\text{Fe})_{\text{ini}}$  less Fe(III) is available for the precipitation as lepidocrocite. Based on observations by Wolthoorn et al. (2004) we assume that lepidocrocite is a more potent surface catalyst than Fe hydroxyphosphates. The dependency of the pseudo-first-order rate constant after  $\text{PO}_4$  depletion on  $(\text{P}/\text{Fe})_{\text{ini}}$  and the extent of Fe(II) oxidation rates after  $\text{PO}_4$  consumption can then be attributed to the different extent of lepidocrocite formed per oxidised Fe(II) after  $\text{PO}_4$  depletion.

### 3.5.2.4 Dependency of Fe(II) oxidation kinetics on oxygen concentration and pH

The rate law for Fe(II) oxidation, as established by Stumm and Lee (1961), is second-order with respect to  $[\text{OH}^-]$  while the rate law by Tamura et al. (1976) is first-order with respect to the  $[\text{OH}^-]$  when phosphate is present. According to both rate laws, the reaction is first-order with respect to oxygen concentration. First-order dependency on oxygen concentration is supported by our experimental results. Increasing the oxygen concentration by a factor of 0.7 leads to an increase in the pseudo-second-order rate constant by a factor of about 0.6 (experiment at  $\text{pH} = 6.1$ ,  $\text{O}_2 = 8.5 \text{ mg L}^{-1}$ ;  $k = 1.53 \times 10^{-5} \text{ } \mu\text{mol}^{-1} \text{ L min}^{-1}$ , experiments at  $\text{pH} = 6.1$ ,  $\text{O}_2 = 10.5 \text{ mg L}^{-1}$ ;  $k = 2.48 \times 10^{-5} - 2.78 \times 10^{-5} \text{ } \mu\text{mol}^{-1} \text{ L min}^{-1}$ ).

We have not systematically explored the dependency of the reaction kinetics on pH, but comparing reaction rates obtained at pH 6.1 and pH 6.4 does shed some light on the pH dependency of Fe(II) oxidation in the presence of  $\text{PO}_4$  in our experiments. Experiments at pH 6.1 and pH 6.4 were not performed at the same oxygen concentration and, therefore, the dependency of the rates on oxygen concentration has to be taken into consideration. In the experiments at  $\text{pH} = 6.4$  and  $\text{O}_2 = 3.6 \text{ mg L}^{-1}$ , the  $[\text{OH}^-]$  is twice as high but the  $\text{O}_2$  concentration is almost three times lower compared to the experiments at  $\text{pH} = 6.1$  and  $\text{O}_2 = 10.5 \text{ mg L}^{-1}$ . Second-order dependency on  $[\text{OH}^-]$  would lead to 33% larger rates at  $\text{pH} = 6.4$  and  $\text{O}_2 = 3.6 \text{ mg L}^{-1}$  compared with rates at  $\text{pH} = 6.1$  and  $\text{O}_2 = 10.5 \text{ mg L}^{-1}$ . If the kinetic reaction is first-order with respect to  $[\text{OH}^-]$ , 32% lower rates would be expected. For experiments with  $(\text{P}/\text{Fe})_{\text{ini}}$  ratios of 0.9, 0.3, 0.18 and 0.12, the pseudo-second-order rate constants obtained at  $\text{pH} = 6.4$  and  $\text{O}_2 = 3.6 \text{ mg L}^{-1}$  are between 33% to 27% lower than rate constants at  $\text{pH} = 6.1$  and  $\text{O}_2 = 10.5 \text{ mg L}^{-1}$ . The increase in rates upon increasing the pH from 6.1 to 6.4 is lower than expected from the oxidation kinetics in the absence of  $\text{PO}_4$ . The change in rates is proportional to the increase in  $[\text{OH}^-]$  and this supports the findings of Tamura et al. (1976) that Fe(II) oxidation kinetics in presence of  $\text{PO}_4$  are first-order with respect to  $[\text{OH}^-]$ .

### 3.5.3 Phosphate immobilisation upon aeration of natural groundwater

The third objective of our study was to assess the effectiveness of the formation of Fe- $\text{PO}_4$  phases to immobilise  $\text{PO}_4$  when natural Fe(II) and  $\text{PO}_4$ -containing groundwater is exposed to atmospheric oxygen. Our study shows that experiments with synthetic solutions are suitable to predict Fe(II) oxidation rates and  $\text{PO}_4$  immobilisation dynamics upon aeration of natural groundwater: Fe(II) oxidation initially results in the formation of a Fe hydroxyphosphate phase until  $\text{PO}_4$  is virtually depleted and afterwards Fe(II) oxidation leads to precipitation of a Fe oxyhydroxide phase.

Due to the presence of dissolved carbonate, the pH-stat device could not be used to continuously derive Fe(II) oxidation rates during the aeration experiments with natural groundwater. However, the measured decrease of logarithmised Fe(II) concentration during the groundwater aeration experiments (Figure 3.5) is well predicted by using the rate laws parameterised with results from experiments with synthetic solutions. For this, the decrease of the Fe(II) concentration with time was calculated by using a combination of the second-order-rate law (before  $\text{PO}_4$  depletion) and first-order rate law (after  $\text{PO}_4$  depletion) with rate constants taken from experiments with synthetic solutions under conditions that most closely match those of the groundwater experiments ( $(\text{P}/\text{Fe})_{\text{ini}}$  ratio = 0.12,  $\text{pH} = 6.1$  and  $\text{O}_2 = 10.5 \text{ mg L}^{-1}$ ). In contrast, Fe(II) oxidation rates are overestimated when using the

first-order rate law with a rate constant from  $\text{PO}_4$ -free synthetic solution experiments. Hence, the effects of  $\text{PO}_4$  on Fe(II) oxidation kinetics in natural groundwater experiments are comparable to those of experiments in synthetic solutions. Based on interpolation of the concentration measurements, values for  $t_{3/4}$  fall into the range of 600 to 1500 min which is somewhat lower than the synthetic water experiments at  $(\text{P}/\text{Fe})_{\text{ini}} = 0.12$  and 0.18 (900 to 1800 min). It is known that the presence of other constituents such as carbonate, silicic acid, DOC and alkaline earth metals may also influence the Fe(II) oxidation rate (e.g. Pullin and Cabaniss, 2003; Wolthoorn et al., 2004). As shown by Wolthoorn et al. (2004), surface catalysed oxidation of Fe(II) proceeds slower in presence of silica than in its absence, but rates are still a factor 2 higher than in a  $\text{PO}_4$ -containing solution. The presence of silicate in groundwater may explain the slightly lower  $t_{3/4}$  values in experiments with natural groundwater compared with synthetic solutions. At longer times ( $> 2500$  sec.), the observed Fe(II) concentrations seem to approach a steady state level which is higher than the detection limit (data not shown). Pullin and Cabaniss (2003) observed a similar feature of inhibited Fe(II) oxidation in the presence of fulvic acid after longer reaction times. They explained this feature by the formation of stable Fe(II) organic complexes and chemical reduction of Fe(III) by DOM.

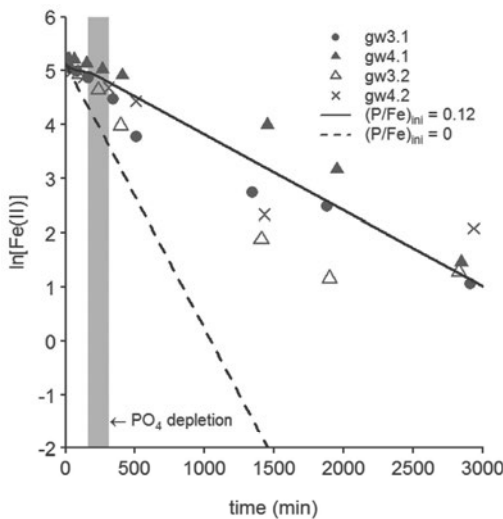


**Figure 3.5.** Measured logarithmised Fe(II) concentrations ( $\mu\text{mol L}^{-1}$ ) as a function of time during groundwater aeration experiments. The lines represent the predicted time evolution of logarithmised Fe(II) concentrations ( $\mu\text{mol L}^{-1}$ ) based on (1) a combination of the 2<sup>nd</sup> rate law constant before  $\text{PO}_4$  depletion and 1<sup>st</sup> order rate law constant after  $\text{PO}_4$  depletion obtained from the synthetic solution experiment with a  $(\text{P}/\text{Fe})_{\text{ini}}$  ratio = 0.12 and  $\text{pH} = 6.1$  and (2) the parameterised 1<sup>st</sup> order rate law obtained from the synthetic solution experiment in the absence of  $\text{PO}_4$  ( $(\text{P}/\text{Fe})_{\text{ini}}$  ratio = 0).

A remarkable difference between experiments with natural groundwater and synthetic solutions is that Fe(II) oxidation results in the formation of stable  $\text{PO}_4$ -rich colloids while in the experiments with synthetic solutions the precipitates agglomerate and flocculate. The formation of stable  $\text{PO}_4$ -rich iron colloids can be attributed to the chemical composition of the groundwater (Table S3.1), that has relatively high DOC concentrations (30–40  $\text{mg L}^{-1}$  expressed as NPOC) and low salinity (chloride concentrations from 18 to 33  $\text{mg L}^{-1}$ ). Colloidal Fe(III) particles can be stabilised against aggregation in the presence of DOC (Gaffney et al., 2008; Neal et al., 2008; Pizarro et al., 1995; Pullin and Cabaniss, 2003). Low ionic strength favours the stability of colloidal suspensions as electrostatic repulsion between equally charged colloidal particles can be attenuated at high ionic strength (Gunnars et

al., 2002; Mosley et al., 2003). Furthermore,  $\text{PO}_4$  itself has a positive effect on the colloidal stability (He et al., 1996) but presence of  $\text{PO}_4$  alone, as shown by the low Fe(III) concentration of the filtrates of the experiments with synthetic solutions, appears not to be sufficient to suppress coagulation (Figure S3.1).

### 3.5.4 Predictive modelling of $\text{PO}_4$ immobilisation during groundwater seepage

The applicability of our experimental results for predicting  $\text{PO}_4$  immobilisation during groundwater seepage was further evaluated by modelling the experimentally derived data of  $\text{PO}_4$  immobilisation of groundwater aeration experiments from the study of Griffioen (2006). The residual  $\text{PO}_4$  concentrations after aeration were modelled based on solubility calculations with Eq. 3.4. The experimentally observed critical  $(\text{P}/\text{Fe})_{\text{ini}}$  value at which  $\text{PO}_4$  remains dissolved after complete Fe(II) oxidation is well reproduced when assuming that a homogeneous Fe hydroxyphosphate phase is formed with a molar ratio of  $\approx 0.6$  ( $\text{Fe}_{1.67}\text{PO}_4(\text{OH})_{2.01}$ ) (Figure 3.6). Below that ratio,  $\text{PO}_4$  concentrations in 0.45 mm filtered solutions are within a range of 1.5 to 10.5  $\mu\text{mol L}^{-1}$  at the end of the aeration experiments. In these solutions, total-Fe concentrations are detected within a range of 2.5 to 35  $\mu\text{mol L}^{-1}$  after 1 day of aeration. This indicates that, similar to our groundwater experiments, these measured Fe and  $\text{PO}_4$  concentrations can be ascribed to the presence of colloidal particles. For the groundwater samples with  $(\text{P}/\text{Fe})_{\text{ini}}$  values from  $\approx 0.6$  to 1.5, a good resemblance is obtained between the experimental  $\text{PO}_4$  concentration after aeration and the modelled  $\text{PO}_4$  concentration after precipitation of  $\text{Fe}_{1.67}\text{PO}_4(\text{OH})_{2.01}$ .

For the majority of groundwater samples with  $(\text{P}/\text{Fe})_{\text{ini}} > 1.5$ , more  $\text{PO}_4$  immobilisation occurred than could be explained by precipitation of Fe hydroxyphosphates. The experiments with  $(\text{P}/\text{Fe})_{\text{ini}} > 1.5$  and little  $\text{PO}_4$  immobilisation also show small decrease of Ca concentrations. This indicates that formation of Ca phosphates, Ca carbonates and/or Ca-Fe-phosphates, which is induced by degassing of the groundwater, contributes to the removal of dissolved  $\text{PO}_4$  in experiments with substantial  $\text{PO}_4$  immobilisation and  $(\text{P}/\text{Fe})_{\text{ini}} > 1.5$ . The role of  $\text{PO}_4$  co-precipitation with Ca precipitates in  $\text{PO}_4$  immobilisation has been demonstrated by Griffioen (2006) and Senn et al. (2015).

Up to initial aqueous P/Fe ratios of 1.5, precipitation of a Fe hydroxyphosphate phase with P/Fe ratio of 0.6 can be used for predictive modelling of fast ( $< 1$  day)  $\text{PO}_4$  immobilisation upon aeration of anoxic natural groundwater. The groundwater samples from the experiments of Griffioen (2006) with  $(\text{P}/\text{Fe})_{\text{ini}}$  ratios  $> 1.5$  can all be considered as nutrient-rich ( $\text{PO}_4 > 50 \mu\text{mol L}^{-1}$ ). The occurrence of nutrient-rich groundwater in the Netherlands is limited to the Holocene coastal lowland areas (Griffioen et al., 2013) and nutrient-rich groundwater is usually not found in Pleistocene areas. As an illustration, 79% of the groundwater samples from the Dutch National Groundwater Quality Monitoring Network (Van Duijvenbooden et al., 1985) taken between 2000 and 2009 have P/Fe ratios  $< 1.5$ . Hence, a model based on the precipitation of an Fe hydroxyphosphate with a  $(\text{P}/\text{Fe})_{\text{ppt}}$  of  $\approx 0.6$  seems suitable to estimate  $\text{PO}_4$  removal during Fe(II) oxygenation in a wide range of streams, ditches and channels that receive anoxic Fe-rich groundwater. These findings provide a solid basis for further studies on transport and bioavailability of  $\text{PO}_4$  in surface water systems.

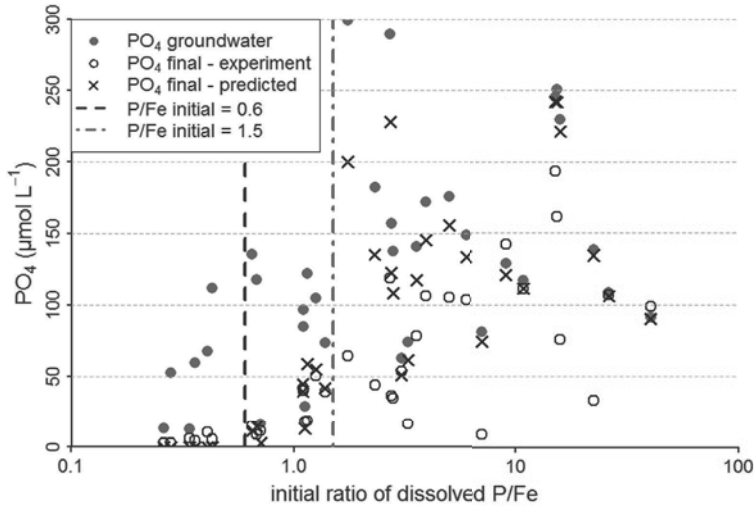


**Figure 3.6.** Measured and predicted  $\text{PO}_4$  concentrations against the  $(\text{P}/\text{Fe})_{\text{ini}}$  ratio from groundwater aeration experiments; experimental results as published by Griffioen (2006) and model results for precipitation of a Fe hydroxyphosphate with a solid molar  $\text{P}/\text{Fe}$  ratio of 0.6.

### 3.6 Conclusions

Aeration experiments with Fe(II) containing solutions demonstrate that dissolved  $\text{PO}_4$  can be effectively immobilised in the form of an homogeneous Fe hydroxyphosphate. In the presence of dissolved  $\text{PO}_4$ , oxidation of Fe(II) leads to the formation of Fe hydroxyphosphates whose  $(\text{P}/\text{Fe})_{\text{ppt}}$  ratios remain virtually constant throughout the reaction despite the change in  $\text{P}/\text{Fe}$  ratio in the solution. However, the  $(\text{P}/\text{Fe})_{\text{ppt}}$  ratio varies depending on the  $(\text{P}/\text{Fe})_{\text{ini}}$  ratio and the pH value. Initial aqueous  $\text{P}/\text{Fe}$  ratios ranging from 0.12 to 0.9 result in  $(\text{P}/\text{Fe})_{\text{ppt}}$  ratios from 0.38 to 0.61. Experiments conducted at pH 6.4 form precipitates with  $\text{P}/\text{Fe}$  ratios that are slightly lower than those forming at pH 6.1.

Presence of dissolved  $\text{PO}_4$  exerts influence on the rates of Fe(II) oxidation. In general, Fe(II) oxidation proceeds slower in the presence of dissolved  $\text{PO}_4$  but, conversely, the decrease of the  $\text{PO}_4$  concentration during Fe(II) oxidation due to the formation of Fe hydroxyphosphates causes additional deceleration of the reaction rate. Although the dependency of the reaction rates on  $\text{PO}_4$  concentration might be complicated, the progress of the reaction in our experiments can be described using a pseudo-second-order rate law with first-order dependencies on both  $\text{PO}_4$  and Fe(II) concentrations. The observed effect of pH on Fe(II) oxidation kinetics in presence of  $\text{PO}_4$  is smaller than in the absence of  $\text{PO}_4$ ; the reaction appears to be first-order with respect to  $[\text{OH}^-]$  in the presence of  $\text{PO}_4$  while it is second-order in absence of  $\text{PO}_4$ . After  $\text{PO}_4$  depletion, the Fe(II) oxidation rate increases again and the kinetics shift to a first-order process with respect to the Fe(II) concentration at constant pH and oxygen concentration. The first-order rate constants after  $\text{PO}_4$

depletion are lower compared to those in  $\text{PO}_4$ -free solutions. This implies that the initially formed Fe hydroxyphosphate affects the kinetics of continuing Fe(II) oxidation after  $\text{PO}_4$  depletion which is likely a result of transformation of the initially formed Fe hydroxyphosphate into other Fe phases during continuing Fe(II) oxidation.

Aeration experiments with natural groundwater show formation of Fe hydroxyphosphates during Fe(II) oxidation in presence of  $\text{PO}_4$  and the progress of Fe(II) oxidation can be described with rate-laws obtained from experiments with synthetic solutions. However, the presence of DOC in the groundwater results in the formation of stable Fe hydroxyphosphate colloids that remain in suspension for longer periods. The formation of a Fe hydroxyphosphate phase with a molar P/Fe ratio of 0.6 can be used for predictive modelling of  $\text{PO}_4$  immobilisation upon aeration of pH-neutral natural groundwater with an initial P/Fe ratio up to 1.5.

## Acknowledgements

Deirdre Clark is gratefully acknowledged for her contribution to the experimental work and field-work. Ype van der Velde is thanked for his mathematical assistance. We thank Andreas Voegelin for the helpful discussions and his suggestions for improvement of the manuscript. The useful comments of three anonymous reviewers are greatly appreciated. Funding of the project was provided by Deltares (project SO2015: From catchment to coast).



## 3.7 Supplement

### S.1 Fe(III) concentrations during the oxidation reaction

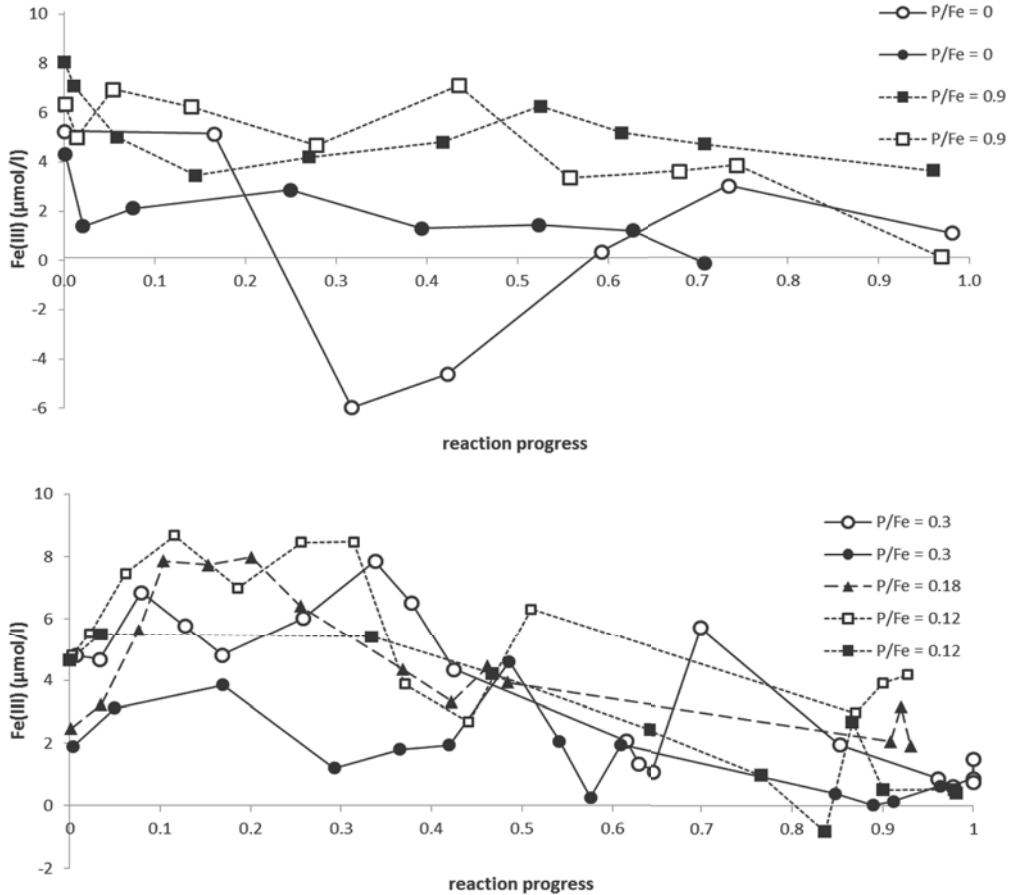
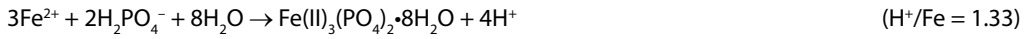


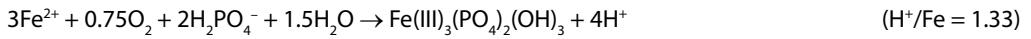
**Figure S3.1.** Fe(III) concentrations vs. the reaction progress. Note that Fe(III) concentrations were calculated from the difference between total-Fe and Fe(II) concentrations. The uncertainty in the Fe(III) concentrations, therefore, ranges between 4 and 6 µmol/l.

## S.2. H<sup>+</sup>/Fe<sup>2+</sup> ratio of the oxidation-precipitation reaction

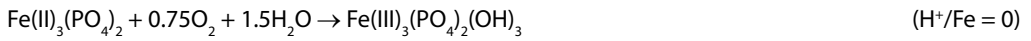
For precipitation of vivianite ((P/Fe)<sub>ppt</sub> = 0.66):



For oxidation of Fe(II) to Fe(III) and precipitation of a Fe(III) hydroxyphosphate with (P/Fe)<sub>ppt</sub> = 0.66



For solid phase oxidation of vivianite to a the Fe(III) hydroxyphosphate with (P/Fe)<sub>ppt</sub> = 0.66:



## S.3. Synthetic water aeration experiments

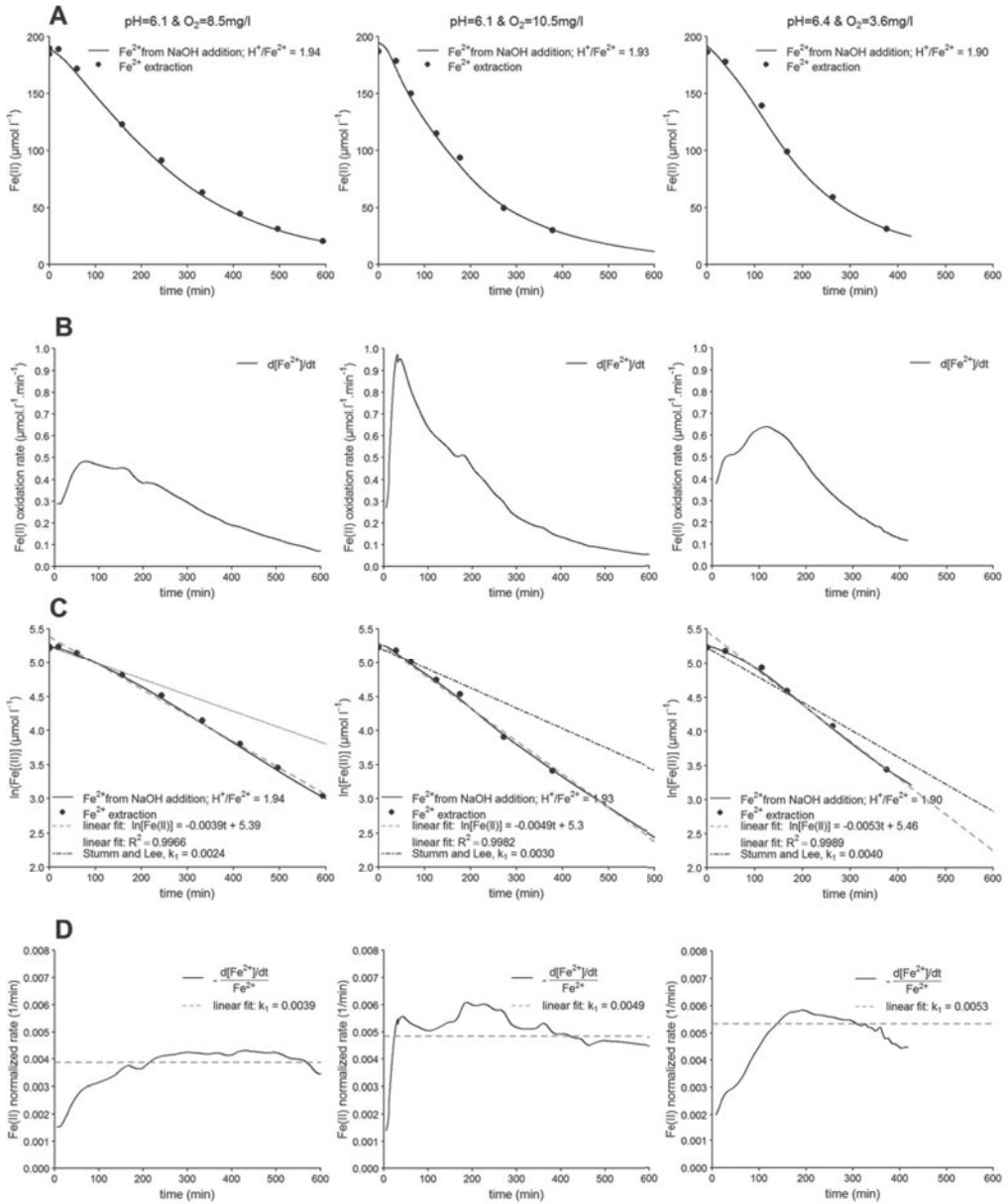


**Figure S3.2.** Progress of Fe(II) oxidation as function of time for experiments with initial aqueous P/Fe ratio of 0. (Row A) Fe(II) concentration. (Row B) Fe(II) oxidation rate. (Row C) semi logarithmic plot of the time evolution of Fe(II) concentration. (Row D) Fe(II) normalised rates as a function of time. The symbols are measurements on discrete samples. Solid lines are computed from the continuously monitored NaOH addition.

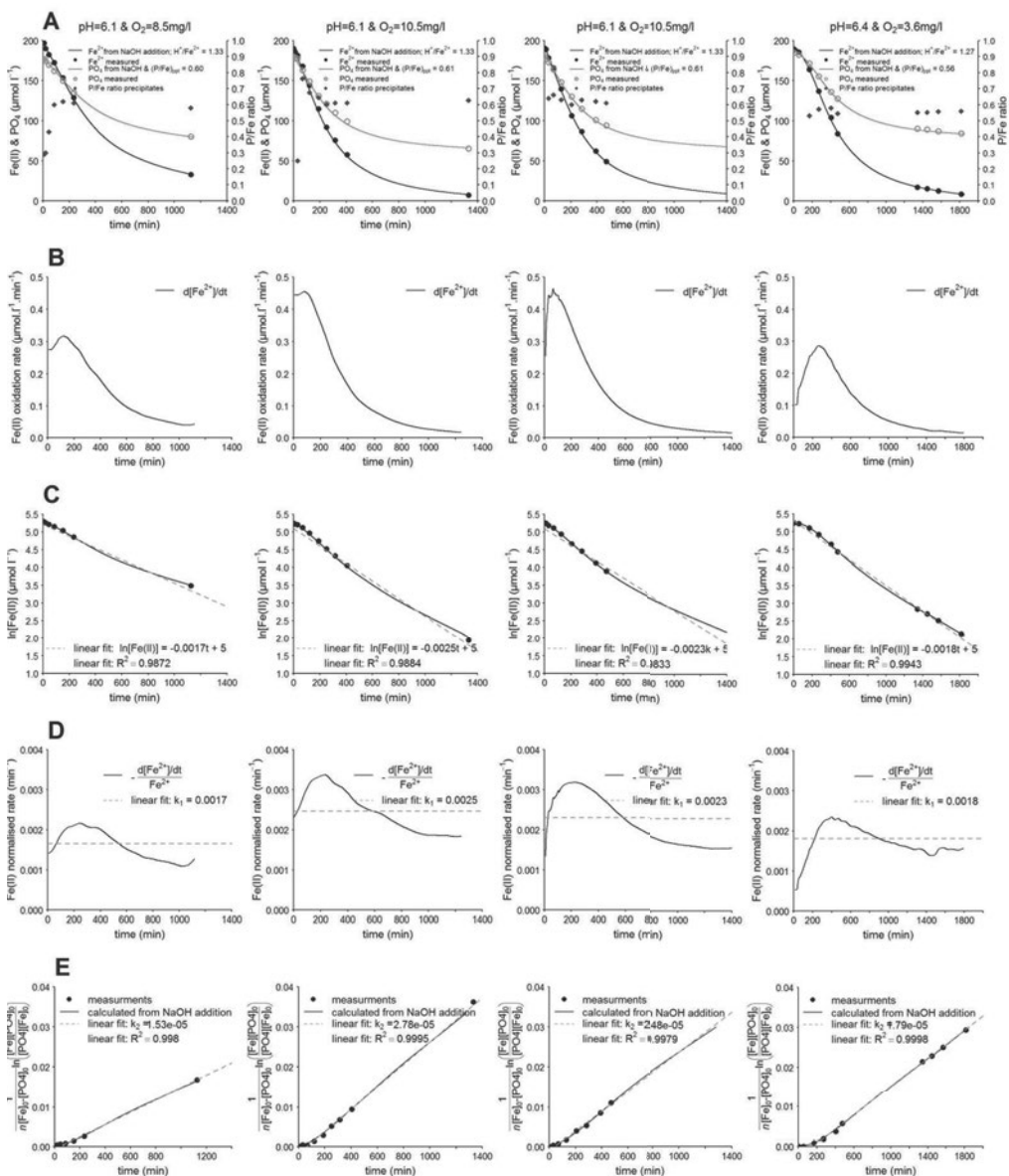


**Figure S3.3.** Progress of Fe(II) oxidation as a function of time for experiments with  $(P/Fe)_{ini}$  ratio of 0.9. (Row A) Fe(II),  $PO_4$  concentration and  $(P/Fe)_{ppt}$  ratio of precipitate. (Row B) Fe(II) oxidation rate. (Row C) semi logarithmic plot of the time evolution of Fe(II) concentration. (Row D) Fe(II) normalised rates as a function of time. (Row E) time evolution of a term derived by integrating the second-order rate law.

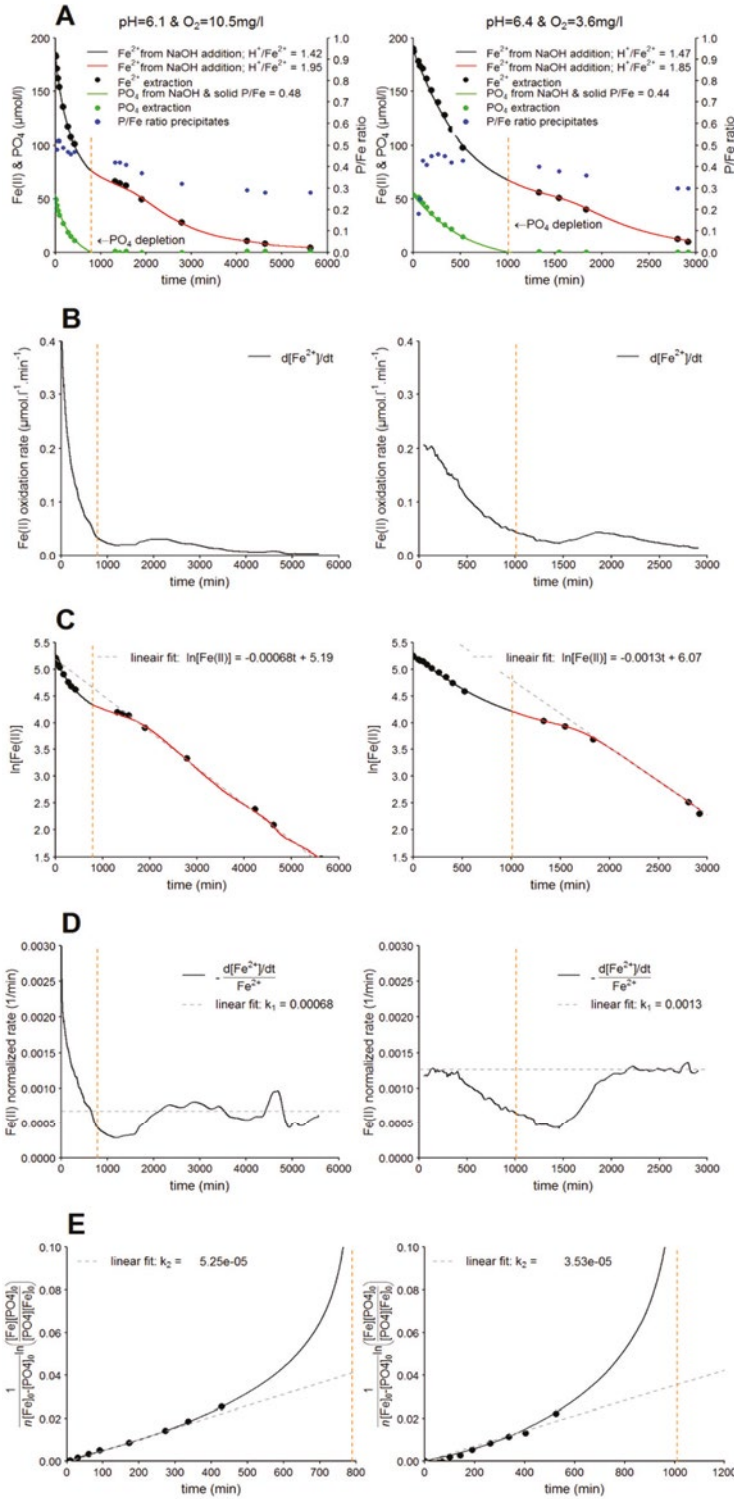


**Figure S3.4.** Progress of Fe(II) oxidation with time for experiments with (P/Fe)<sub>ini</sub> ratio of 0.3. Remarks as for Figure S3.3.

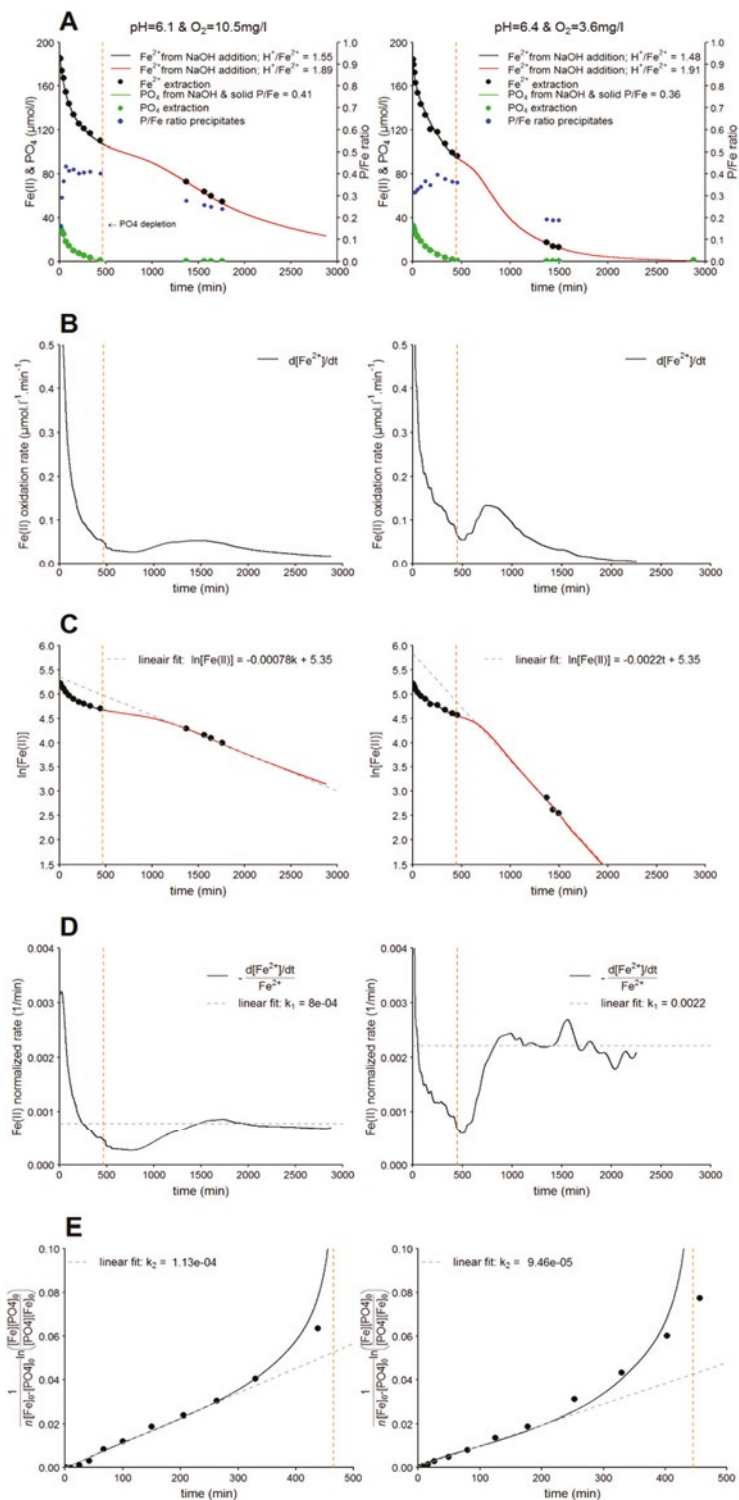


**Figure S3.5.** Progress of Fe(II) oxidation with time for experiments with (P/Fe)<sub>ini</sub> ratio of 0.18. Remarks as for Figure S3.3.

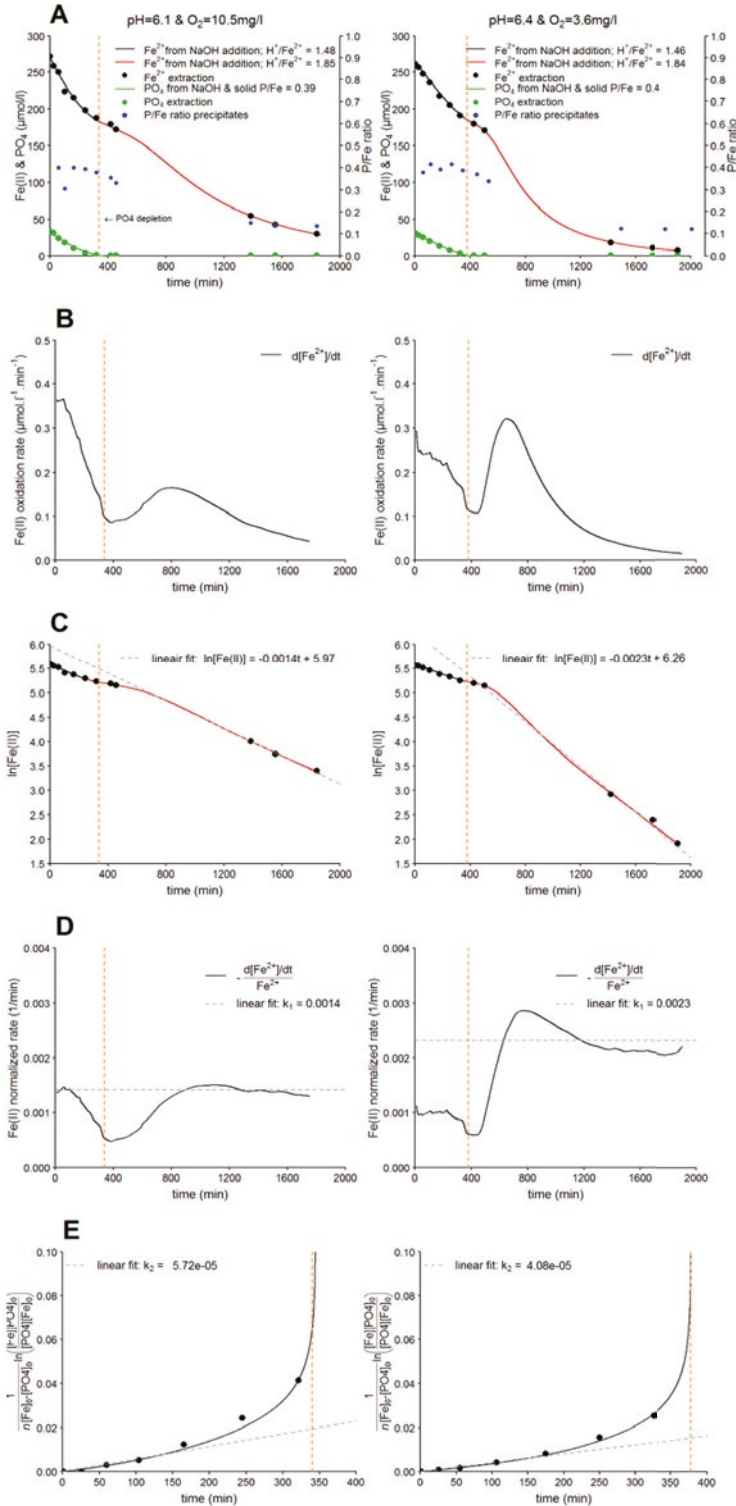


**Figure S3.6.** Progress of Fe(II) oxidation with time for experiments with (P/Fe)<sub>ini</sub> ratio of 0.12. Remarks as for Figure S3.3.

### S.4. Groundwater aeration experiments

**Table S3.1.** Aqueous composition of four groundwater samples from the experimental field site in the Hupsel brook catchment, in  $\text{mmol l}^{-1}$  except when stated otherwise.

Sample	date	$\text{O}_2$ $\text{mg L}^{-1}$	pH	alk $\text{mEq L}^{-1}$	$\text{P}_{\text{CO}_2}$ atm.	Fe	P	(P/Fe) <sub>fm</sub> –	Ca	K	Na	Mg	Mn $\mu\text{mol L}^{-1}$	NH4 $\mu\text{mol L}^{-1}$	Cl	NO3 $\mu\text{mol L}^{-1}$	SO4	NPOC $\text{mg L}^{-1}$
gw3.1	23-06-14	< 0.05	6.10	0.85	0.038	0.178	6.5	0.037	0.77	0.27	0.76	0.33	4.19	20	0.54	< 2	0.51	33.8
gw4.1	23-06-14	< 0.05	5.96	0.48	0.030	0.188	7.4	0.039	0.92	0.34	0.87	0.31	5.64	24	0.91	< 2	1.02	36.8
gw3.2	28-08-13	< 0.05	6.15	1.24	0.050	0.175	12.7	0.073	0.70	0.21	0.63	0.28	8.92	46	0.51	< 2	0.58	35.0
gw4.2	28-08-13	< 0.05	5.84	0.57	0.047	0.184	7.9	0.043	0.72	0.23	0.72	0.32	5.82	69	0.94	14	1.03	41.2



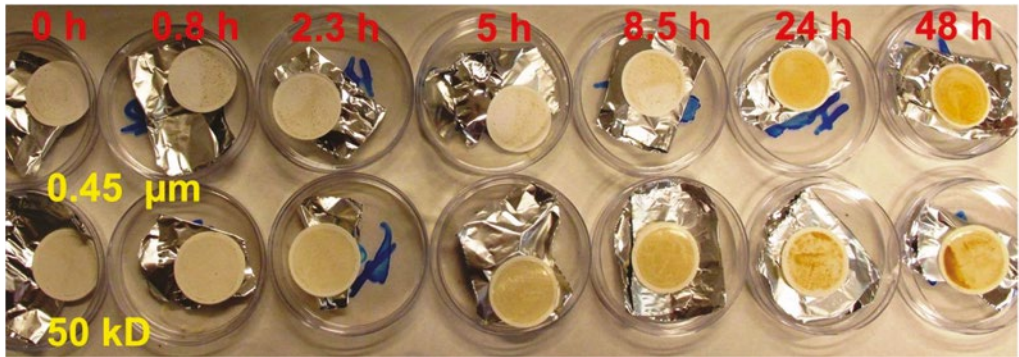


**Figure S3.7.** Photo of the 0.45 µm microfiltration membranes and 50 kD ultrafiltration membranes during the aeration experiment gw4.2. During the first 8.5 h. of the experiment almost no change in the residue on the 0.45 µm membranes was visible. The residue consisted mainly of particulate material that was already present in groundwater before the start of the oxidation experiment. Between 8.5 h. and 24 h. a change in the filter residue was observed that showed the formation of particulate Fe hydroxides during this time interval. The residue on the 50 kD membrane changed between 0.8 h. and 5 h. after the start of the aeration experiment. The colour of the residue became more intense, which indicated a growing amount of colloidal particles during the time interval up to 8.5 h. There was no visible change in the residue on the ultrafiltration membranes after 8.5 h.



# CHAPTER 4

## **Particulate phosphorus speciation in ditches, channels and streams of agriculture-dominated lowland catchments: iron as phosphorus carrier**

Bas van der Grift, Leonard Osté, Paul Schot, Arjen Kratz,  
Emma van Popta, Martin Wassen, Jasper Griffioen

*Under review at Water Research*

## 4.1 Abstract

The fate and environmental effects of phosphorus (P) in natural waters depend on its chemical speciation. The particulate P (PP) concentration is dominant over the dissolved P concentration in agriculture-dominated headwaters in the Netherlands. Routine water quality monitoring programmes worldwide calculate the PP concentration from the difference between total phosphorus (TP) and dissolved reactive phosphorus (DRP) instead of measuring PP. Thus the chemical speciation of PP is not known. To quantify the speciation of PP under various conditions in six agriculture-dominated lowland catchments in the Netherlands, a sequential chemical extraction method was applied to suspended particulate matter (SPM) samples collected by centrifugation or filtration. Sequential chemical extraction of SPM collected by filtration performed better than SPM collected by centrifugation. With an average value of  $8.8 \text{ mg g}^{-1}$ , internationally high P contents of the SPM were found. Iron-bound P was the most important PP fraction in SPM samples (38–95%; median 74%), followed by organic P (2–38%; median 15%). Exchangeable P ranged from 0.2 to 27%, with a median of 4.4%, Ca-P ranged from 0.1 to 11% with a median of 3.9% and detrital P was present in only a small fraction (0–6%; median 1.1%). Iron-bound P dominated the PP speciation throughout the entire range of watercourses (from headwater ditches to catchment outlets) and in samples taken during winter months as well as those taken during summer months. Furthermore, the PP speciation did not change markedly when flow conditions were altered from low to high discharge. The dominance of the Fe-P pool denotes the presence of Fe(III) precipitates in SPM that originate from exfiltration of anoxic groundwater. These Fe(III) precipitates are authigenic and are a major fraction of the total SPM concentration (4 to 67% as  $\text{Fe}(\text{OH})_3$ ; median 18%). The formation of authigenic Fe(III) precipitates results in dissolved P in groundwater rapidly transforming to PP in surface water. We advise including sequential chemical extraction of SPM collected by filtration in large-scale monitoring programmes because the composition of particles is critical for P bioavailability, which is a key driving factor for eutrophication. Authigenic Fe(III) precipitates can be accurately determined in this way, which is important, since these precipitates are a major carrier phase of P in groundwater-fed lowland catchments.

### Keywords

Phosphate binding; Suspended particulate matter; Sequential chemical extraction; Iron hydroxides; Natural water; Filtration

### Abbreviations

TP – Total Phosphorus; DRP – Dissolved Reactive Phosphorus; PP – Particulate Phosphorus; SPM – Suspended Particulate Matter; Fe-P – Iron-bound Phosphorus; exch-P – Exchangeable Phosphorus; Ca-P – Calcium-bound Phosphorus; res-P – residual P; org-P – Organic Phosphorus

## 4.2 Introduction

Phosphorus (P) is an important driver of the biological activity in surface waters and it needs to be managed to avoid or reduce eutrophication. Phosphorus occurs in numerous chemical forms that are distributed throughout the aqueous and solid media, including living organisms (Holtan et al., 1988; Poulernard et al., 2008). Consequently, the fate and environmental effects of P supply (concentration and flux) in flowing water cannot be established unless the biogeochemical reactivity of P associated with different chemical compounds is understood (Pacini and Gächter, 1999) 1999. In aquatic systems, P species are found in 'dissolved', 'colloidal' and 'particulate' fractions (Robards et al., 1994; Worsfold et al., 2005). Particulate P (PP) may be bound to Fe, Mn, Al and Ca, either sorbed onto the surfaces of particles or precipitated as a mineral. Organic P compounds are also associated with PP. Hence, PP is present in a range of compounds with highly diverse stabilities, bondings and exchangeabilities (Poulernard et al., 2008), which influences its bioavailability, the latter being defined as the fraction of PP available for biological uptake. The bioavailability of P is a key parameter associated with eutrophication; it depends on the overall ability of PP to release phosphate in response to an uptake demand by plants or algae (Worsfold et al., 2005).

The composition of particles plays a critical role for P bioavailability (Poulernard et al., 2008). However, routine surface water quality monitoring programmes worldwide, including in the Netherlands, only analyse dissolved reactive phosphorus (DRP) and total phosphorus (TP) (CIW, 2001; Jarvie et al., 2002). Separation of 'dissolved' and 'particulate' P phases is based mainly on filtration using 0.45  $\mu\text{m}$  or 0.7  $\mu\text{m}$  membrane filters. Colloidal P that is not retained by filtration is included in DRP concentration if it is 'reactive' during this analysis. The PP concentration is calculated from the difference between total phosphorus (TP) and dissolved reactive phosphorus (DRP) (Jarvie et al., 2002). Not measuring the chemical speciation of PP in water quality monitoring programmes may be a serious source of uncertainty in addressing eutrophication problems.

Particulate P is vital for understanding the P dynamics in flowing waters in lowland delta areas. Environmental measures to reduce P point sources (e.g. implementation of a third step in wastewater treatment plants and a ban in the use P in detergents) have contributed to a decrease of dissolved P concentrations in major rivers and coastal seas (Burson et al., 2016; EEA, 2015; Grizzetti et al., 2012). As a result, the relative contribution from agricultural sources has risen in recent years in northwest Europe, and commercial fertilisers and animal manure are typically the primary sources of nutrient enrichment in freshwater systems (EEA, 2005). Particulate P is the dominant P fraction in many agriculture-dominated headwaters in the Netherlands. This may be due to the highly particulate nature of P loads to surface water from soil surface and field drain runoff (Van der Salm et al., 2012; Withers et al., 2009). However, P loads commonly leach to surface water via subsurface flow, i.e. through interflow, tube drain discharge or, in well-drained lowlands with shallow groundwater tables (as is the case in much of the Netherlands), through groundwater (Schoumans and Groenendijk, 2000) Type. These P loads have a more dissolved or colloidal nature (King et al., 2015; Regelink et al., 2013) but, as will be explained below, they are expected to be converted to PP during discharge to the surface water system or immediately thereafter.

A typical characteristic of the water bodies that drain agricultural areas in the Netherlands is that they are fed by groundwater from a reactive subsurface with high contents of organic matter and reactive minerals like sulphides and carbonates (Griffioen et al., 2016). Influxes of poorly oxygenated, CO<sub>2</sub>-rich groundwater containing high concentrations of dissolved Fe(II) and Ca provide a continuous supply of Fe(II) and Ca to the surface water. During oxygenation and degassing of this exfiltrated groundwater, solid Fe(III) and Ca phases will precipitate (Griffioen, 2006; van der Grift et al., 2016a). As a result, fine solid aggregates are formed at the sediment/water interface or in the water column (Baken et al., 2013; Van der Grift et al., 2014). Dissolved phosphate present during the oxidation process is removed from the water column into Fe(III) or Ca phases (Senn et al., 2015; van der Grift et al., 2016a; Voegelin et al., 2013). Therefore, we hypothesise that the chemical speciation of P in surface water in lowland catchments is critically dependent on such biogeochemical processes occurring at the groundwater/surface water interface.

Several studies have used P fractionation (inorganic P, organic P, algal available P, total P) or sediment fingerprinting techniques to trace the chemical speciation of P loads and source of suspended particulate matter (SPM) in groundwater-dominated catchments (e.g. Ballantine et al., 2008; Walling et al., 2008). However, these studies only distinguish SPM that originates from soil erosion and resuspension (or erosion) of particles from the streambed or channel bank sediment. They ignore SPM formed in the surface water as a result of aeration and degassing of groundwater. Despite recent research on P behaviour in water systems where authigenic SPM may be formed by aeration and degassing of exfiltrated groundwater (Baken et al., 2016a; Baken et al., 2015a; Baken et al., 2015b; van der Grift et al., 2016a; Van der Grift et al., 2014), we still lack knowledge about the chemical speciation of PP and therefore about its biogeochemical reactivity.

Despite recent developments in the application of advanced spectroscopic techniques such as X-ray Absorption Near Edge Structure spectroscopy (XANES) and Nuclear Magnetic Resonance (NMR) spectroscopy (Li et al., 2015; Liu et al., 2013), the generally accepted and widely used method to determine the chemical speciation of P in sediments is sequential chemical extraction. As it is an indirect method, it has some shortcomings, but nonetheless it is acknowledged to be useful as it allows for comparisons of P pools in sediments (Li et al., 2015). This P speciation (also referred to as fractionation) by means of sequential chemical extraction is an analytical method to fractionate the overall P content of a solid phase sample into groups of compounds with similar chemical release patterns (e.g. Ruttenberg, 1992). It can be used to evaluate the various PP fractions, including labile fractions (loosely bonded or easily exchangeable) and the fractions associated with Al, Fe and Mn oxides and hydroxides, Ca, organic material and residual matter (Pardo et al., 2003). Sequential chemical extraction is widely applied to marine sediments (e.g. Dijkstra et al., 2014; Ruttenberg, 1992; Slomp et al., 1996) and lacustrine sediments (e.g. Golterman, 1996; Gu et al., 2016; Hieltjes and Lijklema, 1980) but only a few studies (Berner and Rao, 1994; Jordan et al., 2008; Subramanian, 2000; Van Eck, 1982) have used sequential chemical extraction to fractionate P pools in SPM from estuaries and rivers. These studies applied sequential chemical extraction to characterise riverine P loads into coastal seas. Studies that use sequential chemical extraction on SPM in small surface water in catchments are even rarer. To our knowledge, those by Pacini and Gächter (1999) and Poulenard et al. (2008) are the only ones to use this method to determine different inorganic PP fractions in

SPM from freshwater catchments. The streams in these studies were located on the northern rims of the Alps in Switzerland and France – a very different geographical setting compared with the Netherlands.

Observations on SPM and associated substances are critically dependent on sampling and processing procedures (Duinker et al., 1979). Samples of SPM for chemical analysis are usually obtained by continuous-flow centrifugation (e.g. Horowitz, 2008; Van Eck, 1982). Large water samples are dewatered by centrifugation, either on site or by returning large bulk samples to the laboratory for processing (Walling, 2013). In the Netherlands, continuous-flow centrifugation is used to sample SPM for routine chemical analysis (CIW, 2001). The disadvantage of centrifugation is, however, that it requires a large volume of water and is time consuming. Additionally, the recovery efficiency for fine particles is not optimal. Time-integrated SPM samplers like the one designed by Phillips et al. (2000) are relatively easy to handle but also have the drawback that the fine fraction does not settle out in the sampler. The routine method for measuring the SPM concentration itself in freshwater systems is sampling by filtration (ISO, 2005). It is an easy method, requiring a small amount of water, but has limitations for chemical analyses. For example, only a small amount of SPM can be sampled and particles cannot be separated from the filters after filtration. Consequently, the filter itself has to be included in the chemical analysis. As these aspects may adversely affect the reliability of the chemical analysis of SPM, experiments on the effects of filtration and centrifugation on substances associated with SPM should be carried out on identical natural samples.

The PP speciation in the water phase may be influenced by several biogeochemical and hydrodynamic processes, including the formation of authigenic SPM. Other processes are the uptake and release of P by plants and algae and loadings by other sources of SPM such as soil erosion or remobilisation of bed sediment. We therefore expect PP speciation will be dynamic in space and time: firstly, a spatial difference in PP speciation in lowland catchments from headwater ditches to catchment outlets; secondly, a seasonal difference between winter and summer in response to biological growth and decay; and thirdly, a rapid temporal change following variation in flow velocities.

The objective of this study was to characterise the chemical speciation of PP as present in small surface waters in the geographical setting of agriculture-dominated lowland catchments in the Netherlands. The three specific objectives of this study were to: (1) validate the widely recognised sequential chemical extraction procedure applied on SPM sampled with filters instead of a continuous-flow centrifuge for the determination of the PP speciation in small surface waters; (2) determine the P content of SPM and the PP speciation in different types of lowland catchments and explore the spatial variation within catchments from headwater ditches to catchment outlets; (3) assess the temporal variation in PP speciation from winter to summer and (4) explore the temporal variation in PP speciation and TP concentrations during changes in flow velocities that are typical for a lowland water system. We expect that insight into PP speciation would help improve understanding of the properties of PP and thereby contribute to the improvement of water quality management in catchments.

## 4.3 Materials and Methods

### 4.3.1 Study areas

To analyse the spatial and temporal PP speciation in surface water of agriculture-dominated lowland catchments in the Netherlands, samples were collected during field surveys in six areas: the Noordplas polder, the Lissentocht polder, the Quarles van Ufford polder, the Langbroekerwetering polder, the Lage Vaart polder and the Hunze catchment (Figure 4.1). These areas differ with respect to type of lowland catchment (free drainage or polder catchment), sampling procedure and period, and flow velocities (Table 4.1). Maps of the study areas with the sampling locations and a short description of the sampling locations, including the order of the watercourse are given in Table S4.1. All study areas are dominated by agricultural land use. The Hunze catchment is a free drainage catchment whereas the other areas are in polders (embanked catchments where water levels are managed by discharge via pumping stations and via the inlet of diverted river water during dry periods). Such polder catchments are found in many delta areas worldwide and are important urban and agricultural areas.



Figure 4.1. Location of the study areas.



**Table 4.1.** Characteristics of the six study areas.

Study area	Type of area	Size (km <sup>2</sup> )	Soil type	Objective of PP speciation	No. of sampling locations	Period of sampling	Type of SPM sampling
Hunze (Hun)	Free drainage catchment	300	sand	spatial	22	March	filtration
Lissentocht polder (LT)	Polder	10	marine clay	spatial	9	April	filtration
Quarles van Ufford polder (QvU)	Polder	120	fluvial clay	spatial and temporal	8	February-June	filtration
Langbroekerwetering polder (LB)	Polder	180	fluvial clay	spatial and temporal	6	February-April	filtration
Lage Vaart (LV)	Polder	243	marine clay	temporal	1	January-August	filtration
Noordplas polder (NPP)	Polder	45	marine clay	flow-induced and spatial	3	February-March	centrifugation and filtration

Regional water authorities provided time series of DRP and TP concentrations from their routine monitoring programmes for the main watercourse of the study area at or near the outlet of the catchment.

### ***Hunze catchment***

The Hunze catchment is a rural, free drainage catchment in the northeast of the Netherlands. It is drained by the small river Hunze (average discharge 3–5 m<sup>3</sup> sec<sup>-1</sup>) and its two major tributaries, the Voorste Diep and the Achterste Diep. Surface elevations range from 0.8 to 25 m above mean sea level (MSL) from north to south. The catchment mainly consists of sandy soils, with peat in the riparian zones. An intensive drainage system with artificial ditches and weirs is used to regulate water levels in the catchment. During dry winter conditions on 21 and 22 March 2013, surface water samples were taken from 22 locations in the catchment, ranging from headwater ditches to the outlet where the river Hunze discharges into Zuidlaardermeer (a lake).

### ***Lissentocht polder***

The Lissentocht polder is part of the Haarlemmermeer polder, created by reclaiming a lake in 1852. It lies 25 km southwest of Amsterdam and contains marine clay soils. The main channel draining the area is the artificial Lissentocht channel. Relief in the polder is flat, with an altitudinal range of 6–3.5 m below MSL. Excess precipitation is quickly drained through an extensive system of tile drains and ditches. A pumping station at the end of the Lissentocht channel maintains water levels throughout the catchment at a relatively constant level. During dry early spring conditions on 6 April 2013, surface water samples were taken from nine locations in the polder, ranging from headwater ditches to the outlet location at the pumping station.

### ***Quarles van Ufford polder***

Quarles van Ufford is a fluvial clay polder in the central part of the Netherlands, located between two rivers: the Meuse (south) and the Waal (north) (the Waal is the main branch of the river Rhine system in the Netherlands). Most (80%) of the area is agricultural. Surface elevations in this relatively flat area range from 3 to 7 m above MSL from west to east. Water discharge from the area mostly flows freely through watercourses westwards and drains into the river Meuse at one outlet location at the western side of the polder. When water levels in the Meuse are high, the water flow is controlled by the Quarles van Ufford pumping station. Inlet of water is possible through five human-controlled inlet locations (Rozemeijer et al., 2012). On 24 February and 2 March 2016, surface water was collected at eight locations in the polder catchment, ranging from headwater ditches to the outlet location at the pumping station. The sampling was repeated at four locations on 25 April and 6 June 2016.

### ***Langbroekerwetering polder***

The Langbroekerwetering polder is situated in the central part of the Netherlands at the transition between the elevated Pleistocene sandy region of the ice-pushed ridge known as Utrechtse Heuvelrug and the lower Holocene fluvial clay soils along the river Kromme Rijn, which was once the main distributary of the river Rhine. The surface elevations range from 0.5 to 10 m above MSL from southwest to northeast. The area is mainly agricultural and about 30% is designated as nature reserve. Rainwater that infiltrates into the ridge may emerge as seepage at the foot of the ridge or locally further west. Rain, seepage and inlet water are discharged into the Kromme Rijn directly and indirectly through a system of watercourses, with the Langbroekerwetering as main channel. Regulation by weirs, pumps and inlets is needed, due to differences in altitude and surface water levels. The Kromme Rijn itself is mainly fed by inlet of river Rhine water. On 10 March 2016, surface water samples were taken from six locations in the catchment, ranging from headwater ditches to the Langbroekerwetering main channel. The sampling was repeated at four locations on 6 June 2016.

### ***Lage Vaart***

The Lage Vaart is the main channel draining the Lage Afdeling polder, which is part of the Flevo polder, the most recent and also the biggest land reclamation project in the Netherlands, which lies between 3 and 5 m below MSL. The land cover in the Lage Afdeling is dominated by agriculture (76%), followed by woodland and marsh (18%) and urban or semi-urban areas (6%). Samples were taken every two to four weeks (January–August 2015) from the Lage Vaart at the Blocq van Kuffeler pumping station, one of the three outlet locations of the Lage Afdeling where excess water is pumped into the Markermeer.

### ***Noordplas polder***

The Noordplas polder, land reclaimed from a lake, is a marine clay polder of about 45 km<sup>2</sup> in the west of the Netherlands, lying 4 to 5 m below MSL. It is characterised by significant exfiltration of groundwater rich in Cl, P and Fe (De Louw et al., 2011). Surface water levels are controlled by two

pumping stations. Time differentiated sampling was performed at three locations in the Noordplas polder during flow events: (1) on 25 February 2014 in the main channel 375 m upstream from the pumping station (PLS), (2) on 25 February 2014 in a secondary channel in a long (5 km) open flow connection with the pumping station (SLT) and (3) on 6 March 2014 in a secondary channel, 25 m upstream from a weir that separates its polder from the influence of the pumping station (STW). The water level in this polder is 20 cm higher than that in the polder. Samples were taken during flow events created by the pumping station (PLS and SLT) or by removing a 20-cm high plank from the weir (STW).

### 4.3.2 Sampling and measurement techniques

#### 4.3.2.1 General sample treatment and field measurements

The surface water samples were collected with peristaltic pumps from a depth of approximately 10 to 20 cm. Sub-samples were filtered in the field (0.45 µm cellulose nitrate filter). A sub-sample was collected in a 60 ml HDPE vial and acidified to a pH of 1, using suprapur nitric acid. This sample was analysed for metals by ICP-OES. Another sub-sample was collected in a 100 ml PE vial, analysed for Cl, NO<sub>3</sub> and SO<sub>4</sub> by ion chromatography and analysed for DRP by using the colorimetric molybdate blue method (Koroleff, 1983). The TP concentration was measured in an unfiltered sub-sample that was digested before analysis by using persulfate and sulphuric acid (Koroleff, 1983). Another set of sub-samples was collected for analysis of the SPM concentration and for sequential chemical extraction either by filtration (2 L glass bottles) or centrifugation (15–25 L plastic tanks), as explained in the following sections.

The flow velocities during the field experiments in the Noordplas polder were measured using electromagnetic flow velocity meters. The device used at locations 1 and 3 is an automated continuous measurement system, which was set to log at a 5-second interval. The flow velocities were measured throughout the field experiments. The device used at location 2 had no data logging capabilities. Flow velocities were only measured at the sampling times.

The particle size distribution and volume concentration of the SPM in the surface water at location PLS in the Noordplas polder was measured in-situ at 10-minute intervals using a LISST-100 Particle Size Analyzer (supplement 3)

#### 4.3.2.2 Suspended particulate matter sampling

All samples for SPM extraction were transferred to a refrigerator (4°C) within 6 hours of collection and processed within 48 hours. For extraction by centrifugation we used a single-speed continuous-flow centrifuge (20,000 RPM) in which the water sample is introduced from above through a funnel and directed to the centre of the column at a flow rate of 0.65 L min<sup>-1</sup> using a peristaltic pump. Centrifugal forces then push the water out from the centre against the walls of the column. The column walls are covered with removable Teflon™ collection sheets which capture the particles on impact. The SPM samples obtained from the Teflon™ sheets were immediately transferred to a freezer and freeze-dried at the earliest opportunity, mostly within 3 days. Sample weights and water volumes were tracked throughout the entire procedure.

Filtration of the water samples from the 2 L glass bottles was performed in the laboratory, using pre-dried, pre-weighed 0.7  $\mu\text{m}$  glass fibre filters (Whatman GF/F) and vacuum pumps. The filters with SPM were dried at 50°C and reweighed, to measure the SPM concentration. The average and standard deviation of the SPM concentration at each location were calculated from three to six filters. The filters plus SPM were stored dry prior to sequential chemical extraction. Photos of the filters with SPM are shown in supplement 2 (Figure S4.2–Figure S4.4).

#### 4.3.2.3 Sequential phosphorus extraction

Phosphorus speciation of the SPM was determined by using the SEDEX method as proposed by Ruttenberg (1992) and modified by Slomp and Epping (1996), but including the exchangeable P step. The dried filters were folded into 15 mL Greiner tubes, placed approximately in the middle of the tube and then submerged by adding the extraction solution. To determine the possibility of P leaching from the GF/F filters, the SEDEX method was applied to a series of four blank filters (only filtered with 500 ml UHQ). The extraction started with loosely bound, exchangeable P (exch-P) (1M  $\text{MgCl}_2$ , pH = 8.0, 0.5 h, 20°C). The filter was subsequently treated with citrate dithionite bicarbonate buffer (1M CDB, pH = 7.5, 8 h, 20°C) to extract P associated with iron oxyhydroxides (Fe-P), followed by a second and third rinse with 1M  $\text{MgCl}_2$  solution (0.5 h, 20°C). The filters were then treated with a sodium acetate buffer (1M, pH = 4, 6 h, 20°C) and another  $\text{MgCl}_2$  rinse (0.5 h, 20°C) to extract calcium-bound P, i.e. authigenic carbonate fluorapatite + biogenic apatite +  $\text{CaCO}_3$ -associated P (Ruttenberg, 1992). The remaining inorganic P was subsequently extracted with 1M HCl (24 h, 20°C). This fraction was referred to as detrital apatite P of igneous or metamorphic origin in Ruttenberg (1992). Because detrital P is also used to refer to P associated with the remains of algae, we prefer to call this fraction residual inorganic P (res-P). For determination of organic P, the sample was dried for 48 h at 50°C. Next, the sample was ashed (2 h, 550°C) and the filter was subjected to another HCl rinse (24 h, 20°C).

In all solutions except for the CDB extracts and the first  $\text{MgCl}_2$  rinse after the CDB step, P concentrations were determined using colorimetric analysis. A standard series was created from a stock solution. For the standard series and the samples, the stock solution was diluted in a combination of UHQ and the matrix of the extract for which the standard series was created. The amount of matrix equalled the volume of sample used. In this way, matrix effects that may obscure the signal were prevented. Phosphorus concentrations in the CDB extracts and the first  $\text{MgCl}_2$  rinse after the CDB step were measured with ICP-OES, in order to prevent the citrate from interfering with the reduction of the molybdate complex.

A separate series of filter samples was treated with aqua regia for determining the total P and total Fe content of the SM. For this destruction, a filter was put in a Teflon™ vessel and concentrated HCl and concentrated  $\text{HNO}_3$  were added in the ratio 3:1. The closed vessel was left overnight on a hot plate at 90°C and then condensed at 160°C. The extract was diluted with a 5%  $\text{HNO}_3$  solution prior to analysis with ICP-OES.

## 4.4 Results

### 4.4.1 Validity of sequential chemical extractions on filter samples

The PP speciation of SPM samples determined by the SEDEX method was performed on 96 filter samples, 19 centrifuge samples and four blank filters as a control. The analysis was performed in duplicate. For 26 of the 96 filter samples (Figure 4.2A). The average difference between both samples for these 26 duplicates was  $0.1 \pm 4.5\%$ .

Except for the org-P step, the P extraction of the blank filters was below the detection limit and did not differ from that of the blanks without filters. Between 0.9 and 1.8  $\mu\text{g P}$  was extracted from the glass fibre filters (Whatman GF/F) in the org-P step. This was approximately one order of magnitude lower than the median value of P extracted during the org-P step in the 96 SPM samples (16  $\mu\text{g P}$ ). The org-P content of the SPM samples was corrected for the recovery of the blank filters.

The sum of the PP fractions from the centrifuge samples was on average lower than the sum of the PP fractions from the filter samples (Figure 4.2B). With the exception of the Fe-P fraction, in all fractions the P contents for the centrifuge samples were lower than those for the filter samples (Table 4.2). The average Fe-P pool was identical, with  $8.1 \pm 1.4 \text{ mg P g}^{-1}$  SPM for the filter samples and  $8.2 \pm 1.7 \text{ P g}^{-1}$  SPM for the centrifuge samples. This indicates that the recovery efficiency of the centrifuge samples is not the same for all fractions. The lower P contents for the exch-P, Ca-P, res-P and org-P fractions resulted in a P content of the SPM that was on average 10% lower in the centrifuge samples than in the filter samples.

We evaluated the performance of the SEDEX method applied to filter samples by comparing the sum of the PP fractions of the SEDEX with the total P content measured after the aqua regia destruction (Figure 4.2C). When plotted against each other, the samples followed the 1:1 line almost perfectly. Linear fitting revealed a slope of 0.998 and an  $R^2$  of 0.93. The average residual content ( $\Sigma\text{SEDEX PP fractions} - \text{PP aqua regia}$ ) was  $-0.38 \text{ mg g}^{-1}$  SM, which resulted in an average error of 4% (for individual samples the residual concentration ranged up to a maximum of 5.8  $\text{mg g}^{-1}$  SPM, resulting in an error up to 28%). In addition, we found a reasonably good match between the 'routinely' calculated PP concentrations in the water phase (TP – DRP concentration) and the sum of the SEDEX PP fractions converted to aqueous concentrations (Figure 4.2D). Although there was more variation around the 1:1 line in comparison with the total P content from the aqua regia destruction, linear regression modelling revealed a slope of 0.954 and an  $R^2$  of 0.87.

Given that the precision of spectrophotometrically quantified dissolved P concentration is generally 2–3% (Monaghan and Ruttenberg, 1999) and that the precision of SPM concentration measurements is about 9%, the results showed that the SEDEX method performed on filters is a robust method for reliable determination of the PP fractionation in SM. The results obtained by this method are used for the next sections of this paper.

### 4.2.2 General characteristics of P fractions and suspended particulate matter in six areas

Total P concentrations in the six areas ranged between 0.06 and 0.61  $\text{mg L}^{-1}$  except for two locations in the Lissertocht polder (LT4 and LT8), which had TP concentrations of 2.98 and 1.49  $\text{mg L}^{-1}$  (Table S4.2). The ditch water at these locations is strongly influenced by boils, where deep nutrient-rich

groundwater discharges directly into the ditch through preferential flow paths (Delsman et al., 2013). Groundwater sampled from a groundwater piezometer located 2 km outside the Lissertocht polder and part of the national groundwater quality monitoring network (no. 2211) has a P concentration of  $3 \text{ mg L}^{-1}$  and a Fe concentration around  $20 \text{ mg L}^{-1}$ . The lowest average TP concentrations were found in the Hunze catchment, Quarles van Ufford and Langbroekerwetering, followed by the Lage Vaart, Lissertocht polder and Noordplas polder (Table 4.3). The latter three are all marine clay polders (Table 4.1).

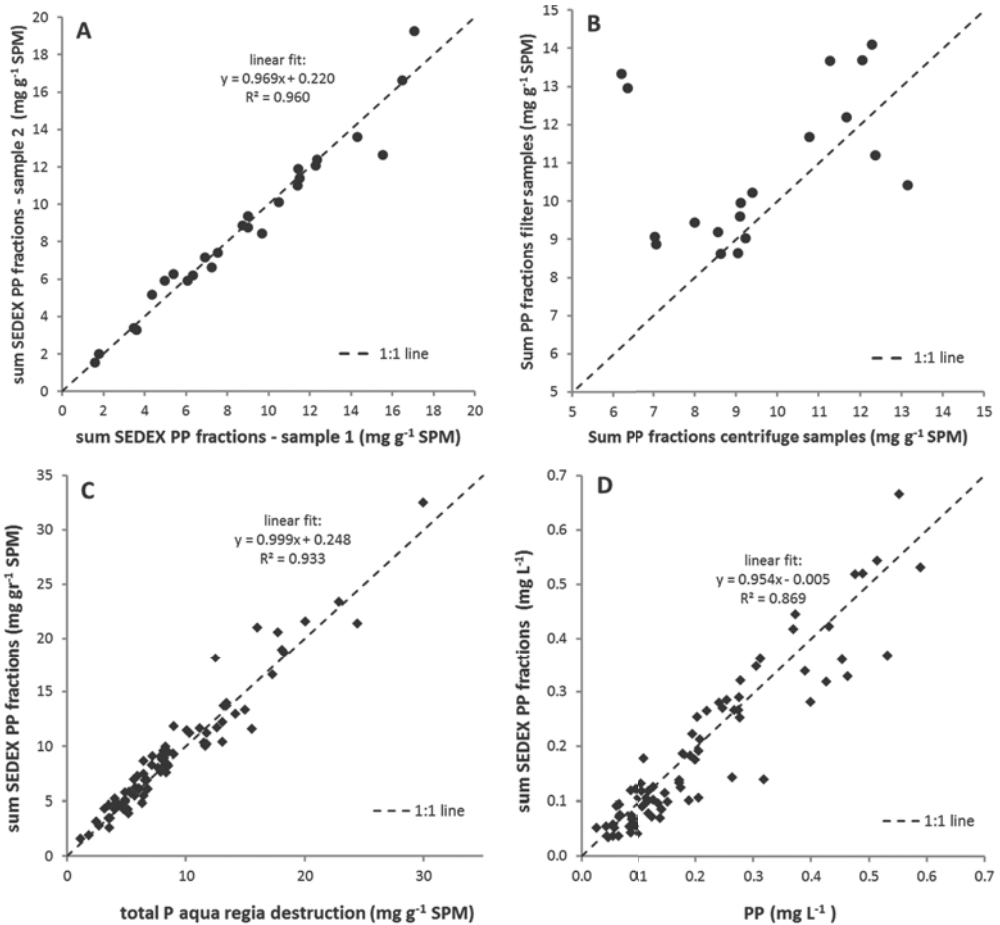


**Figure 4.2.** Validity of sequential chemical extractions: (A) sum of the SEDEX PP fractions of duplicate samples, (B) sum of the SEDEX PP fractions from the centrifuge samples plotted against those of the filter samples, data from the Noordplas polder, (C) total P content of suspended particulate matter samples from aqua regia destruction plotted against the sum of the SEDEX PP fractions and (D) particulate P concentration calculated as difference between TP and DRP concentrations versus sum of the SEDEX PP fractions converted to the aqueous concentrations (by multiplying the sum SEDEX PP fractions by the measured SPM concentration).

**Table 4.2.** Average content and standard deviation of particulate P fractions in the suspended particulate matter collected by filtration and centrifugation of identical samples from the Noordplaspolder (in mg P g<sup>-1</sup> SPM), N = number of samples.

	N	exch-P	Fe-P	Ca-P	res-P	Org-P	Sum of all fractions
Filter samples	19	0.51±0.35	8.14±1.42	0.35±0.20	0.14±0.03	1.47±0.65	10.6±1.93
Centrifuge samples	19	0.16±0.05	8.22±1.75	0.18±0.09	0.07±0.03	0.91±0.46	9.54±2.09

On average, dissolved reactive P concentrations were low, which implies strong dominance of PP in the TP concentration in all areas (Table 4.3 and Figure S4.1 for PP/TP ratios at individual locations). The average PP contribution to the TP concentration was 83%. The dominance of PP in the TP concentration is also clearly apparent in the monthly average values of DRP and TP at the outlets of the areas (Figure 4.3). Substantial DRP concentrations were measured in only a limited number of samples from the Lissertocht polder and the Lage Vaart. Two samples from the Lissertocht polder that were influenced by boils had DRP concentrations of 2.47 mg L<sup>-1</sup> (LT4) and 0.3 mg L<sup>-1</sup> (LT8). No concentrations of this magnitude were found at other locations in the Lissertocht polder, indicating a quick turnover from DRP to PP during aeration of exfiltrated groundwater (Van der Grift et al., 2014). The monthly average DRP and TP concentrations of channel water in the Haarlemmermeer polder 1 km outside the Lissertocht polder revealed TP concentrations similar to those measured in the Lissertocht polder (approximately 0.1–0.4 mg L<sup>-1</sup>). DRP concentrations were low during winter (Figure 4.3), but higher DRP concentrations were measured in this channel during the summer and early autumn months.

**Table 4.3.** Characteristics of P fractionation in the six areas: total P, dissolved reactive P and suspended particulate matter concentrations (in mg L<sup>-1</sup>) and P content of the suspended particulate matter calculated as sum of the SEDEX PP fractions (in mg g<sup>-1</sup>).

	Hunze	Lissertocht	Quarles van Ufford	Langbroekerwetering	Lage Vaart	Noordplaspolder
TP – average	0.14	0.78	0.17	0.18	0.23	0.39
TP – min	0.07	0.06	0.11	0.11	0.08	0.21
TP – max	0.49	2.98	0.27	0.28	0.46	0.61
DRP – average	0.03	0.33	0.02	0.03	0.07	0.03
DRP – min	0.01	0.01	0.01	0.01	0.01	0.01
DRP – max	0.08	2.47	0.04	0.06	0.28	0.06
SPM – average	15	71	34	11	22	34
SPM – min	3	8.3	4	2	13	19
SPM – max	71	222	76	33	37	60
P content SPM – average	7.2	9.2	8.9	14.2	6.1	10.6
P content SPM – min	2.6	4.2	1.6	3.4	3.4	8.2
P content SPM – max	21.4	28.5	23.4	32.5	9.2	14.1

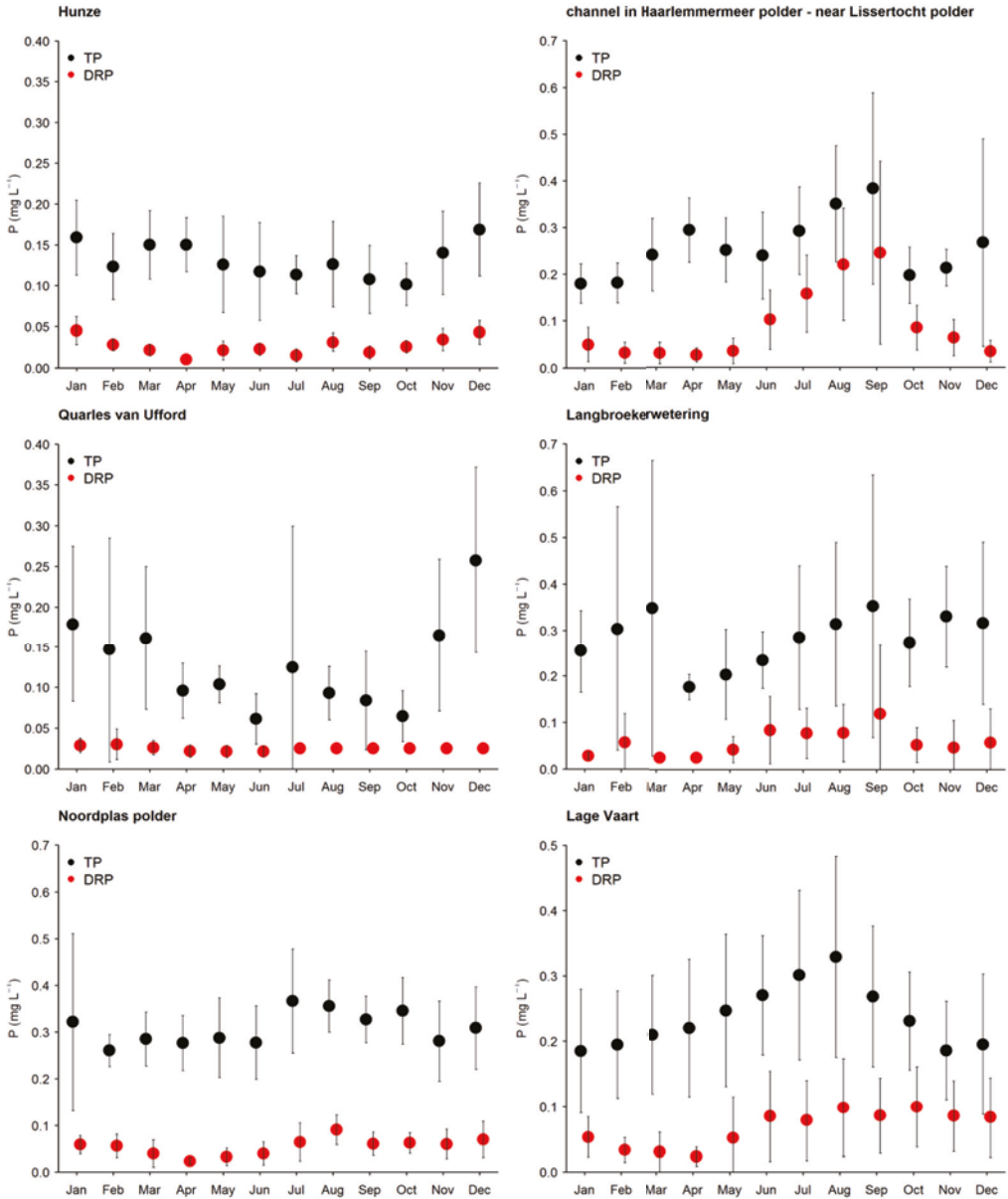


**Figure 4.3.** Monthly average dissolved reactive phosphorus (DRP) and total phosphorus (TP) concentrations for the main watercourse in each of the six study areas at or near the catchment outlet, calculated from time series of concentrations measured from 2005 to 2014. The difference between the TP and DRP concentrations is particulate P (PP). Data from the regional water authorities: Hunze en Aa's, Rivierenland, de Stichtse Rijnlanden, Zuiderzeeland and Rijnland. The monitoring location in the Haarlemmermeer polder is located 1 km outside the Lissertocht polder.



During the sampling campaign, the TP concentration in the samples from the Lage Vaart channel in the Flevo polder increased from 0.09 mg L<sup>-1</sup> in January to 0.46 mg L<sup>-1</sup> in August (Table S4.2). This increase could partly be attributed to the relatively high DRP concentrations in the samples from June (0.11 mg L<sup>-1</sup>) and early August (0.28 mg L<sup>-1</sup>). The PP concentration also increased from 0.06 to 0.27 mg L<sup>-1</sup>. The dominance of PP in the TP concentration during winter months and the increase of DRP concentrations during the summer months are both apparent in the monthly average DRP and TP concentrations in the Lage Vaart (Figure 4.3). Conversely, time series from the Hunze river showed higher DRP concentrations at several sampling moments in the winter.

Suspended particulate matter concentrations ranged from 2 to 76 mg L<sup>-1</sup>, except for the boil location LT4 in the Lissertocht area, which had an exceptionally high SPM concentration of 222 mg L<sup>-1</sup>. The P content of the SPM samples (as sum of the SEDEX PP fractions) ranged between 1.6 and 32.5 mg g<sup>-1</sup>. The SPM from the Langbroekerwetering had the highest P content and the Lage Vaart the lowest.

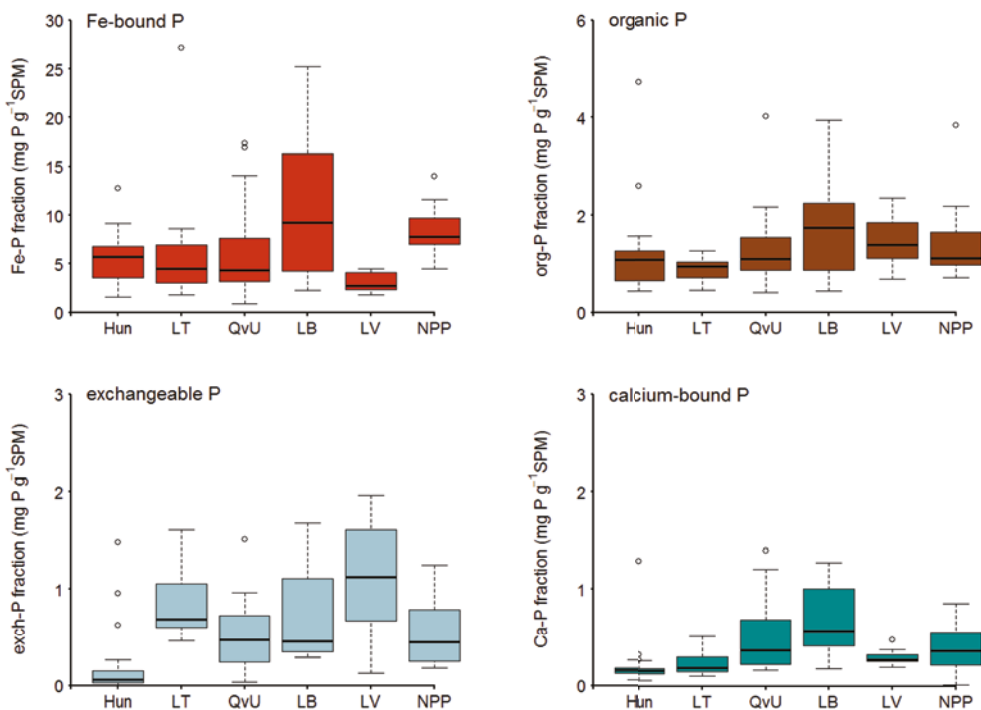


**Figure 4.4.** Boxplots of chemical speciation of particulate P in suspended particulate matter samples from the six study areas. Note the difference in scale of the y-axis. The bold solid line within each box plot is the median concentration. The bottom and top of the box represent the 0.25 and 0.75 quantiles, respectively. Whiskers extend to the maximum and minimum value unless the values exceed 1.5 times the box height. Open circles are extreme values. For abbreviations of the study area, see Table 4.1.

### 4.4.3 Spatial variation particulate P speciation

In all in all SPM samples the most important PP fraction was iron-bound P (Table S4.2 and Table S4.3). The Fe-P content of the SPM ranged from 0.6 to 27.1 mg g<sup>-1</sup> (Figure 4.4). The Fe-P fraction as percentage of total PP ranged from 38 to 95%. The contents of the other PP fractions were much lower and showed less variation as well. Organic P was the second largest PP pool, with values ranging from 0.4 to 4.7 mg g<sup>-1</sup> (2–38% as percentage of total PP). Suspended particulate matter with the highest org-P content was sampled at location H12, a channel in the Hunze catchment that received effluent discharge from a waste water treatment plant (WWTP) (Table S4.1). The exch-P content ranged from 0.01 to 2.0 mg g<sup>-1</sup> (0.2–27% as percentage of total PP). Calcium-bound P ranged from 0.01 to 1.39 mg g<sup>-1</sup> (0.1–11% as percentage of total PP). Residual inorganic P was present only as a minor fraction (0–6% as percentage of total PP).

#### 4.4.3.1 Differences between areas

Although Fe-bound P was the dominant PP fraction (Figure 4.4), the Fe-P content differed appreciably between the areas: median values range from 2.7 mg g<sup>-1</sup> for the Lage Vaart to 9.2 mg g<sup>-1</sup> for the Langbroekerwetering. Suspended particulate matter from the Lage Vaart had the lowest Fe-bound P content (range 1.8–4.5 mg g<sup>-1</sup>). Suspended particulate matter samples with a Fe-P content above 10 mg g<sup>-1</sup> were collected from the Hunze catchment, and the Quarles van Ufford, Langbroekerwetering and Noordplas polders.

The largest variation in the Fe-P fraction was observed in the Lissertocht polder (1.8–27 mg g<sup>-1</sup>), with the highest Fe-P contents being for samples LT4 and LT8, i.e. the boil locations. However, it should be noted that the samples were not in equilibrium with atmospheric conditions at the time of sampling (which can be seen from by the high DRP concentrations) and also that they were not kept under anaerobic conditions between sampling and processing in the lab. Hence, oxidation of the recently exfiltrated groundwater continued after sampling and some of the SPM in samples LT4 and LT8 must have formed after sampling, due to aeration and degassing of the water (van der Grift et al., 2016a). The high SPM concentration of 222 mg L<sup>-1</sup> cannot solely be explained by the formation of P-rich Fe hydroxides and indicates the incorporation of other solutes such as calcium, natural organic matter in the precipitate. In addition, these two samples contained the smallest org-P fraction (0.47 and 0.45 mg g<sup>-1</sup>) and exch-P fraction (0.60 and 0.48 mg g<sup>-1</sup>). Exchangeable P and org-P were, however, more significant PP pools in the other samples from the Lissertocht polder, with values between 0.72 and 1.3 mg g<sup>-1</sup> for org-P and between 0.59 and 1.6 mg g<sup>-1</sup> for exch-P.

The exch-P fraction was also abundant in four other study areas: Quarles van Ufford, Langbroekerwetering, Noordplas polder and the Lage Vaart. The Hunze catchment contained only a marginal exch-P fraction. The org-P fraction did not vary greatly between the areas: median values ranged from 0.95 mg g<sup>-1</sup> for the Lissertocht polder to 1.7 mg g<sup>-1</sup> for the Langbroekerwetering and Lage Vaart.

#### 4.4.3.2 Differences within areas

The Hunze catchment and the Lissertocht polder had the highest spatial sampling densities. For these areas, we determined whether there was a difference in PP speciation between drainage ditches,

secondary channels and the main watercourse (Figure 4.5). There was no structural difference in PP speciation between the different orders of watercourses in either the Hunze catchment or the Lissertocht polder: iron-bound P was already the dominant PP fraction in the drainage ditches and this remained in the secondary channels and the main channel. The high Fe-P contents (8.6 and 27 mg g<sup>-1</sup>) of the two boil locations in the Lissertocht polder resulted in a difference between the Fe-P boxplots for the watercourses in this area.

Results from the other three study areas with sampling locations from smaller headwaters to polder outlets matched the results from the Hunze catchment and the Lissertocht polder. Although the total PP content of the SPM from Quarles van Ufford and Langbroekerwetering ranged between 1.5 and 32 mg g<sup>-1</sup> there is strong dominance of Fe-P (Figure S4.5). Hence, there is only a modest difference in the chemical speciation of PP between sampling locations within catchments, except for a limited number of samples with lower Fe-P contents (locations Q3 and Q7 sampled in February and LB2 sampled in March).

#### 4.4.4 Temporal variation in particulate P speciation

To assess the temporal variation in PP speciation from winter to summer, samples were taken every two to four weeks from the Lage Vaart channel at the Blocq van Kuffeler pumping station from January to August 2015. The P content of the SPM samples from the Lage Vaart (as sum of the SEDEX PP fractions) increased gradually, from 3.4 mg g<sup>-1</sup> in January to approximately 7.5 mg g<sup>-1</sup> in August, except for the sample from April, which had a P content of 9.2 mg g<sup>-1</sup> (Figure 4.6). The largest PP pool in the SPM sampled from the Lage Vaart was iron-bound P (Figure 4.6). Throughout the measuring period, Fe-P varied from 1.8 to 4.5 mg g<sup>-1</sup>, with the lowest value on 20 February and the highest value on 8 April. The second largest fraction was organic P (0.68 to 2.4 mg g<sup>-1</sup>). The highest org-P content was in the sample from 8 April, the lowest was in the sample from 15 January. The exch-P fraction increased from 0.13 to 2.0 mg g<sup>-1</sup> during January-August. The Ca-P fraction varied between 0.20 and 0.48 mg g<sup>-1</sup>, with its highest value on 8 April.

The two other study areas with multiple sampling moments (Quarles van Ufford and Langbroekerwetering) showed no structural trend in the Fe-P fraction during the period from February to June (Figure S4.5). The org-P content at all sampling locations in Langbroekerwetering and at three locations in Quarles van Ufford was higher in February/March than in June. The exch-P contents showed no structural increase or decrease from February/March to June.

#### 4.4.5 Flow-induced changes in particulate P speciation

The Noordplas polder field experiment had a different focus than the other studies: at three locations, it focused specifically on the effect of changes in flow conditions on the SPM and TP concentrations and the distribution of the different PP fractions of the SPM (Figure 4.7). Before the start of the experiment, the TP concentration of the surface water at the three locations was dominated by PP (Table 4.1). This dominance is also apparent in the time series of DRP and TP concentrations in the main channel at the outlet of the Noordplas polder (location PLS) (Figure 4.3).

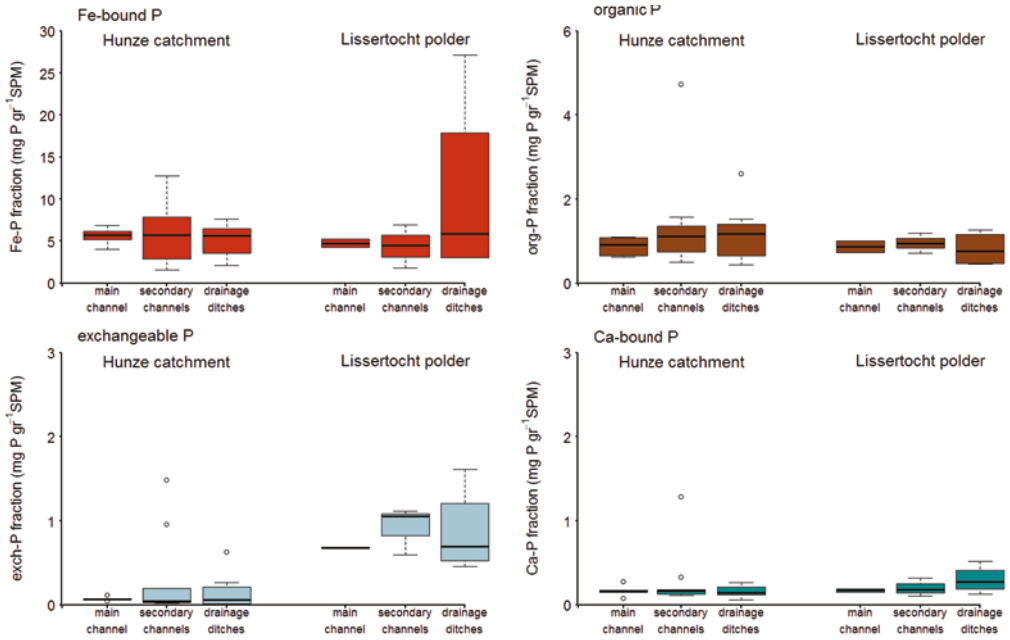


**Figure 4.5.** Boxplots of chemical speciation of particulate P in different orders of watercourses in the Hunze catchment and the Lissertocht polder. Note the difference in scale of the y-axis. Remarks as for Figure 4.4.

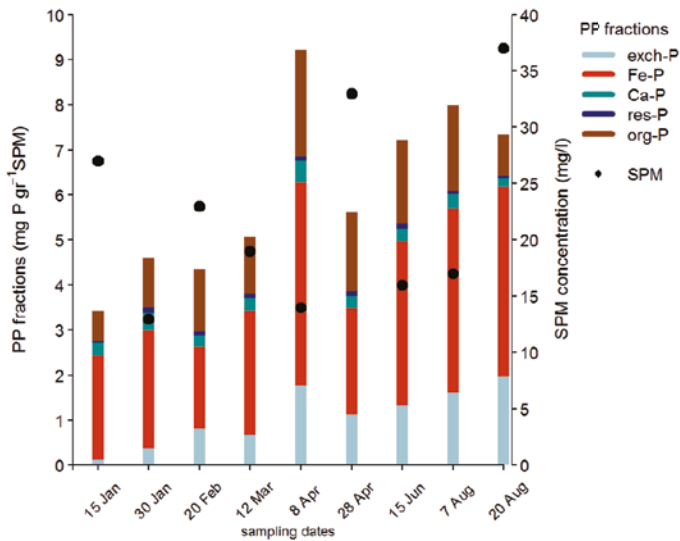


**Figure 4.6.** Chemical speciation of particulate P and suspended particulate matter concentrations in samples from the Lage Vaart channel at the Blocq van Kuffeler pumping station of the Flevo polder.

#### 4.4.5.1 Main channel near pumping station (PLS)

Activation of the pumping station resulted in a quick change in flow velocities in the main channel nearby the pumping station. The flow velocity with one pump in operation was around  $0.1 \text{ m s}^{-1}$  and with two pumps in operation it was  $0.3 \text{ m s}^{-1}$  (Figure 4.7 top). The flow velocity induced by two pumps had a strong influence on SPM and TP concentrations as well as on the particle size distribution. The highest SPM concentration during pumping was almost double the pre-pumping concentration (Figure 4.7 top). Both particle size distribution and particle volume concentration (as measured with the LISST-100) changed markedly upon pumping. The particle volume concentration increased from  $100$  to  $300 \mu\text{L L}^{-1}$  and the mean particle size from  $90$  to  $150 \mu\text{m}$  (supplement S.4). The TP concentration of a sample taken at minute 88 showed a response to pumping but the SPM did not. The large difference between the TP and the SPM concentrations of this sample suggests that the SPM concentration measurement is erroneous. The DRP concentrations remained close to the detection limit. Subtracting the DRP concentration from the TP concentrations revealed that approximately 91–98% of the TP consisted of PP. Similar to the SPM concentration, the PP concentrations doubled during operation of the pumping station. Other dissolved species showed little variation during the experiment, indicating that there was no major change origin of the water that could have influenced the SMP and TP concentration (Table S4.3).

The PP content of the SPM varied between  $8.8$  and  $9.4 \text{ mg g}^{-1}$  and did not show a significant change during operation of the pumping station. The P speciation of the SPM is strongly dominated by Fe-P ( $6.9$ – $7.7 \text{ mg g}^{-1}$ ), followed by org-P ( $1.0$ – $1.1 \text{ mg g}^{-1}$ ). Exchangeable P ( $0.18$ – $0.25 \text{ mg g}^{-1}$ ) and Ca-P ( $0.28$ – $0.58 \text{ mg g}^{-1}$ ) are minor P pools in the SPM (Figure 4.7 top). The contribution of the different PP fractions remained fairly constant during the experiment and was largely unaffected by changes in flow velocity and the SPM concentration. Hence, the SPM did not change markedly in composition.

Suspended particulate matter remobilised by the pumping station showed a decrease in concentration to approximately 75% of its peak value less than 30 minutes after the pumps were stopped. This indicates relatively high fall velocities of the SPM eroded by the increase of flow velocity. The particle size distribution as measured with the LISST-100 device (supplement 3) and the TP concentration (Figure 4.7 top) follow a similar pattern, but 30 min after stopping the pumps the values were even closer to pre-pumping levels.

#### 4.4.5.2 Secondary channel in open connection with pumping station (SLT)

The headwater secondary channel (location SLT) was sampled simultaneously with the main channel near the pumping station. The pull effect of the pumping station was also observed at this location, although flow velocities were lower and lagged behind in time (Figure 4.7 middle). The maximum velocity was  $0.12 \text{ m s}^{-1}$ , which is less than half the maximum velocity at PLS. The SPM concentration initially showed a decrease over time. The TP concentration also slightly decreased during the initial period of the field experiment. Hence, changes in flow velocity did not result in resuspension of particles from the channel bed. The DRP concentration ( $0.04$ – $0.06 \text{ mg L}^{-1}$ ) varied little during the experiment: although slightly higher than in the main channel, it was still a small fraction of the TP concentration.

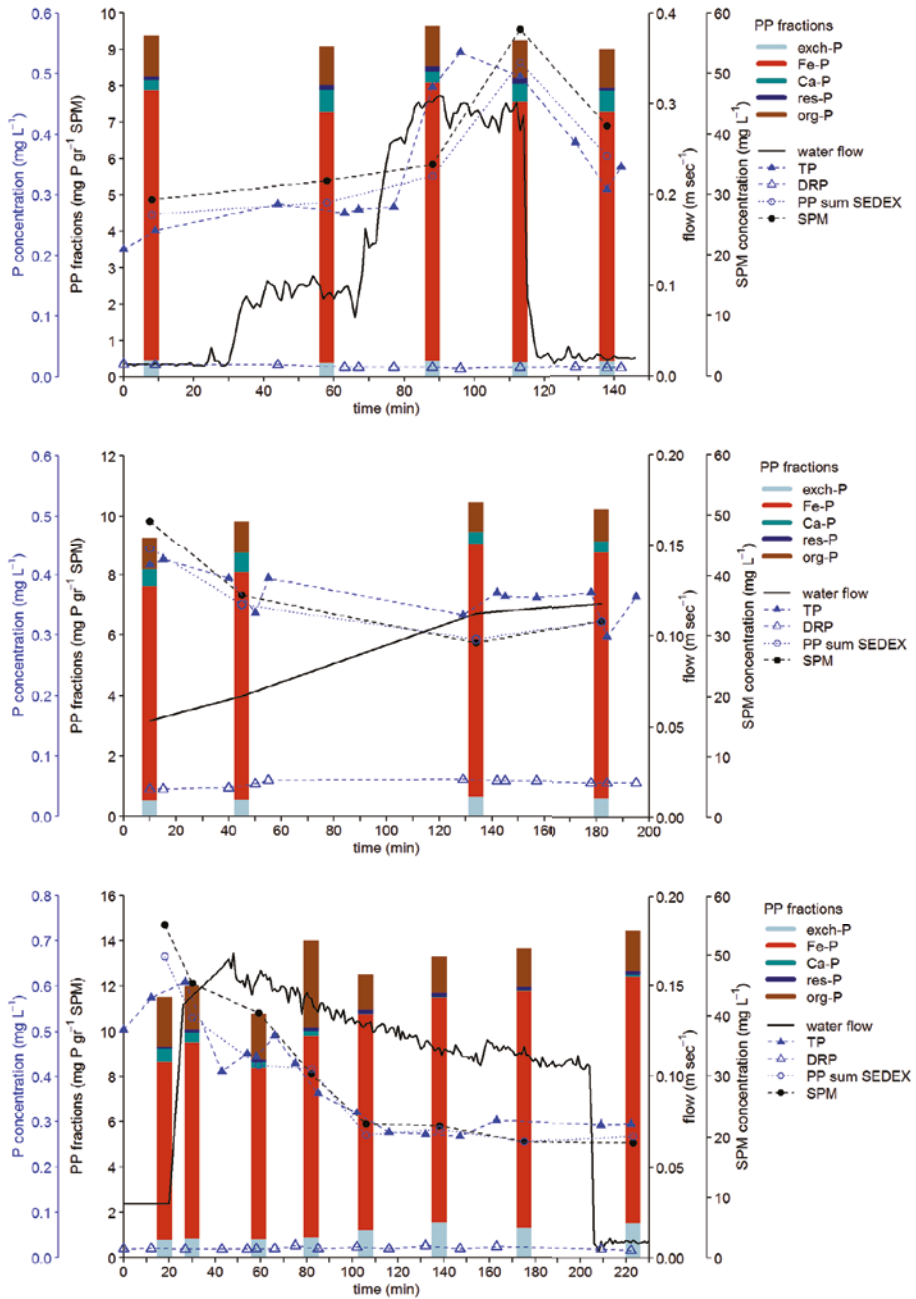


**Figure 4.7.** Particulate P speciation distribution, flow velocities, TP concentrations, DRP concentrations and SPM concentrations during the field experiments in the Noordplas polder: (top) in the main channel near Palenstein pumping station during pumping event (PLS), (middle) in a secondary channel during pumping event (SLT) and (bottom) in a secondary channel during a discharge event generated by lowering of a weir (STW).

The results of sequential chemical extraction indicate that the relative contribution of PP fractions and the P content of the SPM did not vary during the experiment (Figure 4.7 middle). Once more, the largest PP fraction was Fe-P (7.1–8.4 mg g<sup>-1</sup>), followed by org-P (0.85–1.0 mg g<sup>-1</sup>).

#### 4.4.5.3 Secondary channel with weir (STW)

Lowering the weir by 20 cm in another secondary channel at minute 25 caused flow velocity in this channel to increase suddenly from 0.03 m s<sup>-1</sup> to approximately 0.16 m s<sup>-1</sup>, thereafter diminishing gradually over the next three hours to approximately 0.11 m s<sup>-1</sup> (Figure 4.7 bottom). The highest SPM concentrations were observed before the opening of the weir and declined steadily after the weir was lowered. This showed that the increased flow did not result in resuspension of particles from the channel bed. The concentrations of dissolved species changed during the experiment (Table S4.3): the water became less saline, while the SO<sub>4</sub> concentration increased from 290 to 380 mg L<sup>-1</sup>. This indicates a gradual change in source of the water during the experiment.

The most dominant fraction was iron-bound P (7.6–10.9 mg g<sup>-1</sup>): an increase was observed from the first stage (60 min) to the last stage of the experiment. This increase was accompanied by an increase in the exch-P fraction (from 0.46 to 1.24 mg g<sup>-1</sup>) and a decrease in the Ca-P fraction (from 0.57 to 0.01 mg g<sup>-1</sup>). The org-P fraction was lower during the second stage of the experiment (after 100 min) than in the first stage (0–100 min). The concentration change in PP fractions during the experiment resulted in the P content of the SPM increasing from 11 mg P g<sup>-1</sup> during the initial stage to 14 mg P g<sup>-1</sup> SPM during the final stage.

## 4.5 Discussion

### 4.5.1 Validity of sequential chemical extractions on filter samples

We employed sequential chemical extraction on SPM to gain a better understanding of the PP speciation in streams, ditches and channels of agriculture-dominated lowland water systems. Suspended particulate matter was sampled by flow-through centrifugation and filtration. Our results show that despite the small amount of SPM that can be sampled by filtration, this method of SPM sampling outperforms the centrifugation method (Figure 4.2A). The recovery efficiency of centrifugation samples is generally lower than that of filtration samples, largely because the finer and less dense particles may not be included in particulate matter obtained by centrifugation (Duinker et al., 1979). For example, Van Eck (1982) reported the recovery efficiency of a continuous-flow centrifugation was 85–95% of 0.45 µm filtration. The recovery efficiency becomes even more important when dealing with low SPM concentrations (< 30 mg L<sup>-1</sup>), which are typically the case for streams and ditches in lowland catchments and which also applies to a large majority of the samples in our study (Table S4.2 and Table S4.3). Moreover, Duinker et al. (1979) showed that compared with centrifugation as procedure to collect SPM, filtration results in higher contents of metals (Cu, Cd, Pb and Zn) that are associated with the smaller and less dense particles. We found the largest difference between the centrifugation and filtration samples for the exch-P fraction. This is in line with results

from Poulenard et al. (2008) and Pacini & Gächter (1999), who reported that the exch-P fraction is most abundant in the finest particles, which presumably are not captured by the centrifuge.

Sequential chemical extraction, a traditional technique for characterising sediment P speciation, is known to have some limitations. Besides the risk of particulate matter loss during the sequential chemical extraction procedure (Ruttenberg et al., 2009), two other limitations may impact the results of SEDEX extractions. Firstly, some forms of PP could be missed by the SEDEX analysis (Jordan et al., 2008). Any organic P dissolved by extractions for exch-P, auth Ca-P and detr-P would not be measured by the subsequent colorimetric analysis of  $\text{PO}_4$ . In contrast, organic P dissolved by the extraction for Fe-P would be included by the subsequent ICP analysis of total P, resulting in an overestimate of Fe-P. Secondly, the CDB extraction could represent P species that are bound to reduced Fe minerals (at least vivianite) as well (Dijkstra et al., 2014). However, such reduced Fe minerals are not expected in SPM sampled from oxygenated surface water. Despite these potential limitations, sequential chemical extraction continues to be widely used method. When applied to SPM sampled by filtration, the method is amenable to large-scale sampling and analysis programmes of the PP speciation in freshwater systems.

## 4.5.2 Chemical speciation of PP in lowland catchments

### 4.5.2.1 P content of suspended particulate matter

There is consensus about the correlation between SPM and PP concentration (e.g. Beusen et al., 2005; Kronvang et al., 1997). This correlation was also apparent in the present study and this implies that variation in P content of the SPM is limited (Figure 4.8A). The average P content of all SPM samples in our study was  $8.8 \text{ mg g}^{-1}$  but ranged from  $1.5$  to  $32.5 \text{ mg g}^{-1}$ . This average P value is higher than the annual average value of  $5.7 \text{ mg g}^{-1}$  reported during the pollution peak of the early 1980s for an estuary in the southwest of the Netherlands receiving water from the river Rhine (Van Eck, 1982). Also, it is double the value reported by Kronvang et al. (1997) for a Danish arable catchment ( $4.2 \text{ mg g}^{-1}$ ). Other studies reported even lower values. Evans et al. (2004b) found an average value of  $1.7 \text{ mg g}^{-1}$  for two lowland streams in England. Owens and Walling (2002) compiled a table of P content in SPM based on a substantial number of studies. They reported values ranging between  $0.1$  and  $4.4 \text{ mg g}^{-1}$ , except for one study in France that had values up to  $13.5 \text{ mg g}^{-1}$ . The latter is still a factor 2.5 lower than the highest values we found. Huisman et al. (2013) found values between  $1.7$  and  $2.7 \text{ mg g}^{-1}$  in an agricultural watershed in the US. Martínez-Carreras et al. (2012) observed P contents of SPM between  $0.7$  and  $2.1 \text{ mg g}^{-1}$  in several catchments in Luxembourg. Finally, Ballantine et al. (2008) reported average P contents of SPM samples between  $0.1$  and  $2.5 \text{ mg g}^{-1}$  for three groundwater-dominated lowland catchments in the UK. The contents we observed are thus internationally high. This observation, in combination with low observed DRP concentrations, can be explained by a strong tendency for biogeochemical transformation of dissolved P tot PP during exfiltration of groundwater in lowland catchments in the Netherlands (Griffioen, 2006; Van der Grift et al., 2014). This will be elaborated on in the following sections.

Phosphorus contents above  $15 \text{ mg g}^{-1}$  were mostly found in samples with low SPM concentrations ( $< 15 \text{ mg L}^{-1}$ ) (Figure 4.8B). Finer particles have lower fall velocities and remain longer in the water column. Therefore, it can be assumed that SPM collected from surface water with low



SPM concentration consists of finer particles than SPM collected from surface water with higher concentrations. This indicates that finer particles are relatively more enriched with P, which is in line with the results from Evans et al. (2004b).

#### 4.5.2.2 Fe-bound P

The Fe-P content strongly dominates the total P content of the SPM in all six study areas, evidenced by a linear trend line between both parameters with a slope of 0.79 (Figure 4.8C). The slope of the trend lines of the second and third largest PP pools, org-P and exch-P were with 0.10 and 0.038 much lower. Because the DRP concentrations are commonly low in the water systems studied, this all implies that TP concentrations in surface water in agriculture-dominated lowland catchments are strongly determined by the concentration of particulate Fe-bound P (Figure 4.8D). The dominance of Fe-P is independent of the study area, the sampling location within the study area (from headwater ditch to outlet of the catchment), the time of sampling (winter or summer) and the increase in flow conditions typical for channels and ditches in polder catchments. Only during the summer months in the Lage Vaart did DRP become the most important TP fraction instead of Fe-P. Multi-year time series of DRP and TP concentrations in the Lage Vaart channel and in the Haarlemmermeer tocht (near Lissertocht polder) revealed comparable results: an increase of DRP concentration during the late summer and early autumns (Figure 4.3). This is likely due to release of DRP from bed sediments or mineralisation of organic P from algae or plant debris (Van der Grift et al., 2016b) (see also section 4.3).

The dominance of the Fe-P pool indicates the presence of Fe(III) precipitates in the SPM, which is also visible from the colours in the yellow/orange/red/brown range in the photos of the SPM (Figure S4.2–Figure S4.4). These Fe(III) precipitates originate from groundwater exfiltration. After exfiltration of anaerobic Fe-rich groundwater to surface water, oxidation of Fe(II) to Fe(III) by atmospheric oxygen will lead to the formation of authigenic particles, i.e. particles formed when compounds in solution precipitate due to changing environmental conditions (Baken et al., 2013; Vanlierde et al., 2007). Dissolved phosphate that is present during oxidation of Fe(II) will immediately be immobilised, due to precipitation as Fe(III) hydroxyphosphates (van der Grift et al., 2016a; Voegelin et al., 2013). Iron-bound P is already the dominant chemical PP fraction in the headwater ditches we sampled, which implies fast turnover of dissolved P to particle-bound P during exfiltration and subsequent oxygenation of anoxic groundwater (Griffioen, 2006; Van der Grift et al., 2014). Exfiltration of anoxic Fe-rich groundwater is thus a major control on P speciation in surface waters of lowland catchments. This should be taken into account in research on transport and/or ecological effects of P in streams, ditches and channels.

#### 4.5.2.3 Organic P

The organic P fraction, the second largest PP pool, did not differ noticeably between the areas. In the three areas where samples were taken during different seasons, the highest org-P fraction as percentage of total P was present in samples from the end of the winter or early spring. Although we have no hard evidence, we suspect this could be due to recent manure application. One of the measures in the Netherlands to reduce the risk of nutrient leaching to groundwater and surface

water is to restrict manure application: on arable land it is permitted from 1 February to 1 August and on grassland from 15 February to 31 August (LNV, 2009). Van der Grift et al. (2016b) showed that manure application during the end of February and early March resulted in losses of  $\text{NO}_3$  to the surface water. Although we did not detect an effect on the TP concentrations, recent manure application might have affected the chemical speciation of PP by increasing the org-P pool. Two SPM samples from tube drains in Quarles van Ufford collected in February 2016 at the same time as the surface water samples also had high org-P fractions (40 and 47%).

#### **4.5.2.4 Exchangeable P**

The most remarkable difference in P speciation among the study areas and in the temporal trends during the season is apparent in the exch-P fraction, which is negligible in most samples from the Hunze catchment but is significantly higher in the polder catchment (range 2%–26%) (Figure 4.4). The low exch-P fraction in the Hunze catchment compared to the higher fraction in the polder catchments is likely the result of differences in soil types between these areas. Whereas the Hunze catchment consists mostly of sandy soils, the polder catchments are dominated by marine clay soils (Lissertocht polder and Noordplas polder) or fluvial clay soils (Quarles van Ufford and Langbroekerwetering). Particulate P associated with clay particles is expected to be loosely sorbed (Froelich, 1988) and thus extracted by the exch-P step. These particles are vulnerable to being lost from soil as a result of water discharge through trenches or drainage tubes (Regelink et al., 2013; Van der Salm et al., 2012).

The increase from 4 to 27% in the exch-P fraction in the Lage Vaart samples from winter to summer may be associated with mineralisation of organic P from algae or plant debris or dissolved P release from bed sediment which then is available for sorption on suspended particles. Baken et al. (2016a) argued that the sequence of dissolved P and Fe(II) loads to the surface water may influence the P immobilisation process. If P is present during oxidation of Fe(II) to Fe(III) it will precipitate as an Fe hydroxyphosphate (van der Grift et al., 2016a), which results in formation of Fe-P. In contrast, if Fe(III) particles are formed before mixing with P, e.g. P released from mineralisation, this may then be adsorbed to the surface of existing particles, which leads to formation of exch-P. We therefore hypothesise that this may explain the increase in exch-P during spring and summer.

#### **4.5.2.5 Ca-bound P**

A small but detectable fraction was present in most SPM samples. Griffioen (2006) found uptake of phosphate by Ca phosphates and/or Ca carbonates that form upon degassing of exfiltrated groundwater and we expected that this would also play a role in groundwater-fed catchments like ours. After degassing, this water becomes supersaturated in calcium phosphates and these phases may, therefore, precipitate. The amount of Ca-P in the polder catchments was, however, less than expected, given the calcareous nature of the areas. Recently, Senn et al. (2015) showed that immobilisation of phosphate during oxidation of Fe(II) in the presence of Ca can be attributed to (Ca-)Fe(III) phosphate precipitation. It is possible that minerals of this type are extracted during the earlier Fe-P step.

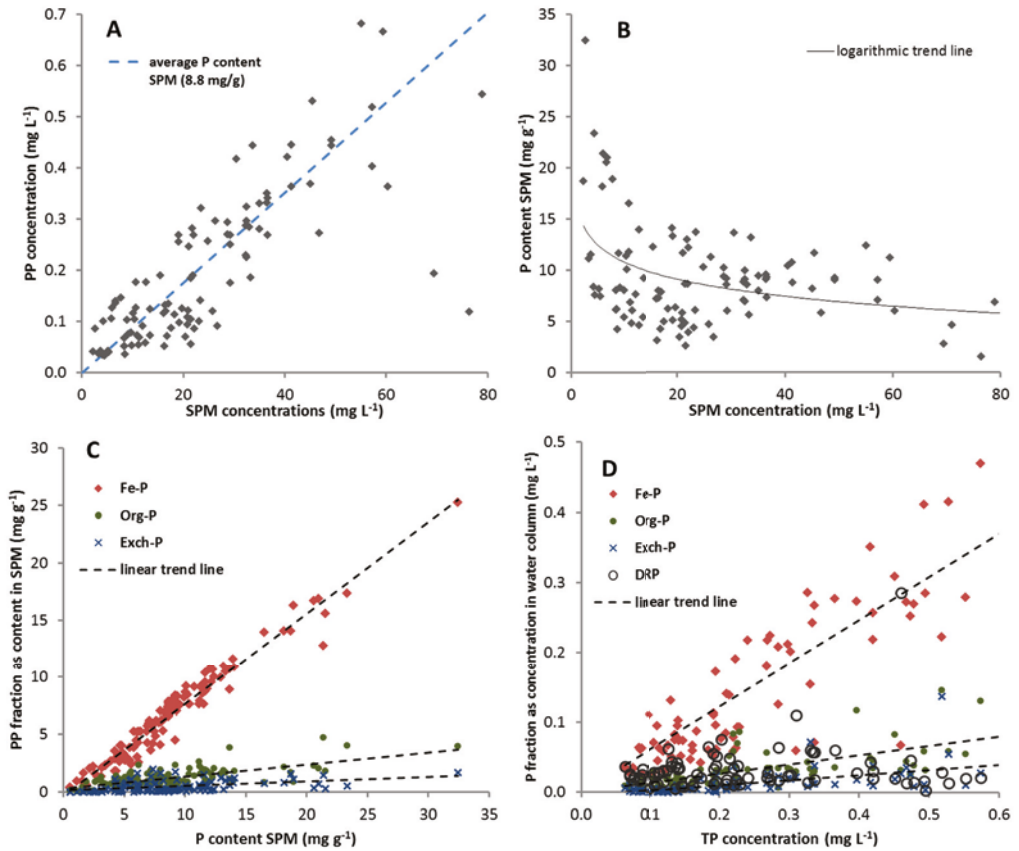


**Figure 4.8.** Particulate P speciation and suspended particulate matter concentration in agriculture-dominated catchments in the Netherlands: (A) particulate P concentration in the water column (sum of the SEDEX PP fractions) versus SPM concentration, (B) particulate P content of SPM (sum of the SEDEX PP fractions) versus SPM concentration, (C) extracted PP fractions versus total P content of the SPM (sum of the SEDEX PP fractions) and (D) P fractions as concentration in the water column versus TP concentration in water column.

The measured decrease of the Ca-P fraction during flow in the two secondary channels studied in the Noordplaspolder (SLT and STW) may be explained by the residence time of the ditch water. The secondary channels act like a reservoir, with limited inflow from the headwater ditches and outflow over the weir. Hence, 'older' almost stagnant water was sampled before the increase in flow conditions. Both degassing of groundwater and precipitation of calcium phosphates and/or calcium carbonates are kinetically controlled processes, which means that the age of the surface water is a factor that influences the occurrence of Ca-P. The water in the headwater ditches that discharge to the secondary channels during the field experiment is likely younger in apparent age and thus would have had less time to undergo kinetically controlled processes. A pool of org-P may also be built up in this virtually stagnant water, due to early spring algal growth. This water was flushed out

during the field experiment, which might explain the decrease of the SPM concentration and the org-P fraction during the experiment.

### 4.5.3 Bioavailability of particulate P

The PP fractions distinguished by sequential chemical extraction differ in bioavailability. While the  $\text{MgCl}_2$  step represents a fully exchangeable and therefore bioavailable fraction, the bioavailability of other phases will depend on geochemical transformations and time allowed for diagenesis (Pacini and Gächter, 1999). Limited bioavailability of colloidal Fe-P was shown by Baken et al. (2014). The consensus is that Fe-P can only be considered largely bioavailable under anoxic conditions, due to the reductive dissolution of Fe oxyhydroxides (Golterman, 2001; Pacini and Gächter, 1999). The greatest risk of mass release of P is during the end of the summer season, when anoxic conditions occur most frequently, due to the decomposition of the primary production during summer. Except for water systems with a full cover of duckweed or a floating mat of algae, which create light limitation, the water column in streams, channels and ditches of lowland catchments is unlikely to become anoxic during summer. This means that before it can become bioavailable, Fe-bound P must settle out and be buried in the sediment layer. Iron-bound P in SPM that is too fine-grained to settle by gravity will not become readily bioavailable. This also applies to Fe-bound P in the easily erodible top layer of the bed sediment, which may become eroded during an increase in flow velocity. The experiment in the Noordplaspolder showed that the PP speciation of this material does not deviate from that of the SPM present originally. Hence, the bioavailability of PP depends on the sedimentation and resuspension behaviour of the SPM.

Once it has been buried in the sediment layer, the entire Fe-bound P pool does not become bioavailable. Phosphorus-rich Fe(III) phases have been detected in anoxic sediments that are resistant to reductive dissolution (Canavan et al., 2006; Hyacinthe and Van Cappellen, 2004). Moreover, 'P trap' layers rich in Fe oxyhydroxides have been reported to develop at the surface of bed sediments, which are capable of sorbing DRP from upward diffusion from sediment porewater (Baken et al., 2015b; Jarvie et al., 2008). However, the increase of DRP concentrations during the end of summer and early autumn we observed in time series from the Lage Vaart channel and the Haarlemmermeer tocht (Lissertocht polder) (Figure 4.4) indicates that release of Fe-bound P is a possibility in lowland areas.

### 4.5.4 Authigenic suspended particulate matter

Assuming the Fe that is extracted by the aqua regia destruction (Table S4.2 and Table S4.3) is mostly present as Fe hydroxide ( $\text{Fe}(\text{OH})_3$ ), we can stoichiometrically calculate the contribution of authigenic Fe particles to the total SPM concentration. The area with the highest average contribution of Fe hydroxides in the SPM was the Hunze catchment (32%; range 5–57%), followed by the Quarles van Ufford polder (average 27% and range 11–67%) and the Langbroekerwetering polder (average 25%; range 18–51%) (Figure 4.9). The average  $\text{Fe}(\text{OH})_3$  content of the SPM samples from the Noordplaspolder was 17%. During the field experiment the  $\text{Fe}(\text{OH})_3$  fraction at location STW increased from 11% to 21%. This indicates that prior to the experiment, SPM consisting of material other than

Fe hydroxides increased in the stagnant water. As described in section 4.2 this material could be carbonates or organic matter (algae).

The individual study areas showed a larger Fe-P pool at higher  $\text{Fe}(\text{OH})_3$  contents (Figure 4.9). All SPM samples with  $\text{Fe}(\text{OH})_3$  contents below 10% had Fe-P fractions below 60%. Hence, PP fractions other than Fe-P may become the dominant fraction in SPM with low  $\text{Fe}(\text{OH})_3$  contents.

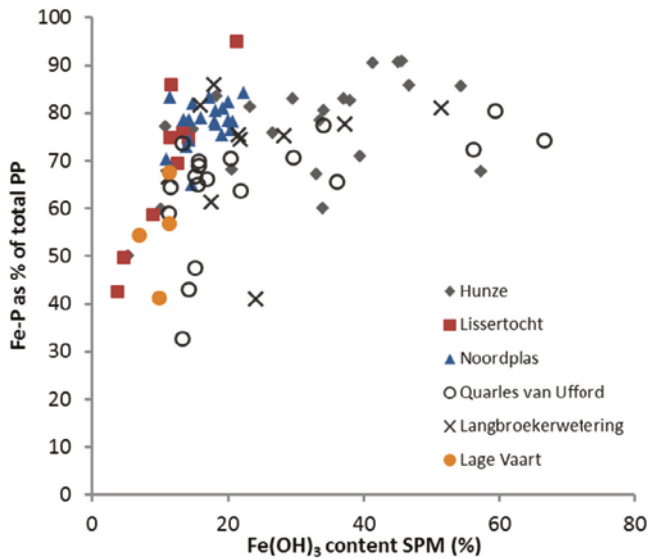


**Figure 4.9.** Fe hydroxide content of suspended particulate matter as extracted by the aqua regia destruction versus Fe-P fraction as percentage of total particulate P.

The Fe content as determined by the aqua regia destruction indicates that a significant amount of the SPM in all six areas is authigenic. At international level, little is known about the contribution of authigenic matter to the total sediment load. The only studies we know on authigenic SPM formed by oxidation of Fe-rich groundwater in fresh water are Baken et al. (2013) and Vanlierde et al. (2007). They reported an average authigenic matter contribution to the total SPM flux of between 31% and 75% for a catchment in Belgium. The limited focus on authigenic production of SPM and related impact on PP in freshwater catchments is probably because the hilly or mountainous regions studied are often characterised by soil erosion, which will decrease the contribution of authigenic sediments to the total sediment load transported by a river. Moreover, in these regions, geological conditions are unlikely to favour the production of authigenic sediment, i.e. discharge of groundwater rich in anoxic Fe may be lacking (Vanlierde et al., 2007). However, authigenic SPM becomes the key sorbent for immobilising dissolved P in lowland catchments that drain anoxic groundwater. When studying P dynamics and transport in such systems it is important to consider the origin and behaviour of authigenic versus detrital particles.

## 4.6 Conclusions

This study characterised the chemical speciation of particulate P in six groundwater-fed lowland catchments in the Netherlands. To do so, suspended particulate matter (SPM) collected by either filtering or centrifuging surface water samples was analysed by means of sequential chemical extractions.

The main conclusions from this study are:

- Sequential chemical extraction of SPM collected by filtration is an appropriate method for determination of the chemical speciation of particulate P in large-scale sampling and analysis programmes.
- The P content of suspended particulate matter in these samples from agriculture-dominated lowland catchments in the Netherlands ranged from 1.5 to 32.5 mg g<sup>-1</sup>. The values observed in this study are high compared with groundwater-fed lowland catchments elsewhere in Europe and North America.
- Iron-bound P was the most important particulate P fraction in SPM sampled from surface water during various conditions in agriculture-dominated lowland catchments. Total P concentration (and therefore the transport of P) in surface water is strongly determined by the concentration of Fe-bound P, except for locations where DRP increases during the summer (especially late summer).
- P speciation distribution in surface water did not change considerably from headwater ditches to the catchment outlet; this indicates a fast turnover of dissolved P to particle-bound P during the exfiltration and subsequent oxygenation of anoxic groundwater.
- The dominance of the Fe-P pool denotes the presence of Fe(III) precipitates in the SPM. These Fe(III) precipitates are authigenic and contribute considerably to the total SPM concentration. Authigenic Fe(III) precipitates are thus a major carrier of P in groundwater-fed lowland catchment. This should be taken into account in P studies of lowland catchments.

Based on these conclusions, it is advisable to include sequential chemical extraction of SPM collected by filtration in large-scale monitoring programmes, because particle composition is critical for P bioavailability, which is a key steering factor for eutrophication.

## Acknowledgements

The Regional Water Authorities Hunze & Aa's, Zuiderzeeland, Rivierenland, Stichtse Rijnlanden and Rijnland are gratefully acknowledged for providing the water quality data. Jelle Molenaar is thanked for his assistance with the electromagnetic flow velocity meters and the LISST device. Joy Burrough was the language editor. Funding of the project was provided by Deltares (project SO2015: From catchment to coast).

## 4.7 Supplement

### S.1 Sampling locations

**Table S4.1.** Description of the sampling locations and order of the watercourse.

Location	Description	Order watercourse
<i>Hunze catchment</i>		
H1	Hunze river outlet	main channel
H2	outlet of channel that drains lower part of the Hunze catchment	main channel
H3	ditch in the lower stretch of the Hunze catchment (east bank)	drainage ditch
H4	middle reach Hunze river	main channel
H5	channel draining middle stretch of the Hunze catchment (east bank)	secondary channel
H6	ditch in middle stretch of the Hunze catchment (east bank)	drainage ditch
H7	ditch in lower stretch of the Hunze catchment (west bank)	drainage ditch
H8	ditch in middle stretch of the Hunze catchment (east bank)	drainage ditch
H9	De Beek tributary of Hunze river	secondary channel
H10	ditch in upstream part of De Beek subcatchment	drainage ditch
H11	channel draining middle stretch of the Hunze catchment (west bank)	secondary channel
H12	ditch downstream of WWTP	secondary channel
H13	channel draining upstream stretch of the Voorste diep catchment	secondary channel
H14	ditch in upstream stretch of the Voorste diep catchment	drainage ditch
H15	upper reach of the Hunze river Achterste diep	secondary channel
H16	ditch in the catchment of the Achterste diep	drainage ditch
H17	ditch in the catchment of the Achterste diep	drainage ditch
H18	outlet of upper reach Hunze river Achterste diep	main channel
H19	outlet of upper reach Hunze river Voorste diep	main channel
H20	tributary in upstream stretch of the Voorste diep catchment	secondary channel
H21	ditch in the catchment of the Voorste diep	drainage ditch
H22	tributary of the Voorste Diep	secondary channel
<i>Quarles van Ufford polder</i>		
Q1	channel in eastern area of the polder	secondary channel
Q2	Broekgraaf channel in the central area of the polder	secondary channel
Q3	channel in the central area of the polder	secondary channel
Q4	ditch in the northwestern area of the polder	drainage ditch
Q5	Grote Wetering main channel near polder outlet and pumping station	main channel
Q6	Grote Wetering main channel in the central area of the polder	main channel
Q7	channel in southern area of the polder	secondary channel
Q8	channel near river Meuse	secondary channel

**Table S4.1.** *Continued*

<b>Location</b>	<b>Description</b>	<b>Order watercourse</b>
<i>Langbroekerwetering polder</i>		
LB1	Rijsbruggerwetering channel in the western area of the polder	secondary channel
LB2	Wijkersloot secondary channel in the southern area of the polder near river Rhine	secondary channel
LB3	Amerongsewetering secondary channel, near river Rhine	secondary channel
LB4	Langbroekerwetering main channel, upstream stretch	main channel
LB5	Gooyerwetering secondary channel, in the northern area of the polder	secondary channel
LB6	Langbroekerwetering main channel, downstream stretch	main channel
<i>Lissericht polder (part of Haarlemmermeer polder)</i>		
LT1	Lissericht main channel near polder outlet	main channel
LT2	ditch in northeastern area of the polder	drainage ditch
LT3	channel in northeastern area of the polder	secondary channel
LT4	dead end of ditch where water from a seepage well (boil) flows into the ditch	drainage ditch
LT5	Kagertocht secondary channel in the central area of the polder	secondary channel
LT6	main channel in the central part of the polder	main channel
LT7	field ditch in the southern area of the polder	drainage ditch
LT8	field ditch in the southern area of the polder with seepage boils in bank	drainage ditch
LT9	Slotertocht channel in the southern area of the polder	secondary channel
<i>Noordplas polder</i>		
PLS	main channel near Palenstein pumping station	main channel
SLT	secondary channel upstream part of the polder	secondary channel
STW	secondary channel in separate sub-polder	secondary channel
<i>Lage Vaart (part of Flevo polder)</i>		
LV	main channel near Blocq van Kuffeler pumping station	main channel



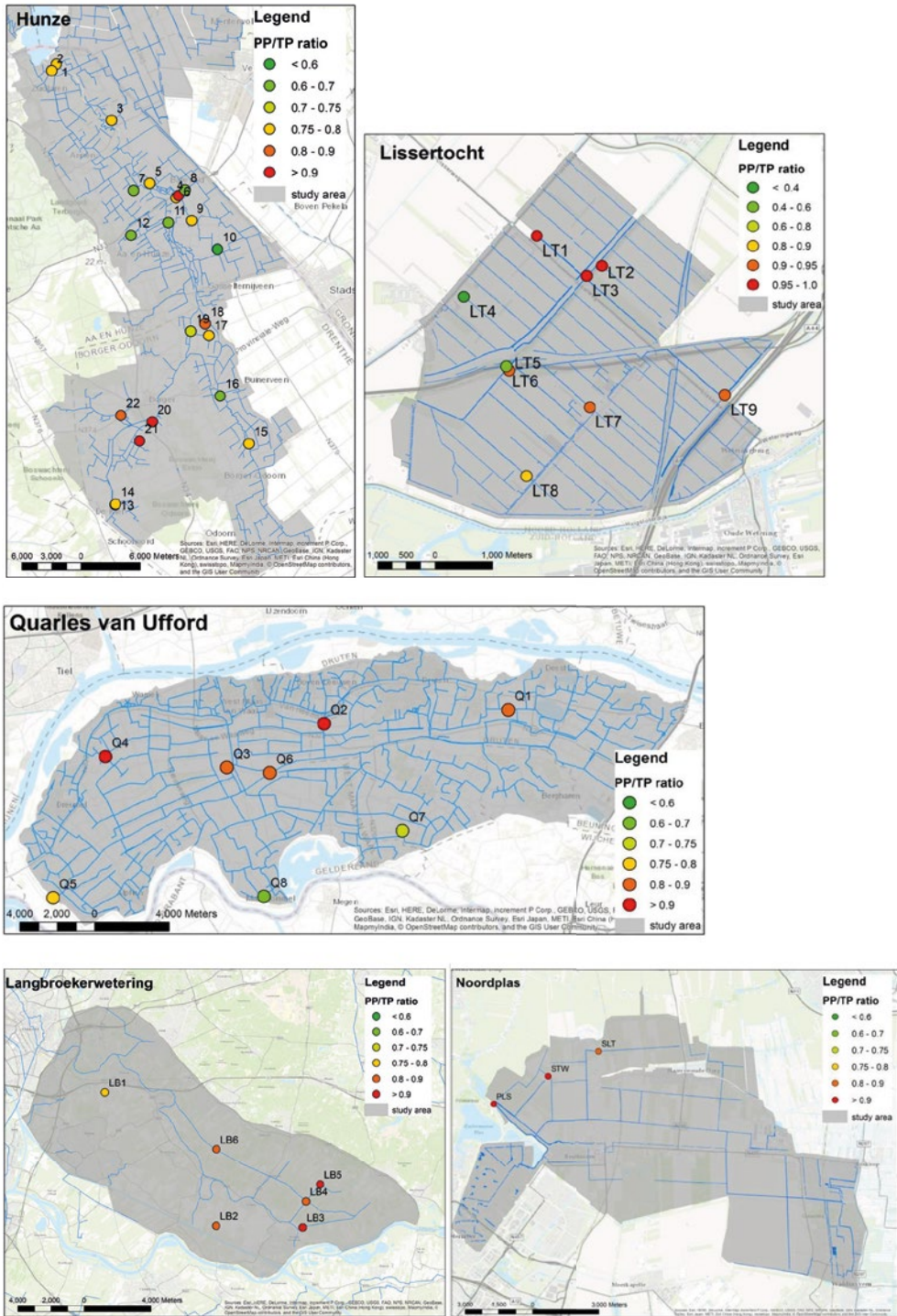


Figure S4.1. Sampling locations and PP/TP ratios in study areas.

### S.2 Photos of suspended sediment

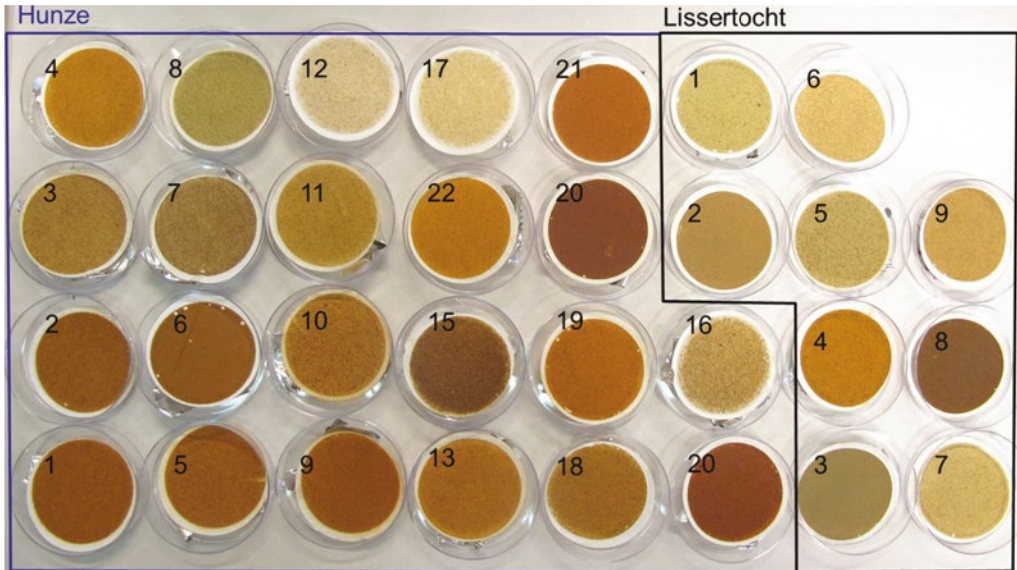


Figure S4.2. Filters with filtered suspended sediment sampled in the Hunze catchment and Lissertocht polder in March/April 2013.

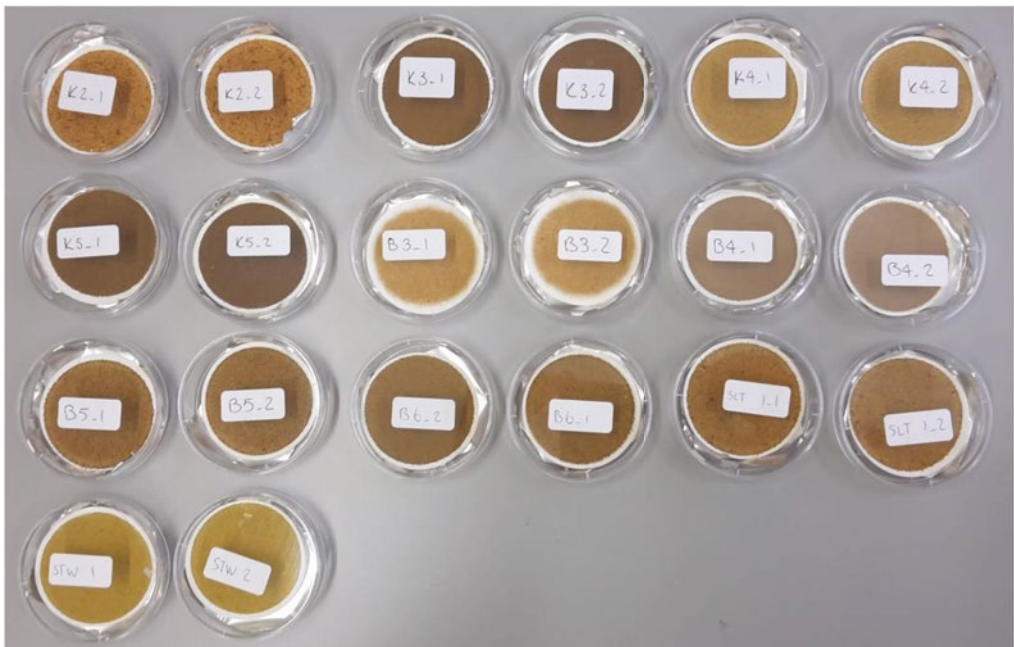


Figure S4.3. Filters with filtered suspended sediment sampled in the Quarles van Ufford polder and Langbroekerwetering in June 2016.

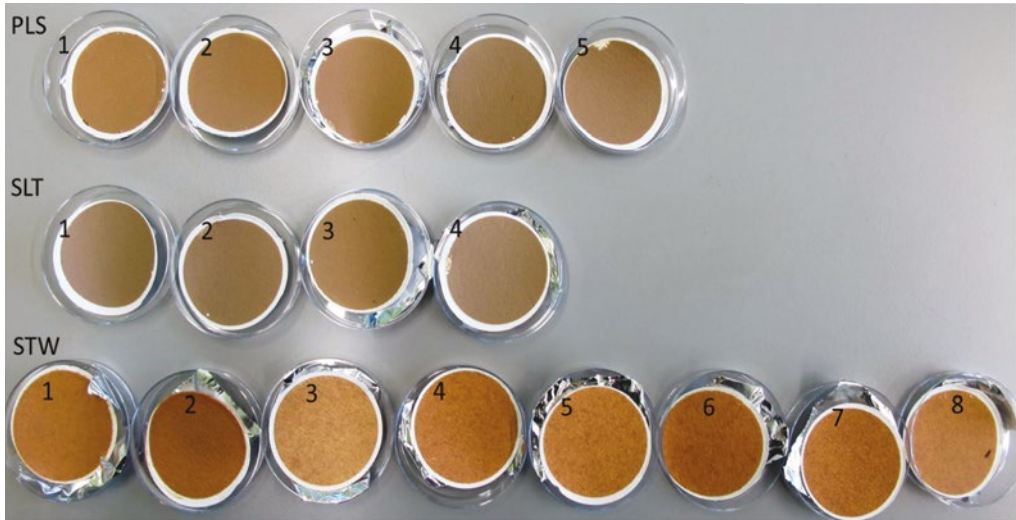
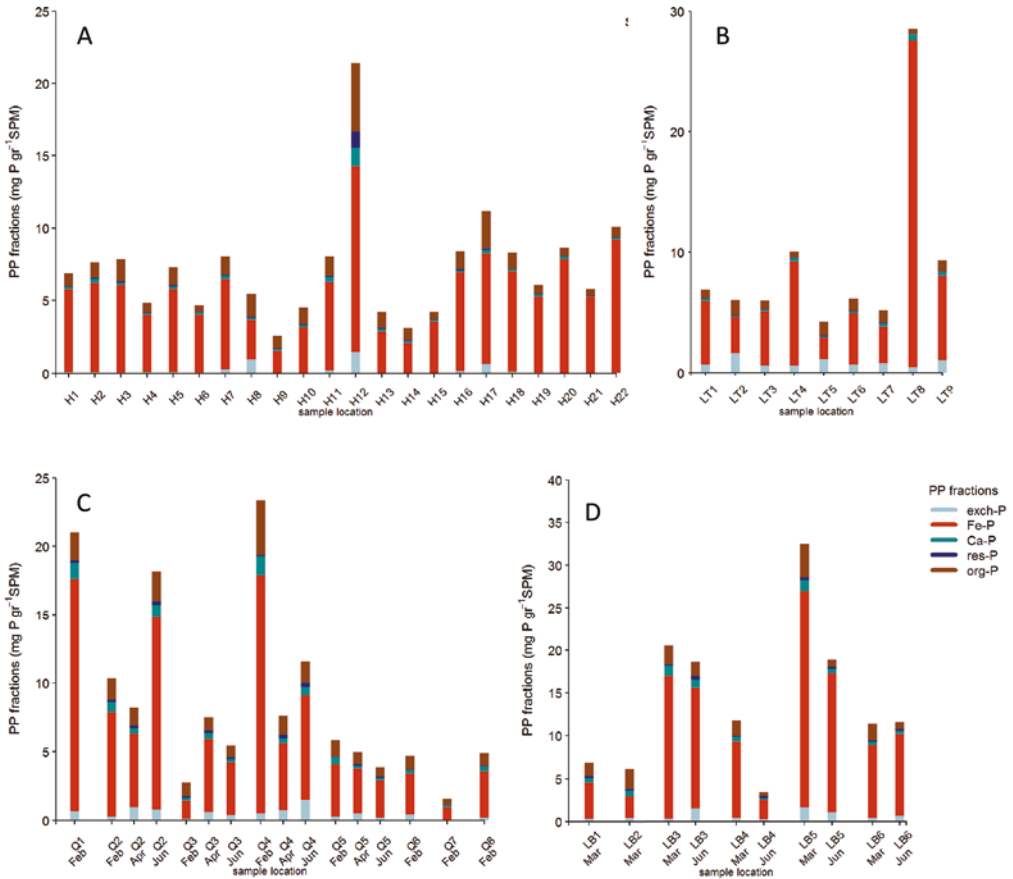


Figure S4.4. Filters with filtered suspended sediment sampled in the Noordplas polder in February/March 2014.

### S.3 Chemical speciation of particulate phosphorus



**Figure S4.5.** Chemical speciation of particulate P in suspended particulate matter samples from (A) Hunze catchment, (B) Lissertocht polder, (C) Quarles van Ufford and (D) Langbroekerwetering.

#### S.4 Particle size distribution during pumping in the Noordplaspolder

A few days before the start of the field experiment in the Noordplaspolder on 25 February 2014, the particle size distribution in the surface water at location PLS was measured in-situ at 10-minute intervals using a LISST-100 Particle Size Analyzer (Laser In-Situ Scattering and Transmissometry, Sequoia Scientific, Inc.) (Figure S4.6). The LISST-100 uses the principle of laser diffraction to obtain the size distribution and volume concentration of suspended particulate matter in 32 size classes logarithmically spaced between 1.25 and 250  $\mu\text{m}$  (Gartner et al., 2001).

The particle size distribution and volume concentration of the SPM at location PLS as measured with the LISST-100 device changed considerably upon pumping. The 375 m stretch between the pumping station and the monitoring location resulted in a lag time of approximately 20 min. Before pumping, the particle volume concentration was approximately  $100 \mu\text{L}^{-1}$  and was relatively uniformly distributed over the particle size range. The mean particle size was approximately  $90 \mu\text{m}$ . An increase of the particle concentration in size ranges larger than  $20 \mu\text{m}$  was measured during pumping. The total particle volume concentration increased to  $300 \mu\text{L}^{-1}$  and the mean particle size increased to  $150 \mu\text{m}$ . Within half an hour after pumping stopped, the particle volume concentration decreased again and the particle size distribution returned to a distribution similar to the pre-pumping situation. These results indicate that particle size distributions and volume concentration respond rapidly to changing flow conditions.

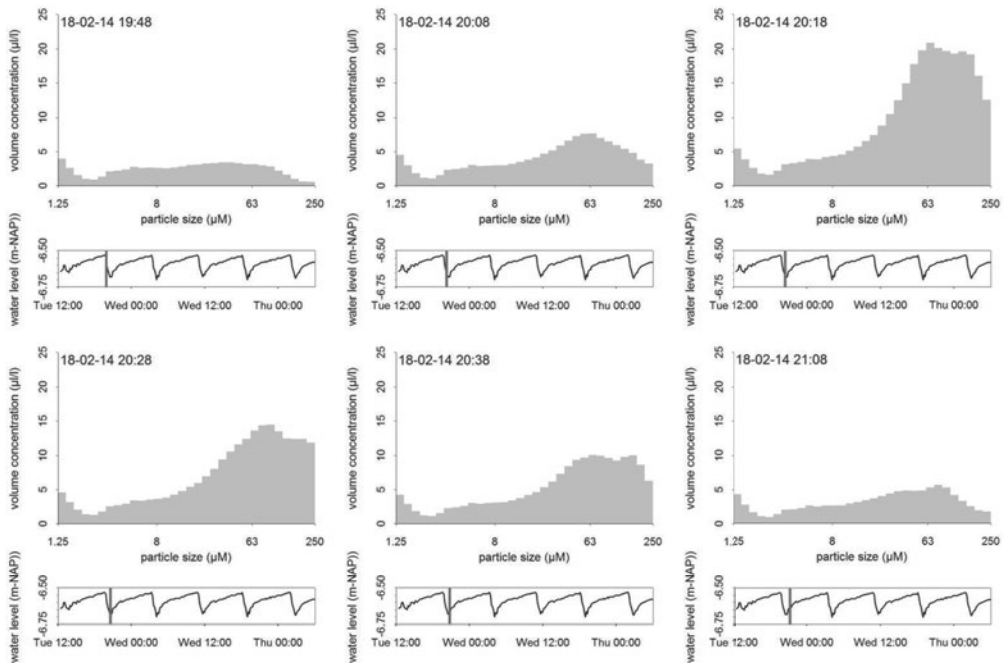


**Figure S4.6.** Evolution of the particle size distribution of the suspended sediment in the main channel of the Noordplaspolder (location PLS, located 375 m upstream of the pumping station) during a pumping event on 18 February 2014 measured with the LISST-100 Particle Size Analyzer. The water level is measured at the pumping station and clearly shows when pumping starts and ends. Particle size distribution of SS at during other pumping events showed similar patterns to the one shown here.

### S.5 Water quality data and sequential chemical extraction data

**Table S4.2.** Results from the field survey in the Hunze catchment, Lissertocht polder, Quarles van Ufford, Langbroekerwetering and Lage Vaart; suspended sediment, DRP, PP and TP concentration; SEDEX extraction and Aqua regia destruction.

area	location	date	water samples										SEDEX					Aqua regia		
			SS mg L <sup>-1</sup>	DRP mg L <sup>-1</sup>	PP mg L <sup>-1</sup>	TP mg L <sup>-1</sup>	Exch-P mg g <sup>-1</sup>	Fe-P mg g <sup>-1</sup>	Ca-P mg g <sup>-1</sup>	auth mg g <sup>-1</sup>	Detr-P mg g <sup>-1</sup>	Org-P mg g <sup>-1</sup>	PP ΣSEDEX mg g <sup>-1</sup>	fractions mg L <sup>-1</sup>	PP ΣSEDEX fractions mg L <sup>-1</sup>	PP ΣSEDEX regia mg g <sup>-1</sup>	PP ΣSEDEX regia mg g <sup>-1</sup>	Fe aqua regia mg g <sup>-1</sup>		
Hunze	H1	22/03/2013	11	0.4	0.03	0.09	0.12	0.07	5.70	0.18	0.03	0.91	6.9	0.07	0.07	6.6	193			
Hunze	H2	22/03/2013	12	0.7	0.03	0.11	0.15	0.07	6.16	0.27	0.07	1.08	7.6	0.09	0.09	7.9	174			
Hunze	H3	22/03/2013	14	1.0	0.04	0.11	0.14	0.06	6.01	0.18	0.07	1.53	7.8	0.07	0.07	7.9	76			
Hunze	H4	22/03/2013	12	1.0	0.03	0.09	0.11	0.08	4.00	0.08	0.04	0.62	4.8	0.07	0.07	6.3	188			
Hunze	H5	22/03/2013	17	0.7	0.03	0.11	0.14	0.07	5.71	0.18	0.06	1.26	7.3	0.10	0.10	6.0	171			
Hunze	H6	22/03/2013	71	11	0.00	0.49	0.49	0.05	4.00	0.14	0.02	0.44	4.7	0.33	0.33	4.4	238			
Hunze	H7	22/03/2013	8	0.8	0.06	0.12	0.19	0.27	6.19	0.25	0.06	1.26	8.0	0.10	0.10	7.7	55			
Hunze	H8	22/03/2013	9	1.3	0.03	0.04	0.07	0.96	2.73	0.13	0.06	1.57	5.4	0.06	0.06	6.5	27			
Hunze	H9	22/03/2013	21	2.0	0.03	0.10	0.13	0.02	1.55	0.12	0.04	0.86	2.6	0.03	0.03	3.6	173			
Hunze	H10	22/03/2013	20	1.3	0.06	0.07	0.13	0.01	3.19	0.15	0.03	1.11	4.5	0.08	0.08	4.1	201			
Hunze	H11	22/03/2013	8	0.7	0.04	0.09	0.13	0.20	6.08	0.33	0.06	1.36	8.0	0.07	0.07	8.0	135			
Hunze	H12	22/03/2013	6	1.1	0.08	0.13	0.21	1.48	12.78	1.28	1.11	4.73	21.4	0.14	0.14	24.5	51			
Hunze	H13	23/03/2013	7	0.6	0.03	0.06	0.09	0.03	2.88	0.17	0.06	1.11	4.2	0.04	0.04	4.8	291			
Hunze	H14	23/03/2013	15	2.4	0.02	0.06	0.07	0.01	2.11	0.14	0.03	0.86	3.1	0.04	0.04	2.5	168			
Hunze	H15	23/03/2013	16	1.5	0.02	0.07	0.09	0.03	3.55	0.14	0.03	0.50	4.3	0.07	0.07	4.1	93			
Hunze	H16	23/03/2013	4	0.1	0.02	0.05	0.07	0.15	6.81	0.11	0.09	1.23	8.4	0.04	0.04	8.4	118			
Hunze	H17	23/03/2013	3	0.1	0.02	0.07	0.09	0.63	7.60	0.27	0.08	2.59	11.2	0.05	0.05	11.8	104			
Hunze	H18	23/03/2013	9	0.3	0.02	0.07	0.09	0.11	6.88	0.17	0.04	1.10	8.3	0.08	0.08	7.2	150			

Table S4.2. (Continued)

area	location	date	water samples										SEDEX					Aqua regia	
			SS mg L <sup>-1</sup>	std SS mg L <sup>-1</sup>	DRP mg L <sup>-1</sup>	PP mg L <sup>-1</sup>	TP mg L <sup>-1</sup>	Exch-P mg g <sup>-1</sup>	Fe-P mg g <sup>-1</sup>	auth Ca-P mg g <sup>-1</sup>	Detr-P mg g <sup>-1</sup>	Org-P mg g <sup>-1</sup>	PP fractions mg g <sup>-1</sup>	PP fractions mg L <sup>-1</sup>	PP fractions mg L <sup>-1</sup>	PP aqua regia mg g <sup>-1</sup>	Fe aqua regia mg g <sup>-1</sup>		
Hunze	H19	23/03/2013	10	1.1	0.03	0.09	0.12	0.04	5.19	0.15	0.04	0.65	6.1	0.06	6.8	276			
Hunze	H20	23/03/2013	23	3.1	0.02	0.18	0.20	0.02	7.84	0.17	0.03	0.56	8.6	0.20	6.5	232			
Hunze	H21	23/03/2013	20	4.3	0.01	0.10	0.10	0.01	5.24	0.06	0.03	0.46	5.8	0.14	4.9	210			
Hunze	H22	23/03/2013	11	0.4	0.01	0.10	0.11	0.04	9.15	0.12	0.04	0.74	10.1	0.10	11.6	229			
Lissertocht	LT1	06/04/2013	38	1.7	0.01	0.32	0.34	0.69	5.24	0.19	0.03	0.74	6.9	0.17	6.8	68			
Lissertocht	L 2	06/04/2013	23	1.3	0.02	0.51	0.53	1.61	3.01	0.13	0.03	1.27	6.1	0.13	6.8	24			
Lissertocht	LT3	06/04/2013	59	4.4	0.01	0.45	0.47	0.59	4.49	0.18	0.03	0.72	6.0	0.21	6.0	58			
Lissertocht	LT4	06/04/2013	260	87	2.47	0.51	2.98	0.60	8.64	0.31	0.03	0.47	10.0	2.61	11.6	59			
Lissertocht	LT5	06/04/2013	55	7.3	0.03	0.49	0.52	1.12	1.81	0.11	0.03	1.19	4.2	0.14	5.1	19			
Lissertocht	LT6	06/04/2013	8	0.4	0.04	0.03	0.06	0.67	4.27	0.15	0.05	1.01	6.2	0.11	6.1	64			
Lissertocht	LT7	06/04/2013	24	3.8	0.02	0.21	0.22	0.80	3.05	0.25	0.06	1.04	5.2	0.08	4.0	46			
Lissertocht	LT8	06/04/2013	68	13.9	0.30	1.19	1.49	0.46	27.13	0.52	-0.01	0.45	28.5	1.20	22.7	108			
Lissertocht	LT9	06/04/2013	34	4.8	0.03	0.39	0.42	1.05	6.98	0.32	0.04	0.94	9.3	0.20	9.0	72			
Quarles van Ufford	Q1	24/02/2016	7	0.4	0.03	0.16	0.19	0.70	16.91	1.20	0.17	2.01	20.99	0.14	16.0	301			
Quarles van Ufford	Q2	24/02/2016	25	5.0	0.02	0.20	0.22	0.27	7.60	0.74	0.19	1.51	10.30	0.26	11.6	67			
Quarles van Ufford	Q2	25/04/2016	5	0.9				0.96	5.33	0.39	0.24	1.27	8.18	0.04	8.5	79			
Quarles van Ufford	Q2	06/06/2016	6	1.6	0.04	0.10	0.14	0.78	14.06	0.87	0.26	2.17	18.15	0.11	12.5	172			
Quarles van Ufford	DQ2	24/02/2016	94	6.8	0.03	0.19	0.22	0.08	0.62	0.22	0.08	0.88	1.88	0.18	1.8	67			
Quarles van Ufford	Q3	24/02/2016	70	9.6	0.04	0.19	0.23	0.11	1.33	0.24	0.10	1.00	2.79	0.19	2.7	77			
Quarles van Ufford	Q3	25/04/2016	5	1.0				0.63	5.28	0.41	0.19	0.97	7.47	0.04	6.5	104			
Quarles van Ufford	Q3	06/06/2016	13	2.0	0.01	0.14	0.15	0.39	3.86	0.22	0.12	0.85	5.44	0.07	5.7	151			
Quarles van Ufford	DQ3	24/02/2016	69	8.8	0.01	0.22	0.23	0.14	1.35	0.21	0.17	1.25	3.12	0.21	2.5	72			
Quarles van Ufford	Q4	24/02/2016	4	1.7	0.01	0.13	0.14	0.53	17.34	1.39	0.07	4.02	23.36	0.10	22.9	338			

Table S4.2. (Continued)

area	location	date	water samples					SEDEX					Aqua regia				
			SS mg L <sup>-1</sup>	std SS mg L <sup>-1</sup>	DRP mg L <sup>-1</sup>	PP mg L <sup>-1</sup>	TP mg L <sup>-1</sup>	Exch-P mg g <sup>-1</sup>	Fe-P mg g <sup>-1</sup>	auth Ca-P mg g <sup>-1</sup>	Detr-P mg g <sup>-1</sup>	Org-P mg g <sup>-1</sup>	PP ΣSEDEX fractions mg g <sup>-1</sup>	PP ΣSEDEX fractions mg L <sup>-1</sup>	PP aqua regia mg g <sup>-1</sup>	Fe aqua regia mg g <sup>-1</sup>	
Quarles van Ufford	Q4	25/04/2016	4	1.0					0.76	4.85	0.36	0.23	1.41	7.60	0.03	8.4	111
Quarles van Ufford	Q4	06/06/2016	4	1.2	0.02	0.08	0.11	1.51	7.60	0.62	0.26	1.58	11.56	0.04	15.6	183	
Quarles van Ufford	DQ4	24/02/2016	8	1.8	0.03	0.10	0.13	0.31	15.61	3.86	0.02	1.78	21.58	0.18	20.1	285	
Quarles van Ufford	Q5	24/02/2016	47	3.6	0.04	0.22	0.27	0.29	3.85	0.44	0.05	1.20	5.82	0.27	5.3	86	
Quarles van Ufford	Q5	25/04/2016	18	0.4				0.51	3.30	0.18	0.14	0.81	4.95	0.09	4.9	77	
Quarles van Ufford	Q5	06/06/2016	22	2.7	0.01	0.15	0.16	0.22	2.69	0.21	0.10	0.67	3.89	0.09	5.2	80	
Quarles van Ufford	Q6	24/02/2016	26	3.9	0.01	0.13	0.14	0.42	3.02	0.26	0.01	0.97	4.68	0.12	4.2	59	
Quarles van Ufford	Q7	24/02/2016	76	8.1	0.03	0.08	0.11	0.03	0.92	0.17	0.03	0.40	1.56	0.12	1.2	57	
Quarles van Ufford	Q8	24/02/2016	22	2.0	0.01	0.14	0.15	0.20	3.40	0.37	0.02	0.87	4.86	0.10	4.1	79	
Langbroekerwetering	LB1	10/03/2016	33	1.8	0.05	0.17	0.21	0.34	4.25	0.55	0.20	1.59	6.93	0.23	5.7	89	
Langbroekerwetering	LB2	10/03/2016	8	1.4	0.01	0.10	0.11	0.46	2.54	0.65	0.22	2.32	6.18	0.05	5.8	122	
Langbroekerwetering	LB3	10/03/2016	7	2.3	0.01	0.18	0.19	0.33	16.68	1.25	0.07	2.25	20.58	0.14	17.8	261	
Langbroekerwetering	LB3	06/06/2016	2	0.1	0.02	0.10	0.12	1.55	14.08	1.00	0.39	1.69	18.72	0.04	18.3	143	
Langbroekerwetering	LB4	10/03/2016	11	3.0	0.04	0.16	0.20	0.44	8.92	0.57	0.09	1.80	11.81	0.13	9.0	109	
Langbroekerwetering	LB4	06/06/2016	21	1.9	0.02	0.14	0.16	0.29	2.28	0.18	0.24	0.44	3.43	0.07	3.7	57	
Langbroekerwetering	LB5	10/03/2016	3	0.0	0.01	0.15	0.16	1.68	25.23	1.27	0.35	3.94	32.47	0.09	30.0	189	
Langbroekerwetering	LB5	06/06/2016	8	1.1	0.06	0.22	0.28	1.10	16.27	0.49	0.20	0.86	18.93	0.15	18.1	91	
Langbroekerwetering	LB6	10/03/2016	10	1.6	0.03	0.14	0.17	0.42	8.53	0.42	0.10	1.96	11.44	0.12	10.1	111	
Langbroekerwetering	LB6	06/06/2016	9	0.8	0.01	0.20	0.21	0.71	9.52	0.40	0.21	0.83	11.67	0.10	11.2	81	
Lage Vaart	LV1	15/01/2015	27	2.1	0.03	0.06	0.09	0.13	2.32	0.27	0.03	0.68	3.43	0.09	3.5	58	
Lage Vaart	LV2	31/01/2015	13	1.2	0.02	0.05	0.08	0.37	2.62	0.38	0.12	1.12	4.62	0.06	3.5	58	
Lage Vaart	LV3	20/02/2015	23	2.1	0.02	0.15	0.17	0.91	1.78	0.24	0.09	1.73	4.75	0.11	3.2	50	



Table S4.2. (Continued)

area	location	date	water samples										SEDEX					Aqua regia	
			SS mg L <sup>-1</sup>	std SS mg L <sup>-1</sup>	DRP mg L <sup>-1</sup>	PP mg L <sup>-1</sup>	TP mg L <sup>-1</sup>	Exch-P mg g <sup>-1</sup>	Fe-P mg g <sup>-1</sup>	auth Ca-P mg g <sup>-1</sup>	Detr-P mg g <sup>-1</sup>	Org-P mg g <sup>-1</sup>	PP SEDEX fractions mg g <sup>-1</sup>	PP SEDEX fractions mg L <sup>-1</sup>	PP SEDEX fractions mg g <sup>-1</sup>	PP aqua regia mg g <sup>-1</sup>	Fe aqua regia mg g <sup>-1</sup>		
Lage Vaart	LV4	12/03/2015	19	1.7	0.06	0.14	0.19	0.67	2.76	0.28	0.10	1.27	5.07	0.10	4.9	35			
Lage Vaart	LV5	08/04/2015	14	1.0	0.05	0.14	0.20	1.76	4.51	0.48	0.11	2.35	9.21	0.12	-	-			
Lage Vaart	LV6	28/04/2015	33	2.2	0.01	0.21	0.22	1.12	2.37	0.26	0.11	1.74	5.60	0.19	-	-			
Lage Vaart	LV7	15/06/2015	16	1.2	0.11	0.20	0.31	1.32	3.64	0.28	0.11	1.85	7.22	0.12	-	-			
Lage Vaart	LV8	07/08/2015	17	0.9	0.28	0.18	0.46	1.61	4.08	0.33	0.07	1.90	7.99	0.13	-	-			
Lage Vaart	LV9	24/08/2015	37	2.8	0.06	0.27	0.33	1.96	4.22	0.20	0.05	0.91	7.34	0.27	-	-			

Table S4.3. Results from the field experiments in Noordplas polder; suspended sediment, DRP, PP and TP concentration; SEDEX extraction and Aqua regia destruction.

sample	Water samples										SEDEX					Aqua Regia	
	SS mg.L <sup>-1</sup>	std SS mg.L <sup>-1</sup>	DRP mg.L <sup>-1</sup>	PP mg.L <sup>-1</sup>	TP mg.L <sup>-1</sup>	Cl mg.L <sup>-1</sup>	SO4 mg.L <sup>-1</sup>	Ca mg.L <sup>-1</sup>	Exch-P mg.gr <sup>-1</sup>	Fe-P mg.gr <sup>-1</sup>	auth Ca-P mg.gr <sup>-1</sup>	Detr-P mg.gr <sup>-1</sup>	Org-P mg.gr <sup>-1</sup>	PP SEDEX fractions mg.gr <sup>-1</sup>	PP SEDEX fractions mg.L <sup>-1</sup>	PP aqua regia mg.gr <sup>-1</sup>	Fe aqua regia mg.gr <sup>-1</sup>
pls1	29	0.73	0.02	0.22	0.24	341	193	219	0.25	7.40	0.29	0.11	1.12	9.2	0.27	8.0	92
pls2	32	2.6	0.02	0.25	0.27	347	199	220	0.18	6.90	0.58	0.14	1.07	8.9	0.29	8.2	92
pls3	35	0.79	0.01	0.46	0.48	377	193	223	0.24	7.65	0.28	0.16	1.09	9.4	0.33	8.5	98
pls4	57	4.6	0.02	0.49	0.50	306	205	222	0.19	7.15	0.51	0.17	1.02	9.1	0.52	7.2	82
pls5	41	2.2	0.01	0.29	0.31	315	208	225	0.20	6.88	0.56	0.10	1.05	8.8	0.36	8.0	91
slt1	49	0.4	0.04	0.38	0.42	252	202	214	0.29	7.09	0.54	0.11	1.00	9.0	0.44	7.9	69
slt3	37	4.9	0.06	0.28	0.34	238	196	206	0.28	7.54	0.64	0.15	0.95	9.6	0.35	8.1	73
slt5	29	4.1	0.06	0.30	0.36	280	195	217	0.41	8.42	0.40	0.14	0.85	10.2	0.29	11.8	102
slt7	33	4.1	0.06	0.24	0.30	280	195	217	0.37	8.17	0.34	0.14	0.94	10.0	0.32	8.3	76
stw1	55	11.4	0.02	0.56	0.58	462	289	257	0.46	7.88	0.57	0.10	2.19	11.2	0.67	12.6	68
stw2	46	3.4	0.02	0.59	0.61	508	286	261	0.51	8.67	0.44	0.13	1.92	11.7	0.53	12.6	73

Table S4.3. (Continued)

sample	Water samples											SEDEX				Aqua Regia		
	SS mg.L <sup>-1</sup>	stdSS mg.L <sup>-1</sup>	DRP mg.L <sup>-1</sup>	PP mg.L <sup>-1</sup>	TP mg.L <sup>-1</sup>	Cl mg.L <sup>-1</sup>	SO4 mg.L <sup>-1</sup>	Ca mg.L <sup>-1</sup>	Exch-P mg.gr <sup>-1</sup>	Fe-P mg.gr <sup>-1</sup>	auth Ca-P mg.gr <sup>-1</sup>	Detr-P mg.gr <sup>-1</sup>	Org-P mg.gr <sup>-1</sup>	PP fractions mg.gr <sup>-1</sup>	PP fractions mg.L <sup>-1</sup>	SEDEX fractions mg.gr <sup>-1</sup>	PP aqua regia mg.gr <sup>-1</sup>	Fe aqua regia mg.gr <sup>-1</sup>
stw3	41	4.3	0.02	0.44	0.42	334	300	248	0.47	7.59	0.26	0.12	2.04	10.4	0.42	0.42	13.1	70
stw4	31	1.9	0.03	0.40	0.42	288	339	263	0.58	8.90	0.20	0.15	3.84	13.7	0.42	0.42	13.2	75
stw5	22	1.7	0.02	0.32	0.30	188	385	265	0.88	9.54	0.01	0.18	1.57	12.2	0.27	0.27	13.1	105
stw6	22	2.9	0.03	0.24	0.24	178	382	260	1.24	9.92	0.04	0.18	1.58	13.0	0.28	0.28	14.2	104
stw7	19	1.9	0.02	0.30	0.27	179	358	257	0.99	10.46	0.02	0.16	1.70	13.3	0.26	0.26	15.0	102
stw8	19	3.9	0.02	0.30	0.27	192	366	258	1.22	10.85	0.08	0.17	1.78	14.1	0.27	0.27	-	-
pls1_c	26	-	-	-	-	-	-	-	0.12	7.37	0.21	0.09	0.78	8.6	-	-	-	-
pls2_c	32	-	-	-	-	-	-	-	0.16	6.18	0.04	0.09	0.60	7.1	-	-	-	-
pls3_c	39	-	-	-	-	-	-	-	0.06	7.01	0.11	0.10	0.73	8.0	-	-	-	-
pls4_c	55	-	-	-	-	-	-	-	0.20	5.93	0.18	0.11	0.61	7.0	-	-	-	-
slt1_c	28	-	-	-	-	-	-	-	0.09	8.36	0.16	0.09	0.52	9.2	-	-	-	-
slt3_c	31	-	-	-	-	-	-	-	0.09	8.13	0.27	0.10	0.50	9.1	-	-	-	-
slt5_c	22	-	-	-	-	-	-	-	0.16	8.31	0.33	0.10	0.49	9.4	-	-	-	-
slt7_c	24	-	-	-	-	-	-	-	0.18	8.06	0.25	0.11	0.52	9.1	-	-	-	-
stw1_c	33	-	-	-	-	-	-	-	0.24	9.99	0.08	0.04	2.03	12.4	-	-	-	-
stw2_c	25	-	-	-	-	-	-	-	0.19	9.08	0.11	0.04	1.37	10.8	-	-	-	-
stw3_c	19	-	-	-	-	-	-	-	0.23	10.96	0.11	0.02	1.83	13.2	-	-	-	-
stw4_c	17	-	-	-	-	-	-	-	0.17	9.08	0.38	0.10	1.56	11.3	-	-	-	-
stw5_c	15	-	-	-	-	-	-	-	0.08	10.36	0.13	0.03	1.07	11.7	-	-	-	-
stw7_c	24	-	-	-	-	-	-	-	0.19	5.25	0.06	0.04	0.65	6.2	-	-	-	-
stw8_c	21	-	-	-	-	-	-	-	0.19	10.63	0.16	0.03	1.27	12.3	-	-	-	-

# CHAPTER 5

## **High-frequency monitoring reveals nutrient sources and transport processes in an agriculture-dominated lowland water system**

Bas van der Grift, Hans Peter Broers, Wilbert Berendrecht,  
Joachim. Rozemeijer, Leonard Osté and Jasper Griffioen

*Hydrology and Earth System Sciences 20, 1851-1868*

## 5.1 Abstract

Many agriculture-dominated lowland water systems worldwide suffer from eutrophication caused by high nutrient loads. Insight in the hydrochemical functioning of embanked polder catchments is highly relevant for improving the water quality in such areas or for reducing export loads to downstream water bodies. This paper introduces new insights in nutrient sources and transport processes in a polder in the Netherlands situated below sea level using high-frequency monitoring technology at the outlet, where the water is pumped into a higher situated lake, combined with a low-frequency water quality monitoring programme at six locations within the drainage area. Seasonal trends and short-scale temporal dynamics in concentrations indicated that the  $\text{NO}_3$  concentration at the pumping station originated from N loss from agricultural lands. The  $\text{NO}_3$  loads appear as losses via tube drains after intensive rainfall events during the winter months due to preferential flow through the cracked clay soil. Transfer function-noise modelling of hourly  $\text{NO}_3$  concentrations reveals that a large part of the dynamics in  $\text{NO}_3$  concentrations during the winter months can be related to rainfall. The total phosphorus (TP) concentration and turbidity almost doubled during operation of the pumping station which points to resuspension of particulate P from channel bed sediments induced by changes in water flow due to pumping. Rainfall events that caused peaks in  $\text{NO}_3$  concentrations did not result in TP concentration peaks. The rainfall induced and  $\text{NO}_3$  enriched quick interflow, may also be enriched in TP but retention of TP due to sedimentation of particulate P then results in the absence of rainfall induced TP concentration peaks. Increased TP concentrations associated with run-off events is only observed during a rainfall event at the end of a freeze-thaw cycle. All these observations suggest that the P retention potential of polder water systems is primarily due to the artificial pumping regime that buffers high flows. As the TP concentration is affected by operation of the pumping station, timing of sampling relative to the operating hours of the pumping station should be accounted for when calculating P export loads, determining trends in water quality or when judging water quality status of polder water systems.

### Keywords

Nitrate, Phosphorus, Nutrient retention, High-frequency monitoring, Time series analysis, Lowland water system, Polder, Nutrient dynamics.

## 5.2 Introduction

Many surface water bodies suffer from eutrophication caused by high nutrient loads. Eutrophication of surface waters can lead to turbid waters with decreased oxygen levels (hypoxia), toxin production by algae and bacteria, and fish kills (Bouwman et al., 2013a). Policy makers of national governments, the European Union and other authorities aim to improve water quality in surface water bodies that receive nutrient load from agriculture or other sources like sewage effluent (EC, 2000). A sound assessment of pressures and impacts on the aquatic ecosystem and a reliable assessment of water status in catchments is, therefore, a topic of major importance. If the assessment of pressures is flawed, the action plans will be ill founded and there is a risk that EU member states will not carry out their work where it is most needed and in a cost-effective way (EC, 2015). This holds strongly for the Netherlands where nutrient surpluses and leaching are higher than elsewhere in Europe (van Grinsven et al., 2012) and the world (Bouwman et al., 2013b), due to a highly concentrated and productive agricultural sector.

For the evaluation of action programmes and pilot studies, water authorities invest heavily in the monitoring of  $\text{NO}_3$  and P concentrations in surface water. Regional surface water quality networks in EU member states are commonly sampled 12 times a year (Fraters et al., 2005). However, the interpretation of grab sample data in terms of loads and fluxes is often problematic from such monitoring networks (Rozemeijer et al., 2010). Grab sample frequencies are generally not sufficient to capture the dynamical behaviour of surface water quality and hydrological functioning of the catchment (Johnes, 2007; Kirchner et al., 2004). It is increasingly recognised that incidental losses and peak flows play an important role in the nutrient loads of surface water systems in the Netherlands (Regelink et al., 2013; Van der Salm et al., 2012) and elsewhere (Withers et al., 2003). Such incidental losses are considered to be related to peak flows after heavy rain storms and due to overland flow or quick interflow via drains and cracked clay soils and related leaching of manure and erosion of soil particles (Kaufmann et al., 2014). Some authors observed a lowering of  $\text{NO}_3$  concentrations shortly after peak flow (e.g. Poor and McDonnell, 2007; Shrestha et al., 2013) caused by dilution with  $\text{NO}_3$ -poor precipitation water. Others detected concentration peaks in response events (e.g. Rozemeijer and Broers, 2007; Tiemeyer et al., 2008). Therefore, the  $\text{NO}_3$  response to rainfall events depends on the hydrochemical properties of the catchment (Rozemeijer et al., 2010). In addition, the capacity of surface water bodies to retain nutrients is spatially and temporally variable (e.g. Cirmo and McDonnell, 1997; Withers and Jarvie, 2008).

As a consequence of the dynamic behaviour of nutrient transfer from land to surface water and in-stream processes that impact nutrient retention combined with increasing demands for sound assessments of the water system, there is an increasing interest in continuous or semi-continuous monitoring of water quality at catchment outlets during the last decade (e.g. Bieroza et al., 2014; Bowes et al., 2015; Cassidy and Jordan, 2011; Jordan et al., 2007; Kirchner et al., 2004; Palmer-Felgate et al., 2008; Rozemeijer et al., 2010; Skeffington et al., 2015; Wade et al., 2012). These studies showed catchment-dependent non-stationary behaviour of the concentration-discharge relationships. High-frequency monitoring has proven to be a powerful tool to improve estimations of annual export loads (e.g. Cassidy and Jordan, 2011; Rozemeijer et al., 2010), nutrients sources (Bowes et

al., 2015) and the hydrochemical functioning of a catchment (e.g. Bieroza et al., 2014; Halliday et al., 2012; Wade et al., 2012). High-frequency nutrient monitoring has revealed the presence of diurnal nutrient cycles in rivers and streams caused by biological processes or by P and N inputs from sewage treatment works (e.g. Bowes et al., 2015; Halliday et al., 2012; Neal et al., 2012). Large changes in concentrations or fluxes of materials over relatively short time periods are increasingly recognised as important pathways of nutrient delivery to surface water bodies (Kaushal et al., 2014). In the Netherlands, there is a still debate about the risk of incidental losses associated with manure application (Akkermans and Hermans, 2014). The Netherlands adopted the European Nitrate Directive in 1991 (EC, 1991b), which regulates the use of nitrogen in agriculture through national action plans. Among other measures, the regulation includes the period of manure application. To reduce the risk of nutrient leaching to groundwater and surface water, manure application on arable land is allowed from 1 February to 1 August and on grassland from 15 February to 31 August (LNV, 2009). The potential risk for incidental nutrient losses after manure application in February and March (before the start of the growing season) is not known. High-frequency monitoring is a powerful tool to detect such incidental losses.

In many low-lying areas worldwide, water levels are managed by inlet of diverted river water in dry periods and discharge via pumping stations in wet periods. Such an embanked land with a human controlled water regime is called a 'polder'. In the Netherlands, these regulated polder catchments cover 60% of the land surface (Van de Ven, 2004). The dense network of subsurface drains, ditches, weirs, channels, pumping stations and the dynamic mixing of water from different sources (see page, precipitation and water inlet) results in a relatively complex hydrology. Many studies on nutrient dynamics in natural catchments showed a relation between nutrient concentrations and discharge, and this significantly improved the insight in the nutrient sources and pathways in the catchment. The water flow in polders is, however, not a function of free discharge but is controlled by pumping stations. The maximum discharge is controlled by the capacity of the pumping stations. Due to the presence of a dense surface water system, the water storage capacity and the residence time of the surface water in a polder is also higher when compared to natural, free drainage catchments which may impact biogeochemical or hydrological in-stream processes controlling nutrient retention. Insight in the hydrochemical functioning of polder catchments is highly relevant for improving the water quality in the Netherlands.

To our knowledge, high-frequency monitoring of surface water quality has not been applied for polder catchments up to now. Discharge-concentration relationships and short-scale variation in water quality in polder catchments are still unclear while nutrient sources and pathways are poorly understood (Rozemeijer et al., 2014). High-frequency measurements reveal the short-term variability in solute concentrations which may give valuable insight into the contribution of different sources or different flow routes to the surface water pollution in polders.

The general aim of this study is to increase our understanding of the hydrochemical function of an agriculture-dominated water system in a clay polder by analysis of high-frequency monitoring of nutrient concentrations at the polder outlet combined with low-frequency surface water quality data and groundwater quality data from different locations within the polder. The specific objectives of this study are: (1) to increase insight in dynamics of nutrient concentrations and nutrient sources

in polder areas (2) to characterise the importance of incidental losses caused by intensive rainfall events whether or not in combination with recent manure application and (3) to assess potential effects of the operational management of the pumping station on the water quality.

## 5.3 Material and Methods

### 5.3.1 Study area

A continuous monitoring station was established in the Lage Vaart main channel nearby the pumping station Blocq van Kuffeler (A in Figure 5.1). This is one of the three pumping stations that control the water level in Lage Afdeling pumped drainage area located within the Flevoland polder, the most recent and at the same time biggest land reclamation project in The Netherlands (Groen, 1997). The Flevoland polder consists of two pumped drainage areas, which are each drained by a main channel. The Lage Afdeling drainage area drains into the Lage Vaart main channel (Figure 5.1). The size of the Lage Afdeling drainage area is 576 km<sup>2</sup>, with altitude ranging between 3 and 5 m below mean sea level. The Lage Afdeling drainage area is mainly rural. The land cover is dominated by agriculture (76%), followed by woodlands and moors (18%) and urban or semi-urban areas (6%).

The geohydrology of the Flevoland polder area is generally described by a confining layer of Holocene marine sediments, with a thickness of less than 0.5 m in the northeast to over 7 m southwest, overlying a sandy aquifer deposited in the Pleistocene age. The soils consist for 50% of clay soils, for 39% of silty clay loam and for 11% of sandy soils (Van den Eertwegh, 2002). A typical characteristic of the soils in Flevoland is that the clay layer contains permanent and interconnected cracks due to physical and chemical ripening of the soil after reclamation. The shrinkage cracks disappeared in the plough layer by tillage activities, but are permanently present in the subsoil down to about 1.0–1.5 m below the soil surface (Groen, 1997; Van den Eertwegh, 2002). From a depth of 1.2 to 1.5 m below the soil surface, clay deposits, if present, are permanently water saturated and thus not ripened, resulting in a low-permeable soil layer. Due to altitudes below mean sea level and below the water level of the surrounding lakes, there is upward groundwater seepage at most locations within the Lage Afdeling drainage area.

The Lage Vaart main channel is connected via a series of secondary channels to a dense network of field ditches and tube drains. Tube drains are generally installed at 0.95 m depth. The horizontal spacing varies between less than 12 to 48 m, mainly dependent on the soil hydraulic conductivity and groundwater seepage rate. The field ditches receive outflow from the tube drain, direct drainage from subsurface flow, regional groundwater seepage and any surface run-off from the connected field area. They drain freely into the secondary channels. The water level in the Lage Afdeling is regulated by 97 weirs and three pumping stations that pump the excess water to the higher situated Markermeer and Ketelmeer. The total pumping capacity is 11–12 mm d<sup>-1</sup>. The Lage Vaart main channel has a controlled constant water level of 6.2 m below mean sea level. The pumping station Blocq van Kuffeler has four electrically powered pumps. Two pumps with a capacity of 750 m<sup>3</sup> min<sup>-1</sup> each drain the Lage Afdeling. Operation of the pumping stations with one pump causes a flow velocity in the main channel of approximately 0.125 m sec<sup>-1</sup> and with both pumps

the flow velocity is approximately  $0.25 \text{ m sec}^{-1}$ . Up to 2008, the pumping station Blocq van Kuffeler was powered with diesel engines. These diesel engines were replaced with electric engines during the renovation of the pumping station in the autumn of 2008 and this conversion was finished in the beginning of 2009. Since this renovation, the operational management of the pumping station is automatically controlled by a series of water level pressure sensors in the area. The pumps run predominantly during evening or night hours because of cheaper power supply during these hours. The discharge generated by the pumping stations is measured continuously. The Blocq van Kuffeler pumping station drains the south-western part of the Lage Afdeling drainage area. The flow direction of the water in the channels that are drained by pumping station Blocq van Kuffeler is illustrated by arrows in Figure 5.1. Pumping station B is an emergency pumping station and only operates during extremely wet conditions. Although there is no physical boundary between the area drained by Blocq van Kuffeler and pumping station C, location 5 can be considered as the most upstream location in the Lage Vaart that is drained by the Blocq van Kuffeler pumping station under normal meteorological conditions. There is a Wastewater Treatment Plant (WWTP) in the area that discharges its effluent to the Lage Vaart (Figure 5.1). The average effluent discharge is  $0.35 \text{ m}^3 \text{ min}^{-1}$ . The total phosphorus (TP) and  $\text{NO}_3$  concentration in the effluent water is measured weakly. The average TP concentration is  $0.5 \text{ mg L}^{-1}$  and the average  $\text{NO}_3$  concentration is  $1.5 \text{ mg N L}^{-1}$ . The TP load to the Lage Vaart in the period October 2014–October 2015 equals approximately 5,400 kg and the  $\text{NO}_3$  load 16,400 kg N. There are no other sources of sewage discharge to the surface water within the Lage Afdeling drainage area.

### 5.3.2 Low-frequency monitoring

Grab samples were collected every 2 or 4 weeks from January 2014 to October 2015 from the polder outlet and five other monitoring locations within the part of the Lage Afdeling drainage area that is drained by the Blocq van Kuffeler pumping station (Figure 5.1). Four locations are representative for different types of land use (Table 5.1). Electrical conductivity, oxygen concentration, transparency, temperature and pH of the samples were measured directly in the field. Sub-samples for determination of dissolved substances were filtered through a  $0.45 \text{ }\mu\text{m}$  pore size filter (Eijkelpamp). The samples were transported and stored at  $4^\circ\text{C}$ . TP, dissolved reactive P (DRP),  $\text{NO}_3$ ,  $\text{NH}_4$ , and Cl were determined using standard colorimetric methods (APHA-AWWA-WPCF, 1989). Organic N was extracted by Kjeldahl extraction and measured by colorimetric method and sulphate was measured using IC (Ion Chromatography).

The water quality in the Lage Afdeling drainage area showed spatial differences in water quality related to land use (Figure S5.1). High  $\text{NO}_3$  concentrations were observed in water from the agricultural during winter (location 3 and 4 in Figure 5.1). The highest TP concentrations were observed in water from the nature area Oostvaardersplassen (location 6 in Figure 5.1). The DRP concentration of all sampling locations showed a seasonal variation with higher concentrations during the summer months.



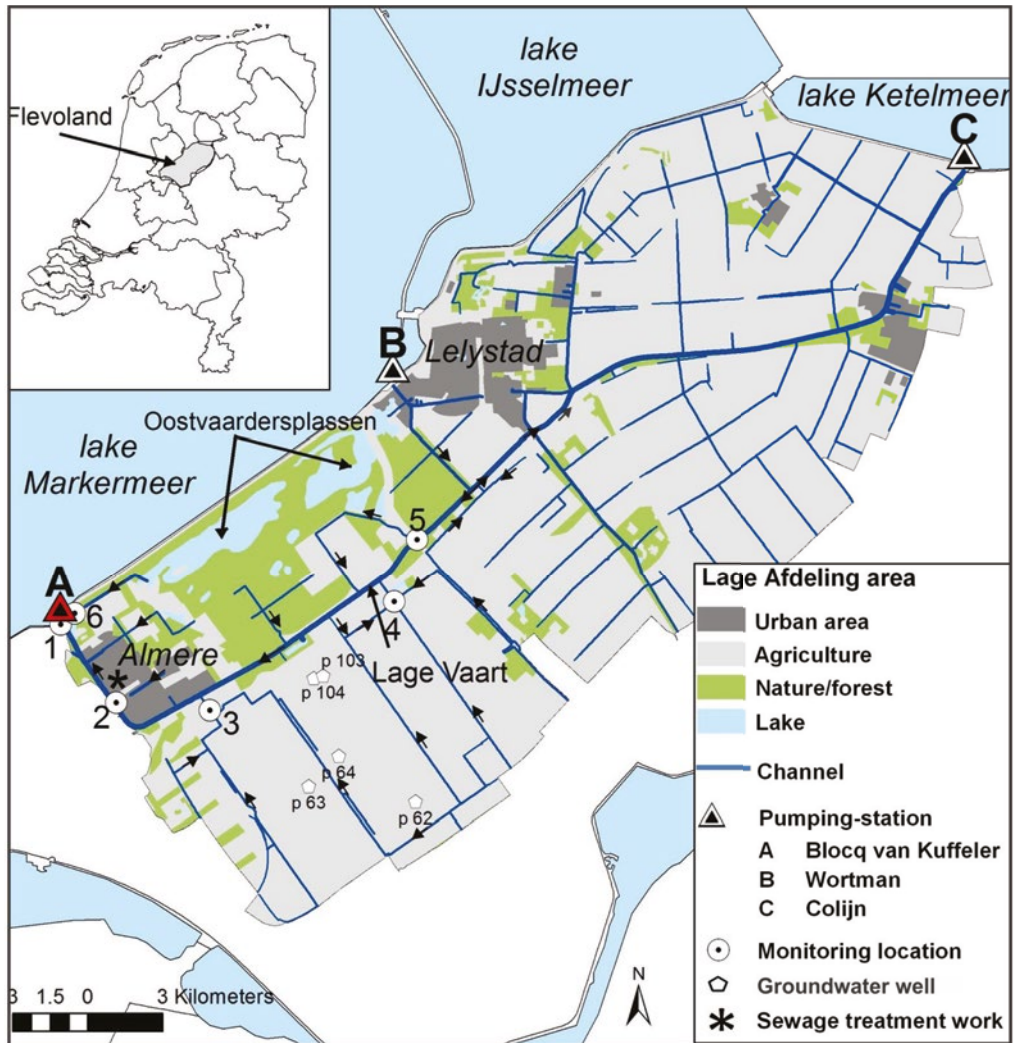


**Figure 5.1.** Map of the Lage Afdeling pumped drainage area, the continuous monitoring station at location A, the low-frequency surface water monitoring locations and the groundwater level monitoring wells. The flow direction of the water in the channels that are drained by pumping station Blocq van Kuffeler is illustrated by arrows.

### 5.3.3 High-frequency measurements

Between October 2014 and October 2015 we measured the TP, total reactive P (TRP) and  $\text{NO}_3$  concentration, turbidity, conductivity, and water temperature semi-continuously at the polder outlet just before the pumping station. TRP include all P forms that are measured with the molybdenum blue method (Murphy and Riley, 1962) in unfiltered samples, those include acid labile phosphorus containing compounds (inorganic and organic) (Worsfold et al., 2005). The flow regime at the

monitoring location is governed almost exclusively by the pumping station. The conductivity was measured continuously with a conductivity, temperature and depth (CTD) sensor (CTD-diver, Van Essen Instruments, Delft, the Netherlands).

**Table 5.1.** Locations of the low-frequency monitoring programme in Lage Afdeling pumped drainage area that is drained by the Blocq van Kuffeler pumping station.

Location	Description
1	Lage Vaart main-channel at pumping station "Blocq van Kuffeler"; outlet of the Lage Afdeling drainage area
2	Outlet of sub-channel that drains the urban area of the city "Almere"
3	Outlet of sub-channel that drains the agricultural "Gruttotocht"
4	Outlet of sub-channel that drains the agricultural "Lepelaartocht"
5	Far end of Lage Vaart main channel that is drained by the pumping station "Blocq van Kuffeler"
6	Outlet of channel that drains the nature area "Oostvaardersplassen"

The  $\text{NO}_3$  concentration was measured using a double wavelength spectrophotometric sensor (DWS), (Nitratax plus sc, Hach Lange GmbH, Düsseldorf, Germany). The DWS measures UV absorbance of dissolved  $\text{NO}_3$  at a wavelength of 218 nm at a measuring receiver (EM – element for measuring) and at 228 nm at a reference receiver (ER – element for reference). The recorded measurements at two different wavelengths are designed to compensate interference of organic and/or suspended matter by interpreting the difference between the absorbance values at EM and ER (Huebsch et al., 2015). The Nitratax sensor covers a  $\text{NO}_x\text{-N}$  detection range of 0.1 to 50.0 mg  $\text{L}^{-1}$ . The  $\text{NO}_3$  concentrations were recorded every 5 minutes. There was a small drift in the signal of the Nitratax sensor (max 0.35 mg  $\text{N L}^{-1}$  per month). We, therefore, corrected the high-frequency  $\text{NO}_3$  data using the  $\text{NO}_3$  concentrations from the bi-weekly grab samples by calculating a linear drift for the separate maintenance intervals of the sensor.

For the TP concentration measurements, we installed a Sigmatax sampler and a Phosphax Sigma auto-analyser (both Hach Lange GmbH, Düsseldorf, Germany). The total-P concentrations were recorded every 20 minutes. The Sigmatax was installed for the automated water sample collection and the pretreatment (ultrasonic homogenisation). Next, the sample was delivered to the Phosphax Sigma auto-analyser. This sample was digested using the sulphuric acid-persulphate method (APHA-AWWA-WPCF, 1989). After mixing and quickly heating and cooling down the sample, the reagents were automatically added and the sample was measured at 880 nm using a LED photometer. The Phosphax Sigma was automatically cleaned and calibrated daily. There was a close agreement between the high-frequency TP data and the TP concentrations of the accompanying two weekly grab samples analysed by standard laboratory assays ( $R^2 = 0.982$ ) and, therefore, no need to correct the high-frequency TP data (Figure S5.2).

The turbidity (formazine turbidity unit, FTU) was measured using a OBS (optical back scatter) sensor (SOLITAX t-line sc, Hach Lange GmbH Düsseldorf, Germany) that receives the reflected light

from the sediment-laden flow. Instead of directly obtaining the suspended sediment concentration, a turbidity sensor measures the turbidity of flow caused by suspended sediment (Gao, 2008). The FTU data were stored with a time interval of 5 minutes. There was a close agreement between the high-frequency turbidity data (FTU) and the suspended sediment (SS) concentrations ( $\text{mg L}^{-1}$ ) of the grab samples ( $R^2 = 0.965$ ) (Figure S5.2). The measured turbidity could thus be taken as a proxy for the SS concentration.

### 5.3.4 Background information

Precipitation data on an hourly basis for the Lage Afdeling were abstracted from HydroNet (<http://portal.hydro.net.nl/>). This is an online database with precipitation data based on calibrated radar images. The precipitation of the radar pixels were averaged over the Lage Afdeling drainage area. Temperature data were retrieved from the Royal Dutch Meteorological Institute (KNMI, De Bilt, the Netherlands) weather station Lelystad, located in the centre of the Lage Afdeling. The Flevoland polder has a moderate maritime climate with an average annual temperature of  $9.9^\circ\text{C}$ , an average annual precipitation of 850 mm and an average of 8 days per year with a maximum temperature below  $0^\circ\text{C}$ . Groundwater levels were monitored continuously with pressure sensors in five phreatic groundwater wells located within the agricultural area of the Lage Afdeling (Figure 5.1).

The groundwater quality data set from Griffioen et al. (2013) was used as background information. This database was assembled from the national database of the TNO Geological Survey of the Netherlands and contains complete groundwater analyses down to a depth of about 30 m with sampling dates later than 1945. The groundwater in the Lage Afdeling is characterised as anoxic fresh to saline (Cl between 7 and  $4500 \text{ mg L}^{-1}$ ) and P rich (TP between 0.01 and  $3.6 \text{ mg P L}^{-1}$ ) with low  $\text{NO}_3$  concentrations (between 0 and  $7 \text{ mg NO}_3 \text{ L}^{-1}$ ) (Figure S5.3).

### 5.3.5 Transfer function-noise modelling

To increase insight in the driving forces of measured dynamics of nutrient concentrations, preliminary research was done on the application of time-series analysis, and more specifically transfer function-noise (TFN) modelling, to estimate the impact of rainfall on  $\text{NO}_3$  concentrations. TFN models are very popular for describing dynamic causal relationships between time series and have been widely applied in the field of groundwater modelling (e.g. Berendrecht et al., 2003; Knotters and van Walsum, 1997). Although a small number of studies have used TFN models to relate streamflow data to nutrient concentrations (Schoch et al., 2009; Worrall et al., 2003) or relate precipitation data to high-frequency observation of dissolved organic carbon (Jones et al., 2014), TFN models have, to our knowledge, not been applied yet on high-frequency monitoring data of nutrients such as those available in this study. Therefore, as a first step, we tried to relate the time series of hourly  $\text{NO}_3$  concentration measurements to rainfall using the following linear TFN model:

$$\log(\text{NO}_3) = \theta(B)p_t + \mu + n_t \quad (5.1)$$

and

$$n_t = \phi n_{t-1} + \varepsilon_t, \quad (5.2)$$

where  $p_t$  is the precipitation at time  $t$ ,  $\theta(B) = \theta_0 + \theta_1 B + \dots + \theta_r B^r$  the transfer function ( $B$  is backward shift operator,  $B^i p_t = p_{t-i}$ ),  $\mu$  the reference or baseline level,  $n_t$  a stochastic first-order autoregressive process,  $\phi$  the autoregressive coefficient ( $0 < \phi < 1$ ), and  $\varepsilon_t$  a zero-mean normally distributed process (Box and Jenkins, 1970). To enhance the parameter estimation process,  $\phi$  is written as  $\phi = 1 - e^{-\alpha}$  and  $\alpha$  is being estimated instead of  $\phi$ . As  $\varepsilon_t$  is assumed to be normally distributed, the time series of  $\text{NO}_3$  data was log-transformed to better satisfy this assumption. For reasons of flexibility and model parsimony, we used a predefined transfer function as described by von Asmuth et al. (2002), which has the form of a Gamma distribution function and has been successfully applied for describing groundwater dynamics:

$$\theta_t = A^* t^{n-1} e^{-at}, \quad A^* = A \frac{a^n}{\Gamma(n)} \quad (5.3)$$

where the parameters  $A^*$ ,  $a$ ,  $n$  and the stochastic model parameter  $\alpha$  are estimated using a log-likelihood function, and  $\Gamma(n)$  is the gamma function.

### 5.3.6 Export loads calculations and trend analysis

True  $\text{NO}_3$  and TP export loads from the drainage area into the Markermeer were based on our high-frequency concentration measurements and discharge data of the pumping station. In addition  $\text{NO}_3$  and TP loads were estimated from linear interpolation of the low-frequency grab sample data combined with the discharge data. Although advanced methods have been developed to improve load estimates from low-frequency concentration data, none of the methods clearly outperformed the methods that were based on simple linear or stepwise interpolation (Rozemeijer et al., 2010). To quantify the event-driven TP export load generated by changes in the water flow due to pumping, a hydrograph separation method was used to separate the high-frequency TP concentration data series into short-term TP concentration peaks and baseline TP concentration. In this study we used the same method as applied by Rozemeijer and Broers (2007). This method, originally developed by (Hewlett and Hibbert, 1963), separates the baseline concentration and the peak concentration by a separation line with a constant slope (Figure S5.5). This line starts whenever the slope of the concentration series exceeds a specified constant separation slope. The separation line ends when it intersects the falling limb of the concentration series. For this study, a constant separation slope of  $0.02 \text{ mg P L}^{-1} \text{ d}^{-1}$  was used. With this relatively low slope value, concentration peaks were also separated from the baseline concentration during situations of upward trends in TP concentrations.

Long-term TP and  $\text{NO}_3$  concentration measurements were available for the polder outlet. We used two frequently applied methods for trend analysis of concentration-time series: (1) seasonal Mann-Kendall tests (Hirsch and Slack, 1984) (2) Theil-Sen robust line (Hirsch et al., 1982) and (3) locally weighted scatter plot smoothing (LOWESS) trend lines (Cleveland, 1979). These methods are relatively insensitive to extreme values and missing data in the time series. The seasonal Mann-Kendall trend test is a robust, non-parametric test on the significance of an upward or downward trend. The Theil-Sen method is a robust non-parametric trend slope estimator. The LOWESS trend

lines were used to examine possible changes in trend slopes within the concentration-time-series period. We refer to Rozemeijer et al. (2014) for details on the statistical methods.

## 5.4 Results

### 5.4.1 Water discharge

The Blocq van Kuffeler pumping station responds rapidly to rainfall events in the drainage area by automatically switching on one or two pumps (Figure 5.2A). The interval in which the pumping station is in operation decreased during the autumn months. During the winter months the pumping station runs almost at a daily basis and continuously for several days during very wet periods. There was a strong decline of the daily pumping hours from mid-April to the end of July. A wet period from mid-August to mid-September resulted in an increase of pumping hours. The pumping station pumped almost  $67 \times 10^6$  m<sup>3</sup> water from the polder into the Markermeer during the period from October 2014 until March 2015 and  $33 \times 10^6$  m<sup>3</sup> during the period from April 2015 until October 2015 (Figure 5.3). This corresponds to approximately 350 mm distributed across the entire drainage area for the winter half year (October–March) and 170 mm for the summer half year (April–September). The sum of the precipitation amounted to 455 mm and 517 mm for the winter half year and summer half year, respectively.

The high-frequency NO<sub>3</sub> concentration ranged from 0.01 to 10.4 mg N L<sup>-1</sup> and showed a seasonal pattern and a response to rainfall with high concentrations in winter and an increase during wet periods (Figure 5.2B). The NO<sub>3</sub> concentration was low from the start of the monitoring until half November. From mid-November to the third week of January, the NO<sub>3</sub> concentration gradually increased to a maximum of 9 mg N L<sup>-1</sup>. During the dry period in the first 3 weeks of February, the NO<sub>3</sub> concentration decreased to a level of 1 mg N L<sup>-1</sup>. Next, the concentration peaked at 24–25 February upon rainfall and gradually decreased towards the end of March where it showed an increase again during the wet period in late March and early April. During April the concentration declined to a level around 0.5 mg N L<sup>-1</sup> or below and stayed at this low level until mid-August. The NO<sub>3</sub> concentration rapidly increased after a wet period during mid-August and gradually decreased afterward.

### 5.4.2 Seasonal trends in high-frequency nutrient data

The high-frequency TP concentration ranged from 0.07 to 1.16 mg P L<sup>-1</sup> (Figure 5.2C). The TP concentration was relatively high during the first 3 weeks of the monitoring period (0.25 to 0.4 mg P L<sup>-1</sup>). In October and November, the TP concentration decreased during wet periods and increased during the dryer periods. During the wet first 2 weeks of December, the TP concentration decreased to a level around 0.1 mg P L<sup>-1</sup> and remained low until halfway through February. During the relatively dry period in February and March the TP concentration increased to a level around 0.2 mg P L<sup>-1</sup> and remained at this level until mid-June. From mid-June to mid-August the TP concentration gradually increased and peaked in mid-August. With higher concentrations during the summer season and a decrease during wet periods, the TP concentration showed a seasonal variation and a response to rainfall that was opposite to the NO<sub>3</sub> concentration.

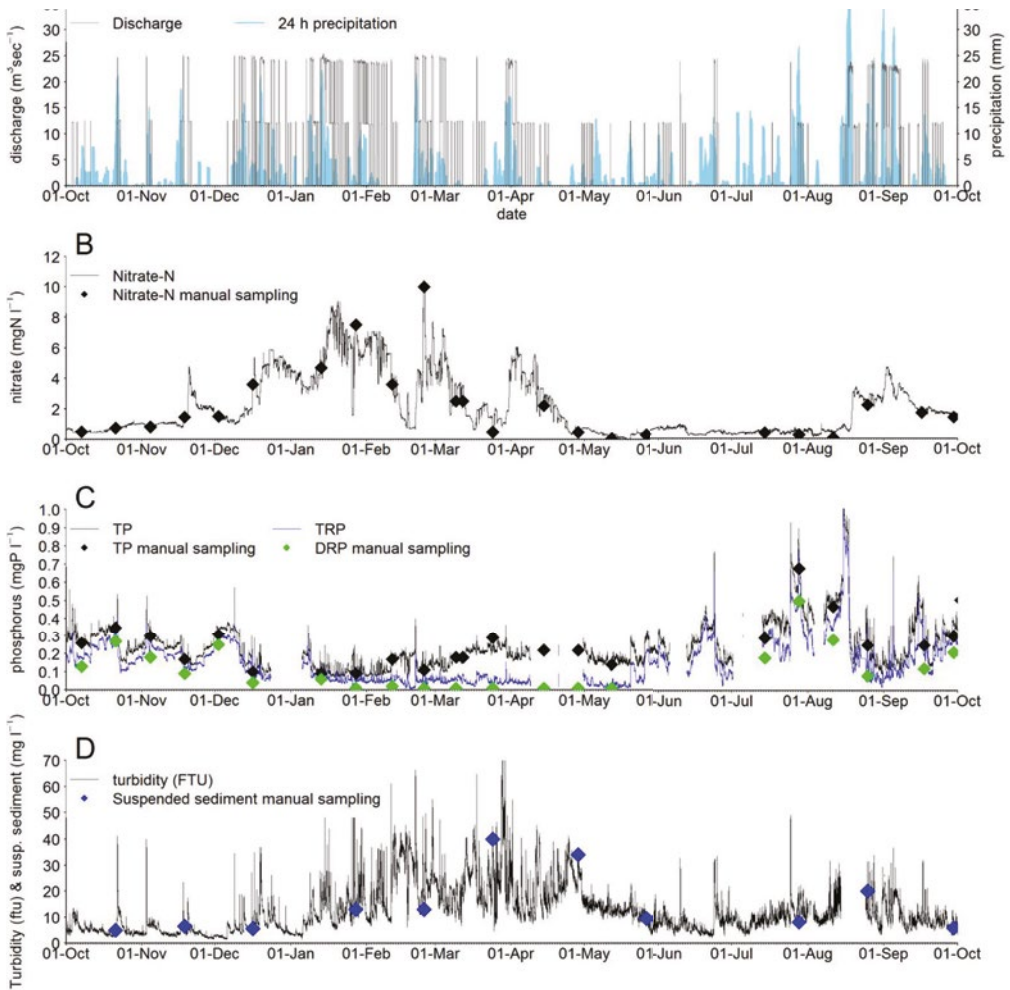
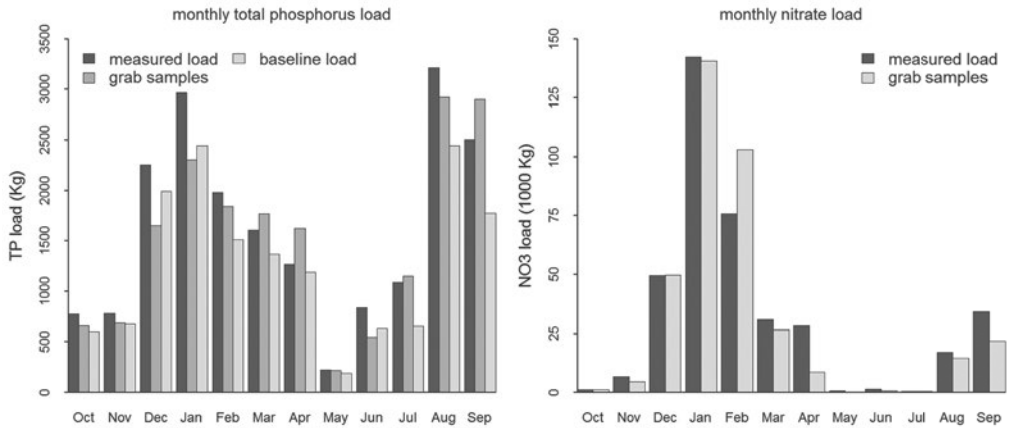
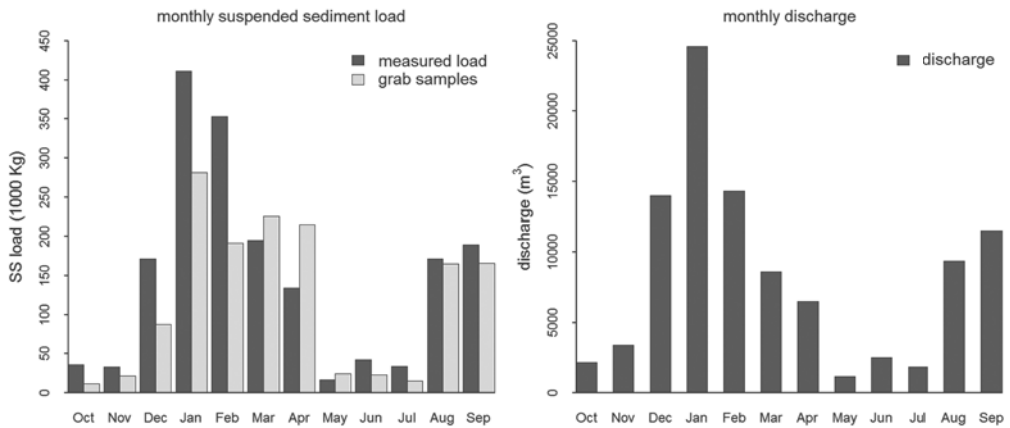


**Figure 5.2.** High-frequency monitoring data for the Lage Vaart channel at the pumping station Blocq van Kuffeler: (A) discharge as generated by the pumping station and 1-day antecedent precipitation; (B) nitrate-N 5 minutes data, with NO<sub>3</sub>-N manual sampled bi-weekly data; (C) total phosphorus and total reactive phosphorus 20 minutes data, with TP and DRP manual sampled bi-weekly data; (D) turbidity 5 minutes data, with suspended sediment manual sampled monthly data.

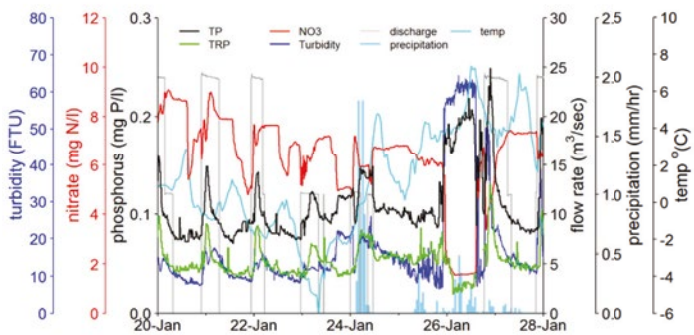
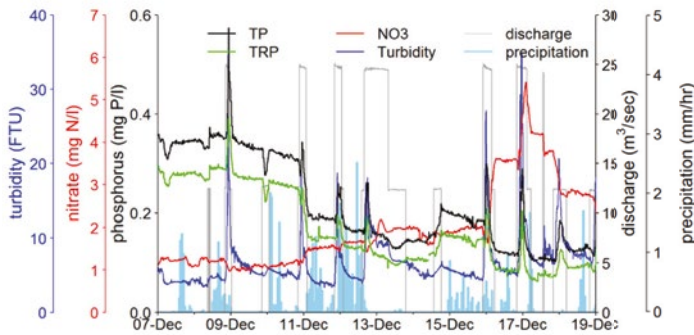
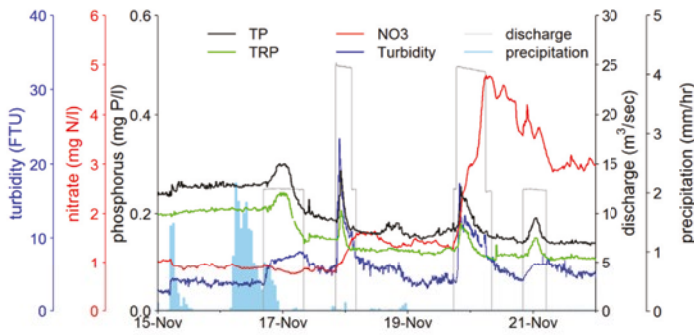
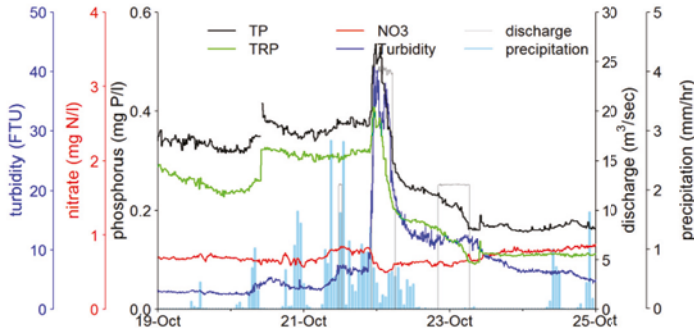


Seasonal and annual load	winter (Oct-Mar)	summer (Apr-Sep)	year	Seasonal and annual load	winter (Oct-Mar)	summer (Apr-Sep)	year
TP (kg)	10350	9150	19500	NO <sub>3</sub> (1000 kg)	306.3	82.3	388.6
TP grab samples (kg)	8900	9350	18300	NO <sub>3</sub> grab samples (1000 kg)	326.2	46.4	372.6
TP baseline (kg)	8600	6900	15500				



Seasonal and annual load	winter (Oct-Mar)	summer (Apr-Sep)	year	Seasonal and annual load	winter (Oct-Mar)	summer (Apr-Sep)	year
SS (1000 kg)	1200	588	1788	Discharge (m <sup>3</sup> )	67000	33000	100000
SS grab samples (1000 kg)	819	609	1428				

**Figure 5.3.** TP, NO<sub>3</sub> and SS export loads and discharge at the pumping station Blocq van Kuffeler. The measured load is calculated from the high-frequency data, the grab sample load is calculated from interpolation of the low-frequency data, the TP baseline load was calculated with the high-frequency TP data after separation of the short-scale concentration peaks generated by the pumping station.





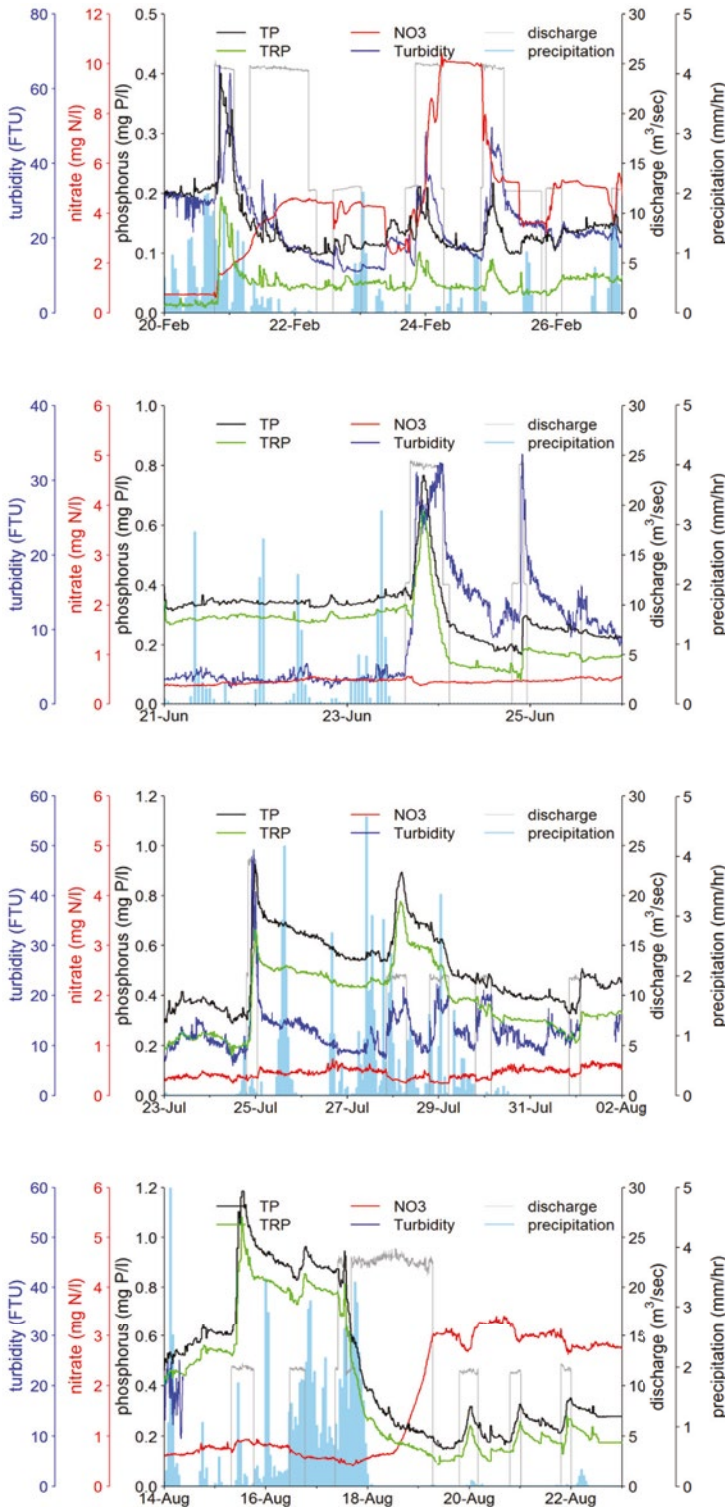


**Figure 5.4.** Examples of surface water  $\text{NO}_3$ , TP and turbidity dynamics at the pumping station Blocq van Kuffeler during meteorological events between October 2014 and August 2015 together with the pumping regime and precipitation (in  $\text{mm hr}^{-1}$ ). The January event demonstrates the effect of freeze-thaw on the nutrient concentrations while the other events show the nutrient dynamics upon rainfall events.

**Table 5.2.** Rainfall events and response of NO<sub>3</sub> concentration (in mg N L<sup>-1</sup>).

Rainfall event	date	mm	NO <sub>3</sub> concentration before event	Maximum NO <sub>3</sub> concentration after event
1	20–23 Oct	31	0.7	0.8
2	3–4 Nov	16	0.8	0.9
3	15–18 Nov	23	0.8	4.6
4	10–12 Dec	29	1.0	5.3
5	19–20 Dec	24	2.4	5.9
6	7–9 Jan	14	3.0	5.8
7	12–14 Jan	24	4.1	9.0
8	20–21 Feb	26	0.8	10.4
9	29 Mar–2 Apr	43	0.8	6.1
10	17–23 June	40	0.2	0.5
11	27–29 July	47	0.5	0.7
12	14–18 Aug	87	0.6	3.4
13	26–31 Aug	59	2.4	4.7

The high-frequency total-reactive P (TRP) data and the dissolved-reactive P (DRP) data from the low-frequency monitoring programme showed rather high concentrations from the start of the monitoring to early December 2014 and then declined to a low level (Figure 5.2C). The TRP and DRP concentration remained low until the second half of May. During the period from mid-May to mid-August the TRP and DRP concentrations followed the trend of the increasing TP concentrations.

The baseline level of the SS concentration was low during the period October to January (Figure 5.2D). In January the SS concentration increase and it stayed at a relative high lever to April. During the end of April and May the SS concentration decreased again.

### 5.4.3 Short-scale dynamics in high-frequency nutrient data

Significant increases of the NO<sub>3</sub> concentration up to 8 mg N L<sup>-1</sup> in short timescales appeared during pumping within 5 days after major rainfall events on 15–18 November, 10–12 December, 19–20 December, 7–9 January, 12–14 January, 21–22 February, 29 March–2 April, 14–18 August, and 26–31 August (Figure 5.4 and Table 5.2) The precipitation during these events was around 20 mm or above. After these NO<sub>3</sub> concentration peaks, the concentration declined during pumping. The increase in NO<sub>3</sub> concentration did not appear after the precipitation events on 20–23 October, 3–4 November 17–23 June and 27–29 July.

There is a structural response of the TP concentration and the turbidity on operation of the pumping station. The TP concentration and turbidity always peaked directly after the start of the pumping engines and decreased again during the period of pumping and afterwards (Figure 5.4). Pumping events with one pump resulted in an average increase of the TP concentration of 0.06 mg L<sup>-1</sup> and turbidity of 4.4 FTU while events with two pumps resulted in an average increase of 0.13 mg L<sup>-1</sup> and turbidity of 22 FTU (Table 5.3). The TP concentration was on average a factor of 1.30

and 1.83 higher during pumping with one pump and two pumps, respectively, compared to the concentration before pumping. The TRP concentrations also showed an increase in concentration during pumping. As the colorimetric measurement of TRP takes place in an acidic solution it is plausible to attribute the increase of the TRP concentration during pumping to the dissolution of particulate Fe or Ca bound inorganic P. The data show the largest increase of TP concentrations (0.16–0.60 mg P L<sup>-1</sup>) during pumping with two pumps after longer periods without pumping (21 October, 2 November, 8 December, 20 February, 23 June, 25 July and 15 August) and decreasing TP peaks were observed with subsequent pumping events (Figure 5.4). Short-term declines of the TP concentrations to values below the pre-pumping concentration were observed during pumping or shortly after pumping induced by rainfall periods in October, June and August (Figure 5.4).

A significant short-term change in NO<sub>3</sub> and TP concentrations and the conductivity that was not linked to pumping appeared during rainfall on 25 and 26 January (Figure 5.4). This period marked the end of a freeze-thaw cycle that started on 20 January. During this period the top soil became frozen. The precipitation during the night of 24 January consisted of snow and this resulted in a snow cover of a few centimetres. Upon rainfall on the frozen soil on 25 January, the NO<sub>3</sub> concentration decreased from 6.1 to 1.5 mg N L<sup>-1</sup> and the TP concentration increased from 0.09 to 0.21 mg P L<sup>-1</sup>. Together with the changes in NO<sub>3</sub> and TP concentrations, the turbidity increased from 8 to 57 FTU, the TRP concentration decrease from 0.06 to 0.02 mg P L<sup>-1</sup> and the conductivity decreased from 235 to 122 mS cm<sup>-1</sup> (Figure S5.4).

**Table 5.3.** Summary of TP and turbidity peaks, calculated as difference between the maximum value during the peak minus the value before the peak, induced by the pumping station.

	$\Delta$ TP (mg L <sup>-1</sup> ) 1 pump	$\Delta$ turbidity (FTU) 1 pump	$\Delta$ TP (mg L <sup>-1</sup> ) 2 pumps	$\Delta$ turbidity (FTU) 2 pumps
n peaks	72	79	59	60
average	0.06	4.4	0.13	22.1
median	0.04	4.4	0.10	21.1
P25	0.01	1.8	0.07	14.0
P75	0.08	8.3	0.14	29.2
max	0.58	26.2	0.61	52.0
min	-0.01	-1.5	0.03	5.9

#### 5.4.4 Decomposition of high-frequency nitrate data

As shown in section 3.2, NO<sub>3</sub> concentrations were low from the start of the monitoring period until the rainfall event on 15 November and during April the NO<sub>3</sub> concentrations decreased again. Precipitation events before mid-November and after April only had a minor influence on the NO<sub>3</sub> concentration. For the period between 15 November and 30 April a transfer function-noise modelling of hourly NO<sub>3</sub> concentrations reveals that the model can relate quite a large part of the dynamics to rainfall: the coefficient of determination  $R^2 = 0.7$ . The measured time series together with the model simulation and the residual series are shown in Figure 5.5.

Overall, the transfer model describes slow dynamics well; short-term dynamics cannot be related to rainfall with the transfer model and are described by the stochastic model. The estimated autoregressive coefficient ( $\phi = 0.98$ ) is quite low given the high sampling interval of 1 hour, indicating that most of the temporal structure in the time series has been captured by the transfer model.

The estimated model parameters and their standard deviation are given in Table S5.1. The estimated impulse response function for transferring an impulse of 1 mm rainfall into log-NO<sub>3</sub> concentration is given in Figure S5.6. The smooth character of the function is due to predefined structure of the function, which is the Gamma distribution function. The time to peak is 5.4 days with a response of 0.033 log(mg NO<sub>3</sub>-N mg L<sup>-1</sup>), while 95% of the total response happens within 43 days. The time to peak as revealed by the TFN model matches well with the delay of approximately 5 days between rainfall events and peak concentrations (Figure 5.4).

The reference or baseline level follows from the model estimation and has a value of  $\mu = -1.13$ , or back-transformed from logarithm:  $e^{-1.13} = 0.32$  mg N L<sup>-1</sup> which means that after a long no-rain period, the NO<sub>3</sub> concentration will decline to 0.32 mg N L<sup>-1</sup>. The current time series does not include seasonal patterns; during spring and summer season the NO<sub>3</sub> concentration cannot be related to rainfall only. The groundwater levels drop below the tube drain levels (i.e. precipitation may not lead to discharge) and denitrification or in-stream nutrient uptake processes reduce the NO<sub>3</sub> concentration, so other driving forces and non-linearity have to be included in the TFN model for modelling the summer season.

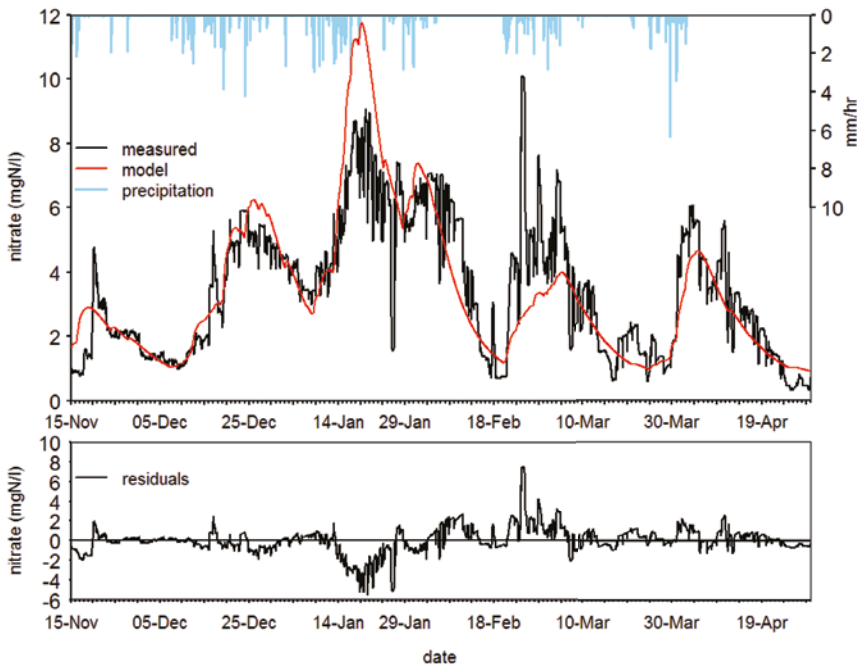


**Figure 5.5.** Measured and simulated NO<sub>3</sub> concentrations and rainfall data (top); and residual NO<sub>3</sub> series (bottom).

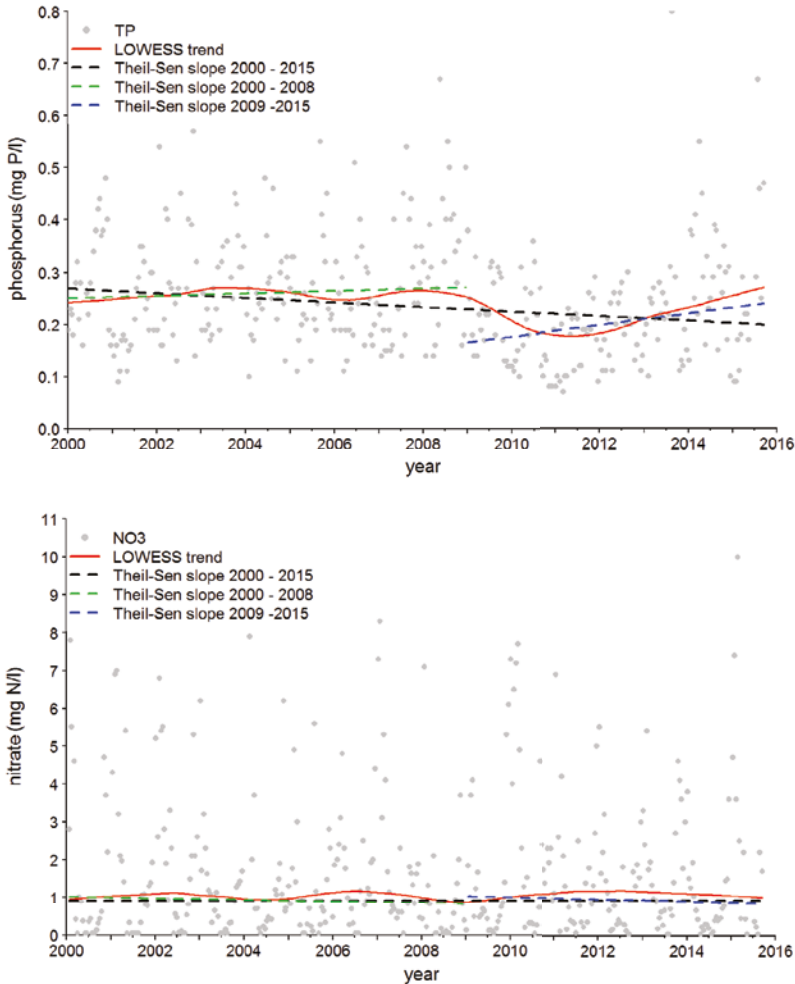


Figure 5.6. Trends in TP and  $\text{NO}_3$  concentrations over the period 2000–2015 at location 1 (*Blocq van Kuffeler*).

#### 5.4.5 Nutrient loads and fluxes at polder outlet

The annual loads based on the high-frequency data set equalled 19,500 kg for TP, 388,500 kg for  $\text{NO}_3\text{-N}$  and 1,788,000 kg for SS which corresponds to  $0.98 \text{ kg ha}^{-1}$  for TP,  $19.4 \text{ kg ha}^{-1}$  for  $\text{NO}_3\text{-N}$  and  $89.4 \text{ kg ha}^{-1}$  for SS (Figure 5.3). The TP load during the winter months (October–March) was almost equal to the load during the summer months (April–September), while for  $\text{NO}_3$  almost 80% of the annual load occurred during the winter months, with January and February as most important months. The annual loads calculated from the grab sample data equalled 18,200 kg for TP and 372,500 kg for  $\text{NO}_3\text{-N}$ . The annual baseline TP load after separation of the TP concentration peaks was 15,400 kg. The difference between the total load and the baseline load equalled 4100 kg; i.e.,

21% of the annual TP load can be attributed to resuspension of TP due to changes in water flow induced by the pumping station.

During the period from 1 October 2014 to 1 April 2015 the cumulative TP load calculated from the grab sample data matched the baseline TP load and underestimated the high-frequency load with 17%. The months December and January showed the largest difference between the grab sample load and the high-frequency load. The winter low-frequency  $\text{NO}_3$  load overestimated the high-frequency load by 6.5%, mainly due to a higher monthly low-frequency load in February. From May to mid-August 2015 there was almost no  $\text{NO}_3$  load. In August and September the grab sample load was lower than the high-frequency load. The annual grab sample load underestimated the high-frequency load with 4%.

Time series of TP and  $\text{NO}_3$  concentrations in grab samples at the Blocq van Kuffeler pumping station over the period 2000–2015 are given in Figure 5.6. The red lines in Figure 5.6 show the LOWESS trend line and the black lines show the Theil-Sen slope over the period 2000–2015. The  $\text{NO}_3$  concentration showed no significant upward or downward trend over the period 2000–2015. The time series of TP concentration showed different trends over the period 2000–2015. After a period with minor increase for 2000 to 2009, the LOWESS trend line reveals a decline in TP concentrations in the period 2009–2010 followed by an increase from 2011 to 2015. The Theil-Sen slope showed a decline of TP concentration ( $-0.0053 \text{ mg P L}^{-1}$  per year) over the years 2000–2015. This downward trend was significant according to the seasonal Mann-Kendall trend tests.

The blue and green lines give the Theil-Sen slopes for the periods 2000–2008 and 2009–2015, respectively, before and after renovation of the pumping station. Where the Theil-Sen slope showed a decline of TP concentration over the years 2000–2015, it showed upward trends of  $0.0023 \text{ mg P L}^{-1}$  per year and  $0.011 \text{ mg P L}^{-1}$  per year over the separate periods 2000–2008 and 2009–2015, respectively. The upward trend for the period 2009–2015 was significant according to the seasonal Mann-Kendall trend tests. The  $\text{NO}_3$  concentrations showed no significant upward or downward trend over the separate periods 2000–2008 and 2009–2015.

## 5.5 Discussion

### 5.5.1 Identification of nutrients sources and dynamics in nutrient concentrations

#### 5.5.1.1 Nitrate

The high-frequency  $\text{NO}_3$  data showed a seasonal trend with higher concentrations during winter compared to summer. Low-frequency surface water data showed high  $\text{NO}_3$  concentrations at the outlet of the agriculture-dominated areas within the drainage area during winter months (Figure S5.1), whereas the groundwater has low  $\text{NO}_3$  concentrations (Figure S5.3). From this, it is clear that  $\text{NO}_3$  in the surface water at the polder outlet has an agricultural source. An increase of  $\text{NO}_3$  concentrations from summer to winter is observed in a large majority of agriculture-dominated headwater in the Netherlands (Rozemeijer et al., 2014) and natural catchments elsewhere (Wade et al., 2012). Catchments where  $\text{NO}_3$  concentrations are controlled by a combination of effluent loads from sewage treatment works and dilution by rainfall commonly show a decline in  $\text{NO}_3$  from summer

to winter (Bowes et al., 2015; Wade et al., 2012). The  $\text{NO}_3$  pattern is therefore thought to be due to a combination of interflow or shallow draining groundwater with high fertiliser or manure inputs and  $\text{NO}_3$  enrichment during autumn and winter. Increased crop uptake of  $\text{NO}_3$  during the growing season combined with the effect of in-stream processes result in declined  $\text{NO}_3$  concentrations during the summer months.

The annual  $\text{NO}_3$  load from the WWTP to the Lage Vaart is approximately 4% of the  $\text{NO}_3$  export load at the polder outlet. The low  $\text{NO}_3$  concentrations during the summer months and the rapid increase after a very wet period during August additionally indicate that the influence of sewage effluent on the  $\text{NO}_3$  concentrations is limited. The discharge from the channel that drains the nature area Oostvaardersplassen (Figure 5.1, location 6) enters the Lage Vaart between the WWTP and the pumping station and is 2 to 3 times higher than the discharge from the WWTP. This implies that there is limited flow of the WWTP effluent towards the pumping station during no pumping conditions.

Beside the seasonal variation, we structurally observed an increase of  $\text{NO}_3$  concentrations after intensive rainfall events during the winter months. A reduction in  $\text{NO}_3$  concentrations coinciding with periods of intensive rainfall is commonly reported in high-frequency monitoring studies in natural catchments and attributed to dilution of the surface water by surface run-off (Bowes et al., 2015; Rozemeijer et al., 2010). Our structurally observed increase implies that run-off, which dilutes the  $\text{NO}_3$  concentration of the surface water does not commonly occur in the polder. Dilution of the  $\text{NO}_3$  concentration upon rainfall was only observed during the thaw on 25 January. Soil freeze-thaw processes significantly increase the potential erosion during run-off events that follow thaw in hill slope areas (Ferrick and Gatto, 2005) but also in relatively flat areas (Gentry et al., 2007). Where during normal conditions rainfall infiltrates into the soil, the thaw and precipitation on 25 January likely resulted in run-off. This temporally diluted the  $\text{NO}_3$  concentration and conductivity and increased the TP concentration and turbidity.

During normal conditions with soil temperatures above  $0^\circ\text{C}$ , rainfall initiates a sudden increase of quick interflow via subsurface tube drains, cracks, or other macropores to the Lage Vaart channel water, which results in leaching for  $\text{NO}_3$  stored in the soil profile to the surface water.

This is confirmed by the TFN model, which showed that quite a large part of the  $\text{NO}_3$  dynamics during the winter months can be related to rainfall. The results in Figure 5.5 show that during no-rain periods the decline in concentration is modelled well. The various periods of rainfall show different results: in December the increase in concentration is modelled well, in January the concentration is overestimated, while in February and March the concentration is underestimated. The overestimation in January can be explained by dilution in combination with a decrease of in the  $\text{NO}_3$  stock stored in the soil profile due to leaching with rain during previous months. The largest positive residuals appeared on 24–26 February. Recent manure application is a plausible explanation for the underestimation of measured concentrations in February and March (see section 3.3). The largest negative residuals appeared during the thaw on 25 and 26 January. The residuals of the TFN model help to get a better understanding of the dynamic  $\text{NO}_3$  behaviour of the polder catchment.

### ***Drainage water***

The tube drain water in the Flevoland polder contains relatively high  $\text{NO}_3$  concentrations. Meinardi and Van den Eertwegh (1997) ran a monitoring programme on tube drain water composition at 14 farms in the Flevoland polder during 1992–1995 and reported concentrations between 5 and 25  $\text{mg N L}^{-1}$ . Another monitoring programme on nutrient concentration of tube drain water at six farms in Flevoland from 2004 to 2008 gave farm-average  $\text{NO}_3$  concentrations of 14–18  $\text{mg N L}^{-1}$  (van Boekel et al., 2012). These concentrations can only explain the observed  $\text{NO}_3$  concentration at the pumping station during wet conditions when the tube drain water is the dominant contributor of the Lage Vaart channel water. Groundwater levels within the polder are commonly low and tube drainage is rare during the summer and early autumn (Groen, 1997; Van den Eertwegh, 2002). In autumn, when evapotranspiration decreases, the groundwater levels rise upon rainfall events to around or above the level of the tube drains, which are present at a depth of 0.95 m below the soil surface, and this initiates drain discharge. This is illustrated by the measured groundwater levels within the Lage Afdeling drainage area (Figure S5.7) that shows a direct response of the groundwater level on rainfall combined with a seasonal trend that shows rising groundwater levels during the months October and November and quite stable levels from December to March. Rainfall events between the start of the monitoring and mid-November and between April and mid-August did not result in tube drain discharge. The low  $\text{NO}_3$  concentration of the surface water during these periods is thus explained by the absence of tube drain discharge. Extensive rainfall during the second half of August resulted in a rising of the groundwater level close to the tube drain level (Figure S5.7) and thus to leaching of  $\text{NO}_3$ , stored in the soil profile, to the surface water. As our TFN model is weak in explaining the processes that might control  $\text{NO}_3$  concentration such as biogeochemical processes in surface waters we did not include the summer period in our model.

### ***Preferential transport***

The high-frequency data showed a quick response of the  $\text{NO}_3$  concentration at the pumping station to rainfall once the groundwater level is at the tube drain level. This can be explained by the presence of cracked clay soils that results in a rapid response of drainage to rainfall events in winter (Groen, 1997; Van den Eertwegh, 2002). Preferential transport of water and nutrients through cracks and macropores is known to play an important role in heavy clay soils (e.g. Van der Salm et al., 2012). Due to regular plowing rainwater easily infiltrates into the top soil layer where exchange of  $\text{NO}_3$  from manure, fertilisers and plant debris occurs. The top soil or plough layer is commonly well aerated and, therefore, quite optimal for conversion of organic nitrogen and ammonium to  $\text{NO}_3$ . After leaching of this water from the plough layer to the cracked soil layer it quickly contributes to tube drain discharge. Due to short residence time of this water in the soil, the influence of denitrification on the  $\text{NO}_3$  concentration is limited. This implies that the  $\text{NO}_3$  concentration at the polder outlet and the related export load from the polder are strongly controlled by quick interflow including tube drain discharge during the winter months.

The period of 5 days between rainfall event and peak in the  $\text{NO}_3$  concentration at the pumping station is representative for the average residence time of water in the Lage Afdeling drainage area during wet conditions. Catchment mean residence times are much shorter during wet periods



compared dry periods (Van der Velde et al., 2012). The 5 days travel time of the water in the field ditches, sub-channels and main channel during wet conditions is in line with model calculated mean annual residence times of water in the Lage Vaart main channel of 6.6 days (Van den Eertwegh, 2002).

### 5.5.1.2 Phosphorus

In contrast to the  $\text{NO}_3$  concentration, the TP concentration at the pumping station decreased after the wet periods (Figure 5.2C). The interflow discharge via subsurface tube drains, cracks or other macropores that resulted in an increase of  $\text{NO}_3$  concentrations diluted the TP concentrations. Likely this can be attributed to the relative decrease of the groundwater contribution to the channel water during periods of increased interflow discharge. This indicates that the sources of TP in the channel water at the polder outlet can largely be attributed to exfiltration of P-rich groundwater that occurs throughout the year, presumably in combination with effluent loads from the WWTP and biogeochemical remobilisation of P from channel sediments during the summer and autumn. The low DRP:TP ratio of the surface water within the Lage Afdeling as observed during the first half-year of 2014 and 2015 (Figure S5.1) can be explained by transition of dissolved P to particulate P at the groundwater-surface water interface. This commonly occurs after exfiltration of anaerobic groundwater into surface water due to oxidation processes (e.g. Baken et al., 2015b; Van der Griff et al., 2014).

The annual TP load from the WWTP to the Lage Vaart is approximately 27% of the TP export load at the polder outlet. As discussed previously for  $\text{NO}_3$ , the effect of the WWTP on the  $\text{NO}_3$  concentration at the pumping station seems to be small. For TP, however, the WWTP load cannot be neglected. The discharge water from the Oostvaardersplassen has relatively high TP concentrations (Figure S5.1) and may contribute to the increase in TP concentration at the pumping station during no pumping periods. The source of the TP in the Oostvaardersplassen is groundwater and feces of wildlife. The Oostvaardersplassen is an important wintering area for birds that import nutrients from elsewhere.

The high DRP:TP ratios of the low-frequency monitoring programme during the second half-year of 2014 and the summer of 2015 indicates that mineralisation of organic P from algae or plant debris, or release of DRP from bed sediments can be considered as an additional P source during summer and autumn when the TP concentration reached a maximum level between 0.8 and 1.2 mg P L<sup>-1</sup>. Mineralisation of organic P mainly occurs after the growing season and the release of DRP from bed sediments is reported during summer and autumn due to temperature and redox-dependent biogeochemical remobilisation processes for lakes (e.g. Boers and van Hese, 1988; Lavoie and Auclair, 2012), wetlands, fens and floodplain soils (e.g. Loeb et al., 2008; Zak et al., 2006) but also for streams and rivers (e.g. Duan et al., 2012; Jarvie et al., 2008). Low  $\text{O}_2$  concentrations in the water column are reported as an indicator for remobilisation of P from bed sediments (Geurts et al., 2013). The surface water at low-frequency monitoring locations showed a decline of the  $\text{O}_2$  concentrations during the summer and autumn months (Figure S5.1), thus, indicating that biogeochemical remobilisation may occur in the channels of the Lage Afdeling.

Surface run-off as a source of P in the surface water was only observed at the end of the freeze-thaw cycle on 25–26 January. The TRP did not increase during this event, suggesting the TP largely existed of non-labile organic P. Run-off is generally not an important transport process controlling P dynamic in the polder catchment.

### ***Resuspension of particulate P***

The increase of the TP concentration and turbidity during operation of the pumping station and the larger increase during pumping with two pumps compared to one pump (Table 5.3) indicate that the increase of the TP concentration is related to resuspension of P from bed sediments due to increased flow velocities. During no-pumping conditions, an erodible layer builds up by sedimentation of particulate P. When the water flow velocities in the main channel increase upon pumping, the P becomes suspended and transported downstream. The largest increase of the TP concentration during pumping with two pumps after longer periods without pumping and the decreasing TP peaks with subsequent pumping events supports this mechanism.

Resuspension of particulate P retained by sediments during high discharge events is an important transport mechanism in natural catchments (e.g. Evans et al., 2004a; Haygarth et al., 2005; Mulholland et al., 1985; Nyenje et al., 2014; Palmer-Felgate et al., 2008). Our data shows that this mechanism is also relevant for P transport in polders where flow velocities vary more abruptly and are maximised by the capacity of the pumping station. The changes in TP concentration during pumping are, however, significantly lower than reported during peak water discharge amongst storms in natural catchments. For an agriculture-dominated lowland catchment in the Netherlands, Rozemeijer et al. (2010) reported a mean increase in TP concentration during discharge from 0.15 to 0.95 mg P L<sup>-1</sup> coming from 47 rainfall events over a year. Particulate P (PP) increases up to a factor of 100 were reported by Stutter et al. (2008) in response to storm events. Evans et al. (2004a) measured PP concentrations up to 3.93 mg P L<sup>-1</sup> in a lowland stream during high discharge conditions while the mean concentration equalled 0.1 mg P L<sup>-1</sup>. Haygarth et al. (2005) reported 10 to 20 times higher mean TP concentrations during storm flow conditions compared to base flow conditions. With data from 76 storms Correll et al. (1999) showed that concentrations of PP increased up to 3 orders of magnitude during storms.

These changes are all considerably larger than the average factor of 1.30 and 1.83 that we observed at the pumping station during pumping with one and two pumps, respectively. The P export from natural catchments during pulses at high flow in less than 10% of the time may amount to about 80% of the annual export (Kaushal et al., 2014). With 143 pumping events during the period from October 2014 to September 2015, discharge-related changes that lead to resuspension of P appear more frequent in this polder catchment compared to natural catchments. As only 21% of the annual TP export load can be related to resuspension this cannot be considered as the dominant P transport mechanism. The artificial pumping regime that buffers high flows in polder area thus results in a high potential of polder areas to retain P by sedimentation of PP. Consequently, this may result in a higher potential of polder areas for DRP release from the bed sediments during summer months by biogeochemical remobilisation which attributes to TP export loads during the summer. Therefore, it can be concluded that P transport mechanisms in polder catchment can be

characterised as less incidental and peak flow controlled and more controlled by biogeochemical remobilisation from bed sediments than those from natural catchments.

### 5.5.2 Incidental nutrient losses to surface water after manure application

The  $\text{NO}_3$  concentration peaked at the polder outlet on 24 February, 4 days after an intensive rainfall event that marked the end of a relative dry period that started early February. The increase of the  $\text{NO}_3$  concentration is almost 2 times higher compared to the other peaks in  $\text{NO}_3$  concentration after a rainfall event (Table 5.2). This suggests that the  $\text{NO}_3$  peak of  $10.4 \text{ mg N L}^{-1}$  was caused by an incidental loss after manure application that started on 1 February. The TFN model revealed high residual  $\text{NO}_3$  concentrations up to almost  $8 \text{ mg N L}^{-1}$  during this  $\text{NO}_3$  peak that cannot be explained by rainfall (Figure 5.5). The  $\text{NO}_3$  concentration peaks on 27 February and 3 March also showed large positive residuals of  $4.2$  and  $3.4 \text{ mg N L}^{-1}$ , respectively. The wet period in January resulted, however, in predicted  $\text{NO}_3$  concentrations that were higher than the measured concentrations. The negative residuals in January can be explained by leaching of the  $\text{NO}_3$  stored in the soil profile during the winter season in combination with the appearance of some degree of dilution of the remaining  $\text{NO}_3$  by precipitation water during this period. Dilution of the  $\text{NO}_3$  concentration upon rainfall events commonly observed in catchments (e.g. Rozemeijer et al., 2010; Wade et al., 2012). A plausible explanation for the large positive residuals in February and March is recent manure application that started on 1 February and temporary soil storage of applied N during the first dry weeks of February.

The TP concentration peaked on 21 February during the beginning of the rainfall event, simultaneously with a turbidity peak after the start-up of the pumps following upon a relatively dry period of more than 1 week without pumping (Figure 5.4). It is, therefore, not likely that this peak was caused by an incidental loss after manure application but caused by hydrodynamic resuspension of the Lage Vaart bed sediment. The absence of a TP peak after the rainfall event on 21–22 February can be attributed to the soil characteristics of the area. We already discussed that the water quality at the polder outlet is strongly controlled by quick interflow via tube drains or cracks and that surface run-off only influenced the water quality when it rained during the end of a freeze-thaw cycle. Although it is known that tube drain discharge after rainfall events in combination with recent manure application on cracked clay soils may contain significant TP concentrations (Van der Salm et al., 2012), these peaks did not appear at the polder outlet. Several other studies ask attention for elevated TP concentrations in drain and trench flow within a few weeks after application of fertilisers or liquid farm manure (Djodjic et al., 2000; Hodgkinson et al., 2002; Simard et al., 2000). It is unknown if these peaks appear after rainfall events in the tube drain discharge or in the receiving field ditches in the Lage Afdeling drainage area. Therefore, it is unclear if the absence of TP peaks simultaneously with the  $\text{NO}_3$  peaks at the polder outlet can be attributed to sedimentation of PP from agricultural sources in the field ditches or sub-channels where it may become a source for DRP release from bed sediments during the summer and autumn months or that there is almost no particulate or dissolved P leaching from the topsoil to the surface water due to the sorption capacity of the topsoil. From other lowland areas it is known that the dissolved P loads to surface water from tube drains and shallow groundwater discharge are low due to precipitation with Fe hydroxides with a high

affinity to retain P, at the oxic/anoxic interface around the tube drains and ditch sediment (Baken et al., 2015b; Van der Grift et al., 2014).

### 5.5.3 Water quality affected by the operational management of the pumping station

Since the renovation of the pumping station in the autumn of 2008, it runs typically overnight during normal meteorological conditions, for reason of cheaper power supply. The low-frequency sampling is always performed during daytime. The distribution of pumping hours and sampling moments over the day during the period October 2014–September 2015 and box plots of measured TP concentrations over the day during the months January and February 2015 are shown in Figure S5.8. These 2 months were selected because box plots for longer time series are dominated by the seasonal trends in the TP concentration. The median, quartile and maximum TP concentrations were higher during night hours than during daytime. As a result, the monitoring programme systematically misses the TP peak that occurs during pumping and consequently does not measure diurnal cycles in water quality caused by the pumping station. The reported time series from the low-frequency sampling programme is, thus, not fully representative for the TP concentration at the polder outlet. As a consequence, export fluxes from the polder as calculated from low-frequency sample data underestimate the true export P-loads (Figure 5.3). The  $\text{NO}_3$  concentration showed no structural response on pumping, further illustrating the importance of resuspension of P by pumping.

The preferred timing of sampling during regular working-hours is also critical for trend detection in the resulted data set time series (Figure 5.6). Trend analysis before and after replacement of the diesel engines compared with trend analysis over the years 2000–2015 indicates that the trend of slightly decreasing concentrations over the years 2000–2015 may be caused by the sudden decrease of concentrations after renovation of the pumping station which is an artefact of a change in pumping regimes.

The number of diesel powered pumping stations in the Netherlands has rapidly declined during the last decades. There were around 200 diesel or hybrid (diesel + electric) powered pumping stations in operation in 1990. Currently, there are only 40 remaining and these pumping stations have mainly a function for emergency situations (Gemalen, 2015). During the same period, electric powered pumping stations have been equipped with automatic switching systems. Nowadays, a large majority of pumping stations operates predominantly during night hours. As the pumping station is the outlet of a (artificial) water system it is often a monitoring location for surface water quality as well. The renovation of pumping stations may thus have had a substantial impact on reported trends in water quality on a regional or even a national scale.

## 5.6 Conclusions

High-frequency monitoring at the outlet of an agriculture-dominated lowland water system combined with low-frequency monitoring at several other locations in the polder appears to be an effective tool to reveal difficult to notice responses in surface water quality. P and  $\text{NO}_3$  react differently. Conclusions regarding P are the following:

- The P retention potential of the polder water systems is enhanced compared to natural catchments due to the artificial pumping regime that prevents high discharge flow and therefore limits resuspension of particulate P.
- Groundwater seepage, biogeochemical remobilisation and wastewater treatment plant effluent are sources of TP in the surface water. The relative importance of these sources, however, cannot be determined.
- Rainfall events do not result in TP concentration peaks. Transport of particulate P that originates from groundwater and (agricultural) drains discharge is strongly retained but particulate P can be remobilised due to biogeochemical processes in the sediment layer at other moments. This makes it difficult to link agricultural practice to P concentrations in the surface water and this should be accounted for when judging measures to reduce P loads from agriculture.
- The artificial pumping regime and high retention capacity of polder catchments, however, enables the potential for measures to reclaim P from the water systems after being leached from the soil but before being transported to downstream surface water bodies.

#### Conclusions with respect to N:

- The  $\text{NO}_3$  load to surface water originates from subsurface drains in the agricultural area, likely in combination with quick interflow via clay cracks, that start discharging upon intensive rainfall events and result in a quick response of the  $\text{NO}_3$  concentration at the polder outlet.
- Intensive rainfall events within a few weeks after manure application in February result in incidental losses of  $\text{NO}_3$ .

#### In general it can furthermore be concluded that:

- Surface run-off is generally not an important transport mechanism controlling  $\text{NO}_3$ , P and SS dynamics in the polder catchment, except at the end of a freeze-thaw cycle.
- The timing of sampling relative to the operating hours of a pumping station affects the concentration of TP and SS and this should be accounted for when calculating P export loads, determining trends in water quality or when evaluating water quality against ecological thresholds and standards.

## Acknowledgements

The Regional Water Authority Zuiderzeeland is gratefully acknowledged for the financial support for installation and maintenance of the high-frequency monitoring station and providing the water quality and groundwater level data. The useful comments of two anonymous reviewers are greatly appreciated. Funding of the project was provided by Deltares (project SO2015: From catchment to coast).

## 5.7 Supplement

### 5.1 Water quality within Lage Afdeling drainage area

The low frequency dataset of almost two years with analyses from 6 locations within the Lage Afdeling drainage area showed spatial differences in water quality related to land use and subsurface characteristics. High chloride concentrations were observed at monitoring locations 1, 3 and 5, where location 1 and 3 showed higher concentrations during summer than during winter (Figure S5.1). Chloride is an indicator for the contribution of deep groundwater to the surface water. Chloride concentrations above  $500 \text{ mg L}^{-1}$  were commonly observed in the deeper groundwater in the area upstream of location 3 and 5 (Figure S5.3). Location 3 shows an inverse relation between the  $\text{NO}_3$  and Cl concentrations ( $R^2 = -0.67$ ) which illustrates the soil and shallow groundwater as source of  $\text{NO}_3$  in the surface water. The Lage Vaart channel acts as a drainage channel for groundwater under the confining Holocene layer, which is often brackish/saline (Van den Eertwegh, 2002). This explains the relatively high Cl concentrations of location 1 during summer.

Low  $\text{NO}_3$  concentrations were observed in discharge water from the nature area Oostvaardersplassen (location 6) throughout the year whereas high  $\text{NO}_3$  concentrations were observed in water from the agricultural areas Lepelaartocht and Gruttotocht (location 3 and 4) in the winter ( $8.3$  and  $13 \text{ mg N L}^{-1}$  in February 2014 and 2015, respectively). The  $\text{NO}_3$  concentration in the urban area water (location 2) did not exceed  $2 \text{ mg N L}^{-1}$ . The  $\text{NO}_3$  concentrations of the Lage Vaart channel water at the pumping station (location 1) during the winter months were lower compared to the  $\text{NO}_3$  concentrations at the outlet of the agricultural areas. As denitrification is limited during winter time, this indicates dilution of agriculture-dominated water with water from nature areas or urban areas. This is confirmed by the  $\text{SO}_4$  data that demonstrate some dilution of the agriculture-dominated water as well. The locations with high  $\text{SO}_4$  concentrations exhibit an inverse pattern with the Cl concentration ( $R^2 = -0.45$  for location 3). This shows the occurrence of pyrite oxidation in the shallow subsurface (Griffioen et al., 2013) in the Lage Afdeling drainage area except for location 6 that drains the Oostvaarderplassen which has no tube drains and high groundwater levels throughout the year. The N-Kjeldahl concentrations varied between  $0.77$  and  $5.8 \text{ mg N L}^{-1}$  but showed little variation over the year for the individual agriculture-dominated and urban-dominated sampling locations. The N-Kjeldahl concentration in the water from the Gruttotocht (location 3) was almost twice as high as from the Lepelaartocht (location 4).

The TP concentration of the low-frequency monitoring program varied between  $0.05$  and  $0.72 \text{ mg P L}^{-1}$  (Figure S5.1). From all sampling locations within the Lage Afdeling, the water from the Oostvaardersplassen (location 6) had the highest TP concentrations. The TP concentration of this water ranged between  $0.37$  and  $0.72 \text{ mg P L}^{-1}$  from January to July 2014. The concentration dropped to a level around  $0.3 \text{ mg P L}^{-1}$  or lower in August 2014 and stayed at this level until April 2015. From April 2015 to mid-September 2015 the TP concentration ranged between  $0.35$  and  $0.74 \text{ mg P L}^{-1}$ . The TP concentration at the Oostvaarderplassen and Blocq van Kuffeler were higher during the first months of 2014 compared with the same period in 2015. The long-term data series for Blocq van Kuffeler showed high TP concentrations during the first months of 2014 as well compared with concentrations in other recent years (Figure 5.6). We do not have a clear explanation for this

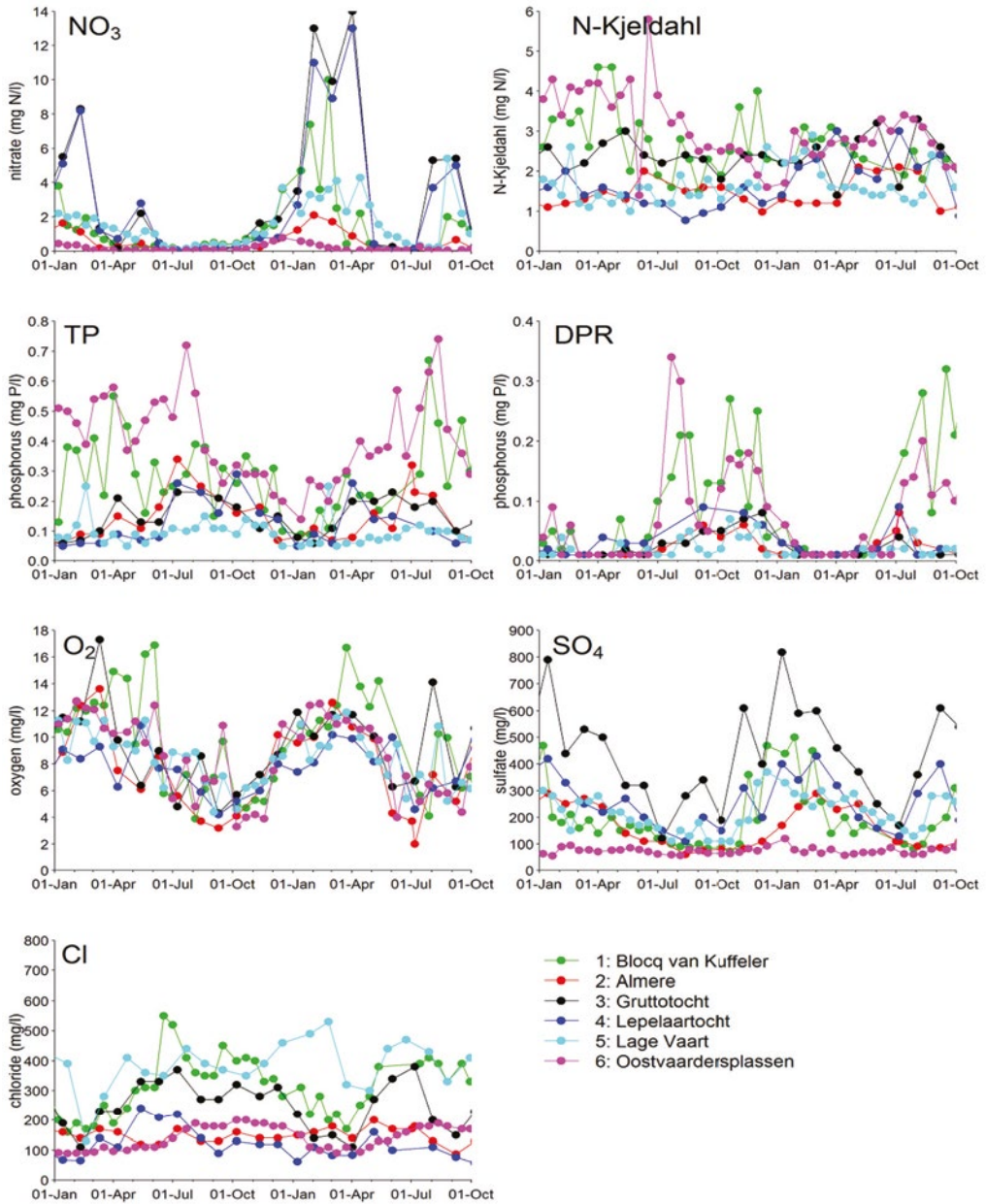


**Figure S5.1.** Low-frequency time series of NO<sub>3</sub>, N-kjeldahl, TP, DRP, O<sub>2</sub>, SO<sub>4</sub> and Cl concentration at surface water sampling location in the Lage Afdeling drainage area during the period January 2014 to October 2015. Figure 5.1 shows the positions of the monitoring locations.

observation. The DRP concentrations were low during the first half year of 2014 and 2015. There was an increase of the DRP concentration in July 2014 and July 2015. During the first half year of 2014 and 2015 the TP concentration was dominated (> 90%) by particulate P while in the second half year about 50% of the TP concentration consisted of DRP.

The seasonal variation of the DRP concentrations of the Lage Vaart channel water at the pumping station (location 1) followed the trend of the Oostvaardersplassen. Although less pronounced, this seasonal variation applied as well for the agriculture-dominated water (location 3 and 4) and the urban water (location 2). The TP concentrations were higher during the summer months than during winter months. The groundwater within the Lage Afdeling drainage area has relatively high dissolved P concentrations (Figure S5.3).

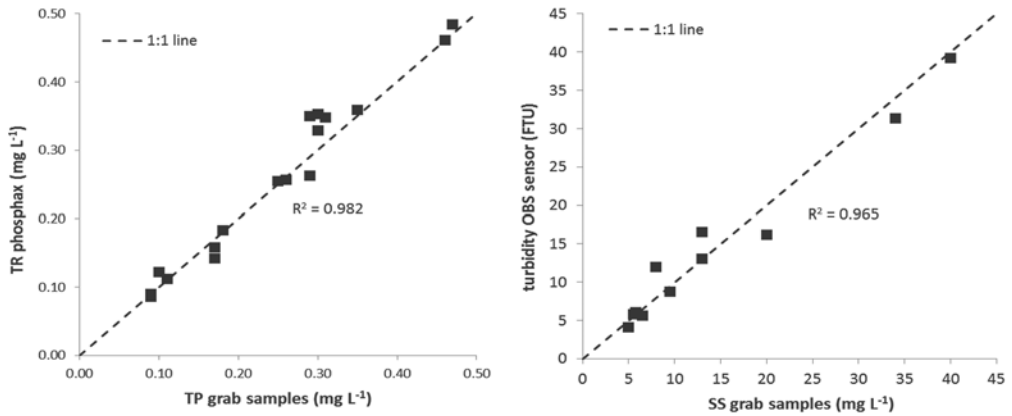


**Figure S5.2.** Total phosphorus (TP) and suspended sediment (SS) concentration from grab samples vs. the concentration measured by the continuous monitoring devices.



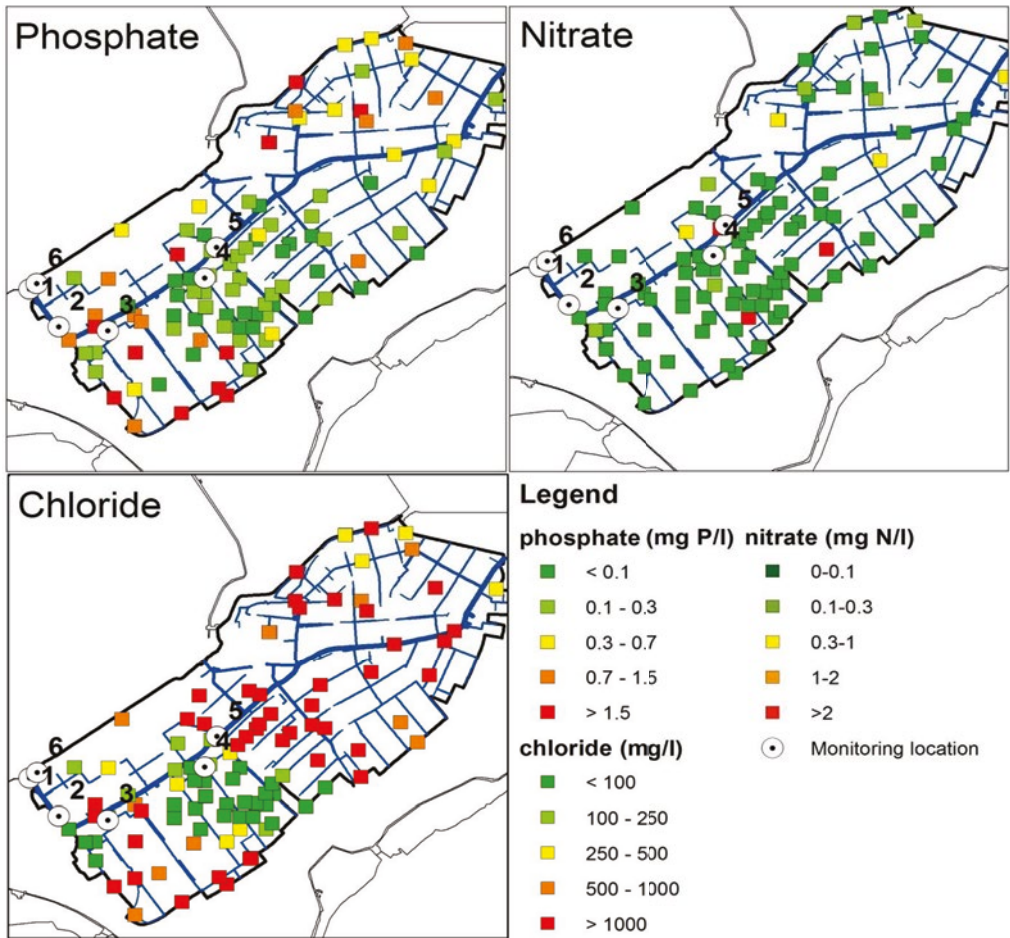
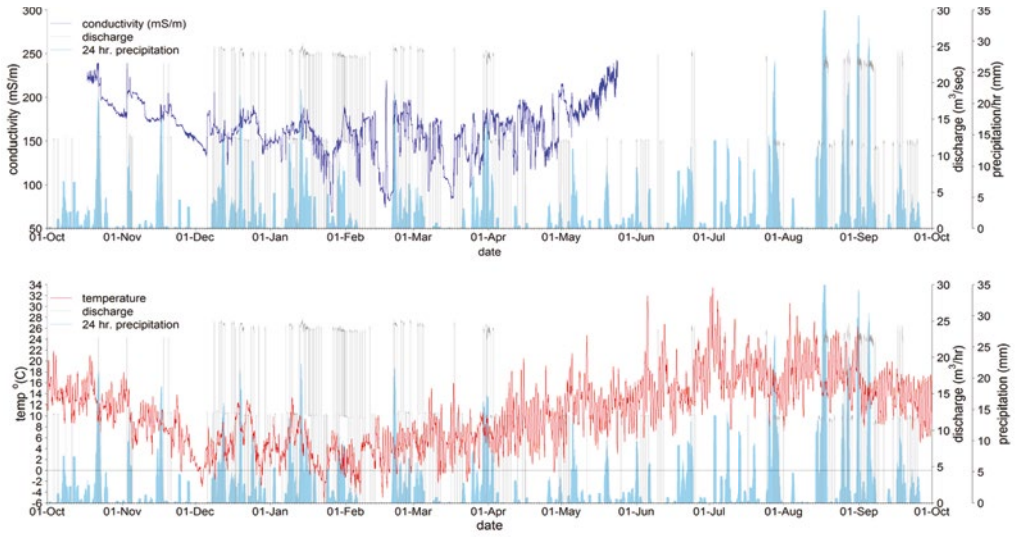
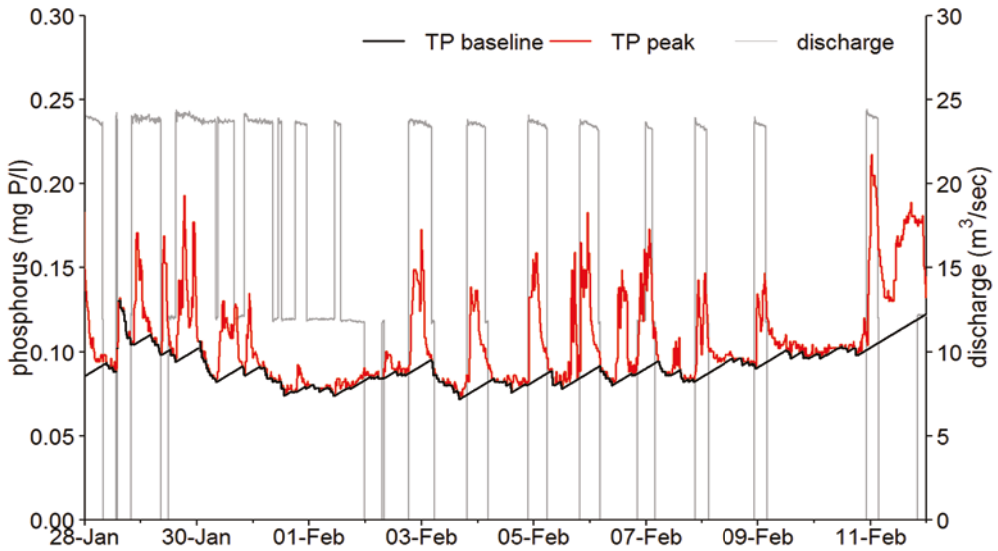


Figure S5.3. Phosphate, nitrate and chloride concentrations in groundwater down to 30 m depth (data from Griffioen et al., 2013).



**Figure S5.4.** Conductivity, air temperature (from KNMI weather station Lelystad). Due to malfunctioning of the CTD divers, conductivity measurements from June 2015 were lost.



**Figure S5.5.** Separation of the high-frequency TP concentration data into baseline concentrations and peak concentrations.

**Table S5.1.** Estimated parameters and associated standard deviations.

Parameter	Value	Standard deviation
A*	0.006956	0.000954
n	1.425	0.03073
a	0.003274	7.70e-05
α	4.311	0.1349

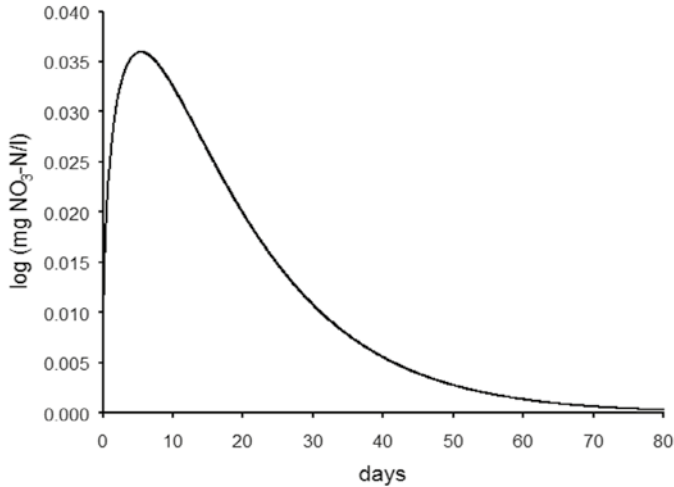


**Figure S5.6.** Impulse response function for log-nitrate concentration resulting from an impulse of 1 mm rainfall.

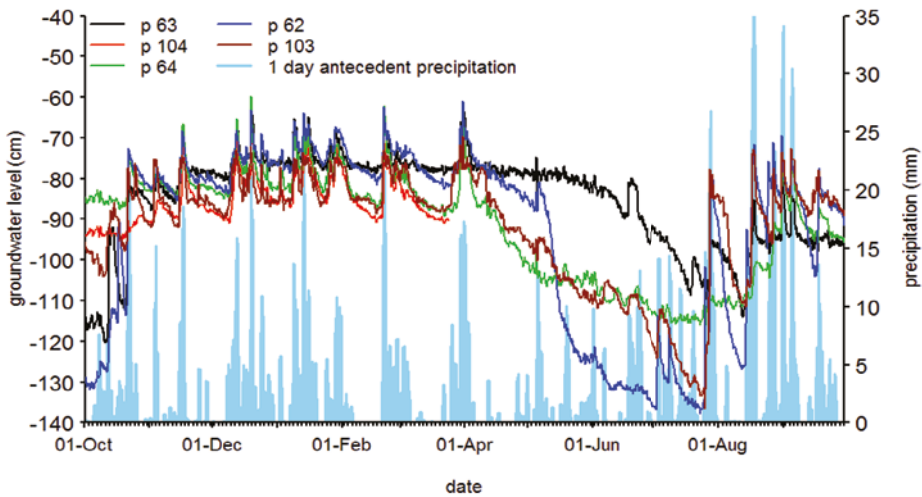


**Figure S5.7.** Groundwater levels (in cm below surface) within the Lage Afdeling drainage area. Figure 5.1 for locations of the groundwater wells.

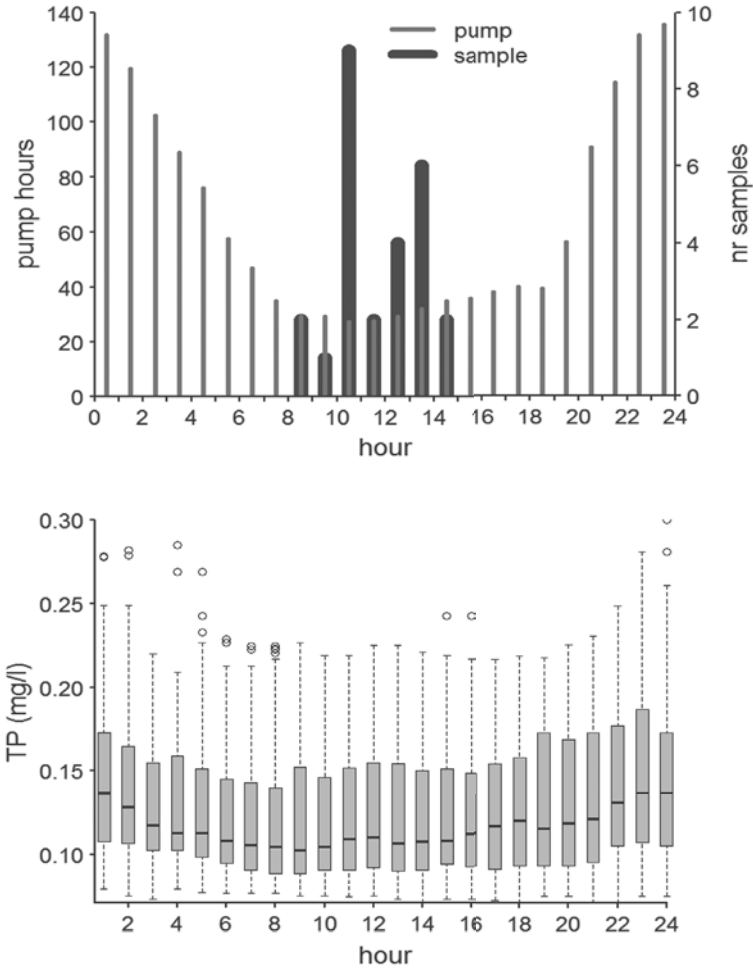


**Figure S5.8.** Hourly distribution of pump hours and water quality sampling during the period October 2014–March–2015 (A) and boxplots of measured TP concentrations during the months January–February 2015. The lower and upper side of the box represent the 0.25 and the 0.75 quantile. Whiskers extend to the maximum and minimum value unless the values are larger than 1.5 times the box length. Open circles are extreme values.

# CHAPTER 6

## **Erodibility of soft sediments from drainage ditches and channels in lowland catchments and associated phosphorus release**

Bas van der Grift, Miguel de Lucas Pardo,  
Leonard Osté, Jasper Griffioen

## 6.1 Abstract

Phosphorus (P) losses from agricultural soils may cause eutrophication problems in surface water. Hydrodynamic resuspension of P stored in bed sediments of watercourses is commonly considered to contribute a high percentage of the annual P flux in lowland catchments. Using a U-GEMS erosion device that quantifies the erosion rate as a function of bed shear stress, we studied the erodibility of soft sediments in drainage ditches, from which P entrainment of the water column can be derived. Experiments with undisturbed sediment cores from field ditches and secondary channels in two polder catchments in the Netherlands revealed that the critical shear stress for erosion ranged between 0.1 and 0.28 Pa. Above the critical shear stress the sediment erosion rate and P release were almost linearly related to the bed shear stress. More easily eroded bed sediments had lower bulk densities and higher water contents and were sampled further downstream. By using a regional hydrodynamic model of a polder, we additionally show that bed shear stresses above 0.1 Pa rarely occur in watercourses of polder catchments. Such catchments typically have a dense network of drainage ditches and the water flow is strongly controlled by weirs and pumping stations. This geographical setting tempers peak flow following rainstorms and thus results in hydrodynamic forces that are not strong enough to cause erosion of bed sediment. A polder can thus be considered as a comprehensive peak flow control system that mitigates P export loads from agricultural fields to downstream surface water bodies. Limited erosion of easily resuspendable matter was, however, observed at bed shear stresses below the critical shear stress. This is often referred to as floc erosion and may contribute to P transport in polder catchments, especially in watercourses near pumping stations, where flow velocities are relatively high.

## 6.2 Introduction

Phosphorus (P) losses from agricultural fields may cause eutrophication of local surface waters or downstream surface water bodies such as lakes, rivers and coastal zones (e.g. Schindler, 2012). This holds strongly for the Netherlands where, for decades, P surpluses on agricultural land were among the highest in Europe (Bouraoui and Grizzetti, 2011; Oenema et al., 2007). However, before P loads applied on agricultural land cause eutrophication of surface waters, they must undergo a series of transport processes. First, P has to be leached from the soil to the surface water. Second, it has to be transported through a series of watercourses, from headwater drainage ditches to downstream regional surface water bodies. Various studies (e.g. Evans and Johnes, 2004; Evans et al., 2004b; Reddy et al., 1999) argue that processes occurring in a watercourse or stream reach (in-stream processes) are critical for determining P transport in catchments. The in-stream transport of P is controlled by a complex interplay between physical advection/diffusion, chemical adsorption/desorption and precipitation/dissolution and biological uptake/release processes which remove and/or transform P during downstream transport and retain it in a form not readily released under normal conditions (Reddy et al., 1999; Withers and Jarvie, 2008). Withers and Jarvie (2008) argue that the importance of various biotic and abiotic in-stream processes on the P retention is typically site-specific and varies with flow velocity, discharge, biological, and chemical characteristics of the water column and the underlying sediments. Consequently, knowledge about the importance of these processes specifically in relation to the typical characteristics of the catchment of interest is essential for the improvement of water quality management in catchments.

The P speciation observed at outlet locations of agriculture-dominated catchments in the Netherlands can be characterised by low ratios of dissolved reactive phosphate (DRP) over total phosphorus (TP), particularly in winter (Van der Grift et al., 2016c). Hence, agricultural P loads to ditches, channels and streams as present in the geographical settings of the Netherlands are dominantly associated with particulate phosphorus (PP). Phosphorus loads to surface water that originate from soil surface or field drain runoff are dominated by PP forms (Van der Salm et al., 2012; Withers et al., 2009). Tube-drain discharge also contains a significant amount of PP (King et al., 2015; Regelink et al., 2013; Ulén, 2004). Furthermore, dissolved P loads from groundwater exfiltration, including tube-drain discharge, can be immobilised to PP along the flow path from groundwater into surface water or in the surface water itself, due to the precipitation of Fe(III) hydroxyphosphates (Baken et al., 2015a; Baken et al., 2015b; van der Grift et al., 2016a; Van der Grift et al., 2014) or Ca solids (Griffioen, 2006; House, 2003) formed during the aeration and degassing of anoxic groundwater. Because PP is subject to sedimentation by gravity during low flow conditions, P losses from agricultural fields may be stored temporarily in the bed sediment of drainage ditches, channels or streams. De Klein (2008) showed that P retention in a small Dutch watercourse was largely determined by sedimentation.

After being stored in the bed sediment, P may be rereleased to the water column, due to biogeochemical remobilisation of PP in the sediment layer followed by diffusion of dissolved P into the water column or by flow-induced resuspension of sediments and associated particulate P during storm flow events (e.g. Withers and Jarvie, 2008). The latter process is commonly accepted to be a

main P transport mechanism during high discharge events in lowland catchments (e.g. Evans et al., 2004a; Haygarth et al., 2005; Kaushal et al., 2014; Kleeberg et al., 2008; Mulholland et al., 1985; Nyenje et al., 2014) and often constitutes a high percentage (up to 88%) of the total annual P flux (e.g. Banner et al., 2009; Kleeberg et al., 2007). A number of studies have additionally reported that DRP concentrations increase during storm events (e.g. Evans et al., 2004a; Roelsma et al., 2011b; Stutter et al., 2008). However, the processes leading to such increases in concentrations are not fully understood. This mobilisation response may be the result of flushing of soil water that is enriched in DRP concentrations, rapid desorption of P from particles that have been resuspended from the bed sediment or eroded from the soil, or release of pore water DRP from the sediment layer during resuspension.

As storm events have been recognised as a key factor for P transport in lowland catchments, it is important to understand the mechanisms that control resuspension of sediment particles and to know how P mobility and concentration (both PP and DRP) change as a result of the resuspension of particles from the bed sediment. This particularly applies to surface water bodies that drain agricultural areas where the P speciation is dominated by PP and bed sediments are typically fine-grained and therefore cohesive. Both the resuspension and transport of fine-grained sediments are largely driven by changes in hydrodynamic forces at the sediment-water interface. These initiate and control the particle exchange between the sediment layer and water column and thus cause erosion (Grabowski et al., 2011; Kleeberg et al., 2008; Winterwerp et al., 2012). To be eroded from the bed sediment, fine particles need to be subjected to higher velocities than expected from their size, due to their cohesive character (Winterwerp et al., 2012). However, once suspended, it can take a long time for these fine particles to resettle and therefore they can also be transported over longer distances than expected (Kleeberg et al., 2008).

In areas such as the Netherlands, which have a flat topography and surface elevation around or below sea level, water levels are mainly regulated by pumping stations, water inlet locations and a dense artificial network of main channels, secondary channels and field ditches. In the Netherlands, polder catchments enclosed by dikes and with pumping stations controlling the water level cover 60% of the land surface (Van de Ven, 2004). Polders are found in all delta areas worldwide and are important agricultural areas with high risks for P surpluses and eutrophication of surface water within the polder or in receiving surface water bodies. The water flow in polders is not a function of free discharge but is controlled by pumping stations. The maximum discharge is determined by the capacity of the pumping stations. An increase of suspended particulate matter (SPM) and PP concentrations has been measured in channels near the pumping station during pumping (Van der Grift et al., 2016b; Van der Grift et al., 2016c). The potential for erosion of bed sediments and resuspension of PP in the secondary channels and ditches connected to the main channel is, however, not clear. Flow velocities of water in these smaller watercourses are typically low, but due to the fluffy nature of the sediments, erosion occurs at a very low bed shear stress even though the force of the water is low.

To our knowledge, the erodibility of bed sediments and P mobility and concentration changes of particulate and dissolved P due to flow-induced resuspension from bed sediments has never been measured in small freshwater channels and ditches in lowland catchments. This limits the



understanding of P transport from agricultural source areas to downstream surface water bodies associated with changing flow conditions in such catchments. Therefore, the aims of the research described here were: (1) to determine the erodibility of soft drainage ditch sediments in polder catchments; (2) to quantify the P entrainment due to resuspension; (3) to assess the potential of polder catchments to retain sedimented P. In this paper, we present the results of a series of resuspension experiments with undisturbed sediment cores from field ditches and secondary channels in two polder catchments in the Netherlands. An erosion device was used to quantify the erosion rate as a function of bed shear stresses.

### 6.3 Theoretical backgrounds

One of the key factors in the transport and fate of SPM is the exchange of fine sediment between the bed sediment and the water column above. For this reason, the erosion and deposition of cohesive sediments has been studied extensively (Winterwerp et al., 2012 and references therein). Erosion of cohesive sediment beds is commonly described as a function of the bed shear stress using the Krone–Partheniades formula (Winterwerp et al., 2012):

$$E = M \left( \frac{\bar{\tau}_b - \tau_{cr}}{\tau_{cr}} \right) \text{ for } \bar{\tau}_b > \tau_{cr} \quad (6.1)$$

where  $E$  ( $\text{g m}^{-2} \text{s}^{-1}$ ) is the erosion or resuspension flux,  $M$  ( $\text{g m}^{-2} \text{s}^{-1}$ ) is an erosion rate parameter,  $\bar{\tau}_b$  (Pa) the mean bed shear stress, and  $\tau_{cr}$  (Pa) a critical (i.e. threshold) shear stress for erosion. Resuspension (or erosion) of particles from the streambed sediment takes place if the shear flow exceeds a critical value for resuspension, the critical (threshold) shear stress for erosion. The critical shear stress for erosion  $\tau_{cr}$  is generally assumed to be a constant material parameter, but may vary with depth and time because of consolidation and physicochemical effects (Winterwerp et al., 2012). As reviewed by Grabowski et al. (2011), a broad range of sediment properties are known to influence the erodibility of the fine sediment beds, including particle size distribution, bulk density, water content, water geochemistry, organic matter content and extracellular polymeric substances produced by sediment inhabitants such as bacteria and diatoms. Other factors known to influence erodibility are bioturbation (De Lucas Pardo et al., 2013) and biofilm growth (Valentine et al., 2014). Typical values for critical bed shear stress for erosion are  $0.1 \text{ Pa} < \tau_{cr} < 5 \text{ Pa}$  (Winterwerp et al., 2012). In addition, the erosion rate parameter  $M$  may vary with time and depth, but is commonly also kept constant. A typical range of values is  $0.01 \text{ g m}^{-2} \text{ s}^{-1}$ – $0.5 \text{ g m}^{-2} \text{ s}^{-1}$  (Winterwerp et al., 2012). Hence, the strength or erodibility of a bed sediment depends on both  $M$  and  $\tau_{cr}$ . Highly erodible sediment would have a low critical shear stress and/or high erosion rate at low excess shear stress, i.e. a high erosion rate parameter.

It is difficult to develop a unifying equation to predict erodibility based on sediment properties because of the lack of a complete mechanistic understanding of how the key sediment properties interact to influence sediment erodibility (Grabowski et al., 2011). The critical shear stress of resuspension and the erosion rate of cohesive and loosely structured sediments must therefore

be obtained by direct measurements (Grabowski et al., 2011; Lau and Droppo, 2000). To measure sediment erodibility and associated nutrient entrainment under conditions of increasing flow, erosion devices have been designed. These devices have been used to investigate nutrient release in marine environments (Couceiro et al., 2013; Kalnejais et al., 2010; Wengrove et al., 2015), freshwater lakes (Kleeberg and Herzog, 2014) and lowland rivers (Kleeberg et al., 2007, 2008). Erosion devices impose a known shear stress at the sediment–water interface, and sampling of the outflowing water allows for the evaluation of both erosion and local chemical transformations associated with a range of shear stresses. The SPM concentration is commonly measured with a turbidity meter.

A typical example of the increase in SPM concentration at the suction outlet of an erosion microcosm system as function of the applied bed shear stress is given in Figure 6.1A. The eroded mass can be calculated from the turbidity data using the following equation:

$$E = c \cdot Q \cdot \Delta t \quad (6.2)$$

where  $E$  is the eroded mass (g),  $c$  is the SPM concentration ( $\text{g L}^{-1}$ ) in the outflowing water,  $Q$  is the discharge ( $\text{L s}^{-1}$ ) of water through the suction outlet, and  $\Delta t$  (s) is the interval between two measurements of the turbidity meter. The erosion rate ( $\text{g m}^{-2} \text{s}^{-1}$ ) can then be calculated by dividing the eroded mass by the area of the microcosm section, and by the number of seconds within each bed shear step. Hence, one erosion rate can be obtained for each bed shear stress step applied.

The critical shear stress for erosion ( $\tau_{cr}$ ) and the erosion rate parameter ( $M$ ) from the Krone–Partheniades formula (Eq. 6.1) can be derived from the experiments by plotting the erosion rate against the applied mean bed shear stress ( $\bar{\tau}_b$ ) as shown in Winterwerp et al. (2012) based on results of Partheniades (1965) (Figure 6.1B):

## 6.4 Material and Methods

### 6.4.1 Sampling and study sites

Undisturbed cylindrical sediment cores were collected from two polder catchments in the Netherlands: Noordplaspolder and Quarles van Ufford polder (Figure 6.2). Two sediment cores were taken at each sampling location, using cylinders with a diameter of 0.1 m and length of 0.2 m. The cylinders were half-filled with sediment and half-filled with ditch water and could be used directly in the erosion experiment without resampling or transferring the sediment. Unfiltered ditch water that was needed for pumping through the chamber was sampled at the same time and the same location. Additionally, water samples were taken for chemical analysis as described in section 2.3. Subsamples for analysis of dissolved concentrations were filtered using 0.45  $\mu\text{m}$  pore size cellulose nitrate filters.

The land use in both polders is dominated by agriculture. Noordplaspolder, a former lake, is in the west of the Netherlands and has marine clay soils. The polder lies 4 to 5 m below mean sea level. It is characterised by significant groundwater exfiltration containing high levels of chloride, phosphorus and iron (De Louw et al., 2011). Surface water levels are controlled through two pumping stations.

Samples were taken at both ends and in the middle of a field ditch 300 m long and in a secondary channel 25 m upstream of a weir that controls the water level in a separate drainage area within the polder.

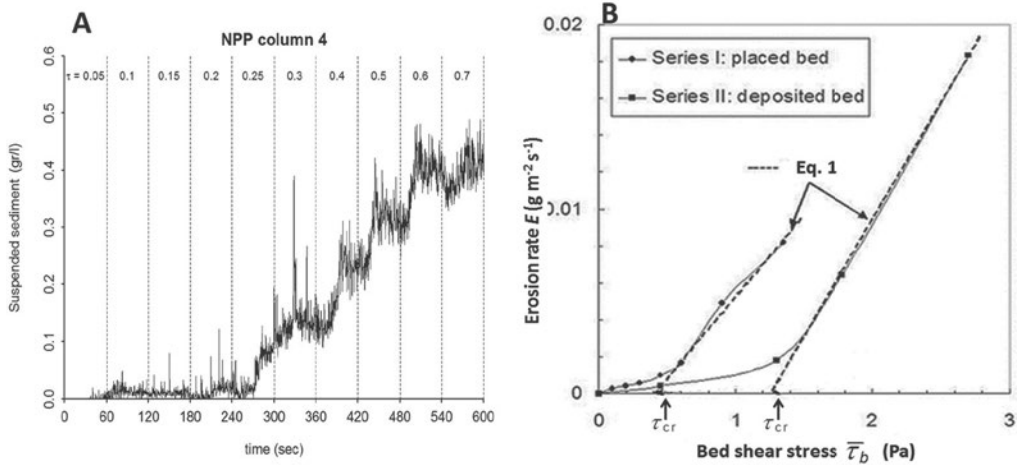


**Figure 6.1.** Results obtained from erosion experiments: (A) Typical example of bed shear stress applied and suspended particulate matter concentration as measured with an erosion microcosm chamber (data from this study) and (B) example showing how the critical bed shear stress ( $\tau_{cr}$ ) and the erosion rate parameter (M) can be calculated from measured erosion rates according to Eq. 6.1 (redrawn from Partheniades (1965)).

Quarles van Ufford is a fluvial clay polder in the centre of the Netherlands, lying between the river Meuse (south) and the main branch of the Rhine known as Waal (north) (Figure 6.7). Surface elevations in the relatively flat area range from 3 to 7m above sea level from west to east. Inlet of water is possible through five human-controlled inlet locations (Rozemeijer et al., 2012). Excess water from Quarles van Ufford drains towards the river Meuse at one outlet location at the western side of the polder. Samples were taken from two secondary channels and one field ditch in the polder.

#### 6.4.2 Erosion experiments

The erosion experiments were performed with an UMCES<sup>1</sup>-Gust Erosion Microcosm System (U-GEMS). U-GEMS is an adaptation of the Gust Microcosm (Gust, 1989, 1990). The U-GEMS can be used to study the erodibility of fine-grained sediment. The characteristic components of this set-up are a spinning disc, as well as a suction inlet in the axis of the spinning disc to provide a continuous suction of ditch water (Figure 6.3). These devices can generate a spatially homogenous bed shear stress by controlling two parameters simultaneously: the rotational speed of the spinning disc and the rate at which water is removed through the suction outlet (Tolhurst et al., 1999). The device

<sup>1</sup> University of Maryland, Centre of Environmental Research

delivers a known shear stress at 8 cm below the spinning disk, which is where the sediment-water interface must be located. The U-GESMS microcosm was calibrated by De Lucas Pardo et al. (2013), using sand of various diameters and Shield/van Rijn's erosion diagram (Van Rijn, 1984). The resulting calibration curve was published in De Lucas Pardo et al. (2013). In every erosion experiment on ditch sediment cores, we applied the following nine bed shear stresses: 0.05, 0.1, 0.15, 0.2, 0.25, 0.3, 0.4, 0.5, 0.6 and 0.7 Pa. Each bed shear stress lasted for 60 s. An OSLIM meter (Optical Silt meter, Deltares, the Netherlands) was installed at the suction outlet of the microcosm to measure light attenuation of the particle-laden outflowing water (Figure 6.3). This OSLIM meter was calibrated with SPM suspensions at different concentrations made of the sediments to be studied. The eroded mass and the erosion parameters  $\tau_{cr}$  and  $M$  were calculated according to the description in section 2.



**Figure 6.2.** Noordplas and Quarles van Ufford study areas and the spatial distribution of polder areas in the Netherlands.

### 6.4.3 Water and sediment analysis

A water sample for chemical analysis was taken throughout each one-minute  $\bar{\tau}_b$  interval. Selected subsamples were immediately filtered through 0.45  $\mu\text{m}$  nylon membranes and acidified to a pH of 1 using suprapure nitric acid. The samples were analysed for dissolved metals by ICP-OES. A second set of subsamples was immediately filtered using 0.45  $\mu\text{m}$  nylon membranes and analysed for DRP by using the colorimetric molybdenum blue method (Koroleff, 1983). Total P and total Fe were determined in unfiltered subsamples after aqua regia digestion and analysis with ICP-OES.

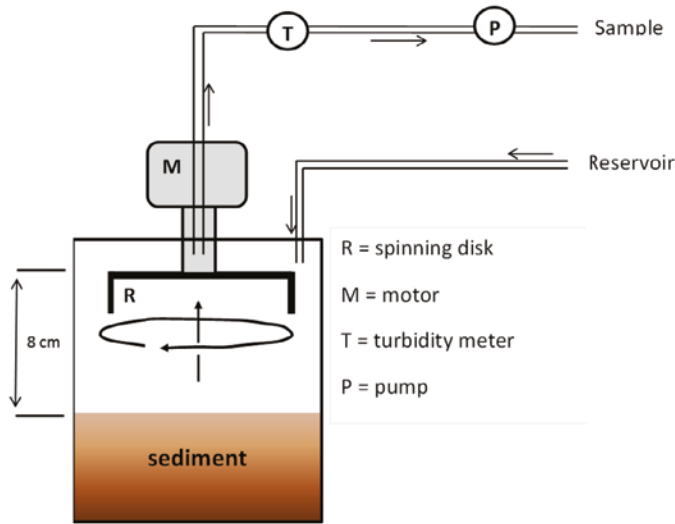


**Figure 6.3.** Experimental laboratory set-up for determining the erodibility of bed sediments and phosphorus resuspension due to erosion.

The composition of the surface sediment (0–1 cm) was determined by standard methods. This surface layer was sampled after completion of the erosion experiment and thus does not fully represent the properties of the eroded matter. The sediment water content was calculated after freeze-drying the samples. Water content ( $W$ ) is a well-known soil mechanics parameter, and is defined as: mass of water/mass of solids. Organic matter (OM) and total carbonates were determined using thermogravimetric analysis (TGA) by slowly heating to 1000°C. The weight loss between 105 and 550°C is a proxy for organic matter and the weight loss between 550 and 800°C is the proxy for total carbonates. The bulk density was calculated as a weighted mean, using the percentage of constituents and their specific density (water 1.0 g cm<sup>-3</sup>, OM 1.4 g cm<sup>-3</sup>, mineral constituents 2.65 g cm<sup>-3</sup>). Total metal contents and total P were analysed with ICP-OES after aqua regia digestion. The particle size distribution of the samples was measured with a laser diffraction particle size analyzer using chemical and ultrasonic dispersion. Two series of samples were analysed: one without treatment and one following pre-treatment with hydrogen peroxide and hydrochloric acid to remove the organic matter and carbonate fractions.

#### 6.4.4 Quarles van Ufford hydrodynamic model

A SOBEK-Delwaq model was used to simulate the water flow and bed shear stress in the main ditches and channels of Quarles van Ufford polder. SOBEK is an integrated model that has multiple modules able to model urban, rural or river flows (Deltares, 2016b). The relevant modules in relation to this study are Rural 1DFLOW, RR and Delwaq (Deltares, 2016a). The SOBEK-Rural 1DFLOW can simulate one-dimensional flow in irrigation and drainage systems. To do this, the complete Saint

Venant equations for one-dimensional problems are solved. The Saint Venant equations are derived from the integration of the Navier-Stokes equations, the most important assumption being that the horizontal length is much greater than the vertical depth, as is the case in shallow waters like ditches and channels. RR is the rainfall–runoff module which is often used to model small agricultural headwater ditches that were not explicitly incorporated in the model but were represented as a lumped storage. The Delwaq module calculates the transport of substances and sediment in water systems and incorporates the dynamics of the water system in its calculations (Deltares, 2016a).

The water in Quarles van Ufford polder originates from groundwater discharge (including subsurface tube drains) and inlet from the river Meuse and from the neighbouring polder. Water stages and flow in main ditches and channels are controlled by admitting and discharging water of water and a series of 10 (small) pumping stations and 178 weirs (Udo and Bakker, 2009). Groundwater inputs were derived from a regional groundwater model (Van der Linden et al., 2008). Precipitation data for this research was derived from a nearby precipitation measurement station of the Royal Dutch Meteorological Institute (KNMI) in Megen. The model was calibrated on measured water levels and discharges at six locations. A detailed description of the model schematisation and input data is given in Udo and Bakker (2009).

The bed shear stress was calculated by the Delwaq module from the water flux ( $\text{m s}^{-1}$ ) using the following equation:

$$\bar{\tau}_b = \frac{\rho \cdot g \cdot q^2}{C^2} \quad (6.3)$$

In which  $\bar{\tau}_b$  is the bed shear stress (Pa),  $\rho$  is the density of the water ( $\text{kg m}^{-3}$ ),  $g$  is the gravitational acceleration ( $\text{m s}^{-2}$ ),  $q$  is the flow velocity ( $\text{m s}^{-1}$ ) and  $C$  is the Chézy bed-friction coefficient ( $\text{m}^{1/2} \text{s}^{-1}$ ). The Chézy coefficient was calculated according to the Bos-Bijkerk formulation for bed friction (De Bos and Bijkerk, 1963), which describes the Chézy coefficient as a function of the water depth, hydraulic radius and the Bos–Bijkerk friction parameter  $\gamma$  (1/s). The latter parameter normally ranges between 20 and 40, so the Chézy coefficient value depends on this parameter, the depth of water and hydraulic radius:

$$C = \gamma^3 \sqrt{d} \sqrt[6]{R} \quad (6.4)$$

In which  $d$  is the water depth (m) and  $R$  is hydraulic radius (m) i.e. the wetted area of the channel cross-section ( $\text{m}^2$ ) divided by the wetted perimeter (m). For the Quarles van Ufford model,  $\gamma$  was set at 34, the value suggested by De Bos and Bijkerk (1963) for channels in the Netherlands during the winter and that is commonly used in hydrodynamic models in this country.

## 6.5 Results

### 6.5.1 Sediment composition

The sediments studied can be characterised as mud-like, with water contents ranging between 1.9 and 4.2 (Table 6.1). The OM content varied between 6.1 and 17.5% (in dry weight). At some locations (e.g. NPP7–NPP8 and Q1–Q2) there was a remarkably large difference in OM content between the two sampled sediment cores. Overall, the carbonate content varied between 0.8 and 4.9% and was lower in sediment from Quarles van Ufford polder than in sediment from Noordplas polder. The carbonate content of the secondary channel sediment in the Noordplas polder was higher than that from the field ditch sediment. The grain size distribution of the sediment treated with hydrogen peroxide and hydrochloric acid was somewhat finer than that of the untreated samples, except for sample NPP7, which is coarser-grained than the other samples. The sediment from Quarles van Ufford was finer-grained and had a lower bulk density and a higher water content than the sediments from Noordplas polder. On the other hand, the sediment from Quarles van Ufford had higher Fe and P contents (on average, 2.2 times higher for Fe and 1.6 times higher for P) than the samples from Noordplas polder.

### 6.5.2 Erosion rate

Figure 6.4 shows the erosion rate as a function of the bed shear stress for the different sediment cores. All sediment cores showed a very small or even absent increase in the erosion rate with increasing bed shear stress until the critical shear stress for erosion was reached. The  $\tau_{cr}$  varied between 0.10 and 0.28 Pa for the different sediments (Table 6.2); between two sediment cores taken from the same location it varied by up to a factor of two. Despite the large variation in the  $\tau_{cr}$  between the duplicates from the field ditch in Noordplas polder,  $\tau_{cr}$  seems to decrease from the beginning to the end of the field ditch. The  $\tau_{cr}$  of the secondary channel sediment from Noordplas polder could not be distinguished from that of the field ditch sediments.

When  $\bar{\tau}_b$  exceeded  $\tau_{cr}$ , the erosion rate ( $E$ ) increased nearly linearly with  $\bar{\tau}_b$  (Figure 6.4). Significant erosion of the bed only occurred at  $\bar{\tau}_b$  above 0.2–0.3 Pa. Four of the 14 experiments showed almost ideal erosion behaviour, with a linear increase of the erosion rate with increase of  $\bar{\tau}_b$  over the shear stress range from  $\tau_{cr}$  to 0.7 Pa. In five of the 14 experiments, the increase in erosion rate levelled off at  $\bar{\tau}_b$  above 0.5 or 0.6 Pa. Three experiments showed a convex increase of erosion rate with increasing  $\bar{\tau}_b$  values, meaning that the erosion rate increased more than expected from the increase in  $\bar{\tau}_b$  above values of 0.4 Pa. During two experiments (Q4, Q6), erosion rates decreased temporarily with the increase of  $\bar{\tau}_b$ . This decrease in erodibility might be attributed to starvation of erodible sediment during the one-minute experimental stage with the applied  $\bar{\tau}_b$ .

The values of erosion rate parameter ( $M$ ) as calculated using Eq. 6.1 varied between 0.056 and 0.45  $\text{g m}^{-2} \text{s}^{-1}$  (Table 6.2). The  $M$  values for the field ditch sediments ranged from 0.056 to 0.159  $\text{g m}^{-2} \text{s}^{-1}$  whereas the secondary channel sediments had  $M$  values that ranged from 0.156 to 0.450  $\text{g m}^{-2} \text{s}^{-1}$ . Thus, the  $M$  values were higher for the secondary channels than for the field ditches in both polders, while  $\tau_{cr}$  did not differ between the field ditches and the secondary channel.

**Table 6.1.** Physical and chemical properties of the surface layer (0–1 cm) of sediment cores from Noordplaspolder (NPP sediment cores) and Quarles van Uffordpolder (Q sediment cores) that were used for the erosion experiments.

Location	sediment core	water content –	bulk density g cm <sup>-3</sup>	organic matter %*	carbo-nates %*	particle size distribution untreated samples		particle size distribution treated samples		Total P mg kg <sup>-1</sup>	Total Fe mg kg <sup>-1</sup>	Fe/P ratio mol/mol		
						d10 (µm)	d50 (µm)	d10 (µm)	d50 (µm)				d90 (µm)	
field ditch beginning	NPP1	2.0	1.49	16.7	1.4	4.8	27	196	2.4	15	100	1282	31265	13.5
	NPP1a	2.7	1.39	14.7	2.2	5.4	29	213	3.0	27	110	854	25214	16.4
field ditch middle	NPP2	1.9	1.51	14.6	3.9	4.6	24	131	3.1	15	174	1190	32331	21.8
	NPP3	3.1	1.35	15.3	2.7	4.6	22	95	2.5	13	94	796	31232	21.8
	NPP4	2.3	1.45	12.3	3.5	4.2	20	108	2.6	13	100	1241	28603	15.1
field ditch end	NPP5	2.0	1.51	12.0	2.2	4.0	21	121	3.0	22	160	673	26395	12.8
	NPP7	2.3	1.48	6.1	4.7	7.2	60	195	7.3	102	220	1281	15633	6.8
secondary channel	NPP8	4.2	1.29	13.3	5.0	4.9	24	177	3.1	21	150	3575	30910	4.8
	Q1	2.8	1.40	9.3	1.9	3.0	16	75	2.9	11	57	2219	53937	13.5
secondary channel	Q2	3.4	1.33	16.8	1.4	3.4	17	182	1.7	8	60	1712	47620	15.4
	Q3	4.2	1.28	16.4	1.3	3.3	15	107	1.7	8	50	1579	51301	18.0
	Q4	3.4	1.34	12.8	2.4	2.9	14	42	2.4	9	48	3287	85264	14.4
	Q5	2.4	1.43	17.5	1.8	2.4	16	107	2.2	10	164	2361	66668	15.7

\* = in dry weight



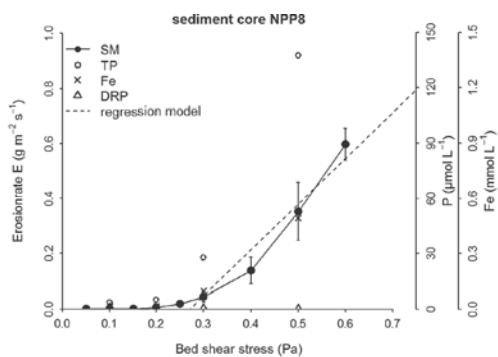
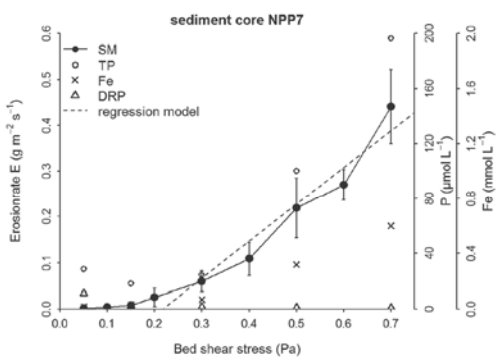
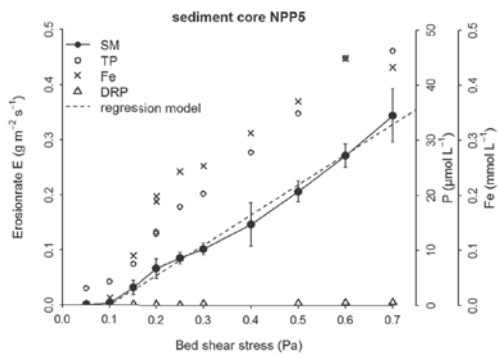
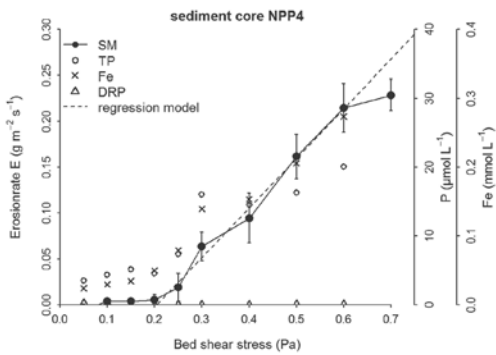
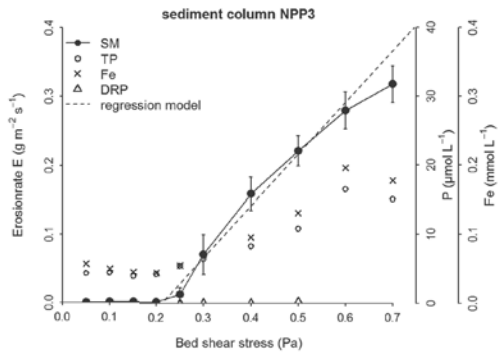
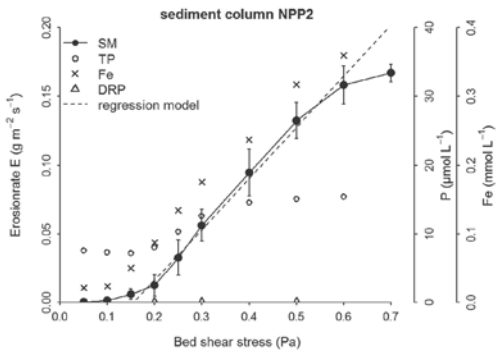
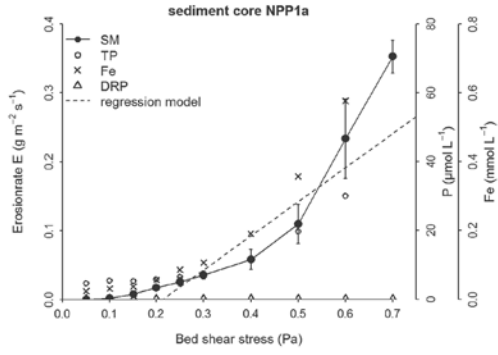
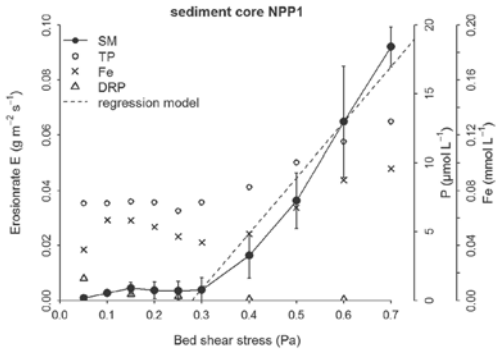
The decrease of the  $\tau_{cr}$  from the beginning to the end of the field ditch in Noordplas polder and the higher  $M$  values for the secondary channels compared with those of the field ditch samples suggest that the erodibility of the bed sediments increased from headwaters to more downstream locations. This is reflected by the sediment water content and the bulk density, which for most secondary channel sediments were lower than those for the field ditch sediments (Table 6.1). Plotting sediment water content against the erosion parameter  $M$  revealed an inverse correlation with an  $R^2$  of 0.75 (Figure 6.5). The bulk density showed a comparable correlation with  $M$ , resulting in an  $R^2$  of 0.60 (not shown). This indicates that with increasing water content or bulk density, the sediment becomes less erodible. No such correlations were found between water content and  $\tau_{cr}$  (Figure 6.5) and between bulk density and  $\tau_{cr}$  (not shown). The values obtained for  $\tau_{cr}$  could not be correlated with these sediment properties. Both erosion parameters,  $M$  and  $\tau_{cr}$  could not be correlated to the particles size of the bed sediment and the organic matter content ( $R^2$  of 0.12 or less).

**Table 6.2.** Critical shear stress for erosion ( $\tau_{cr}$ ) and erosion rate parameter ( $M$ ) as derived from the U-GEMS microcosm chamber experiments.

location	sample	$\tau_b$ regression range (Pa)	$R^2$ regression	$\tau_{cr}$ (Pa)	$M$ ( $\text{g m}^{-2} \text{s}^{-1}$ )
field ditch beginning	NPP1	0.25–0.7	0.96	0.28	0.056
	NPP1a	0.2–0.6	0.86	0.21	0.106
field ditch middle	NPP2	0.2–0.6	0.99	0.16	0.058
	NPP3	0.25–0.7	0.97	0.21	0.159
field ditch end	NPP4	0.2–0.6	0.99	0.20	0.105
	NPP5	0.2–0.7	0.99	0.10	0.055
secondary channel	NPP7	0.2–0.6	0.94	0.22	0.176
	NPP8	0.25–0.6	0.95	0.27	0.450
secondary channel	Q1	0.2–0.6	0.98	0.21	0.268
	Q2	0.15–0.4	0.99	0.15	0.177
secondary channel	Q3	0.2–0.7	0.98	0.22	0.357
	Q4	0.15–0.5	0.98	0.10	0.156
field ditch	Q5	0.15–0.6	0.96	0.12	0.073
	Q8	0.15–0.7	0.92	0.13	0.064

### 6.5.3 Total P, dissolved reactive P and Fe concentrations

The major trends in the plots of TP and total Fe concentrations in the outlet water of the erosion chamber versus  $\bar{\tau}_b$  were similar. When  $\bar{\tau}_b$  increased above the  $\tau_{cr}$  value, the concentrations of both species increased in a similar way as the erosion rate (Figure 6.4). No experiment showed an increase in DRP concentrations during the experimental stage, irrespective of whether  $\bar{\tau}_b$  was higher or lower than  $\tau_{cr}$ . This clearly shows that in our experiments, entrainment of the water column with DRP due to release of pore water DRP or desorption of DRP from eroded particles did not occur.



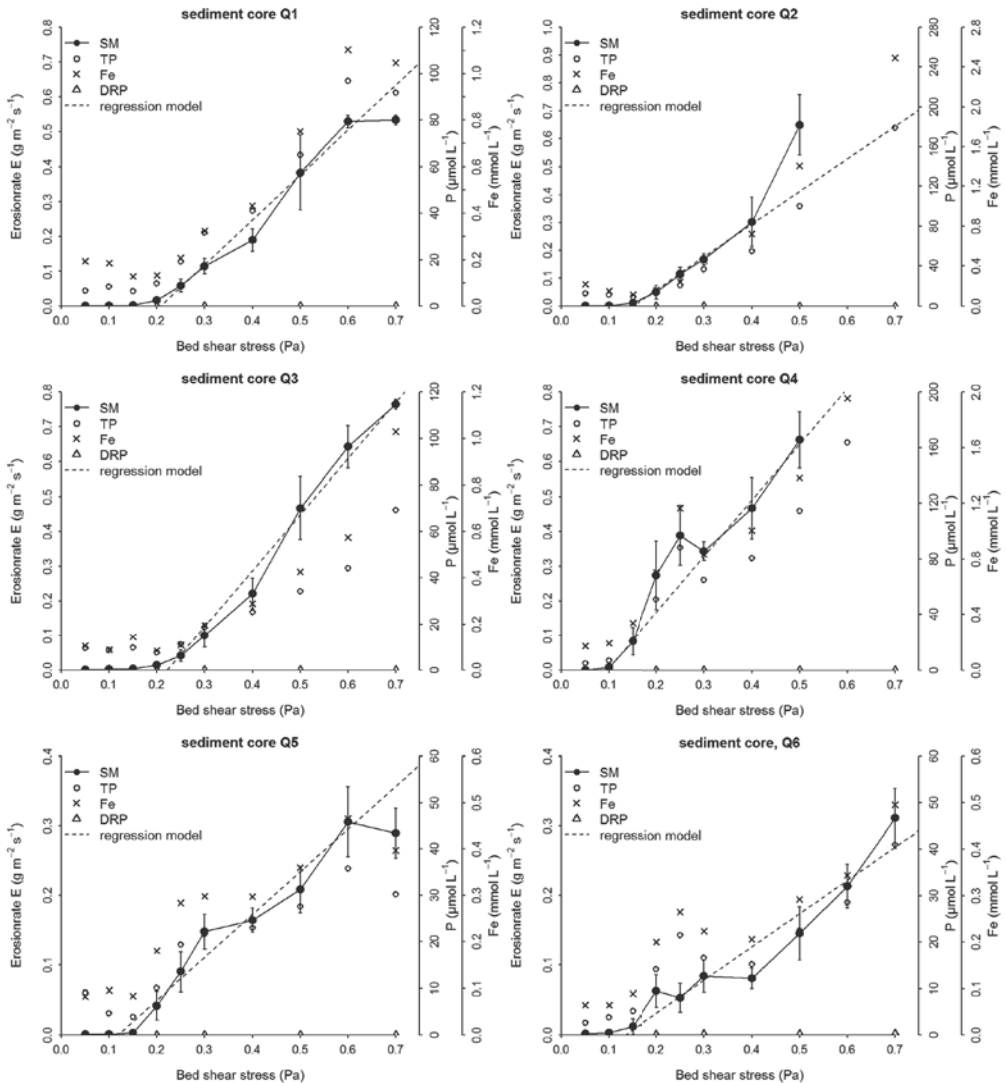


**Figure 6.4.** Erodibility of drainage ditch sediments represented as suspended particulate matter and total P and Fe concentrations at the suction outlet of the U-GEMS microcosm as function of bed shear stress ( $\bar{\tau}_b$ ). The dashed line represents the regression model from which the critical shear stress ( $\tau_{cr}$ ) and the erosion rate parameters ( $M$ ) have been derived (Eq. 6.1). Note the different y-axis scales.

The total Fe concentrations during the initial stage of the experiment were in the range of 0.1–0.2 mmol L<sup>-1</sup> for the Quarles van Ufford columns and 0.01–0.08 mmol L<sup>-1</sup> for the Noordplaspolder samples. The dissolved Fe concentrations, which were below 0.01 mmol L<sup>-1</sup>, were low. The TP concentration during the initial stage did not differ between the two areas and varied between 3.1

(NPP3) and  $12.4 \text{ (Q2)} \mu\text{mol L}^{-1}$ , except for experiment NPP7, which had a higher initial TP concentration ( $28.7 \mu\text{mol L}^{-1}$ ). This sediment core also showed slightly elevated DRP concentrations during the initial stage of the experiment ( $11 \mu\text{mol L}^{-1}$ ), probably as a result of reducing conditions appearing in the top sediment layer before the start of the experiment and the subsequent release of DRP into the water column. The dissolved Fe concentration, which was  $6 \mu\text{mol L}^{-1}$ , was not noticeably higher. In all the other experiments, dissolved reactive P concentrations were low during the initial stage (in most cases below the detection threshold of  $0.3 \mu\text{mol L}^{-1}$ ). The TP and total Fe concentrations measured during the experimental stage where  $\bar{\tau}_b$  was lower than  $\tau_{cr}$  can be explained by very fine-grained or colloidal SPM being present in the water column before the start of the experiment, which had not settled by gravity.

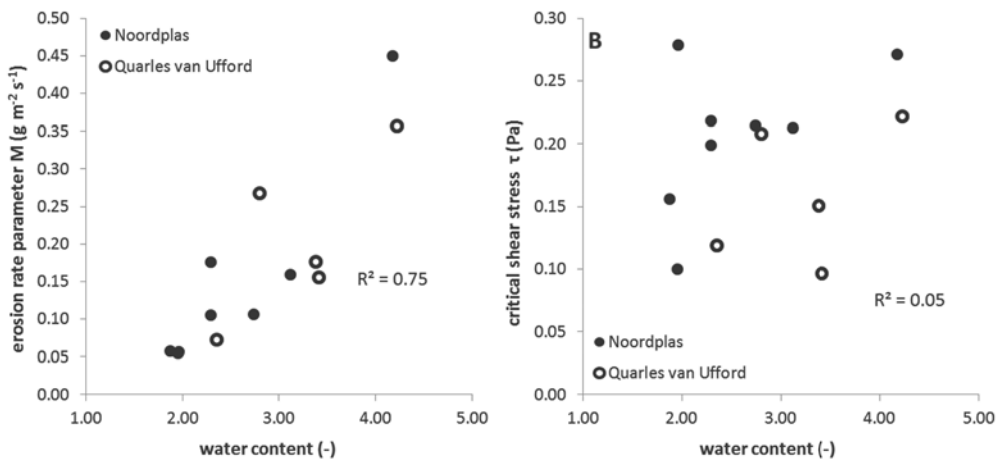


**Figure 6.5.** Relationship between sediment water content and erosion parameters: (A) water content vs. erosion rate parameter, (B) water content vs. critical shear stress.

The highest TP concentrations were measured in the experiments with the sediment cores from the secondary ditches: NPP7 and NPP8 in Noordplas polder and Q2 and Q4 in Quarles van Ufford (Figure 6.4). The latter two cores also showed the highest Fe concentrations.

In most of the experiments, the P content of the eroded matter decreased with increasing erosion rate (Figure 6.6A+B). The P content of the eroded matter from the Quarles van Ufford sediment cores at erosion rates above  $0.1 \text{ g m}^{-2} \text{ s}^{-1}$  was in the range of the P content of the surface sediment layer ( $1.6\text{--}3.3 \text{ mg g}^{-1}$ , see Table 6.1). However, the P content of the eroded matter from the Noordplas polder sediment cores was higher than the P content of the surface sediment layer ( $0.7\text{--}1.3 \text{ mg g}^{-1}$  except for NPP7, with  $3.6 \text{ mg g}^{-1}$ ).

The molar Fe/P ratio of the eroded matter from the Quarles van Ufford sediments was 12.7 on average and ranged between 9.9 and 18 (Figure 6.6C). This is lower than the Fe/P ratio of the surface sediment layer, which was 15.3 on average and ranged between 13.5 and 18 (Table 6.1). The Fe/P

ratio of the eroded matter remained almost constant with increasing erosion rates in experiments Q1 and Q8, decreased in experiments Q4 and Q5 and increased slightly in experiments Q2 and Q3. The final Fe/P ratios of the latter two experiments, which were 14 to 15, were similar to the Fe/P ratio of surface sediment layer, which indicated that this eroded matter was not enriched in P content compared with the surface sediment layer.

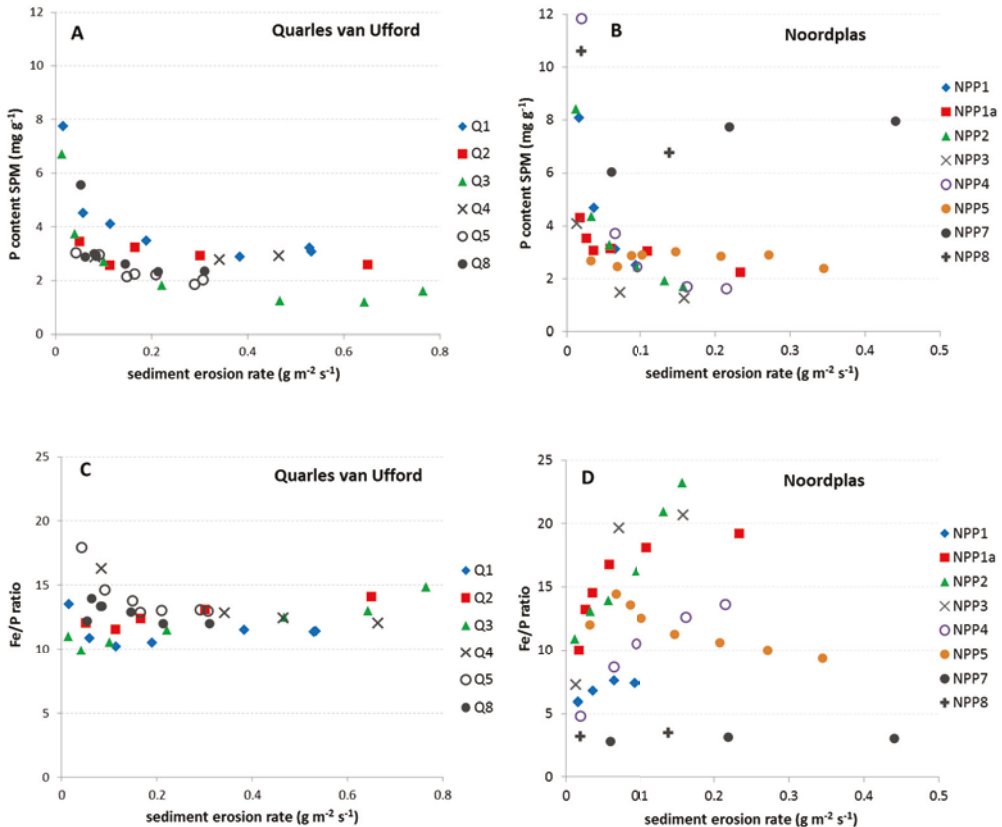


**Figure 6.6.** Sediment erosion rate plotted against phosphorus content of the suspended particulate matter (A+B) and against the molar Fe/P ratio of the suspended particulate matter (C+D).

The eroded matter from the experiments with the sediment cores from Noordplas polder had Fe/P ratios which varied more (Figure 6.6D). Low Fe/P ratios with values of approximately 3 to 3.5 were measured for the secondary ditch (NPP7 and NPP8). This matched with the surface sediment layer, which also had relatively low Fe/P ratios: 6.8 for NPP7 and 4.8 for NPP8. The eroded matter from the field ditch sediments had Fe/P ratios ranging between 6 and 23, and the ratios increased with increasing erosion rates for all sediment cores except NPP5. The Fe/P ratio of the eroded matter during experiments with sediment cores NPP1a, NPP2, NPP3 and NPP4 increased to levels that were

similar to the Fe/P ratio of the surface sediment layer (approximately 15–22, see Table 6.1), but the eroded matter for experiment NPP1 did not reach the level of the surface sediment layer.

## 6.6 Discussion

The experiments clearly revealed that in the watercourses we studied, erosion of particles and associated P release is controlled by bottom shear stress  $\bar{\tau}_b$ . Despite the great variability in the erodibility of the bed sediments, all sediment cores showed a  $\tau_{cr}$  below which there was very little erosion. At  $\bar{\tau}_b$  values above  $\tau_{cr}$  the sediment erosion rate and associated P release were almost linearly related to the  $\bar{\tau}_b$ . The  $\tau_{cr}$  ranged between 0.1 and 0.28 Pa. This range does not deviate greatly from the  $\tau_{cr}$  values reported in the literature. Van Rijn (1993) gives a  $\tau_{cr}$  value of 0.34 for silt sediments with a mean grain size from 31–62  $\mu\text{m}$ . De Lucas Pardo et al. (2013) reported  $\tau_{cr}$  values between 0.2 and 0.3 Pa for bioturbated soft sediment beds from lake Markermeer. Kleeberg et al. (2007) reported higher values of 0.48 and 1.25 Pa for two lowland rivers in northeast Germany with sediments of fine and coarse sand. Winterwerp et al. (2012) reported a range typical values between 0.1 and 5 Pa. The  $M$  values from our experiments ranged between 0.056 and 0.45  $\text{g m}^{-2} \text{s}^{-1}$ . These values are in the range of  $M$  values reported by Winterwerp et al. (2012): 0.01–0.5  $\text{g m}^{-2} \text{s}^{-1}$ . De Lucas Pardo (2014) reported  $M$  values between 0.01 and 0.07  $\text{g m}^{-2} \text{s}^{-1}$  for the soft sediment beds from lake Markermeer, which are thus in the lower range of our measured values.

With respect to the environmental implications regarding the origin of SPM and transport of PP in lowland catchments, the question arises when and how often this  $\tau_{cr}$  will be exceeded in the natural setting of such water systems. The hydrodynamic aspects of sediment erosion and transport are well advanced and, unlike the erodibility of bed sediment, can be predicted by using models (Grabowski et al., 2011). We calculated the maximum  $\bar{\tau}_b$  attained in the watercourses of Quarles van Ufford polder during the period from March 2004 to April 2005 by using the SOBEK-Delwaq model (Figure 6.7). A large majority of watercourses had relatively low maximum  $\bar{\tau}_b$  values. The results from the erosion experiments showed that erosion of bed sediment is likely at  $\bar{\tau}_b$  values above 0.2 and very unlikely at  $\bar{\tau}_b$  below 0.1. The total length of the watercourses in the Quarles van Ufford model was 350 km. The length of watercourses where the maximum  $\bar{\tau}_b$  did not exceed 0.1 Pa was 320 km and the length of watercourses where the maximum  $\bar{\tau}_b$  exceeded 0.2 Pa was 13 km. The channels in which  $\bar{\tau}_b$  exceeded 0.2 Pa are near two main inlet locations in the southeast of the area (indicated by the bold red arrows in Figure 6.7). Some ditches and channels in the western and northern parts of the area also had maximum  $\bar{\tau}_b$  values above 0.2 Pa. The  $\bar{\tau}_b$  values in some of these watercourses might be caused by an incomplete parameterisation of the manually controlled small-scale pumping stations and some weir crest levels.

Small agricultural field ditches were not explicitly incorporated in the model but instead were represented as a lumped storage. Because the flow velocities in these ditches are typically lower than those in the larger ditches and secondary channels that receive the water discharged from a network of field ditches, it is likely that the  $\bar{\tau}_b$  values in these field ditches are lower than those in the explicitly modelled ditches and channels shown in Figure 6.7. Hence, the experimentally

derived  $\tau_{cr}$  values for bed sediments combined with model calculations of maximum  $\bar{\tau}_b$  value in watercourses leads to the conclusion that erosion of bed sediment is not a major process controlling the SPM concentrations and transport of PP in the polder catchment.

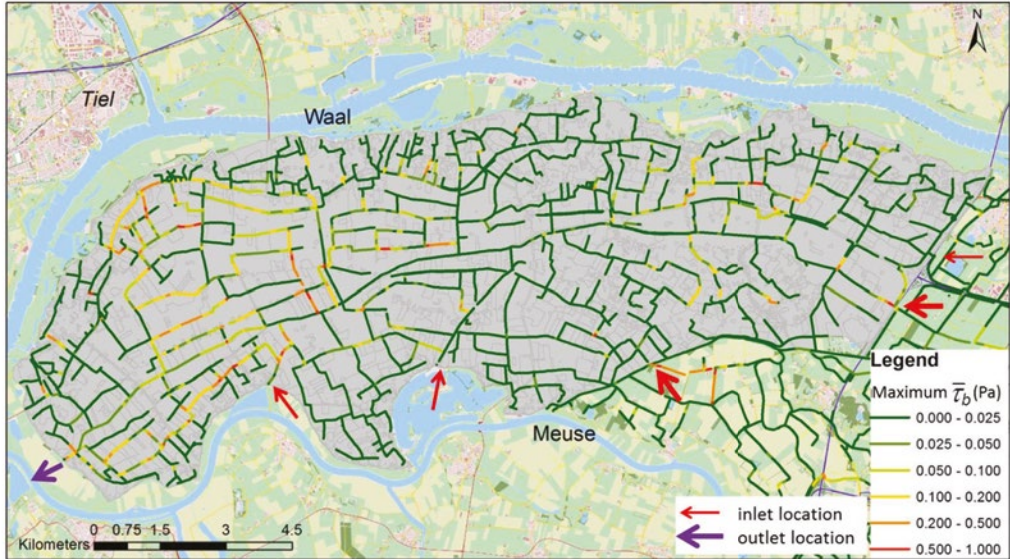


**Figure 6.7.** Maximum bottom shear stress in ditches and channels of the Quarles van Ufford study area during the period from March 2004 to April 2005, showing water inlet and outlet locations.

Despite our general conclusion that erosion of bed sediments is not important for PP transport in polder catchments, previous studies have reported that some erosion can occur at  $\bar{\tau}_b < \tau_{cr}$ , which is often referred to as floc erosion (Winterwerp et al., 2012) but is also attributed to a stochastic distribution of the bed strength (Van Prooijen and Winterwerp, 2010). Although quite limited, this type of erosion was also observed in some experiments in our study: for example, in sediment cores NPP1 and NPP1a (Figure 6.4). This type of eroded matter likely originates from SPM that is produced in the water column due to aeration of exfiltrated Fe-rich groundwater and that settles during low flow conditions (van der Grift et al., 2016a), or due to redox dynamics in the sediment layer causing dissolution and precipitation of Fe(III) precipitates across the sediment–water interface (Baken et al., 2015b) and forming a layer of easily resuspendable matter on the bed surface. The temporary presence of a layer of easily resuspendable Fe-oxide flocs on ditch bottoms has been observed in a drainage ditch of a groundwater-fed lowland catchment in the Netherlands (Van der Grift et al., 2014). In addition, using *in situ* resuspension experiments, Kleeberg et al. (2008) found the presence of such stocks of easily resuspendable matter in surface sediments in a lowland river that were eroded at a low bottom shear stress. This fluffy surface layer was, however, not measured in their laboratory experiments using a comparable set-up to ours. Kleeberg et al. (2008) concluded that

the fluffy surface layer on the river bed was not preserved after sampling. This suggests that our experiments pass by the presence of a fluffy surface layer and its erodability.

Erosion at  $\bar{\tau}_b < \tau_{cr}$  might also be the mechanism that explains the increase in SPM and total P concentration measured during pumping at locations near pumping stations, where water flow velocities are relatively high (Van der Grift et al., 2016b; Van der Grift et al., 2016c). Chemical analysis of SPM showed that the sediment particles eroded during pumping did not deviate in P content and Fe/P ratio from those of the SPM originally present in the water column (Van der Grift et al., 2016c). Data from the current study, however, revealed a difference in P content and Fe/P ratio between bed sediment and SPM in the water column during normal flow conditions.

The molar Fe/P ratios of the surface sediment layer (4.8–21.8, see Table 6.1) are in the range of values for rivers and streams reported in the literature. Kleeberg et al. (2008) obtained a molar ratio of 8.2 in the surface sediment of a lowland river in Germany. Other studies reported values of 9–290 (House and Denison, 2002) and 5–42 (Fox, 1991). Sequential chemical extraction of bed sediment and SPM samples from Quarles van Ufford revealed that in both types of sample, iron-bound P was the dominant particulate P fraction (Van der Grift et al., 2016c; Van Popta, 2016). Between 71–92% of the total P content of the bed sediment was bound to Fe(III) precipitates, 1–19% was organic P and 3–10% was calcium-bound P (Van Popta, 2016). SPM samples from the same locations revealed an Fe-bound P fraction that ranged between 64 and 79% of the total particulate P (Van der Grift et al., 2016c). However, the SPM was generally more enriched in P as dry weight content and had a lower Fe/P ratio than the bed sediment (Figure 6.8). The P content of SPM from Quarles van Ufford was approximately four times higher than the P content of bed sediment, and the Fe/P ratio of the SPM was approximately half that of the bed sediment. Samples from the secondary ditch in Noordplaspolder showed a comparable trend, with SPM that had higher P contents and lower Fe/P ratios in the bed sediment (Figure 6.8).

The P content and Fe/P ratio of the eroded matter were intermediate to the values of the bed sediment and the initially measured SPM (Figure 6.8). Moreover, the P content of the eroded matter decreased during the experiment, and in several experiments the Fe/P ratio increased with increasing erosion rates. These observations show that the first particles released from the bed sediment had a signature which was more similar to that of the SPM than to that of the eroded matter released during higher erosion rates. Thus, compared with the average composition of the bed sediment, finer particles that are easier to erode or are present in the water column as SPM are more enriched with P. The different values of the P content and the Fe/P ratio between the SPM, the bed sediment and the eroded matter also suggest that the SPM did not originate from resuspension of particles from the bed sediment.

### ***Role of retention***

Hydrodynamic resuspension of P stored in bed sediments of watercourses during storm flow events is commonly considered to be the main P transport mechanism in lowland catchments (e.g. Haygarth et al., 2005; Kaushal et al., 2014). Our results revealed contrasting insights for polder catchments. Polder catchments typically have a dense network of drainage ditches and water flow strongly controlled by weirs and pumping stations. This geographical setting tempers peak



flow following rainstorms and thus results in lower maximum hydrodynamic forces that generally may not be strong enough to cause erosion of bed sediment. Hence, the P retention potential in the polder water systems is greater than in natural catchments. It appears that after P has been stored in the bed sediment, it is retained permanently and can only be removed by dredging the watercourses, which normally occurs every six to ten years. If the dredged matter is spread on the soil surface, the P stored in the bed sediment might become available again for plant uptake. We therefore hypothesise that a significant fraction of the P load that leaches from the soil to the surface water in polder catchments is returned to the soil and thus that polder catchment export loads are limited, relative to the scale of P application to the soil and the size of the P pool stored in the soil.

Polders can thus be considered as comprehensive peak flow control systems that attenuate P export loads from agriculture. Polder catchments cover 60% of the land surface in the Netherlands (Van de Ven, 2004). The remaining 40% are free-draining catchments. Although there are no pumping stations in these areas, the water levels are frequently controlled by a network of ditches and weirs, as in polder catchments. Furthermore, the elevation gradient of free-draining lowland catchments is typically shallow (no steep slopes). Although higher flow velocities may occur in main streams in lowland catchments during rainstorms, these are not expected in headwater ditches in free-draining catchments. In the international scientific literature, artificial drainage ditches have been recognised as elements that reduce P export load to downstream water bodies (Kröger et al., 2008; Marttila and Kløve, 2010), especially when they are engineered to reduce the water velocity (i.e. by the construction of weirs or frequent dredging to enhance the water storage capacity), to optimise the stream conditions for sedimentation and uptake of dissolved P (Kröger et al., 2011; Smith, 2009). Dutch surface water systems act thus similarly.

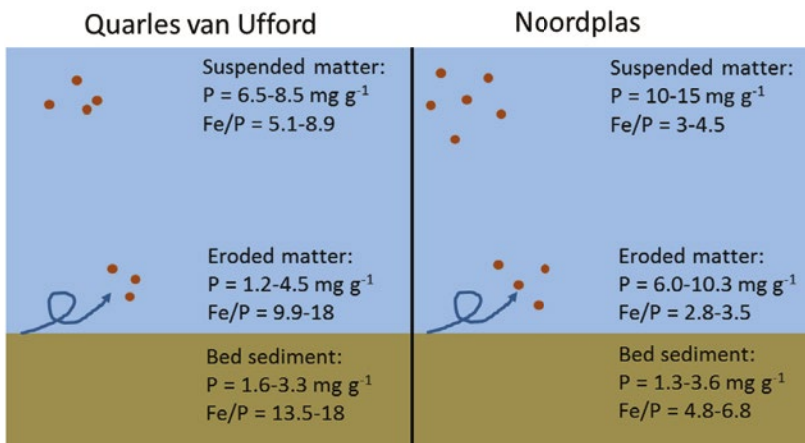


**Figure 6.8.** Phosphorus content and molar Fe/P ratio of bed sediment (0–1 cm), eroded matter and suspended particulate matter in Quarles van Ufford polder and in the secondary channel in Noordplas polder (suspended particulate matter data from Van der Grift et al. (2016c)).

## 6.7 Conclusions

Using an erosion microcosm system, a series of erosion experiments with undisturbed sediment cores was performed to characterise the erodibility of soft sediments from drainage ditches and the P entrainment of the water column that result from hydrodynamic forces in polder catchments.

The main conclusions from this study are:

- Erosion experiments with soft sediments from drainage ditches and channels in polder catchments have revealed a critical shear stress for erosion in the range of 0.1–0.28 Pa.
- At bed shear stresses above the critical shear stress, the sediment erosion rate and P release were almost linearly related to the bed shear stress.
- The erosion rate parameter could be related to the bulk density and water content of the sediment. More easily erodible sediment with lower bulk density and higher water content was found at locations further downstream. The critical shear stress could not be related to these sediment properties.
- The geographical setting of a Dutch polder is such that flow-induced bed shear stress in watercourses seldom exceeds the critical shear stress for erosion. This implies that in the polder catchment, erosion of bed sediment is not a major process controlling SPM concentrations and transport of PP.
- The experiments show that limited erosion of easily resuspendable matter occurred at bed shear stresses below the critical shear stress. This floc erosion may contribute to P transport in polder catchments, especially in watercourses near pumping stations, where flow velocities are relatively high. Additional experiments are needed to assess the importance of this process for P transport in lowland catchments.
- Once particles have settled in a ditch or channel they are trapped and generally recycled on land by cleaning/dredging of watercourses.

## Acknowledgements

Rivierenland Regional Water Authority is gratefully acknowledged for providing their hydrodynamic model for the Quarles van Ufford polder. We thank Thijs van Kessel for the helpful discussions regarding the erosion experiment. Erwin Meijers is thanked for his assistance with the model. The project was funded by Deltares (project SO2015: From catchment to coast). Joy Burrough edited the English of a near-final version of the manuscript.

# CHAPTER

# 7

## Synthesis

Bas van der Grift

## 7.1 Introduction

The research presented in this thesis was motivated by an impact of the agricultural sector in the Netherlands: high phosphorus (P) loads in the soil. Considerable reduction in the use of manure and fertilisers was achieved in the second half of 1980s and 1990s (Rozemeijer et al., 2014) but the accumulation of P in soil has continued during recent years (Smit et al., 2015). Phosphorus loads from agricultural sources may cause eutrophication problems in surface water. However, in lowland areas, P from agricultural sources needs to be transported through a series of ditches, channels and/or streams before it can affect water quality of downstream regional surface water bodies. In this thesis, I report my research results about geochemical and hydrodynamic mechanisms controlling phosphorus (P) speciation and transport in watercourses in agriculture-dominated lowland catchments and polders in the Netherlands. A better insight into these mechanisms contributes to the improvement of our understanding of P retention in watercourses, and this, hopefully, supports water quality management. My research is based on a combination of laboratory and field experiments, field monitoring studies, and surveys in catchments. In the introduction to this thesis, I formulated four research objectives, which were addressed in subsequent chapters. The first two research objectives were to determine the geochemical mechanisms controlling P transformation and speciation in groundwater-fed surface water bodies. The last two research objectives address the hydrodynamic mechanisms controlling P transport in lowland catchments.

In this synthesis, I will first give a short summary and discuss the new insights obtained from this study (section 7.2). The synthesis continues with a discussion of the implications of the research results for water quality management (section 7.3). Next, suggestions are made for further research that may contribute to future water quality management (section 7.4). These suggestions vary from applied environmental research targets to more fundamental biogeochemical and hydrodynamic issues still to be solved. The chapter ends with a final remark regarding the closing of P cycles (section 7.5).

## 7.2 New insights into phosphorus retention mechanisms

The research presented in this thesis has provided new insights into the mechanisms controlling phosphorus speciation and transport in lowland catchments. Two most important key findings will be described below.

### 7.2.1 Formation of phosphate-rich iron precipitates at the groundwater–surface water interface

A key insight obtained is that redox processes taking place when Fe-bearing groundwater discharges into surface water strongly determine the further fate and transport of P in surface water. Aeration of groundwater during exfiltration to surface water results in immobilisation of dissolved inorganic P by formation of Fe hydroxyphosphates upon oxidation of Fe(II) in the soil/sediment surrounding the watercourse or in the water column itself (chapters 2 and 3). To the best of my knowledge, this study

is the first to document the oxidation gradient of naturally occurring Fe(II) in natural catchments at circumneutral pH. Lower pH and lower temperatures in winter (than in summer) resulted in low Fe(II) oxidation rates, albeit that the removal of P by oxidising Fe(II) was highly efficient in all seasons, resulting in low dissolved inorganic P concentrations in the surface water throughout the year. Aeration of anoxic groundwater with a dissolved Fe(II) concentration which is, on a molar basis, at least 1.7 times higher than the phosphate concentration will result in fast and complete transformation of dissolved P into particulate P. Hence, it is a very efficient geochemical process to immobilise phosphate.

The results from the field and laboratory experiments, which showed a strong tendency for dissolved P to transform into particulate P upon aeration of groundwater, were confirmed with data from field surveys in catchments. In chapter 4, we showed that the suspended particulate matter (SPM) sampled during various conditions in six lowland catchments in the Netherlands had high P contents. The average content was about 2-10 higher than the P contents of SPM reported in international studies. Iron-bound P was the dominant P species in the TP concentration in surface water bodies in the lowland catchments. This dominance of the Fe-P pool denotes the presence of Fe(III) precipitates in SPM that originate from exfiltration of anoxic Fe-bearing groundwater. With a range from 4% to 67% and a median of 18%, these authigenic Fe(III) precipitates are a major fraction of the total SPM concentration. This study is the first to address formation of authigenic SPM and its influence on P speciation and transport in catchments in the Netherlands.

This P binding during formation of Fe(III) precipitates is often referred to as co-precipitation; it is a different mechanism than P binding to the surface of existing minerals, which leads to surface-adsorbed P. This new insight is important because the binding mechanism of P affects the reactivity of the particulate P: co-precipitated P is commonly considered as less labile, and becomes available to biota more slowly than surface-adsorbed P (e.g. Baken et al., 2014). There is consensus that Fe-bound P can be considered as largely not bioavailable as long as conditions remain oxic (e.g. Golterman, 2001; Pacini and Gächter, 1999), which is commonly the case as long as the Fe-bound P is present as SPM in the water column. Since this fraction has limited bioavailability, the eutrophication risk associated with it is less than that associated with dissolved (free)  $\text{PO}_4$  or P bound to degradable organic matter. The effect of P loads from agriculture on the ecological status of water bodies is, therefore, reduced compared with that of P loads from agriculture in catchments without exfiltration of Fe-bearing groundwater.

The sequence of Fe(II) and P loading of the surface water may also influence the immobilisation mechanism and, therefore, the bioavailability of P (Baken et al., 2016a). As shown in chapter 3, Fe hydroxyphosphate forms when  $\text{PO}_4$  is present during the oxidation of Fe(II) to Fe(III). In contrast, when Fe(III) particles are formed before mixture with P, e.g. when the P originates from a downstream point source, surface adsorption of  $\text{PO}_4$  by Fe oxyhydroxides is likely the dominant mechanism of P binding (e.g. Ding et al., 2012; Wang et al., 2013). Under such conditions, the capacity to bind P is lower than when P is present during oxidation of Fe(II). Hence, immobilisation of dissolved P in surface water bodies can be more effective if the P is from diffuse sources than if it originates from point sources.

Although this research showed that formation of Fe hydroxyphosphates at natural redox boundaries such as the groundwater–surface water interface is the geochemical process responsible for the immobilisation of dissolved P for diffuse sources (chapter 3), the presence of a separate Fe hydroxyphosphate phase as proof that this is the causal mechanism will be difficult to detect under field conditions because Fe(II) concentrations are commonly much higher than  $\text{PO}_4$  concentrations. In such situations, Fe(II) oxidation and precipitation of Fe(III) phases will continue after  $\text{PO}_4$  depletion. Voegelin et al. (2013) reported that part of the Fe(III) newly formed after  $\text{PO}_4$  depletion contributes to initially precipitated Fe hydroxyphosphate being polymerised into  $\text{PO}_4$ -rich Fe oxyhydroxides with a significantly lower P/Fe ratio than the initial Fe hydroxyphosphates, thus causing the initially present Fe hydroxyphosphate phase to decrease. In addition, Fe(II) oxidation after depletion of  $\text{PO}_4$  that results in the formation of more crystalline Fe oxyhydroxides can mask the Fe hydroxyphosphate phase when these Fe hydroxyphosphates are present as a moderate fraction of the total Fe(III) solids. In this situation, Fe hydroxyphosphates cannot be identified with classical chemical extraction techniques (Hyacinthe and Van Cappellen, 2004) or more advanced X-ray absorption methods (van Genuchten et al., 2014).

### 7.2.2 Retention of particulate phosphorus

After dissolved P has been transformed into Fe-bound particulate P, the transport of P in catchments or polders is controlled by sedimentation and erosion of particles. Hydrodynamic resuspension of P stored in bed sediments of watercourses is commonly considered as being the main P transport mechanism in lowland catchments (e.g. Haygarth et al., 2005; Kaushal et al., 2014). A combination of erosion experiments with undisturbed bed sediment cores and a hydrodynamic model that calculates bed shear stresses in watercourses revealed contrasting insights for polder catchments (chapter 6). Polder catchments typically have a dense network of drainage ditches and a water flow strongly controlled by weirs and pumping stations. This geographic setting tempers peak flow and thus results in lower maximum hydrodynamic forces that generally may not be strong enough to cause erosion of bed sediment. The highest flow velocities in polder catchments occur near pumping stations, but this study showed that flow-induced changes in P concentrations are considerably lower at pumping stations than at outlets of natural catchments (chapters 4 and 5). This also suggests that polders have enhanced potential for P retention.

Polders can thus be considered as comprehensive peak flow control systems that attenuate P export loads from agriculture. Polder catchments cover 60% of the land surface in the Netherlands (Van de Ven, 2004). The remaining 40% are free-draining catchments. Although there are no pumping stations in these areas, the water levels are frequently controlled by a network of ditches and weirs, as in polder catchments. The elevation gradient of free-draining lowland catchments is, furthermore, typically shallow (no steep slopes). Although higher flow velocities may occur in main streams in lowland catchments during rainstorms, these are not expected in headwater ditches in free-draining catchments. In the international scientific literature, artificial drainage ditches have been recognised as elements that reduce P export load to downstream water bodies (Kröger et al., 2008; Marttila and Kløve, 2010), especially when they are engineered to reduce the water velocity (i.e.

by construction of weirs, or frequent dredging to enhance the water storage capacity), to optimise the stream conditions for sedimentation and uptake of dissolved P (Kröger et al., 2011; Smith, 2009).

Based on my results, I hypothesise that a significant fraction of the P load that leaches from soil to surface water in lowland catchments is returned to the soil by the dredging of the drainage channels, which may imply that P recycling in lowland catchments is more effective than acknowledged at present. This insight opens opportunities for increasing the potential to reclaim P from water systems after it has been leached from the soil but before it has been transported to downstream surface water bodies.

### 7.3 Implications for water quality management, modelling and monitoring

The results described in the previous section have two major implications for water quality management:

- (1) Discharge of Fe-bearing groundwater in combination with the limited water flow in artificial and strongly managed watercourses reduces the environmental risk of eutrophication resulting from P loads from diffuse sources. Surface waters in catchments draining Fe-bearing groundwater are less vulnerable to deterioration of ecological status than surface water in catchments that do not drain Fe-bearing water.
- (2) Sedimentation of SPM with high P contents results in a steady accumulation of a pool of 'legacy P' in bed sediments of headwater ditches and in surface water bodies further downstream, such as inland lakes or even estuaries or coastal areas that receive export loads from agricultural areas. This pool of 'legacy P' may again become available for aquatic organisms at a later stage but could also be removed from the surface water system by dredging.

Organisations and legislators involved in water quality management should be aware that P does not behave as a conservative solute at the interface of groundwater and surface water. Instead, P loads from agriculture will be attenuated and retained in watercourses due to the transformation processes during discharge of groundwater and the low flow velocities of water in lowland catchments. Without this capacity of watercourses to retain P loads in surface water, the eutrophication problems would likely be more severe, given the intensive agriculture and the manure surplus in the Netherlands. Although naturally occurring processes mitigate the negative effects of P loads from agriculture to a certain extent, we should realise that the continuous loading of bed sediments with Fe-bound P may adversely affect water quality at longer time scales and this may retard the improvement of water quality in the future, even if the reduction of P loads has been accomplished. Thus, a further enrichment of this P pool is highly undesirable from an environmental point of view.

In my opinion, water quality management in the Netherlands, including actions taken within the EU Water Framework Directive (WFD) and the Dutch manure policy may benefit from my findings. These have implications for the models currently used to support water quality management, the development of mitigation strategies, the derivation of environmental quality standards, and for

water quality monitoring programmes. In the following subsections I will briefly discuss each of these implications. Additionally, I argue that an important consideration for water quality management should be that problems are not passed on to other compartments, other regions, or other periods, because this is in essence unsustainable. First, this means that the risk of potentially negative consequences of the 'legacy P' pool in bed sediments needs to be clarified. And second, additional research questions regarding P speciation, transformation and transport in watercourses should be tackled. Therefore, subsection 7.3.1 starts with a discussion on the environmental implications of continuous loading of bed sediment. Finally, section 7.4 addresses research questions for applied environmental research and more fundamental research.

### **7.3.1 Environmental implications of continuous loading of bed sediments**

Phosphorus stored in bed sediments can be remobilised as a result of biogeochemical processes in the sediment layer, especially during the more ecologically sensitive periods in summer. Reductive dissolution results in the release of Fe-bound P, making Fe(III) precipitates an internal P source to receiving waters. The potential for biogeochemical remobilisation is especially high in water bodies in polder catchments in clay and peat areas where the DRP concentration is typically higher in summer than in winter (see Figure 1.5 in the introduction of this thesis and Text box 7.1). As described in chapter 5, there is enough supporting evidence to assume that this process controls the increase of DRP concentrations in the Lage Vaart channel during the summer. The evidence is in time series of measured oxygen and NO<sub>3</sub> concentrations in the watercourses, which revealed that concentrations were lower during the summer months. This indicates conditions shifting towards being more reducing, i.e. more favourable for reductive dissolution of Fe(III) precipitates. However, release of P from sediments not only depends on reductive dissolution of Fe(III) precipitates, but is also coupled to the cycle of other elements, such as sulphur (Smolders et al., 2006).

Whereas most of the P loads from the soil to the surface water and export from catchment occur during the winter (see Text box 7.2), biogeochemical remobilisation is mainly restricted to the summer. The sequence of immobilisation, storage and remobilisation processes makes it difficult to link agricultural practice to P concentrations in the surface water. When assessing measures to reduce P loads from agriculture we should be aware of the long-term in-stream mechanisms controlling P concentrations in surface waters. A proper assessment of the effects of measures requires detailed and long-term monitoring programmes at different spatial scales from field to catchment outlet. Sedimentation of particles with high contents of Fe-bound P is especially a risk for water quality in lakes that receive discharge water from lowland catchments. Lakes function as huge sediment traps for SPM from upstream catchments. As described earlier, this SPM contains a large fraction of the P load that has been leached from soils and transported through the surface water system, mostly during winter. However, remobilisation of P from bed sediments in lakes may lead to harmful toxic algal blooms during warm weather.

Besides the negative effects of biogeochemical P remobilisation from bed sediments, the huge amount of P stored in bed sediments may also adversely affect the ecological status of lakes may as well be hampered by the huge amount of P stored in bed sediments. In recent years, an increase in the growth of aquatic macrophytes has been observed in many shallow Dutch lakes (Lamers et al.,



2012; van Geest and Noordhuis, 2014). The P pool in bed sediments may contribute to this rampant growth when rooting aquatic macrophytes are able to mobilise particulate P and thus gain access to this huge nutrient pool. Although this system state is far preferable to algae domination, it has negative consequences for the biodiversity of lakes and for the recreational sector.

**Text box 7.1.** Phosphorus remobilisation in the Krimpenerwaard.

An example where remobilisation is clearly apparent is in the Krimpenerwaard: a polder with peat soils, in the west of the Netherlands. High TP concentrations and DRP/TP ratios combined with low  $\text{NO}_3$  concentrations have been measured there during summer (Woestenburg and Van Tol-Leenders, 2011). The average TP concentration in the Krimpenerwaard was  $0.99 \text{ mg L}^{-1}$ , which is about five times the regional environmental quality standard (EQS) of  $0.22 \text{ mg L}^{-1}$  (Figure 7.1). The low  $\text{NO}_3$  concentrations during summer indicate that reductive dissolution of Fe oxyhydroxides may occur. Because peat soils largely consist of organic matter, they naturally contain high nutrient levels. The degradation of the peat soil and the release of dissolved P from ditch sediments during anoxic conditions in warm and dry periods is a plausible explanation for the observed TP concentrations in this area. The same release of DRP from bed sediment during the summer has been reported by other studies (e.g. Evans et al., 2004a). In addition, Kjaergaard et al. (2012) speculated that if P and Fe(II) are released concomitantly from sediments, the export of P may be attenuated by the downstream re-oxidation of Fe(II) and subsequent binding of P. One may speculate that this reduces the environmental risk of biogeochemical remobilisation.

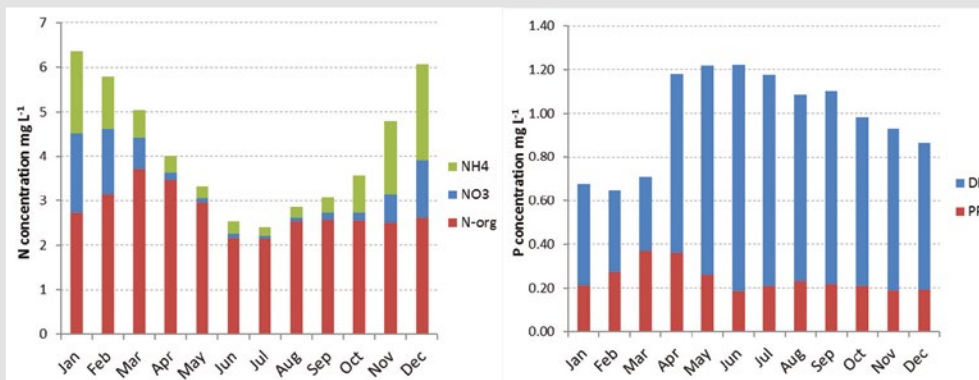


**Figure 7.1.** Average monthly surface water concentrations of N species: ammonium, nitrate and organic N (left) and P species: particulate P and dissolved reactive P (right) over the period 2005–2010 in the Krimpenerwaard (43 sampling locations).

**Text box 7.2.** Dominance of winter period in annual nutrient export loads.

Figure 7.2 gives the cumulative annual N and P loads of the Drentse Aa catchment from 2003 to 2010 (Roelsma et al., 2011a). The plots show a large difference in total annual loads between the years. Furthermore, all individual cumulative load curves are steep during the winter period and much flatter during summer. This indicates that most nutrient export (circa 80–90%) from this catchment towards downstream water bodies occurs during the winter (November–March). The same dominance of winter nutrient exports from agricultural catchments has been reported for various studies in other humid regions (e.g. Petry et al., 2002; Tappin et al., 2013).

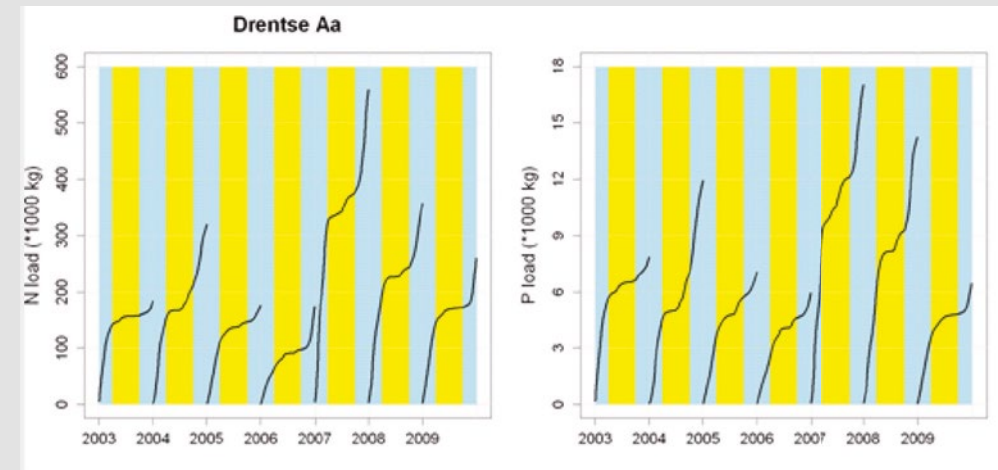


**Figure 7.2.** Cumulative yearly TN and TP loads from the Drentse Aa test catchment. The blue bands indicate the winter months (November–March) and the yellow bands indicate the summer months (April–October) (from Roelsma et al., 2011a).

### 7.3.2 Implications for spatial model systems

Current water quality management in the Netherlands, including the obligations imposed by the Dutch Manure Act and the EU Nitrate Directive and Water Framework Directive, is largely based on the results of spatially explicit model systems. Two model systems are currently used in the Netherlands to support water quality management at national or regional scale: the WFD explorer (Van den Roovaart et al., 2012) and ECHO (Kroes et al., 2011). Both use the results from the same STONE model (Wolf et al., 2003) for leaching and runoff of nutrients from soil. Additionally, both rely on the same data on emission from point sources: the Pollutant Release and Transfer Register ([www.prtr.nl](http://www.prtr.nl)). Phosphorus retention in surface water bodies is implemented somewhat simplistically in both model systems, but the approach differs.

The WFD explorer as a national application is used for assessments of the current water quality status and ex-ante evaluations of the river basin management plans of the Netherlands as outcome of the WFD (Van Gaalen et al., 2016). It uses a different approach for retention, depending on whether

the catchment is a polder or is free draining. For free-draining catchments, the retention factors are derived for individual water bodies. They are calculated with a first-order decay function in which the retention factor for a water system  $i$  ( $R_{f,i}$ ) is dependent on the hydraulic residence time ( $HRT$  in d) and a retention coefficient ( $k$ ).

$$R_{f,i} = (1 - e^{-k \cdot HRT})$$

The HRT for the individual water systems is calculated by the flow model of the WFD explorer. A general value of 0.15 is used as retention coefficient for all free-draining catchments in the Netherlands. The retention factor for polder catchments is not water system specific and, therefore, not calculated with the first-order decay function. A retention factor of 0.5 is always used for these areas.

ECHO is used at the national scale for evaluation of surface water quality for the Dutch Manure Act (Groenendijk et al., 2012; van Boekel et al., 2013), for assessments of the contribution of the agricultural sector to the failure to achieve nutrient standards in regional surface water (Groenendijk et al., 2016) and for regional studies on nutrient sources in surface water (e.g. Van Boekel et al., 2015). Similar to the WFD explorer, ECHO sets the retention factor for P from leaching and runoff in polder catchments at 0.5. This value is based on retention estimates for major river basins in Denmark (Van Boekel et al., 2015). For free-draining catchments, the retention factors are, similar to the WFD explorer, derived for individual water bodies. The retention factor ( $R_{f,i}$ ) for free-draining catchments is a function of the specific discharge ( $SR$  in  $\text{m}^3 \text{s}^{-1} \text{ha}^{-1}$ ), which is the quotient of the discharge ( $\text{m}^3 \text{s}^{-1}$ ) and the surface area ( $\text{ha}^{-1}$ ) of a catchment and the absolute retention  $R$  (%) (van Boekel et al., 2013):

$$R_{f,i} = a \cdot SR^b$$

The coefficients  $a$  and  $b$  are derived for the winter and summer periods from calculations of the absolute retention and specific discharge in four free-draining pilot catchments (van Boekel et al., 2013). The absolute retention is calculated by subtracting P export loads from the catchments from P loads from the soil to the surface water system. The P export loads are determined by concentration and discharge measurements and the P loads to the surface water are derived from the national STONE model or regional model for leaching and runoff (ANIMO-SWAP model).

In my research, I showed that Fe-controlled P retention is the dominant mechanism controlling P speciation and transport in lowland catchments. The processes as described in this thesis are, however, not represented in the equations and retention factor as described above. Because the results of operational spatial model systems like ECHO and the WFD explorer have major implications for management and policy analysis in the Netherlands, I would argue for a more process-based implementation of P retention mechanisms in such model systems, which takes account of the key processes controlling P transport. Water quality management at national and regional scale would be strengthened by implementation of these P retention mechanisms in spatially explicit model systems.

A convenient framework within which developments on P retention can take place is the Netherlands Hydrological Instrument (NHI). This is an operational, multi-scale, multi-model system for consensus-based, integrated water management and policy analysis (De Lange et al., 2014). The NHI consists of various physical models at appropriate temporal and spatial scales for all parts of the water system and for both water quantity and water quality. Intelligent connectors provide transfer between different scales and fast computation, by coupling model codes at a deep level in software (De Lange et al., 2014). Model codes for water quality, like Delwaq (Deltares, 2016a) and PCDitch (Janse, 1998; van Gerven, 2016), allow Fe-controlled P retention mechanisms to be implemented (see also section 7.4.3) and are already coupled to model codes that are currently part of the NHI. The detail required in the model set-up and parameterisation, and also the accompanying computational requirements need attention but are not considered as major obstacles, given that computational power is growing. To facilitate the implementation of Fe-controlled P retention mechanisms in this modelling framework, a number of research questions have to be addressed: see section 7.4.

### 7.3.3 Implications for programmes of measures

Knowledge about geochemical and hydrodynamic P retention mechanisms can contribute to the development of more effective programmes of measures for water quality improvement. The knowledge that P from diffuse sources is strongly retained in watercourses by subsequent transformation of dissolved P into Fe-bound P and sedimentation of this particulate P in bed sediment is valuable information for the design or optimisation of water quality measures. I therefore advocate that measures to be implemented take into consideration the behaviour of P in the surface water system.

Three possible measures will be briefly described below:

- (1) More frequent dredging of watercourses: this could reduce the environmental risk of P remobilisation from bed sediment and, if the dredged material is applied to fields, this may help maintain the soil fertility. From the perspective of optimal P recycling, the dredging should be done at the end of the leaching season i.e. during early spring, which is not current practice.
- (2) Smart operation of pumping stations. In chapter 5 we showed that P export loads from polder catchments are affected by the operation of the pumping station. Pumping at maximum power will result in more pronounced resuspension of particulate P. If the water from a polder catchment could be discharged by pumping for longer at a lower discharge rate, more P will remain in the polder and thus be available for re-use.
- (3) Construction of sedimentation basins or floodplains. Particulate Fe-bound P is the dominant species in the TP concentration in lowland catchments. Enhanced sedimentation of the particulate P near outlets of catchments is, therefore, an effective measure to mitigate P export loads from catchments. This requires low flow conditions. Note that this technique is already being used in the Dommel Brook in Noord Brabant, although not targeted at P but to diminish transport of cadmium and zinc.

### 7.3.4 Implication for environmental quality standards

During the implementation of the WFD in the Netherlands it was decided to base the EQS for P on summer average TP concentrations (1 April–30 September) (Heinis and Evers, 2007b). The P concentration itself is not a primary goal for the WFD but a supporting variable that must be achieved in order to achieve ‘good ecological status’ in natural water bodies or ‘good ecological potential’ in *artificial* or *heavily modified* water bodies. The EQSs for P are, therefore, based on a national assessment of ecosystem vulnerability and are dependent on water type and location. Details and background on EQSs are presented in Heinis and Evers (2007a) and (Evers et al., 2012).

Briefly, the EQSs for streams and small rivers are based on a dataset of such water bodies in the Netherlands, which are, to use WFD terminology, neither *artificial* nor *heavily modified* and which have a ‘good ecological status’. The EQSs for P are set at the 90 percentile of measured TP concentrations in these waters (Heinis and Evers, 2007b). The EQSs for most types of ditches and channels are EQSs that were derived for shallow lakes (Evers et al., 2012). The EQSs for lakes were derived from analyses that establish the relationships between measured chlorophyll-a and TP concentrations in Dutch lakes during the summer period. Ratios between chlorophyll-a and TP were derived for a different type of lake and used to set a maximum TP concentration at a desired chlorophyll-a concentration (Portielje et al., 2005). Not surprisingly, the dataset used is characterised by a large range in measured TP concentrations at a certain chlorophyll-a level. It was claimed by the authors that this is due to factors other than P that often limit algal growth (Heinis and Evers, 2007b). However, this claim ignores the fact that TP is a sum parameter consisting of both organic and inorganic P that can either be dissolved in the water column or be present as suspended matter. Hence, total P is present in a range of compounds with highly diverse stabilities, bondings and exchangeabilities, which influence its biological availability (e.g. Poulenard et al., 2008).

In scientific literature there is agreement that using TP as an indicator of P limitation may be flawed without concomitant measurement of bioavailable P (e.g. Baken et al., 2014; Steinman et al., 2016). This means that relationships between chlorophyll-a and TP as derived for lakes are not an ideal way of setting EQSs for P in ditches and channels in which a ‘good ecological potential’ should be achieved. Therefore, I argue that the chemical speciation of TP should be measured and knowledge about the chemical speciation should be implemented in the EQSs for P. An interesting suggestion for overcoming the shortcomings of the current framework of EQSs, such as the bioavailability of the TP concentration, is the development of a system of EQSs which is based on critical loads and takes into account the processes that control the P speciation. The basic idea and main advantage of working with critical loads is that nutrient loads are more predictive for the ecosystem functioning than nutrient concentrations. This holds for all water systems where nutrient concentrations are a response variable of biogeochemical and biological uptake and release processes. Statutory requirements for water quality in the United States is already based on total maximum daily loads (Copeland, 2012). Thus, the processes must be taken into account when deriving critical loads for water bodies and this implies that critical loads will be based, at least partially, on model calculations. When the critical and actual loads are known, it is much easier to assess the effort needed to reduce the load. However, the difficulty of developing such a system should not be underestimated, especially for water systems that receive their loads from the soil/

groundwater domain. The good news is that empirical evidence on lake ecosystems' response to reducing nutrient loads (Jeppesen et al., 2005) indicates that loads are a good driver for ecosystem functioning; satisfying results for deriving critical loads have also already been obtained for lakes (Janse et al., 2010; Rast and Lee, 1978). Moreover, work on critical load in ditches where the shift of a submerged vegetation to duckweed coverage has been simulated (van Liere et al., 2007), seems to be promising.

### 7.3.5 Implications for water quality monitoring

In chapter 4 we recommended that chemical analysis of SPM collected by filtration should be included in large-scale monitoring campaigns to characterise the chemical speciation of particulate P. This is because particulate P is present in a range of compounds with highly diverse stabilities, bondings and exchangeabilities that influence its biological availability. Additional spatial and temporal data on P speciation will contribute to the improvement of water quality management because it improves assessments of the ecological effects of P in surface water and the refinement of water quality models, e.g. for assessments of critical loads. Moreover, authigenic Fe(III) precipitates can be accurately determined in this way, which is important since these provide an important contribution to the SPM concentration and are a major carrier phase of P in groundwater-fed lowland catchments.

In chapter 5 we showed that the TP concentration is affected by operation of the pumping station. Nowadays, most pumping stations in the Netherlands operate predominantly during the night, whereas sampling for water quality always occurs during daytime. As the pumping station is the outlet of an (artificial) water system, it is often a location for monitoring surface water quality as well. The timing of sampling should thus be synchronised with the operating hours of the pumping station when calculating P export loads or when determining trends in water quality or when judging water quality status of polder water systems.

## 7.4 Suggestions for further research

### 7.4.1 Assessment of iron loads from groundwater to surface water

I have shown that discharge of Fe-bearing groundwater into surface water strongly determines the speciation and transport of P in lowland catchments. In catchments or polders with Fe-rich groundwater, Fe is likely present in large excess of P and thus able to sequester a major proportion of the available dissolved P. However, it is unknown if an Fe excess is present in the different types of catchments and polders in the Netherlands. It is therefore important to carry out spatial assessments of dissolved Fe(II) loads from groundwater to surface water. A feasible approach is to generate maps of Fe concentrations in groundwater and incorporate these maps in groundwater transport models that calculate fluxes to the surface water domain. An example of such an approach is given in Text box 7.3. The assessment of dissolved Fe(II) loads will also help to assess the contribution of authigenic Fe(III) precipitates to the total SPM. These Fe(III) precipitates may significantly contribute to the composition, concentration and fluxes of SPM, and are also a sorbent for dissolved substances other than P. Hence, Fe(II) loads to surface water are also important for studies that consider SPM.

### 7.4.2 Spatial characterisation of phosphorus immobilisation at the groundwater–surface water interface

Both leaching of P and discharge of Fe-bearing groundwater into surface water are spatially very heterogeneous within a catchment. This implies that whereas at catchment scale there may be enough Fe to immobilise all dissolved phosphate that leaches into surface water, this need not be the case at local scales where groundwater exfiltrates via a tube drain or drainage ditch. A spatial characterisation of P sequestration during discharge of groundwater into surface water at local scales is, therefore, highly relevant. Fully understanding such transformation processes requires data at local scales on concentrations of relevant parameters in groundwater, tube drain water and ditch water. A feasible approach would be to use the data from the Minerals Policy Monitoring Programme (LMM; Landelijk Meetnet effecten Mestbeleid). As this dataset contains all relevant parameters at different domains from groundwater to surface water from a large number of farms in the Netherlands, it is an excellent source for such a systematic study on spatial dynamics in transformation processes of dissolved P during flow from groundwater into surface water. The transformation can be characterised using a relationship between the initial molar P/Fe ratio of shallow groundwater and the final “dissolved” (< 0.45  $\mu\text{m}$ ) P and Fe concentrations in drainage ditches after complete oxidation of the Fe(II). Parameters that influence the transformation process such as calcium and DOC may provide additional information for characterisation of the transformation process.

### 7.4.3 Challenges for water quality models

Many catchment-scale P models have been developed during recent decades. They have been used extensively in hydrological science and environmental management research for a number of tasks, including estimating diffusive source pollutant inputs to receiving water bodies and their source areas and predicting the effects of climate and land-use change on water quality (Rode et al., 2010). However, the interaction between P and Fe is lacking in existing models that describe P transport in catchments or river basins and/or impact of P on the aquatic ecosystem. For example, the Integrated Catchment model for Phosphorus (INCA-P) is a so-called process-based, mass balance model that simulates the P dynamics in both the plant/soil system and the stream. Together with SWAT, AGNPS/AnnAGNPS, HSPF and E-HYPE, it is one of the top five catchment water quality models used worldwide (Wellen et al., 2015). In the release of the most recent version of the INCA-P model, the authors say that omitting the interaction of Fe with P is one of the limitations of the INCA-P model (Jackson-Blake et al., 2016). Because the impact of redox and pH on P mobility is not taken into account in the INCA-P model, the authors state that it is unlikely the model will perform well in catchments fed by anoxic Fe-bearing groundwater. The other models have similar representations of nutrient biogeochemistry, with a small number of pools with reaction rates treated as calibration parameters and no interaction between nutrient cycles included (Wellen et al., 2015), and thus they face the same limitation. In addition, they do not account for suspended matter formed in the surface water by discharge of anoxic Fe-bearing groundwater. This indicates that there is currently no adequate catchment model that can be used for the assessment of P speciation and transport in catchments fed by anoxic Fe-bearing groundwater.

**Text box 7.3.** Example of a feasible approach to assess iron loads from groundwater to surface water.

Assessments of Fe loads to surface water require data on Fe concentrations in groundwater and groundwater fluxes to surface water. Figure 7.3 is the result of a spatial mapping of the Fe concentration in groundwater in the Drentse Aa catchment at three depths (Van der Grift et al., 2011). The Drentse Aa catchment is in the north of the Netherlands and borders the Hunze catchment (chapter 4). The monitoring data used for this map originate from the national and provincial groundwater quality monitoring networks, which assess groundwater quality using piezometers in so-called *homogeneous areas* that have homogeneous land use, soil type and geohydrology (Broers, 2002). Average Fe concentrations were calculated for the different homogeneous areas, using data from wells within these areas. It is clear that the Fe concentration increases with depth. The highest Fe concentrations ( $> 15 \text{ mg L}^{-1}$ ) were observed below the brook valleys, whereas the lowest concentrations were found in the drier and more upstream parts of the catchment. Iron fluxes towards the surface water system can be derived from such maps by multiplying the concentration by the modelled groundwater fluxes to surface water. For the Drentse Aa catchment, the annual average Fe flux to surface water derived in this way is  $650 \cdot 10^3 \text{ kg yr}^{-1}$ . Based on the maximum molar P/Fe ratio of Fe hydroxyphosphates of 0.6, this can theoretically sequestrate  $215 \cdot 10^3 \text{ kg P yr}^{-1}$  from the water phases. This amount is almost ten times higher than the modelled P flux from the soil to the surface water of  $25 \cdot 10^3 \text{ kg P yr}^{-1}$  (Roelsma et al., 2011a). There is thus enough Fe to immobilise all dissolved P in this catchment. For comparison, the annual average Cl surface water flux is  $2100 \cdot 10^3 \text{ kg yr}^{-1}$  (based on flow-proportional monitoring at the outlet location), while the Cl flux based on groundwater concentrations and groundwater flow equals  $2400 \cdot 10^3 \text{ kg yr}^{-1}$ . This indicates that such an approach provides a reasonable estimate of Fe(II) fluxes to surface water.

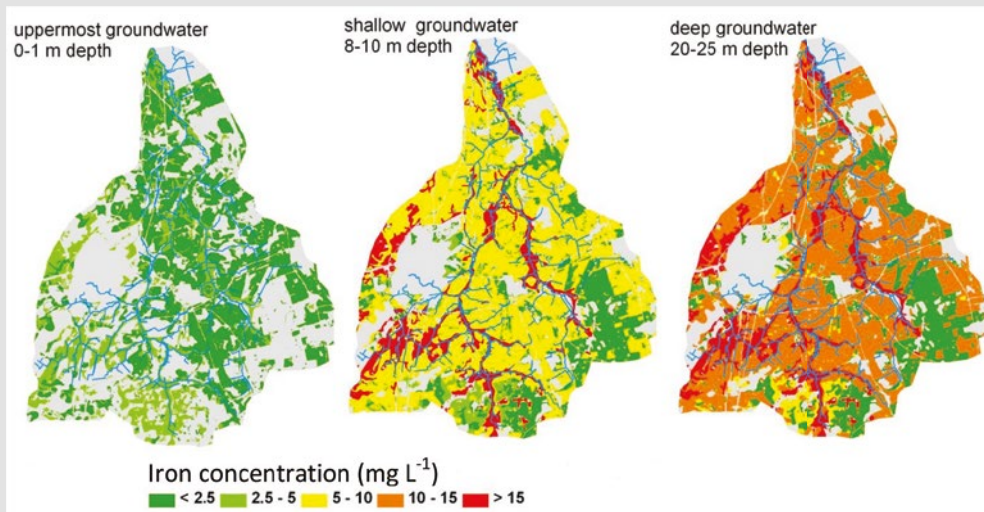


**Figure 7.3.** Iron concentrations in groundwater at three depth intervals in the Drentse Aa catchment (adapted from Van der Grift et al. (2011)).



A development that should be mentioned is the work of Vanlierde (2013). In that research, a catchment model named Model for Authigenic River Sediment (MARS) was developed. This model predicts the flux of authigenic sediment produced by groundwater seepage, while taking settling, erosion and accumulation processes into account. According to this model, the average annual contribution of authigenic sediment accounts for 65 to 75% of the total sediment flux in a lowland river in Belgium. However, binding of P by Fe(III) precipitates is not incorporated in the current version of this model.

The integration of (nonlinear) biogeochemistry with any surface water transport model is still one of the fundamental problems in catchment-scale water quality modelling (e.g. Rode et al., 2010). Mechanistic geochemical packages like PHREEQC (Parkhurst and Appelo, 2013) and ORCHESTRA (Meeussen, 2003) are frequently applied for groundwater studies but to a very limited extent in surface water quality modelling studies. Nevertheless, the results presented in this thesis merit further development of process-based catchment models that use a mechanistic geochemical sub-model to calculate P speciation in surface water (abiotic controls) coupled to the existing model formulations for P transfers in biological mechanisms like phytoplankton growth or grazing by zooplankton (biotic controls). In chapter 3 we showed that the formation of a Fe hydroxyphosphate with a molar P/Fe ratio of 0.6 can be used for predictive modelling of  $\text{PO}_4$  immobilisation upon aeration of pH-neutral natural groundwater with an initial P/Fe ratio up to 1.5. This demonstrates that a complex natural process can be described mathematically in a simplified form and likewise can be properly parameterised by the available data (see section 7.4.2) and implemented in existing water quality model codes such as Delwaq (Deltares, 2016a) or PCDitch (Janse, 1998) (see section 7.3.2). In this way, continuous production of Fe hydroxyphosphates at the groundwater–surface water interface may be included in spatially explicit model systems. Information generated by further work in line with the research suggestions described in the two previous sections can be used to parameterise such model systems.

#### 7.4.4 Dynamics in redox boundaries at the groundwater–surface water interface

Iron-rich layers with high P contents have been found at the interface between soil/sediment and surface water, such as in bed sediments of drainage ditches (Baken et al., 2015b; Foppen and Griffioen, 1995) or in the soil surrounding tube drains (Van den Eertwegh, 2002). In addition, drain tubes have to be flushed repeatedly to maintain their function, which releases much red iron hydroxide and indicates that at least some of the Fe(II) load from groundwater has been oxidised and removed from solution before it enters the surface water system. Hence, at least some of the immobilisation of dissolved P occurs in the soil/sediment domain. Then the question of whether this P should be considered as loads to the surface water domain becomes relevant. Conversely, oxidation of Fe(II) in the water column can be proved by the presence of SPM that originates from aeration of exfiltrated groundwater, i.e. the surface water in many watercourses in groundwater-fed catchments has the typical orange-brown colour of iron hydroxides.

In chapter 2 we showed that the Fe(II) oxidation rate and residence time in drainage reservoirs vary seasonally. In winter, it took a couple of days to more than a week before complete oxidation of Fe(II) was reached. In summer, Fe oxidation rates were much higher. The Fe concentrations in the exfiltrated groundwater were low, indicating that dissolved Fe(II) had been completely oxidised

prior to inflow into a ditch. Seasonal variations in dissolved Fe concentrations have been observed in lowland streams in Flanders as well (Baken et al., 2015a). These observations suggest that Fe(II) oxidation occurs predominantly in the surface water domain during winter as a result of lower oxidation rates in combination with increased flow. During summer, Fe(II) oxidation in the soil/sediment domain is more likely, because groundwater levels are lower and this favours penetration of atmospheric oxygen in the soil surrounding the tube drains and enables infiltration of oxic surface water into the sediment layer. Moreover, the abundant growth of grasses and reeds in the ditches is likely to actively transfer oxygen through the groundwater–surface water interface during summer. Thus, I hypothesise that the position of the redox gradient in the groundwater–surface water interface is dynamic in time as a result of dynamics in hydrological conditions and temperature. This process strongly controls the SPM concentration and, consequently, P transport in lowland catchments. Detailed knowledge the dynamics of the fluctuating redox gradient in such systems is lacking. I therefore recommend further research on this topic. Opportunities for the next steps in this research would be created by integrating information from multiple sources. Spatial data from earth observation techniques (satellite, remote sensing, drones) can be used to assess temporal and spatial changes in the turbidity and colour of water in watercourses (Figure 1.6). In combination with information from in-situ sensing techniques, such as networks of turbidity sensors and optical fibres for temperature measurements, this would facilitate a better understanding of the biogeochemical functioning of a ditch and the controls on SPM concentrations and, therefore, would improve the prediction of P transport in catchments.

#### **7.4.5 Coagulation behaviour of colloidal particles and associated settling velocities**

In chapter 4 we showed that Fe precipitates present as SPM in the water column are the major carrier phase of P in lowland catchments. Chapter 6 revealed the insight that once stored in the bed sediment, flow-induced remobilisation does not occur at a large scale in such areas. Hence, a critical aspect that determines P transport in lowland catchments is the sedimentation behaviour of particulate Fe-bound P that is formed in the water column. This sedimentation behaviour is critically dependent on the polymerisation and coagulation behaviour of the Fe-rich nanoparticles that are formed initially. Flocs formed by coagulation are less dense but settle faster than their constituent particles, thus affecting their depositional characteristics. A high colloidal stability, which implies a low rate of coagulation, will result in less effective retardation of P in watercourses because particles are too small for sedimentation by gravity.

It is known that the aqueous composition of water in which the Fe-rich particles are formed affects the mineralogy and morphology of the particles (Châtellier et al., 2004; Senn et al., 2015; Voegelin et al., 2010) but this may also influence colloidal stability. In chapter 3 we found that Fe(II) oxidation at high DOC concentrations and low salinity led to the formation of Fe-rich particles that were colloidally stable. These results were confirmed recently by Bollyn et al. (2016), who studied the influence of natural organic matter (NOM) on the environmental stability of  $\text{PO}_4$ -bearing colloidal Fe oxyhydroxides. Moreover, solutes such as calcium, magnesium or silicate interfere with Fe(III) polymerisation and may influence the aggregation of colloidal particles (Baken et al., 2016b; Mayer and Jarrell, 2000; Senn et al., 2015; van Genuchten et al., 2014; Voegelin et al., 2010). But it is still difficult to predict the size of Fe-rich particles.

**Text box 7.4.** Transparency of surface water shows seasonal dynamics.

Figure 7.4 shows the results of daily measurement of the transparency of a groundwater-fed channel in the Netherlands over a period of almost 2.5 years. The transparency exhibits a clear seasonal variation and, as illustrated by photos of this channel in March and June (Figure 7.5), the colour of the surface water is characterised as orange-brown in autumn, winter and spring and black during the summer. This phenomenon is explained by the seasonal dynamics of Fe(II) oxidation in the soil/sediment versus in surface water domains.

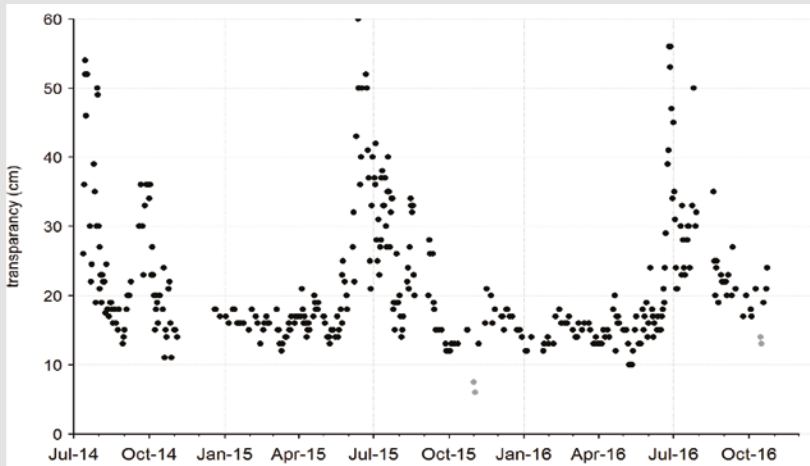


**Figure 7.4.** Time series of transparency measurements in a small channel that is fed by anoxic Fe-bearing groundwater in Soest, the Netherlands (*data supplied by Sjef Meekes*).



**Figure 7.5.** Colour of surface water in a small channel on 11 March (left) and 22 June 2015 (right) in Soest, the Netherlands (*Courtesy: Sjef Meekes*).

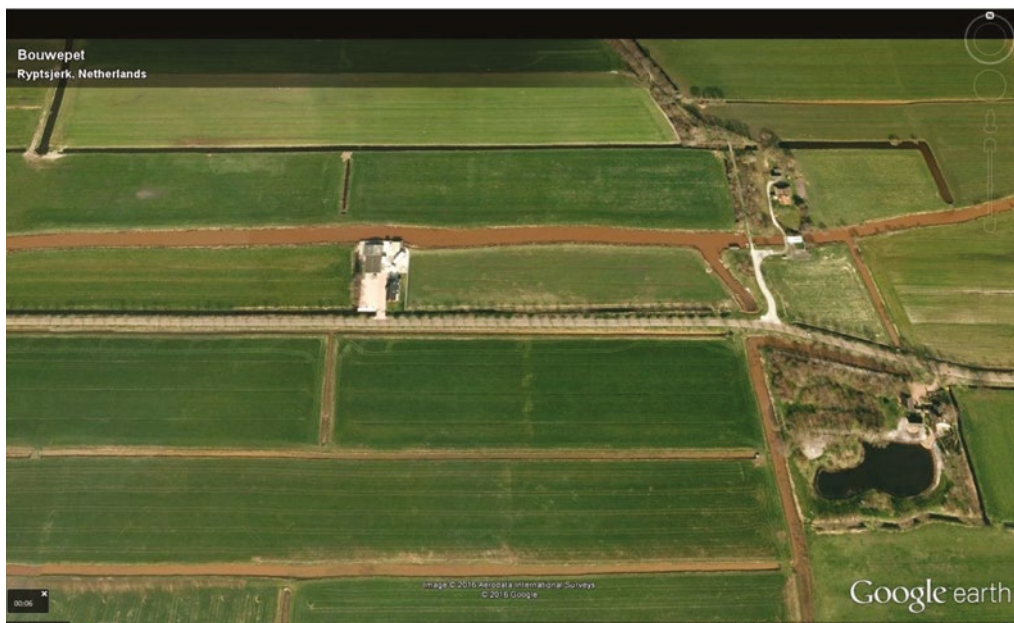


**Figure 7.6.** Google Earth image showing an alteration in colour of the surface water in watercourses in a polder near Ryptsjerk, the Netherlands. Processing of earth observation data in combination with in-situ sensing techniques enables detection of spatial and temporal dynamics in redox boundaries. Ultimately, this helps to gain a better understanding of P transport in catchments.

In agreement with suggestions for further research made by Baken (2015), I argue that a systematic and quantitative study is needed on how the particle size of Fe-rich particles formed in surface water depends on the NOM concentration, particle concentration, NOM quality, water hardness,  $\text{PO}_4$  concentration, ionic strength and pH. A feasible approach would be to perform a sampling and analysis campaign in different catchments with a range in values of the parameters as described above. If the controls on the sizes of Fe-rich particles formed in surface water are known, the typical particle sizes can be predicted and translated into effective settling velocities. Such insights can be incorporated in models; this is essential for a more quantitative description of P transport in catchments. The fate of P-containing colloidal particles is especially of concern when they reach brackish water. In estuaries, small particles commonly aggregate to larger sizes because the increased salinity promotes settling of particles to the bottom sediments and removes much of the Fe and the particle-bound P from the water column (Jordan et al., 2008; Mylon et al., 2004).

#### 7.4.6 Floc erosion

One of the general conclusions of my thesis is that due to the limited flow velocities in watercourses in lowland catchments as present in the Netherlands, hydrodynamic forces are generally not strong enough to cause erosion of bed sediment. However, in chapters 4 and 5 we showed that some resuspension of particulate P from channel bed sediments occurs, induced by changes in water flow

due to pumping. This resuspension accounted for 21% of the annual TP export load from the polder. Furthermore, we observed limited erosion of easily resuspendable material at bed shear stresses below the critical shear stress (chapter 6). The erosion that already occurs at bed shear stresses less than the critical shear stress is often referred to as floc erosion (Winterwerp et al., 2012) but is also attributed to a stochastic distribution of the bed strength (Van Prooijen and Winterwerp, 2010).

Iron-rich particles formed in the water column that are big enough to settle by gravity accumulate on top of the bed sediment during low flow conditions (Baken et al., 2015b; Rozemeijer et al., 2014). These precipitates may be very fluffy, and may contribute to floc erosion during relatively low water flow velocities which are typical for lowland catchments. I therefore hypothesise that the increase of TP concentrations we observed in watercourses near pumping stations during pumping hours can be attributed to erosion of particles that formed in the water column and settled on the bed sediment during non-pumping conditions forming a fluffy layer on top of the bed sediment. The extent of floc erosion in secondary channels and drainage ditches that connect to pumping stations or catchment outlets and its contribution to P transport in lowland catchments are, however, unclear. As floc erosion may be a relevant P transport mechanism in catchments, this needs additional research. A feasible approach would be to combine continuous sediment, phosphorus and water flow measurements in groundwater-fed drainage ditches while flow conditions were being altered, with erosion experiments (in-situ or elsewhere) and erosion modelling.



**Figure 7.7.** Iron precipitates in two groundwater-fed mountain streams in the Pyrenees, Spain (Courtesy: Jasper Griffioen).

### 7.4.7 Assessment of iron-controlled phosphate retention in other areas than lowland catchments

My research adds to insights that redox cycling of Fe strongly controls P mobility at the groundwater–surface water interface in lowland catchments as present in the Netherlands. Comparable results have been found for catchments in Flanders (Baken, 2015). Many delta systems have aquifers with reducing conditions and associated Fe-bearing groundwater. A typical example is the delta system of Bangladesh. A comprehensive survey of well water in Bangladesh showed that the majority of groundwater samples had characteristics that are typical of reducing groundwater with high Fe concentrations (median  $1.1 \text{ mg L}^{-1}$ , maximum  $61 \text{ mg L}^{-1}$ ,  $n = 3534$ ) (Kinniburgh and Smedley, 2001). Iron-controlled P retention is thus likely in surface water bodies in Bangladesh and other deltaic areas too. The outcomes of my research thus have relevance for sedimentary basins worldwide.

Aquifers with reducing conditions and Fe-bearing groundwater are not restricted to delta systems. This is clearly illustrated by the photographs in Figure 7.7, which show typical Fe precipitates in two groundwater-fed mountain streams in the Spanish Pyrenees. As exfiltration of Fe-bearing groundwater is a key process controlling the fate and transport of P in surface water systems, discharge of Fe-bearing groundwater should be paid more attention to in further studies on transport and bioavailability of P in streams and rivers worldwide.

## 7.5 Final remark

In the research presented in this thesis, I studied environmental issues associated with excess P in the Netherlands. Besides these issues, concerns about P being a non-renewable natural resource are another motive for optimising P use efficiency and for reducing P losses from agricultural soils via surface waters towards the oceans. During the late 2000s, great concern arose about the global reserves of phosphate rock. Cordell et al. (2009) estimated that the recoverable reserves of P would be depleted within 50–100 years. This information, in combination with the awareness that three countries control more than 85% of the known global P reserves worldwide, with Morocco clearly as main player, resulted in a 700% increase in phosphate rock prices during this period (Elser and Bennett, 2011). Later assessments of global P reserves, which incorporated previously overlooked geological reports from the 1980s, increased the estimated reserves for Morocco by more than fourfold. However, the size of the remaining P deposits remains under discussion (Edixhoven et al., 2014) and the availability of P fertiliser is still a major concern for food production, especially for low-income, food-deficient countries where farmers cannot afford fertilisers (Obersteiner et al., 2013). As a consequence, the sustainable use and recycling of P have been key policy issues over the past few years, and will likely continue to be so in the near future (e.g. ESPP, 2014). However, despite these efforts to achieve more sustainable use of P, we should realise that robust P recycling pathways are still lacking (Elser and Bennett, 2011). The lack of a robust P recycling pathway is also clearly demonstrated by a flow analysis of P in the Netherlands, which showed that less than 0.5% of the total P import was reused in 2011 (Smit et al., 2015).

Strategies that sustain food production while protecting water quality and taking into account concerns about the global recoverable resource of P should thus focus on closing P cycles in catchments by reducing P inputs. The national P balance of the Netherlands is characterised by large quantities of animal feed imports (Smit et al., 2015). Limiting these imports would be beneficial for long-term water quality developments in the Netherlands and also for P availability in feed-producing countries such as Argentina and Brazil, where P is becoming an increasingly valuable resource. More explicitly, this implies that the P input via manure and fertilisers in catchments should not exceed the P output via surface water and export of food/feed (and manure), and at the same time the loss to waste should be minimised. Such an approach requires high quality data on P flows, including on export loads from catchments via surface water.





# References

- Act on Pollution of Surface Water. (1970). Wet verontreiniging oppervlaktewateren. The Hague, the Netherlands.
- Akkermans, S., & Hermans, B. (2014). Position paper manure. Stichting Natuur & Milieu, Utrecht, the Netherlands.
- Allard, T., Menguy, N., Salomon, J., Calligaro, T., Weber, T., Calas, G., & Benedetti, M. F. (2004). Revealing forms of iron in river-borne material from major tropical rivers of the Amazon Basin (Brazil). *Geochimica et Cosmochimica Acta*, 68(14), 3079-3094. doi: <http://dx.doi.org/10.1016/j.gca.2004.01.014>
- APHA-AWWA-WPCF. (1989). *Standard Methods for the Examination of Water and Waste Water* (Vol. 17th ed). Washington, D.C: American Public Health Association.
- Baken, S. (2015). The effect of iron-rich particles on the fate and bioavailability of phosphorus in streams. PhD thesis, KU Leuven.
- Baken, S., Moens, C., van der Grift, B., & Smolders, E. (2016). Phosphate binding by natural iron-rich colloids in streams. *Water Research*, 98, 326-333. doi: <http://dx.doi.org/10.1016/j.watres.2016.04.032>
- Baken, S., Nawara, S., Van Moorleghem, C., & Smolders, E. (2014). Iron colloids reduce the bioavailability of phosphorus to the green alga *Raphidocelis subcapitata*. *Water Research*, 59(0), 198-206. doi: <http://dx.doi.org/10.1016/j.watres.2014.04.010>
- Baken, S., Regelinck, I. C., Comans, R. N. J., Smolders, E., & Koopmans, G. F. (2016). Iron-rich colloids as carriers of phosphorus in streams: A field-flow fractionation study. *Water Research*, 99, 83-90. doi: <http://dx.doi.org/10.1016/j.watres.2016.04.060>
- Baken, S., Salaets, P., Desmet, N., Seuntjens, P., Vanlierde, E., & Smolders, E. (2015). Oxidation of Iron Causes Removal of Phosphorus and Arsenic from Streamwater in Groundwater-Fed Lowland Catchments. *Environmental Science & Technology*, 49(5), 2886-2894. doi: 10.1021/es505834y
- Baken, S., Sjöstedt, C., Gustafsson, J. P., Seuntjens, P., Desmet, N., De Schutter, J., & Smolders, E. (2013). Characterisation of hydrous ferric oxides derived from iron-rich groundwaters and their contribution to the suspended sediment of streams. *Applied Geochemistry*, 39(0), 59-68. doi: <http://dx.doi.org/10.1016/j.apgeochem.2013.09.013>
- Baken, S., Verbeeck, M., Verheyen, D., Diels, J., & Smolders, E. (2015). Phosphorus losses from agricultural land to natural waters are reduced by immobilization in iron-rich sediments of drainage ditches. *Water Research*, 71, 160-170.
- Ball, J. W., & Nordstrom, D. K. (1991). User's manual for wateq4f, with revised thermodynamic data base and text cases for calculating speciation of major, trace, and redox elements in natural waters USGS Open-File Report: 91-183. U.S. Geological Survey, Menlo Park, California, United States.
- Ballantine, D. J., Walling, D. E., Collins, A. L., & Leeks, G. J. L. (2008). The phosphorus content of fluvial suspended sediment in three lowland groundwater-dominated catchments. *Journal of Hydrology*, 357, 140-151.
- Banner, E., Stahl, A., & Dodds, W. (2009). Stream Discharge and Riparian Land Use Influence In-Stream Concentrations and Loads of Phosphorus from Central Plains Watersheds. *Environmental Management*, 44(3), 552-565.
- Benedetti, M. F., Ranville, J. F., Allard, T., Bednar, A. J., & Menguy, N. (2003). The iron status in colloidal matter from the Rio Negro, Brasil. *Colloids and Surfaces A: Physicochemical and Engineering Aspects*, 217(1-3), 1-9. doi: [http://dx.doi.org/10.1016/S0927-7757\(02\)00553-8](http://dx.doi.org/10.1016/S0927-7757(02)00553-8)
- Berendrecht, W. L., Heemink, A. W., van Geer, F. C., & Gehrels, J. C. (2003). Decoupling of modeling and measuring interval in groundwater time series analysis based on response characteristics. *Journal of Hydrology*, 278(1-4), 1-16. doi: [http://dx.doi.org/10.1016/S0022-1694\(03\)00075-1](http://dx.doi.org/10.1016/S0022-1694(03)00075-1)
- Berner, R. A., & Rao, J. L. (1994). Phosphorus in sediments of the Amazon River and estuary: Implications for the global flux of phosphorus to the sea. *Geochimica et Cosmochimica Acta*, 58(10), 2333-2339. doi: 10.1016/0016-7037(94)90014-0
- Beusen, A. H. W., Dekkers, A. L. M., Bouwman, A. F., Ludwig, W., & Harrison, J. (2005). Estimation of global river transport of sediments and associated particulate C, N, and P. *Global Biogeochemical Cycles*, 19(GB4S05), GB4S05. doi: 10.1029/2005GB002453

- Bieroza, M. Z., Heathwaite, A. L., Mullinger, N. J., & Keenan, P. O. (2014). Understanding nutrient biogeochemistry in agricultural catchments: The challenge of appropriate monitoring frequencies. *Environmental Sciences: Processes and Impacts*, 16(7), 1676-1691. doi: 10.1039/c4em00100a
- Boers, P. C. M., & van Hese, O. (1988). Phosphorus release from the peaty sediments of the Loosdrecht Lakes (The Netherlands). *Water Research*, 22(3), 355-363.
- Boesch, D. F. (2002). Challenges and opportunities for science in reducing nutrient over-enrichment of coastal ecosystems. *Estuaries*, 25(4), 886-900. doi: 10.1007/BF02804914
- Bollyn, J., Nijssen, M., Baken, S., Joye, I. J., Waegeneers, N., Cornelis, G., & Smolders, E. (2016). Polyphosphates and fulvates enhance environmental stability of PO<sub>4</sub> bearing colloidal iron oxyhydroxides. *Journal of Agricultural and Food Chemistry*. doi: 10.1021/acs.jafc.6b02425
- Bonneville, S., Van Cappellen, P., & Behrends, T. (2004). Microbial reduction of iron(III) oxyhydroxides: effects of mineral solubility and availability. *Chemical Geology*, 212(3-4), 255-268. doi: 10.1016/j.chemgeo.2004.08.015
- Bonte, M. (2013). Impacts of shallow geothermal energy on groundwater quality; A hydrochemical and geomicrobial study of the effects of ground source heat pumps and aquifer thermal energy storage. PhD thesis, Vrije Universiteit Amsterdam.
- Botter, G., Bertuzzo, E., & Rinaldo, A. (2011). Catchment residence and travel time distributions: The master equation. *Geophysical Research Letters*, 38(11), L11403. doi: <http://dx.doi.org/10.1029/2011GL047666>
- Bouraoui, F., & Grizzetti, B. (2011). Long term change of nutrient concentrations of rivers discharging in European seas. *Science of The Total Environment*, 409(23), 4899-4916. doi: 10.1016/j.scitotenv.2011.08.015
- Bouwman, A. F., Bierkens, M. F. P., Griffioen, J., Hefting, M. M., Middelburg, J. J., Middelkoop, H., & Slomp, C. P. (2013). Nutrient dynamics, transfer and retention along the aquatic continuum from land to ocean: towards integration of ecological and biogeochemical models. *Biogeosciences*, 10(1), 1-22. doi: 10.5194/bg-10-1-2013
- Bouwman, L., Goldewijk, K. K., Van Der Hoek, K. W., Beusen, A. H. W., Van Vuuren, D. P., Willems, J., . . . Stehfest, E. (2013). Exploring global changes in nitrogen and phosphorus cycles in agriculture induced by livestock production over the 1900–2050 period. *Proceedings of the National Academy of Sciences*, 110(52), 20882-20887. doi: 10.1073/pnas.1012878110
- Bowes, M. J., Jarvie, H. P., Halliday, S. J., Skeffington, R. A., Wade, A. J., Loewenthal, M., . . . Palmer-Felgate, E. J. (2015). Characterising phosphorus and nitrate inputs to a rural river using high-frequency concentration–flow relationships. *Science of The Total Environment*, 511(0), 608-620. doi: <http://dx.doi.org/10.1016/j.scitotenv.2014.12.086>
- Bowes, M. J., Smith, J. T., Hilton, J., Sturt, M. M., & Armitage, P. D. (2007). Periphyton biomass response to changing phosphorus concentrations in a nutrient-impacted river: A new methodology for phosphorus target setting. *Canadian Journal of Fisheries and Aquatic Sciences*, 64(2), 227-238. doi: 10.1139/F06-180
- Box, G. E. P., & Jenkins, G. M. (1970). *Time Series Analysis: Forecasting and Control*. Holden-Day, San Francisco, U.S.
- Broers, H. P. (2002). *Strategies for regional groundwater quality monitoring*. PhD thesis, Utrecht University.
- Buffle, J., De Vitre, R. R., Perret, D., & Leppard, G. G. (1989). Physico-chemical characteristics of a colloidal iron phosphate species formed at the oxic-anoxic interface of a eutrophic lake. *Geochimica et Cosmochimica Acta*, 53(2), 399-408.
- Burson, A., Stomp, M., Akil, L., Brussaard, C. P. D., & Huisman, J. (2016). Unbalanced reduction of nutrient loads has created an offshore gradient from phosphorus to nitrogen limitation in the North Sea. *Limnology and Oceanography*, 61(3), 869–888. doi: 10.1002/lno.10257
- Canavan, R. W., Slomp, C. P., Jourabchi, P., Van Cappellen, P., Laverman, A. M., & van den Berg, G. A. (2006). Organic matter mineralization in sediment of a coastal freshwater lake and response to salinization. *Geochimica et Cosmochimica Acta*, 70(11), 2836-2855. doi: <http://dx.doi.org/10.1016/j.gca.2006.03.012>
- Carlyle, G. C., & Hill, A. R. (2001). Groundwater phosphate dynamics in a river riparian zone: effects of hydrologic flowpaths, lithology and redox chemistry. *Journal of Hydrology*, 247(3&4), 151-168.
- Cassidy, R., & Jordan, P. (2011). Limitations of instantaneous water quality sampling in surface-water catchments: Comparison with near-continuous phosphorus time-series data. *Journal of Hydrology*, 405(1–2), 182-193. doi: <http://dx.doi.org/10.1016/j.jhydrol.2011.05.020>

- Chardon, W. J., Aalderink, G. H., & Van Der Salm, C. (2007). Phosphorus leaching from cow manure patches on soil columns. *Journal of Environmental Quality*, 36(1), 17-22.
- Chardon, W. J., & Schoumans, O. F. (2007). Soil texture effects on the transport of phosphorus from agricultural land in river deltas of Northern Belgium, The Netherlands and North-West Germany. *Soil Use and Management*, 23, 16-24. doi: 10.1111/j.1475-2743.2007.00108.x
- Châtellier, X., Grybos, M., Abdelmoula, M., Kemner, K. M., Leppard, G. G., Mustin, C., . . . Paktunc, D. (2013). Immobilization of P by oxidation of Fe(II) ions leading to nanoparticle formation and aggregation. *Applied Geochemistry*, 35, 325-339. doi: 10.1016/j.apgeochem.2013.04.019
- Châtellier, X., West, M. M., Rose, J., Fortin, D., Leppard, G. G., & Ferris, F. G. (2004). Characterization of iron-oxides formed by oxidation of ferrous ions in the presence of various bacterial species and inorganic ligands. *Geomicrobiology Journal*, 21(2), 99-112.
- Cirno, C. P., & McDonnell, J. J. (1997). Linking the hydrologic and biogeochemical controls of nitrogen transport in near-stream zones of temperate-forested catchments: a review. *Journal of Hydrology*, 199(1-2), 88-120. doi: [http://dx.doi.org/10.1016/S0022-1694\(96\)03286-6](http://dx.doi.org/10.1016/S0022-1694(96)03286-6)
- CIW. (2001). Leidraad Monitoring [Guidance Monitoring]. Institute for Inland Water Management and Wast Water Treatment (RIZA), Lelystad, the Netherlands.
- Cleveland, W. S. (1979). Robust locally weighted regression and smoothing scatterplots. *Journal of the American Statistical Association*, 74, 829-836.
- Copeland, C. (2012). Clean Water Act and Pollutant Total Maximum Daily Loads (TMDLs) CRS Report for Congress Prepared for Members and Committees of Congress (Vol. 7-5700). Congressional Research Service, United States.
- Cordell, D., Drangert, J.-O., & White, S. (2009). The story of phosphorus: Global food security and food for thought. *Global Environmental Change*, 19(2), 292-305. doi: <http://dx.doi.org/10.1016/j.gloenvcha.2008.10.009>
- Correll, D. L. (1998). The role of phosphorus in the eutrophication of receiving waters: A review. *Journal of Environmental Quality*, 27(2), 261-266.
- Correll, D. L., Jordan, T. E., & Weller, D. E. (1999). Transport of nitrogen and phosphorus from Rhode River watersheds during storm events. *Water Resources Research*, 35(8), 2513-2521.
- Couceiro, F., Fones, G. R., Thompson, C. E. L., Statham, P. J., Sivyer, D. B., Parker, R., . . . Amos, C. L. (2013). Impact of resuspension of cohesive sediments at the Oyster Grounds (North Sea) on nutrient exchange across the sediment-water interface. *Biogeochemistry*, 113(1-3), 37-52. doi: 10.1007/s10533-012-9710-7
- Cumplido, J., Barron, V., & Torrent, J. (2000). Effect of phosphate on the formation of nanophase lepidocrocite from Fe(II) sulfate. *Clays and Clay Minerals*, 48(5), 503-510.
- Dahlke, H. E., Easton, Z. M., Lyon, S. W., Todd Walter, M., Destouni, G., & Steenhuis, T. S. (2012). Dissecting the variable source area concept - Subsurface flow pathways and water mixing processes in a hillslope. *Journal of Hydrology*, 420-421, 125-141.
- Dahm, C. N., Grimm, N. B., Marmonier, P., Valett, H. M., & Vervier, P. (1998). Nutrient dynamics at the interface between surface waters and groundwaters. *Freshwater Biology*, 40(3), 427-451. doi: 10.1046/j.1365-2427.1998.00367.x
- Davison, W., & Seed, G. (1983). The kinetics of the oxidation of ferrous iron in synthetic and natural waters. *Geochimica et Cosmochimica Acta*, 47(1), 67-79. doi: [http://dx.doi.org/10.1016/0016-7037\(83\)90091-1](http://dx.doi.org/10.1016/0016-7037(83)90091-1)
- De Bos, W. P., & Bijkerk, C. (1963). Een nieuw nomogram voor het berekenen van waterlopen [A new nomograph for the calculation of watercourses]. *Cultuurtechnisch Tijdschrift*, 3(4), 149-155.
- De Klein, J. J. M. (2008). From Ditch to Delta, Nutrient retention in running waters. PhD thesis, Wageningen University.
- De Lange, W. J., Prinsen, G. F., Hoogewoud, J. C., Veldhuizen, A. A., Verkaik, J., Oude Essink, G. H. P., . . . Kroon, T. (2014). An operational, multi-scale, multi-model system for consensus-based, integrated water management and policy analysis: The Netherlands Hydrological Instrument. *Environmental Modelling & Software*, 59(0), 98-108. doi: <http://dx.doi.org/10.1016/j.envsoft.2014.05.009>
- De Louw, P. G. B., Van der Velde, Y., & Van der Zee, S. E. A. T. M. (2011). Quantifying water and salt fluxes in a lowland polder catchment dominated by boil seepage: A probabilistic end-member mixing approach. *Hydrology and Earth System Sciences*, 15(7), 2101-2117. doi: 10.5194/hess-15-2101-2011

- De Lucas Pardo, M. A. (2014). Effect of Biota on Fine Sediment Transport Processes: A Study of Lake Markermeer. PhD thesis, Technische Universiteit Delft.
- De Lucas Pardo, M. A., Bakker, M., Van Kessel, T., Cozzoli, F., & Winterwerp, J. C. (2013). Erodibility of soft freshwater sediments in Markermeer: The role of bioturbation by meiobenthic fauna Topical Collection on the 11th International Conference on Cohesive Sediment Transport. *Ocean Dynamics*, 63(9-10), 1137-1150. doi: 10.1007/s10236-013-0650-0
- De Vet, W. W. J. M., Dinkla, I. J. T., Rietveld, L. C., & van Loosdrecht, M. C. M. (2011). Biological iron oxidation by *Gallionella* spp. in drinking water production under fully aerated conditions. *Water Research*, 45(17), 5389-5398.
- Delsman, J. R., Oude Essink, G. H. P., Beven, K. J., & Stuyfzand, P. J. (2013). Uncertainty estimation of end-member mixing using generalized likelihood uncertainty estimation (GLUE), applied in a lowland catchment. *Water Resources Research*, 49(8), 4792-4806. doi: 10.1002/wrcr.20341
- Deltares. (2016a). D-Water quality processes library description, technical reference manual 1D/2D/3D Modelling suite for integral water solutions (Vol. version 5.01, pp. 473). Deltares, Delft, the Netherlands.
- Deltares. (2016b). SOBEK. Hydrodynamics, Rainfall Runoff and Real Time Control. User Manual. Suitable for Sobek 2.14 1D/2D modelling suite for integral water solutions (Vol. version 1.0, pp. 854). Deltares, Delft, the Netherlands.
- Deng, Y. (1997). Formation of iron(III) hydroxides from homogeneous solutions. *Water Research*, 31(6), 1347-1354.
- Deppe, T., & Benndorf, J. (2002). Phosphorus reduction in a shallow hypereutrophic reservoir by in-lake dosage of ferrous iron. *Water Research*, 36(18), 4525-4534. doi: [http://dx.doi.org/10.1016/S0043-1354\(02\)00193-8](http://dx.doi.org/10.1016/S0043-1354(02)00193-8)
- Dijkstra, N., Kraal, P., Kuypers, M. M., Schnetger, B., & Slomp, C. P. (2014). Are iron-phosphate minerals a sink for phosphorus in anoxic black sea sediments? *PLoS ONE*, 9(7), e101139. doi: doi:10.1371/journal.pone.0101139
- Ding, X., Song, X., & Boily, J.-F. (2012). Identification of Fluoride and Phosphate Binding Sites at FeOOH Surfaces. *The Journal of Physical Chemistry C*, 116(41), 21939-21947. doi: 10.1021/jp3083776
- Djodjic, F., Ulén, B., & Bergström, L. (2000). Temporal and spatial variations of phosphorus losses and drainage in a structured clay soil. *Water Research*, 34(5), 1687-1695. doi: [http://dx.doi.org/10.1016/S0043-1354\(99\)00312-7](http://dx.doi.org/10.1016/S0043-1354(99)00312-7)
- Duan, S., Kaushal, S. S., Groffman, P. M., Band, L. E., & Belt, K. T. (2012). Phosphorus export across an urban to rural gradient in the Chesapeake Bay watershed. *Journal of Geophysical Research: Biogeosciences*, 117(1), G01025. doi: 10.1029/2011JG001782
- Duinker, J. C., Nolting, R. F., & van der Sloot, H. A. (1979). The determination of suspended metals in coastal waters by different sampling and processing techniques (filtration, centrifugation). *Netherlands Journal of Sea Research*, 13(2), 282-297. doi: [http://dx.doi.org/10.1016/0077-7579\(79\)90007-3](http://dx.doi.org/10.1016/0077-7579(79)90007-3)
- Dunne, E. J., Reddy, K. R., & Clark, M. W. (2006). Phosphorus release and retention by soils of natural isolated wetlands. *International Journal of Environment and Pollution*, 28(3-4), 496-516.
- Dutch Manure Act. (1986). *Meststoffenwet (Manure act)*. The Hague, The Netherlands.
- Dzombak, D. A., & Morel, F. M. (1990). *Surface complexation modeling: hydrous ferric oxide (Vol. 393)*: Wiley New York.
- EC. (1991a). Council Directive 91/271/EEC of 21 May 1991 concerning urban waste-water treatment Brussels: European Commission.
- EC. (1991b). Council Directive 91/676/EEC of 12 December 1991 concerning the protection of waters against pollution caused by nitrates from agricultural sources. Brussels: European Commission.
- EC. (2000). Council Directive of 23 October 2000 establishing a framework for Community action in the field of water policy. (Vol. Directive number 2000/60/EC). Brussel: European Commission.
- EC. (2015). *The Water Framework Directive and the Floods Directive: Actions towards the 'good status' of EU water and to reduce flood risks (COM(2015) 120 final ed., Vol. COM(2015) 120 final)*. Brussels: European Commission.
- Edixhoven, J. D., Gupta, J., & Savenije, H. H. G. (2014). Recent revisions of phosphate rock reserves and resources: a critique. *Earth Syst. Dynam.*, 5(2), 491-507. doi: 10.5194/esd-5-491-2014
- EEA. (2005). *Source apportionment of nitrogen and phosphorus inputs into the aquatic environment*. EEA report nr7/2005.
- EEA. (2015). *State of the Environment Report 2015*.

- Einsele, W. (1934). Über chemische und kolloidchemische Vorgänge in Eisen-Phosphat-Systemen unter limnochemischen und limnogeologischen Gesichtspunkten. *Arch. Hydrobiol.*, 33, 361-387.
- Elser, J., & Bennett, E. (2011). Phosphorus cycle: A broken biogeochemical cycle. *Nature*, 478(7367), 29-31.
- Elser, J. J., Bracken, M. E. S., Cleland, E. E., Gruner, D. S., Harpole, W. S., Hillebrand, H., . . . Smith, J. E. (2007). Global analysis of nitrogen and phosphorus limitation of primary producers in freshwater, marine and terrestrial ecosystems. *Ecology Letters*, 10(12), 1135-1142. doi: 10.1111/j.1461-0248.2007.01113.x
- ESPP. (2014). Joint declaration for a European sustainable phosphorus platform. European Sustainable Phosphorus Platform, Brussels, Belgium.
- Evans, D. J., & Johnes, P. J. (2004). Physico-chemical controls on phosphorus cycling in two lowland streams. Part 1 – the water column. *Science of The Total Environment*, 329(1-3), 145-163. doi: <http://dx.doi.org/10.1016/j.scitotenv.2004.02.018>
- Evans, D. J., Johnes, P. J., & Lawrence, D. S. (2004a). Physico-chemical controls on phosphorus cycling in two lowland streams. Part 2–The sediment phase. *Science of The Total Environment*, 329(1-3), 165-182. doi: 10.1016/j.scitotenv.2004.02.023
- Evans, D. J., Johnes, P. J., & Lawrence, D. S. (2004b). Physico-chemical controls on phosphorus cycling in two lowland streams. Part 2 -The sediment phase. *Science of The Total Environment*, 329(329), 165-182. doi: doi: 10.1016/j.scitotenv.2004.02.023
- Evers, C. H. M., Knoben, R. A. E., & Van Herpen, F. C. J. (2012). Omschrijving MEP en maatlatten voor sloten en kanalen voor de Kaderrichtlijn Water 2015-2021 (in Dutch). STOWA rapport 2012-34, Utrecht, the Netherlands.
- Ferrick, M. G., & Gatto, L. W. (2005). Quantifying the effect of a freeze-thaw cycle on soil erosion: Laboratory experiments. *Earth Surface Processes and Landforms*, 30(10), 1305-1326. doi: 10.1002/esp.1209
- Filippelli, G. M. (2008). The global phosphorus cycle: Past, present, and future. *Elements*, 4(2), 89-95.
- Foppen, J. W., & Griffioen, J. (1995). Contribution of groundwater outflow to the phosphate balance of ditch water in a dutch polder. *IAHS Publications-Series of Proceedings and Reports-Intern Assoc Hydrological Sciences*, 230, 177-184.
- Fox, L. E. (1988). The solubility of colloidal ferric hydroxide and its relevance to iron concentrations in river water. *Geochimica et Cosmochimica Acta*, 52(3), 771-777.
- Fox, L. E. (1989). A model for inorganic control of phosphate concentrations in river waters. *Geochimica et Cosmochimica Acta*, 53(2), 417-428.
- Fox, L. E. (1991). Phosphorus chemistry in the tidal Hudson River. *Geochimica et Cosmochimica Acta*, 55(6), 1529-1538. doi: [http://dx.doi.org/10.1016/0016-7037\(91\)90125-O](http://dx.doi.org/10.1016/0016-7037(91)90125-O)
- Frapporti, G., Vriend, S. P., & van Gaans, P. F. M. (1993). Hydrogeochemistry of the shallow dutch groundwater: Interpretation of the National Groundwater Quality Monitoring Network. *Water Resources Research*, 29(9), 2993-3004. doi: 10.1029/93WR00970
- Fraters, B., Kovar, K., Willems, W., Stockmarr, J., & Grant, R. (2005). Monitoring effectiveness of the EU Nitrates Directive Action Programmes. Results of the international MonNO3 workshop in the Netherlands, 11-12 June 2003 RIVM report 500003007/2005 (pp. 290 pp.). National Institute for Public Health and the Environment (RIVM), Bilthoven, the Netherlands.
- Frei, S., Knorr, K. H., Peiffer, S., & Fleckenstein, J. H. (2012). Surface micro-topography causes hot spots of biogeochemical activity in wetland systems: A virtual modeling experiment. *Journal of Geophysical Research G: Biogeosciences*, 117(4), G00N12. doi: 10.1029/2012JG002012
- Friedman, J. H. (1984). A variable span scatterplot smoother Stanford University Technical Report No. 5 (Vol. Stanford University Technical Report No. 5): Laboratory for Computational Statistics, Stanford University, Stanford University Technical Report No. 5.
- Froelich, P.N. (1988). Kinetic control of dissolved phosphate in natural rivers and estuaries: a primer on the phosphate buffer mechanism. *Limnology & Oceanography*, 33(4), 649-668.
- Fytianos, K., Voudrias, E., & Raikos, N. (1998). Modelling of phosphorus removal from aqueous and wastewater samples using ferric iron. *Environmental Pollution*, 101(1), 123-130. doi: 10.1016/S0269-7491(98)00007-4
- Gaffney, J. W., White, K. N., & Boulton, S. (2008). Oxidation state and size of Fe controlled by organic matter in natural waters. *Environmental Science and Technology*, 42(10), 3575-3581.

- Gao, P. (2008). Understanding watershed suspended sediment transport. *Progress in Physical Geography*, 32(3), 243-263.
- Gartner, J. W., Cheng, R. T., Wang, P.-F., & Richter, K. (2001). Laboratory and field evaluations of the LISST-100 instrument for suspended particle size determinations. *Marine Geology*, 175(1-4), 199-219. doi: [http://dx.doi.org/10.1016/S0025-3227\(01\)00137-2](http://dx.doi.org/10.1016/S0025-3227(01)00137-2)
- Gemalen. (2015). Available from: <http://www.gemalen.nl/> (Accessed 12 May 2015).
- Gerke, J. (1993). Phosphate adsorption by humic/Fe-oxide mixtures aged at pH 4 and 7 and by poorly ordered Fe-oxide. *Geoderma*, 59(1-4), 279-288.
- Geurts, J. J. M., Hetjens, H., & Lamers, L. P. M. (2013). Remobilization of nutrients after un-deepening of lakes (in Dutch) (Vol. Rapportnr 12.VDP.01, pp. 79 pp.). Nijmegen: Radbouduniversiteit Nijmegen,.
- Golterman, H. (1996). Fractionation of sediment phosphate with chelating compounds: a simplification, and comparison with other methods. *Hydrobiologia*, 335(1), 87-95. doi: 10.1007/BF00013687
- Golterman, H. L. (2001). Fractionation and bioavailability of phosphates in lacustrine sediments: A review. *Limnetica*, 20(1), 15-29.
- Grabowski, R. C., Droppo, I. G., & Wharton, G. (2011). Erodibility of cohesive sediment: The importance of sediment properties. *Earth-Science Reviews*, 105(3-4), 101-120. doi: <http://dx.doi.org/10.1016/j.earscirev.2011.01.008>
- Griffioen, J. (1994). Uptake of phosphate by iron hydroxides during seepage in relation to development of groundwater. *Environmental Science & Technology*, 28(4), 675.
- Griffioen, J. (2006). Extent of immobilisation of phosphate during aeration of nutrient-rich, anoxic groundwater. *Journal of Hydrology*, 320(3-4), 359-369. doi: 10.1016/j.jhydrol.2005.07.047
- Griffioen, J., Klaver, G., & Westerhoff, W. E. (2016). The mineralogy of suspended matter, fresh and Cenozoic sediments in the fluvio-deltaic Rhine-Meuse-Scheldt-Ems area, the Netherlands: An overview and review. *Netherlands Journal of Geosciences*, 95(1), 23-107. doi: 10.1017/njg.2015.32
- Griffioen, J., Vermooten, S., & Janssen, G. (2013). Geochemical and palaeohydrological controls on the composition of shallow groundwater in the Netherlands. *Applied Geochemistry*, 39(0), 129-149. doi: <http://dx.doi.org/10.1016/j.apgeochem.2013.10.005>
- Grizzetti, B., Bouraoui, F., & Aloe, A. (2012). Changes of nitrogen and phosphorus loads to European seas. *Global Change Biology*, 18(2), 769-782. doi: 10.1111/j.1365-2486.2011.02576.x
- Groen, K. P. (1997). Pesticide leaching in polders, Field and model studies on cracked clays and loamy sand. PhD Thesis, Wageningen University.
- Groenendijk, P., Renaud, L. V., Schoumans, O. F., Luesink, H. H., Koeijer, T. J. d., & Kruseman, G. (2012). MAMBO- en STONE-resultaten van rekenvarianten Evaluatie Meststoffenwet 2012: eindrapport ex-ante [MAMBO and STONE results of calculation variants: Evaluation Manure Act 2012: final report ex-ante]. Alterra-rapport 2317. Alterra, Wageningen, the Netherlands.
- Groenendijk, P., van Boekel, E., Renaud, L., Greijdanus, A., Michels, R., & de Koeijer, T. (2016). Landbouw en de KRW-opgave voor nutriënten in regionale wateren. Het aandeel van landbouw in de KRW-opgave, de kosten van enkele maatregelen en de effecten ervan op de uit- en afspoeling uit landbouwgronden [Agriculture and WFD task for nutrients in regional waters, the share of agriculture in the WFD task, the cost of some of the measures and their impact on the leaching and run-off from agricultural soils]. Report 2749. Wageningen Environmental Research, Wageningen, the Netherlands.
- Gu, S., Qian, Y., Jiao, Y., Li, Q., Pinay, G., & Gruau, G. (2016). An innovative approach for sequential extraction of phosphorus in sediments: Ferrous iron P as an independent P fraction. *Water Research*, 103, 352-361. doi: <http://dx.doi.org/10.1016/j.watres.2016.07.058>
- Gunnars, A., Blomqvist, S., Johansson, P., & Andersson, C. (2002). Formation of Fe(III) oxyhydroxide colloids in freshwater and brackish seawater, with incorporation of phosphate and calcium. *Geochimica et Cosmochimica Acta*, 66(5), 745-758.
- Gust, G. R. (1989). Method and apparatus to generate precisely-defined wall shearing stresses U.S. Patent No 4884892 A (Vol. US Patent 4884892 A). 5 Dec 1989.
- Gust, G. R. (1990). Method of generating precisely-defined wall shearing stresses U.S. Patent No 4973165. 27 Nov 1990.

- Halliday, S. J., Wade, A. J., Skeffington, R. A., Neal, C., Reynolds, B., Rowland, P., . . . Norris, D. (2012). An analysis of long-term trends, seasonality and short-term dynamics in water quality data from Plynlimon, Wales. *Science of The Total Environment*, 434(0), 186-200. doi: <http://dx.doi.org/10.1016/j.scitotenv.2011.10.052>
- Hardenbicker, P., Rolinski, S., Weitere, M., & Fischer, H. (2014). Contrasting long-term trends and shifts in phytoplankton dynamics in two large rivers. *International Review of Hydrobiology*, 99(4), 287-299. doi: 10.1002/iroh.201301680
- Hayashi, M., & Yanagi, T. (2009). Water and phosphorus budgets in the Yellow River estuary including the submarine fresh groundwater. Paper presented at the in: From Headwaters to the Ocean: Hydrological Change and Water Management - Proceedings of the International Conference on Hydrological Changes and Management from Headwaters to the Ocean, Hydrochange 2008, Kyoto, Japan.
- Haygarth, P. M., Wood, F. L., Heathwaite, A. L., & Butler, P. J. (2005). Phosphorus dynamics observed through increasing scales in a nested headwater-to-river channel study. *Science of The Total Environment*, 344(1-3), 83-106. doi: <http://dx.doi.org/10.1016/j.scitotenv.2005.02.007>
- He, Q. H., Leppard, G. G., Paige, C. R., & Snodgrass, W. J. (1996). Transmission electron microscopy of a phosphate effect on the colloid structure of iron hydroxide. *Water Research*, 30(6), 1345-1352.
- Heathwaite, A. L., & Dils, R. M. (2000). Characterising phosphorus loss in surface and subsurface hydrological pathways. *Science of The Total Environment*, 251-252, 523-538. doi: 10.1016/S0048-9697(00)00393-4
- Hecky, R. E., & Kilham, P. (1988). Nutrient limitation of phytoplankton in freshwater and marine environments: a review of recent evidence on the effects of enrichment. *Limnology and Oceanography*, 33(4), 796-822.
- Heiberg, L., Koch, C. B., Kjaergaard, C., Jensen, H. S., & Hansen, H. C. B. (2012). Vivianite precipitation and phosphate sorption following iron reduction in anoxic soils. *Journal of Environmental Quality*, 41(3), 938-949.
- Heinis, F., & Evers, C. H. M. (2007). Afleiding getalswaarde voor nutriënten voor een goede ecologische toestand voor natuurlijke wateren [Derivation numerical values for nutrients for the good ecological status of natural waters]. STOWA-report 2007-02. STOWA, Utrecht, the Netherlands.
- Heinis, F., & Evers, C. H. M. (2007). Toelichting op ecologische doelen voor nutriënten in oppervlaktewateren (in Dutch). STOWA-report 2007-18. STOWA, Utrecht, the Netherlands.
- Hewlett, J. D., & Hibbert, A. R. (1963). Moisture and energy conditions within a sloping soil mass during drainage. *Journal of Geophysical Research*, 68(4), 1081-1087.
- Hieltjes, A. H. M., & Lijklema, L. (1980). Fractionation of inorganic phosphates in calcareous sediments. *Journal of Environmental Quality*, 9(3), 405-407.
- Hirsch, R. M., & Slack, J. R. (1984). A Nonparametric Trend Test for Seasonal Data With Serial Dependence. *Water Resources Research*, 20(6), 727-732. doi: 10.1029/WR020i006p00727
- Hirsch, R. M., Slack, J. R., & Smith, R. A. (1982). Techniques of trend analysis for monthly water quality data. *Water Resources Research*, 18(1), 107-121. doi: 10.1029/WR018i001p00107
- Hodgkinson, R. A., Chambers, B. J., Withers, P. J. A., & Cross, R. (2002). Phosphorus losses to surface waters following organic manure applications to a drained clay soil. *Agricultural Water Management*, 57(2), 155-173. doi: [http://dx.doi.org/10.1016/S0378-3774\(02\)00057-4](http://dx.doi.org/10.1016/S0378-3774(02)00057-4)
- Holman, I. P., Whelan, M. J., Howden, N. J. K., Bellamy, P. H., Willby, N. J., Rivas-Casado, M., & McConvey, P. (2008). Phosphorus in groundwater—an overlooked contributor to eutrophication? *Hydrological Processes*, 22(26), 5121-5127. doi: 10.1002/hyp.7198
- Holtan, H., Kamp-Nielsen, L., & Stuanes, A. O. (1988). Phosphorus in soil, water and sediment: an overview. *Hydrobiologia*, 170(1), 19-34. doi: 10.1007/BF00024896
- Horowitz, A. J. (2008). Determining annual suspended sediment and sediment-associated trace element and nutrient fluxes. *Science of The Total Environment*, 400(1-3), 315-343. doi: <http://dx.doi.org/10.1016/j.scitotenv.2008.04.022>
- Horowitz, A. J., Elrick, K. A., & Hooper, R. C. (1989). A comparison of instrumental dewatering methods for the separation and concentration of suspended sediment for subsequent trace element analysis. *Hydrological Processes*, 3(2), 163-184. doi: 10.1002/hyp.3360030206
- Houot, S., & Berthelin, J. (1992). Submicroscopic studies of iron deposits occurring in field drains: formation and evolution. *Geoderma*, 52(3-4), 209-222.
- House, W. A. (2003). Geochemical cycling of phosphorus in rivers. *Applied Geochemistry*, 18(5), 739-748.

- House, W. A., & Denison, F. H. (1997). Nutrient dynamics in a lowland stream impacted by sewage effluent: Great Ouse, England. *Science of The Total Environment*, 205(1), 25-49. doi: 10.1016/S0048-9697(97)00086-7
- House, W. A., & Denison, F. H. (2002). Total phosphorus content of river sediments in relationship to calcium, iron and organic matter concentrations. *Science of The Total Environment*, 282-283, 341-351. doi: 10.1016/S0048-9697(01)00923-8
- Huebsch, M., Grimmeisen, F., Zemann, M., Fenton, O., Richards, K. G., Jordan, P., . . . Goldscheider, N. (2015). Technical Note: Field experiences using UV/VIS sensors for high-resolution monitoring of nitrate in groundwater. *Hydrology and Earth System Sciences*, 19(4), 1589-1598. doi: 10.5194/hess-19-1589-2015
- Hug, S. J., & Leupin, O. (2003). Iron-Catalyzed Oxidation of Arsenic(III) by Oxygen and by Hydrogen Peroxide: pH-Dependent Formation of Oxidants in the Fenton Reaction. *Environmental Science & Technology*, 37(12), 2734-2742. doi: 10.1021/es026208x
- Hug, S. J., Leupin, O. X., & Berg, M. (2008). Bangladesh and Vietnam: Different groundwater compositions require different approaches to arsenic mitigation. *Environmental Science and Technology*, 42(17), 6318-6323. doi: 10.1021/es7028284
- Huisman, N. L. H., Karthikeyan, K. G., Lamba, J., Thompson, A. M., & Peaslee, G. (2013). Quantification of seasonal sediment and phosphorus transport dynamics in an agricultural watershed using radiometric fingerprinting techniques. *Journal of Soils and Sediments*, 13(10), 1724-1734. doi: 10.1007/s11368-013-0769-0
- Hyacinthe, C., & Van Cappellen, P. (2004). An authigenic iron phosphate phase in estuarine sediments: composition, formation and chemical reactivity. *Marine Chemistry*, 91(1-4), 227-251. doi: <http://dx.doi.org/10.1016/j.marchem.2004.04.006>
- ISO. (2005). Liquid flow in open channels — Sediment in streams and canals — Determination of concentration, particle size distribution and relative density International Standard ISO 4365:2005. Geneva: International Organization for Standardization.
- Iuliano, M., Ciavatta, L., & De Tommaso, G. (2007). On the solubility constant of strengite. *Soil Science Society of America Journal*, 71(4), 1137-1140.
- Jackson-Blake, L. A., Wade, A. J., Futter, M. N., Butterfield, D., Couture, R. M., Cox, B., . . . Whitehead, P. G. (2016). The INtegrated CAtachment model of phosphorus dynamics (INCA-P): Description and demonstration of new model structure and equations. *Environmental Modelling & Software*, 83, 356-386. doi: <http://dx.doi.org/10.1016/j.envsoft.2016.05.022>
- Janse, J. H. (1998). A model of ditch vegetation in relation to eutrophication. *Water Science and Technology*, 37(3), 139-149. doi: 10.1016/S0273-1223(98)00065-1
- Janse, J. H., Scheffer, M., Lijklema, L., Van Liere, L., Sloot, J. S., & Mooij, W. M. (2010). Estimating the critical phosphorus loading of shallow lakes with the ecosystem model PCLake: Sensitivity, calibration and uncertainty. *Ecological Modelling*, 221(4), 654-665. doi: <http://dx.doi.org/10.1016/j.ecolmodel.2009.07.023>
- Jarvie, H. P., Mortimer, R. J. G., Palmer-Felgate, E. J., Quinton, K. S., Harman, S. A., & Carbo, P. (2008). Measurement of soluble reactive phosphorus concentration profiles and fluxes in river-bed sediments using DET gel probes. *Journal of Hydrology*, 350(3-4), 261-273.
- Jarvie, H. P., Withers, J. A., & Neal, C. (2002). Review of robust measurement of phosphorus in river water: Sampling, storage, fractionation and sensitivity. *Hydrology and Earth System Sciences*, 6(1), 113-132.
- Jeppesen, E., Søndergaard, M., Jensen, J. P., Havens, K. E., Anneville, O., Carvalho, L., . . . Winder, M. (2005). Lake responses to reduced nutrient loading – an analysis of contemporary long-term data from 35 case studies. *Freshwater Biology*, 50(10), 1747-1771. doi: 10.1111/j.1365-2427.2005.01415.x
- Johnes, P. J. (2007). Uncertainties in annual riverine phosphorus load estimation: Impact of load estimation methodology, sampling frequency, baseflow index and catchment population density. *Journal of Hydrology*, 332(1-2), 241-258. doi: <http://dx.doi.org/10.1016/j.jhydrol.2006.07.006>
- Jones, T. D., Chappell, N. A., & Tych, W. (2014). First Dynamic Model of Dissolved Organic Carbon Derived Directly from High-Frequency Observations through Contiguous Storms. *Environmental Science & Technology*, 48(22), 13289-13297. doi: 10.1021/es503506m
- Jordan, P., Arnscheidt, A., McGrogan, H., & McCormick, S. (2007). Characterising phosphorus transfers in rural catchments using a continuous bank-side analyser. *Hydrology and Earth System Sciences*, 11(1), 372-381.



- Jordan, P., Melland, A. R., Mellander, P. E., Shortle, G., & Wall, D. (2012). The seasonality of phosphorus transfers from land to water: Implications for trophic impacts and policy evaluation. *Science of The Total Environment*, 434(0), 101-109.
- Jordan, T. E., Cornwell, J. C., Boynton, W. R., & Anderson, J. T. (2008). Changes in phosphorus biogeochemistry along an estuarine salinity gradient: The iron conveyor belt. *Limnology and Oceanography*, 53(1), 172-184. doi: 10.4319/lo.2008.53.1.0172
- Kaegi, R., Voegelin, A., Folini, D., & Hug, S. J. (2010). Effect of phosphate, silicate, and Ca on the morphology, structure and elemental composition of Fe(III)-precipitates formed in aerated Fe(II) and As(III) containing water. *Geochimica et Cosmochimica Acta*, 74(20), 5798-5816. doi: <http://dx.doi.org/10.1016/j.gca.2010.07.017>
- Kalnejs, L. H., Martin, W. R., & Bothner, M. H. (2010). The release of dissolved nutrients and metals from coastal sediments due to resuspension. *Marine Chemistry*, 121(1-4), 224-235. doi: <http://dx.doi.org/10.1016/j.marchem.2010.05.002>
- Kaufmann, V., Pinheiro, A., & Castro, N. M. d. R. (2014). Simulating transport of nitrogen and phosphorus in a Cambisol after natural and simulated intense rainfall. *Journal of Contaminant Hydrology*, 160(0), 53-64. doi: <http://dx.doi.org/10.1016/j.jconhyd.2014.02.005>
- Kaushal, S. S., Mayer, P. M., Vidon, P. G., Smith, R. M., Pennino, M. J., Newcomer, T. A., . . . Belt, K. T. (2014). Land use and climate variability amplify carbon, nutrient, and contaminant pulses: A review with management implications. *Journal of the American Water Resources Association*, 50(3), 585-614. doi: 10.1111/jawr.12204
- Kersting, K., & Kouwenhoven, P. (1989). Annual and diel oxygen regime in two polder ditches. *Hydrobiological Bulletin*, 23(2), 111-123. doi: 10.1007/BF02256728
- King, K. W., Williams, M. R., Macrae, M. L., Fausey, N. R., Frankenberger, J., Smith, D. R., . . . Brown, L. C. (2015). Phosphorus transport in agricultural subsurface drainage: A review. *Journal of Environmental Quality*, 44(2), 467-485. doi: 10.2134/jeq2014.04.0163
- Kinniburgh, D., & Smedley, P. (2001). Arsenic contamination of groundwater in Bangladesh. BGS Technical Report WC/00/19. British Geological Survey, Keyworth, UK.
- Kirchner, J. W., Feng, X., Neal, C., & Robson, A. J. (2004). The fine structure of water-quality dynamics: the (high-frequency) wave of the future. *Hydrological Processes*, 18(7), 1353-1359. doi: 10.1002/hyp.5537
- Kjaergaard, C., Heiberg, L., Jensen, H. S., & Hansen, H. C. B. (2012). Phosphorus mobilization in rewetted peat and sand at variable flow rate and redox regimes. *Geoderma*, 173-174(0), 311-321. doi: 10.1016/j.geoderma.2011.12.029
- Kleeberg, A., & Herzog, C. (2014). Sediment microstructure and resuspension behavior depend on each other. *Biogeochemistry*, 119(1-3), 199-213. doi: 10.1007/s10533-014-9959-0
- Kleeberg, A., Hupfer, M., & Gust, G. (2007). Phosphorus entrainment due to resuspension in a lowland river, Spree, NE Germany - A laboratory microcosm study. *Water, Air, and Soil Pollution*, 183(1-4), 129-142. doi: 10.1007/s11270-007-9362-8
- Kleeberg, A., Hupfer, M., & Gust, G. (2008). Quantification of phosphorus entrainment in a lowland river by in situ and laboratory resuspension experiments. *Aquatic Sciences*, 70(1), 87-99. doi: 10.1007/s00027-007-0935-9
- Klein, J., & Rozemeijer, J. C. (2015). Meetnet Nutriënten Landbouw Specifiek Oppervlaktewater; Update toestand en trends tot en met 2014 (in Dutch) Deltares raport 1220098-007-BGS-0001 (pp. 86). Deltares, Delft, the Netherlands.
- Knotters, M., & van Walsum, P. E. V. (1997). Estimating fluctuation quantities from time series of water-table depths using models with a stochastic component. *Journal of Hydrology*, 197(1-4), 25-46. doi: [http://dx.doi.org/10.1016/S0022-1694\(96\)03278-7](http://dx.doi.org/10.1016/S0022-1694(96)03278-7)
- Koroleff, E. (1983). Determination of phosphorus. In K. Grasshoff, M. Ehrhardt & K. Kremling (Eds.), *Methods of Seawater Analysis*, (pp. 117-122). Weinheim: Verlag Chemie.
- Krause, S., Heathwaite, L., Binley, A., & Keenan, P. (2009). Nitrate concentration changes at the groundwater-surface water interface of a small Cumbrian river. *Hydrological Processes*, 23(15), 2195-2211.
- Kroes, J., van Boekel, E., van der Bolt, F., Renaud, L., & Roelsma, J. (2011). ECHO, een methodiek ter ondersteuning van waterbeleid; methodiekbeschrijving en toepassing Drentse Aa [ECHO, a methodology to support water policy: methodology description and application Drenthe Aa] Altera rapport 1913. Alterra, Wageningen, the Netherlands.

- Kröger, R., Holland, M. M., Moore, M. T., & Cooper, C. M. (2008). Agricultural drainage ditches mitigate phosphorus loads as a function of hydrological variability. *Journal of Environmental Quality*, 37(1), 107-113. doi: 10.2134/jeq2006.0505
- Kröger, R., Moore, M. T., Farris, J. L., & Gopalan, M. (2011). Evidence for the Use of Low-Grade Weirs in Drainage Ditches to Improve Nutrient Reductions from Agriculture. *Water, Air, & Soil Pollution*, 221(1), 223. doi: 10.1007/s11270-011-0785-x
- Kronvang, B., Bechmann, M., Lundekvam, H., Behrendt, H., Rubæk, G. H., Schoumans, O. F., . . . Hoffmann, C. C. (2005). Phosphorus losses from agricultural areas in river basins: Effects and uncertainties of targeted mitigation measures. *Journal of Environmental Quality*, 34(6), 2129-2144. doi: 10.2134/jeq2004.0439
- Kronvang, B., Behrendt, H., Andersen, H. E., Arheimer, B., Barr, A., Borgvang, S. A., . . . Larsen, S. E. (2009). Ensemble modelling of nutrient loads and nutrient load partitioning in 17 European catchments. *Journal of Environmental Monitoring*, 11(3), 572-583.
- Kronvang, B., Laubel, A., & Grant, R. (1997). Suspended sediment and particulate phosphorus transport and delivery pathways in an arable catchment, Gelbæk Stream, Denmark. *Hydrological Processes*, 11(6), 627-642.
- Kronvang, B., Vagstad, N., Behrendt, H., Bøgestrand, J., & Larsen, S. E. (2007). Phosphorus losses at the catchment scale within Europe: an overview. *Soil Use and Management*, 23, 104-116. doi: 10.1111/j.1475-2743.2007.00113.x
- Lamers, L., Schep, S., Geurts, J., & Smolders, A. (2012). Erfenis fosfaatrijk verleden: helder water met woekerende waterplanten [Heritage phosphate rich past: clear water with invasive aquatic plants]. *H2O*, 29-31.
- Lau, Y. L., & Droppo, I. G. (2000). Influence of antecedent conditions on critical shear stress of bed sediments. *Water Research*, 34(2), 663-667. doi: [http://dx.doi.org/10.1016/S0043-1354\(99\)00164-5](http://dx.doi.org/10.1016/S0043-1354(99)00164-5)
- Lavoie, M., & Auclair, J.-C. (2012). Phosphorus Mobilization at the Sediment-Water Interface in Softwater Shield Lakes: the Role of Organic Carbon and Metal Oxyhydroxides. *Aquatic Geochemistry*, 18(4), 327-341. doi: 10.1007/s10498-012-9166-3
- Ler, A., & Stanforth, R. (2003). Evidence for Surface Precipitation of Phosphate on Goethite. *Environmental Science & Technology*, 37(12), 2694-2700. doi: 10.1021/es020773i
- Li, W., Joshi, S. R., Hou, G., Burdige, D. J., Sparks, D. L., & Jaisi, D. P. (2015). Characterizing phosphorus speciation of Chesapeake Bay sediments using chemical extraction, 31P NMR, and X-ray absorption fine structure spectroscopy. *Environmental Science and Technology*, 49(1), 203-211. doi: 10.1021/es504648d
- Lienemann, C. P., Monnerat, M., Janusz, D., & Perret, D. (1999). Identification of stoichiometric iron-phosphorus colloids produced in a eutrophic lake. *Aquatic Sciences - Research Across Boundaries*, 61(2), 133-149.
- Ligtvoet, W., Beugelink, G. P., & Franken, R. (2008). Evaluation of the Water Framework Directive in the Netherlands; costs and benefits. Netherlands Environmental Assessment Agency (PBL), Bilthoven, the Netherlands.
- Liu, J., Yang, J., Cade-Menun, B. J., Liang, X., Hu, Y., Liu, C. W., . . . Shi, J. (2013). Complementary phosphorus speciation in agricultural soils by sequential fractionation, solution 31P nuclear magnetic resonance, and phosphorus K-edge X-ray absorption near-edge structure spectroscopy. *Journal of Environmental Quality*, 42(6), 1763-1770. doi: 10.2134/jeq2013.04.0127
- LNV. (2009). Fourth Dutch Action Programme (2010-2013) concerning the Nitrates Directive; 91/676/EEC. (pp. 50). Ministry of Agriculture Nature and Food Quality, The Hague, the Netherlands.
- Loeb, R., Lamers, L. P. M., & Roelofs, J. G. M. (2008). Prediction of phosphorus mobilisation in inundated floodplain soils. *Environmental Pollution*, 156(2), 325-331. doi: 10.1016/j.envpol.2008.02.006
- Lofts, S., Tipping, E., & Hamilton-Taylor, J. (2008). The Chemical Speciation of Fe(III) in Freshwaters. *Aquatic Geochemistry*, 14(4), 337-358. doi: 10.1007/s10498-008-9040-5
- Luedecke, C., Hermanowicz, S. W., & Jenkins, D. (1989). Precipitation of ferric phosphate in activated sludge: A chemical model and its verification. *Water Science and Technology*, 21(4-5 -5 pt 1), 325-337.
- Lyvén, B., Hassellöv, M., Turner, D. R., Haraldsson, C., & Andersson, K. (2003). Competition between iron- and carbon-based colloidal carriers for trace metals in a freshwater assessed using flow field-flow fractionation coupled to ICPMS. *Geochimica et Cosmochimica Acta*, 67(20), 3791-3802. doi: [http://dx.doi.org/10.1016/S0016-7037\(03\)00087-5](http://dx.doi.org/10.1016/S0016-7037(03)00087-5)

- Maassen, S., & Balla, D. (2010). Impact of hydrodynamics (ex- and infiltration) on the microbially controlled phosphorus mobility in running water sediments of a cultivated northeast German wetland. *Ecological Engineering*, 36(9), 1146-1155. doi: 10.1016/j.ecoleng.2010.01.009
- Macrae, M. L., Zhang, Z., Stone, M., Price, J. S., Bourbonniere, R. A., & Leach, M. (2011). Subsurface mobilization of phosphorus in an agricultural riparian zone in response to flooding from an upstream reservoir. *Canadian Water Resources Journal*, 36(4), 293-311. doi: 10.4296/cwrj3604810
- Mao, Y., Pham, A. N., Rose, A. L., & Waite, T. D. (2011). Influence of phosphate on the oxidation kinetics of nanomolar Fe(II) in aqueous solution at circumneutral pH. *Geochimica et Cosmochimica Acta*, 75(16), 4601-4610. doi: <http://dx.doi.org/10.1016/j.gca.2011.05.031>
- Martínez-Carreras, N., Krein, A., Gallart, F., Iffly, J.-F., Hissler, C., Pfister, L., . . . Owens, P. N. (2012). The Influence of Sediment Sources and Hydrologic Events on the Nutrient and Metal Content of Fine-Grained Sediments (Attert River Basin, Luxembourg). *Water, Air & Soil Pollution*, 223(9), 5685-5705. doi: 10.1007/s11270-012-1307-1
- Marttila, H., & Kløve, B. (2010). Managing runoff, water quality and erosion in peatland forestry by peak runoff control. *Ecological Engineering*, 36(7), 900-911. doi: <http://dx.doi.org/10.1016/j.ecoleng.2010.04.002>
- Matthiesen, H., Leipe, T., & Laima, M. (2001). A new experimental setup for studying the formation of phosphate binding iron oxides in marine sediments. Preliminary results. *Biogeochemistry*, 52(1), 79-92.
- Mayer, T. D., & Jarrell, W. M. (2000). Phosphorus sorption during iron(II) oxidation in the presence of dissolved silica. *Water Research*, 34(16), 3949-3956. doi: 10.1016/S0043-1354(00)00158-5
- Meeussen, J. C. (2003). ORCHESTRA: an object-oriented framework for implementing chemical equilibrium models. *Environmental Science & Technology*, 37(6), 1175-1182.
- Meinardi, C. R., & Van den Eertwegh, G. A. P. H. (1997). Investigations on tile drains in clayey regions of the Netherlands, Part II: Interpretation of data RIVM report 714801013. National Institute for Public Health and the Environment (RIVM), Bilthoven, the Netherlands.
- Meng, X., Korfiatis, G. P., Bang, S., & Bang, K. W. (2002). Combined effects of anions on arsenic removal by iron hydroxides. *Toxicology Letters*, 133(1), 103-111. doi: [http://dx.doi.org/10.1016/S0378-4274\(02\)00080-2](http://dx.doi.org/10.1016/S0378-4274(02)00080-2)
- Mikutta, C., Schröder, C., & Marc Michel, F. (2014). Total X-ray scattering, EXAFS, and Mössbauer spectroscopy analyses of amorphous ferric arsenate and amorphous ferric phosphate. *Geochimica et Cosmochimica Acta*, 140, 708-719. doi: <http://dx.doi.org/10.1016/j.gca.2014.05.040>
- Millero, F. J. (1985). The effect of ionic interactions on the oxidation of metals in natural waters. *Geochimica et Cosmochimica Acta*, 49(2), 547-553.
- Mitra, A. K., & Matthews, M. L. (1985). Effects of pH and phosphate on the oxidation of iron in aqueous solution. *International Journal of Pharmaceutics*, 23(2), 185-193. doi: [http://dx.doi.org/10.1016/0378-5173\(85\)90008-0](http://dx.doi.org/10.1016/0378-5173(85)90008-0)
- Monaghan, E. J., & Ruttenger, K. C. (1999). Dissolved organic phosphorus in the coastal ocean: Reassessment of available methods and seasonal phosphorus profiles from the Eel River Shelf. *Limnology and Oceanography*, 44(7), 1702-1714.
- Mosley, L. M., Hunter, K. A., & Ducker, W. A. (2003). Forces between Colloid Particles in Natural Waters. *Environmental Science & Technology*, 37(15), 3303-3308. doi: 10.1021/es026216d
- Mulholland, P. J., Newbold, J. D., Elwood, J. W., Ferren, L. A., & Jackson, R. W. (1985). Phosphorus Spiralling in a Woodland Stream: Seasonal Variations. *Ecology*, 66(3), 1012-1023.
- Murphy, J., & Riley, J. P. (1962). A modified single solution method for the determination of phosphate in natural waters. *Analytica Chimica Acta*, 27(C), 31-36.
- Mylon, S. E., Chen, K. L., & Elimelech, M. (2004). Influence of Natural Organic Matter and Ionic Composition on the Kinetics and Structure of Hematite Colloid Aggregation: Implications to Iron Depletion in Estuaries. *Langmuir*, 20(21), 9000-9006. doi: 10.1021/la049153g
- Navrotsky, A., Mazeina, L., & Majzlan, J. (2008). Size-Driven Structural and Thermodynamic Complexity in Iron Oxides. *Science*, 319(5870), 1635-1638. doi: 10.1126/science.1148614
- Neal, C., Jarvie, H. P., Williams, R. J., Neal, M., Wickham, H., & Hill, L. (2002). Phosphorus - calcium carbonate saturation relationships in a lowland chalk river impacted by sewage inputs and phosphorus remediation: an assessment of phosphorus self-cleaning mechanisms in natural waters. *Science of The Total Environment*, 282-283(0), 295-310. doi: 10.1016/S0048-9697(01)00920-2

- Neal, C., Lofts, S., Evans, C. D., Reynolds, B., Tipping, E., & Neal, M. (2008). Increasing Iron Concentrations in UK Upland Waters. *Aquatic Geochemistry*, 14(3), 263-288. doi: 10.1007/s10498-008-9036-1
- Neal, C., Reynolds, B., Rowland, P., Norris, D., Kirchner, J. W., Neal, M., . . . Armstrong, L. (2012). High-frequency water quality time series in precipitation and streamflow: From fragmentary signals to scientific challenge. *Science of The Total Environment*, 434(0), 3-12. doi: <http://dx.doi.org/10.1016/j.scitotenv.2011.10.072>
- Noordhuis, R., van Zuidam, B. G., Peeters, E. T. H. M., & van Geest, G. J. (2015). Further improvements in water quality of the Dutch Borderlakes: two types of clear states at different nutrient levels. *Aquatic Ecology*, 1-19. doi: 10.1007/s10452-015-9521-8
- Nriagu, J. O. (1972). Solubility equilibrium constant of strengite. *American Journal of Science*, 272(5), 476-484. doi: 10.2475/ajs.272.5.476
- Nriagu, J. O., & Dell, C. I. (1974). Diagenetic formation of iron phosphates in Recent lake sediments. *Am. Mineral.*, 59, 934-946.
- Nürnberg, G., & Peters, R. H. (1984). Biological Availability of Soluble Reactive Phosphorus in Anoxic and Oxidic Freshwaters. *Canadian Journal of Fisheries and Aquatic Sciences*, 41(5), 757-765. doi: 10.1139/f84-088
- Nyenje, P. M., Meijer, L. M. G., Foppen, J. W., Kulabako, R., & Uhlenbrook, S. (2014). Phosphorus transport and retention in a channel draining an urban, tropical catchment with informal settlements. *Hydrology and Earth System Sciences*, 18(3), 1009-1025. doi: 10.5194/hess-18-1009-2014
- Obersteiner, M., Peñuelas, J., Ciais, P., van der Velde, M., & Janssens, I. A. (2013). The phosphorus trilemma. *Nat Geosci*, 6(11), 897-898.
- Oenema, O., Oudendag, D., & Velthof, G. L. (2007). Nutrient losses from manure management in the European Union. *Livestock Science*, 112(3), 261-272. doi: <http://dx.doi.org/10.1016/j.livsci.2007.09.007>
- Owens, P. N., & Walling, D. E. (2002). The phosphorus content of fluvial sediment in rural and industrialized river basins. *Water Research*, 36(3), 685-701. doi: [http://dx.doi.org/10.1016/S0043-1354\(01\)00247-0](http://dx.doi.org/10.1016/S0043-1354(01)00247-0)
- Pacini, N., & Gächter, R. (1999). Speciation of riverine particulate phosphorus during rain events. *Biogeochemistry*, 47(1), 87-109. doi: 10.1007/BF00993098
- Palmer-Felgate, E. J., Jarvie, H. P., Williams, R. J., Mortimer, R. J. G., Loewenthal, M., & Neal, C. (2008). Phosphorus dynamics and productivity in a sewage-impacted lowland chalk stream. *Journal of Hydrology*, 351(1-2), 87-97. doi: <http://dx.doi.org/10.1016/j.jhydrol.2007.11.036>
- Pardo, P., Rauret, G., & López-Sánchez, J. F. (2003). Analytical approaches to the determination of phosphorus partitioning patterns in sediments. *Journal of Environmental Monitoring*, 5(2), 312-318. doi: 10.1039/b210354k
- Parkhurst, D. L., & Appelo, C. (1999). User's guide to phreeqc (Version 2): A computer program for speciation, batch-reaction, one-dimensional transport, and inverse geochemical calculations US Geol. Survey, Water-Resour. Inv. Report 99-4259. Denver, Colorado, United States: U.S. Geological Survey.
- Parkhurst, D. L., & Appelo, C. (2013). Description of input and examples for PHREEQC version 3—a computer program for speciation, batch-reaction, one-dimensional transport, and inverse geochemical calculations US geological survey techniques and methods (Vol. 6, pp. 497): US geological survey.
- Partheniades, E. (1965). Erosion and deposition of cohesive soils. *J. Hydraul. Div. Am. Soc. Civ. Eng.*, 91(1), 105-139.
- Pedersen, H. D., Postma, D., Jakobsen, R., & Larsen, O. (2005). Fast transformation of iron oxyhydroxides by the catalytic action of aqueous Fe(II). *Geochimica et Cosmochimica Acta*, 69(16), 3967-3977. doi: <http://dx.doi.org/10.1016/j.gca.2005.03.016>
- Perret, D., Gaillard, J. F., Dominik, J., & Atteia, O. (2000). The diversity of natural hydrous iron oxides. *Environmental Science and Technology*, 34(17), 3540-3546.
- Perry, R. H., Green, D. W., & Maloney, J. O. (1997). *Perry's Chemical Engineers' Handbook*: McGraw-Hill Education.
- Petry, J., Soulsby, C., Malcolm, I. A., & Youngson, A. F. (2002). Hydrological controls on nutrient concentrations and fluxes in agricultural catchments. *Science of The Total Environment*, 294(1-3), 95-110. doi: 10.1016/S0048-9697(02)00058-X
- Phillips, J. M., Russell, M. A., & Walling, D. E. (2000). Time-integrated sampling of fluvial suspended sediment: a simple methodology for small catchments. *Hydrological Processes*, 14(14), 2589-2602. doi: 10.1002/1099-1085(20001015)14:14<2589::AID-HYP94>3.0.CO;2-D

- Pizarro, J., Belzile, N., Filella, M., Leppard, G. G., Negre, J.-C., Perret, D., & Buffle, J. (1995). Coagulation/sedimentation of submicron iron particles in a eutrophic lake. *Water Research*, 29(2), 617-632. doi: [http://dx.doi.org/10.1016/0043-1354\(94\)00167-6](http://dx.doi.org/10.1016/0043-1354(94)00167-6)
- Poor, C. J., & McDonnell, J. J. (2007). The effects of land use on stream nitrate dynamics. *Journal of Hydrology*, 332(1-2), 54-68. doi: <http://dx.doi.org/10.1016/j.jhydrol.2006.06.022>
- Portielje, R., Schipper, C., & Schoor, M. (2005). Effects of hydromorphological pressures on the ecological water quality elements of the WFD RIZA/2005.098X. Institute for Inland Water Management and Wast Water Treatment (RIZA), Lelystad, the Netherlands.
- Poulenard, J., Dorioz, J.-M., & Elsass, F. (2008). Analytical Electron-Microscopy Fractionation of Fine and Colloidal Particulate-Phosphorus in Riverbed and Suspended Sediments. *Aquatic Geochemistry*, 14(3), 193-210. doi: 10.1007/s10498-008-9032-5
- Pratesi, G., Cipriani, C., Giuli, G., & Birch, W. D. (2003). Santabarbarite: a new amorphous phosphate mineral. *European Journal of Mineralogy*, 15(1), 185-192. doi: 10.1127/0935-1221/2003/0015-0185
- Pullin, M. J., & Cabaniss, S. E. (2003). The effects of pH, ionic strength, and iron-fulvic acid interactions on the kinetics of non-photochemical iron transformations. I. Iron(II) oxidation and iron(III) colloid formation. *Geochimica et Cosmochimica Acta*, 67(21), 4067-4077. doi: [http://dx.doi.org/10.1016/S0016-7037\(03\)00366-1](http://dx.doi.org/10.1016/S0016-7037(03)00366-1)
- Rast, W., & Lee, G. F. (1978). Summary analysis of the North American (US Portion) OCED eutrophication project: nutrient loading-lake response relationships and trophic state indices (Vol. EPA-600/3-78-008): United States Environmental Protection Agency.
- Reddy, K. R., Kadlec, R. H., Flaig, E., & Gale, P. M. (1999). Phosphorus Retention in Streams and Wetlands: A Review. *Critical Reviews in Environmental Science and Technology*, 29(1), 83-146.
- Regelink, I. C., Koopmans, G. F., van der Salm, C., Weng, L., & van Riemsdijk, W. H. (2013). Characterization of Colloidal Phosphorus Species in Drainage Waters from a Clay Soil Using Asymmetric Flow Field-Flow Fractionation. *Journal of Environmental Quality*, 42(2), 464-473. doi: 10.2134/jeq2012.0322
- Reid, D. K., Ball, B., & Zhang, T. Q. (2012). Accounting for the Risks of Phosphorus Losses through Tile Drains in a Phosphorus Index. *Journal of Environmental Quality*, 41(6), 1720-1729. doi: 10.2134/jeq2012.0238
- Robards, K., McKelvie, I. D., Benson, R. L., Worsfold, P. J., Blundell, N. J., & Casey, H. (1994). Determination of carbon, phosphorus, nitrogen and silicon species in waters. *Analytica Chimica Acta*, 287(3), 147-190. doi: 10.1016/0003-2670(93)E0542-F
- Roberts, L. C., Hug, S. J., Ruettimann, T., Billah, M., Khan, A. W., & Rahman, M. T. (2004). Arsenic Removal with Iron(II) and Iron(III) in Waters with High Silicate and Phosphate Concentrations. *Environmental Science and Technology*, 38(1), 307-315.
- Rode, M., Arhonditsis, G., Balin, D., Kebede, T., Krysanova, V., Van Griensven, A., & Van Der Zee, S. E. A. T. M. (2010). New challenges in integrated water quality modelling. *Hydrological Processes*, 24(24), 3447-3461. doi: 10.1002/hyp.7766
- Roden, E. E., & Edmonds, J. W. (1997). Phosphate mobilization in iron-rich anaerobic sediments: Microbial Fe(III) oxide reduction versus iron-sulfide formation. *Archiv für Hydrobiologie*, 139(3), 347-378.
- Roelsma, J., Van der Griff, B., Mulder, H. M., & Tol-Leenders, T. P. (2011a). Nutriënthuishouding in de bodem en het oppervlaktewater van de Drentse Aa; bronnen, routes en sturingsmogelijkheden [Nutrient balance in the soil and surface of the Drenthe Aa: sources, pathways and control options] Alterra-report 2218. Alterra, Wageningen, the Netherlands.
- Roelsma, J., Van der Griff, B., Mulder, H. M., & Tol-Leenders, T. P. (2011b). Nutriënthuishouding in de bodem en het oppervlaktewater van de Schuitenbeek; bronnen, routes en sturingsmogelijkheden [Nutrient balance in the soil and surface of the Schuitenbeek: sources, pathways and control options] Alterra-report 2219. Alterra, Wageningen, the Netherlands.
- Rose, J., Manceau, A., Bottero, J. Y., Masion, A., & Garcia, F. (1996). Nucleation and Growth Mechanisms of Fe Oxyhydroxide in the Presence of PO<sub>4</sub> Ions. 1. Fe K-Edge EXAFS Study. *Langmuir*, 12(26), 6701-6707.
- Rozemeijer, J., Siderius, C., Verheul, M., & Pomarius, H. (2012). Tracing the spatial propagation of river inlet water into an agricultural polder area using anthropogenic gadolinium. *Hydrology and Earth System Sciences*, 16(8), 2405-2415. doi: 10.5194/hess-16-2405-2012

- Rozemeijer, J., Van der Velde, Y., De Jonge, H., Van Geer, F., Broers, H. P., & Bierkens, M. (2010a). Application and evaluation of a new passive sampler for measuring average solute concentrations in a catchment scale water quality monitoring study. *Environmental Science and Technology*, 44(4), 1353-1359.
- Rozemeijer, J. C., & Broers, H. P. (2007). The groundwater contribution to surface water contamination in a region with intensive agricultural land use (Noord-Brabant, The Netherlands). *Environmental Pollution*, 148(3), 695-706. doi: 10.1016/j.envpol.2007.01.028
- Rozemeijer, J. C., Klein, J., Broers, H. P., Van Tol-Leenders, T. P., & Van Der Grift, B. (2014). Water quality status and trends in agriculture-dominated headwaters; a national monitoring network for assessing the effectiveness of national and European manure legislation in The Netherlands. *Environmental Monitoring and Assessment*, 186(12), 8981-8995. doi: 10.1007/s10661-014-4059-0
- Rozemeijer, J. C., Van Der Velde, Y., McLaren, R. G., Van Geer, F. C., Broers, H. P., & Bierkens, M. F. P. (2010c). Integrated modeling of groundwater-surface water interactions in a tile-drained agricultural field: The importance of directly measured flow route contributions. *Water Resources Research*, 46(11), W11537. doi: 10.1029/2010WR009155
- Rozemeijer, J. C., Van der Velde, Y., Van Geer, F. C., De Rooij, G. H., Torfs, P. J. J. F., & Broers, H. P. (2010). Improving load estimates for NO<sub>3</sub> and P in surface waters by characterizing the concentration response to rainfall events. *Environmental Science and Technology*, 44(16), 6305-6312.
- Rozemeijer, J. C., Van Der Velde, Y., Van Geer, F. C., De Rooij, G. H., Torfs, P. J. J. F., & Broers, H. P. (2010b). Improving load estimates for NO<sub>3</sub> and P in surface waters by characterizing the concentration response to rainfall events. *Environmental Science and Technology*, 44(16), 6305-6312.
- Ruttenberg, K. C. (1992). Development of a sequential extraction method for different forms of phosphorus in marine sediments. *Limnology & Oceanography*, 37(7), 1460-1482.
- Ruttenberg, K. C., Ogawa, N. O., Tamburini, F., Briggs, R. A., Colasacco, N. D., & Joyce, E. (2009). Improved, high-throughput approach for phosphorus speciation in natural sediments via the SEDEX sequential extraction method. *Limnology and Oceanography: Methods*, 7, 319-333.
- Salminen, R. (2005). FOREGS Geochemical Atlas of Europe, Part 1 - Background information, methodology and maps. Espoo, Finland: Geological Survey of Finland.
- Scanlon, T. M., Kiely, G., & Amboldi, R. (2005). Model determination of non-point source phosphorus transport pathways in a fertilized grassland catchment. *Hydrological Processes*, 19(14), 2801-2814.
- Schaefer, M. V., Gorski, C. A., & Scherer, M. M. (2010). Spectroscopic Evidence for Interfacial Fe(II)–Fe(III) Electron Transfer in a Clay Mineral. *Environmental Science & Technology*, 45(2), 540-545. doi: 10.1021/es102560m
- Scherrenberg, S. M. (2011). Reaching ultra low phosphorus concentrations by filtration techniques. (PhD PhD), Technische Universiteit Delft, Delft.
- Schindler, D. W. (2012). The dilemma of controlling cultural eutrophication of lakes. *Proceedings of the Royal Society of London B: Biological Sciences*, 279(1746), 4322-4333. doi: 10.1098/rspb.2012.1032
- Schoch, A. L., Schilling, K. E., & Chan, K.-S. (2009). Time-series modeling of reservoir effects on river nitrate concentrations. *Advances in Water Resources*, 32(8), 1197-1205. doi: <http://dx.doi.org/10.1016/j.advwatres.2009.04.002>
- Schoumans, O. F., & Chardon, W. J. (2014). Phosphate saturation degree and accumulation of phosphate in various soil types in The Netherlands. *Geoderma*, 237, 325-335.
- Schoumans, O. F., & Chardon, W. J. (2015). Phosphate saturation degree and accumulation of phosphate in various soil types in The Netherlands. *Geoderma*, 237–238, 325-335. doi: <http://dx.doi.org/10.1016/j.geoderma.2014.08.015>
- Schoumans, O. F., & Groenendijk, P. (2000). Modeling Soil Phosphorus Levels and Phosphorus Leaching from Agricultural Land in the Netherlands. *Journal of Environmental Quality*, 29(1), 111-116. doi: 10.2134/jeq2000.00472425002900010014x
- Senn, A. C., Kaegi, R., Hug, S. J., Hering, J. G., Mangold, S., & Voegelin, A. (2015). Composition and structure of Fe(III)-precipitates formed by Fe(II) oxidation in water at near-neutral pH: Interdependent effects of phosphate, silicate and Ca. *Geochimica et Cosmochimica Acta*, 162, 220-246. doi: 10.1016/j.gca.2015.04.032
- Sharpley, A. N., Kleinman, P. J. A., Heathwaite, A. L., Gburek, W. J., Folmar, G. J., & Schmidt, J. P. (2008). Phosphorus loss from an agricultural watershed as a function of storm size. *Journal of Environmental Quality*, 37(2), 362-368.

- Shenker, M., Seittelbach, S., Brand, S., Haim, A., & Litaor, M. I. (2005). Redox reactions and phosphorus release in flooded soils of an altered wetland. *European Journal of Soil Science*, 56(4), 515-525.
- Shrestha, R. R., Osenbrück, K., & Rode, M. (2013). Assessment of catchment response and calibration of a hydrological model using high-frequency discharge nitrate concentration data. *Hydrology Research*, 44(6), 995-1012. doi: 10.2166/nh.2013.087
- Simard, R. R., Beauchemin, S., & Haygarth, P. M. (2000). Potential for preferential pathways of phosphorus transport. *Journal of Environmental Quality*, 29(1), 97-105.
- Skeffington, R. A., Halliday, S. J., Wade, A. J., Bowes, M. J., & Loewenthal, M. (2015). Using high-frequency water quality data to assess sampling strategies for the EU Water Framework Directive. *Hydrology and Earth System Sciences*, 19(5), 2491-2504. doi: 10.5194/hess-19-2491-2015
- Slomp, C. P., & Epping, E. H. G. (1996). A key role for iron-bound phosphorus in authigenic apatite formation in North Atlantic. *Journal of Marine Research*, 54(6), 1179.
- Slomp, C. P., Epping, E. H. G., Helder, W., & Van Raaphorst, W. (1996). A key role for iron-bound phosphorus in authigenic apatite formation in North Atlantic continental platform sediments. *Journal of Marine Research*, 54(6), 1179-1205. doi: <https://doi.org/10.1357/0022240963213745>
- Smit, A. L., van Middelkoop, J. C., van Dijk, W., & van Reuler, H. (2015). A substance flow analysis of phosphorus in the food production, processing and consumption system of the Netherlands. *Nutrient Cycling in Agroecosystems*, 103(1), 1-13. doi: 10.1007/s10705-015-9709-2
- Smith, D. R. (2009). Assessment of in-stream phosphorus dynamics in agricultural drainage ditches. *Science of The Total Environment*, 407(12), 3883-3889. doi: 10.1016/j.scitotenv.2009.02.038
- Smolders, A. J. P., Lamers, L. P. M., Lucassen, E. C. H. E. T., Van Der Velde, G., & Roelofs, J. G. M. (2006). Internal eutrophication: How it works and what to do about it - A review. *Chemistry and Ecology*, 22(2), 93-111. doi: 10.1080/02757540600579730
- Spiteri, C., Regnier, P., Slomp, C. P., & Charette, M. A. (2006). pH-Dependent iron oxide precipitation in a subterranean estuary. *Journal of Geochemical Exploration*, 88(1-3), 399-403. doi: <http://dx.doi.org/10.1016/j.gexplo.2005.08.084>
- Steinman, A., Abdimalik, M., Ogdahl, M. E., & Oudsema, M. (2016). Understanding planktonic vs. benthic algal response to manipulation of nutrients and light in a eutrophic lake. *Lake and Reservoir Management*, 1-9. doi: 10.1080/10402381.2016.1235065
- Stumm, W., & Lee, G. F. (1961). Oxygenation of Ferrous Iron. *Industrial & Engineering Chemistry*, 53(2), 143-146. doi: 10.1021/ie50614a030
- Stumm, W., & Morgan, J. J. (1970). *Aquatic Chemistry: An Introduction Emphasizing Chemical Equilibria in Natural Waters*. New York.
- Stumm, W., & Sigg, L. (1979). Kolloidchemische Grundlagen der Phosphor-Elimination in Fällung, Flockung und Filtration. *Z. Wasser Abwass. Forsch.*, 12, 73-83.
- Stutter, M. I., Langan, S. J., & Cooper, R. J. (2008). Spatial contributions of diffuse inputs and within-channel processes to the form of stream water phosphorus over storm events. *Journal of Hydrology*, 350(3-4), 203-214. doi: 10.1016/j.jhydrol.2007.10.045
- Subramanian, V. (2000). Transfer of phosphorus from the Indian sub-continent to the adjacent oceans. Marine authigenesis: From global to microbial. SEPM (Society for Sedimentary Geology) Special Publication, 66, 77-88.
- Sung, W., & Morgan, J. J. (1980). Kinetics and product of ferrous iron oxygenation in aqueous systems. *Environmental Science & Technology*, 14(5), 561-568. doi: 10.1021/es60165a006
- Tamura, H., Goto, K., & Nagayama, M. (1976). Effect of anions on the oxygenation of ferrous ion in neutral solutions. *Journal of Inorganic and Nuclear Chemistry*, 38(1), 113-117. doi: [http://dx.doi.org/10.1016/0022-1902\(76\)80061-9](http://dx.doi.org/10.1016/0022-1902(76)80061-9)
- Tappin, A. D., Mankasingh, U., McKelvie, I. D., & Worsfold, P. J. (2013). Temporal variability in nutrient concentrations and loads in the River Tamar and its catchment (SW England) between 1974 and 2004. *Environmental Monitoring and Assessment*, 185(6), 4791-4818. doi: 10.1007/s10661-012-2905-5

- Tessenow, U. (1974). Solution diffusion and sorption in the upper layers of lake sediments. IV. Reaction mechanisms and equilibria in the system iron-manganese-phosphate with regard to the accumulation of vivianite in Lake Ursee (In German with English summary). *Arch. Hydrobiol. Suppl.*(47), 1–79.
- Tiemeyer, B., Lennartz, B., & Kahle, P. (2008). Analysing nitrate losses from an artificially drained lowland catchment (North-Eastern Germany) with a mixing model. *Agriculture, Ecosystems & Environment*, 123(1–3), 125–136. doi: <http://dx.doi.org/10.1016/j.agee.2007.05.006>
- Tolhurst, T. J., Black, K. S., Shayler, S. A., Mather, S., Black, I., Baker, K., & Paterson, D. M. (1999). Measuring the in situ Erosion Shear Stress of Intertidal Sediments with the Cohesive Strength Meter (CSM). *Estuarine, Coastal and Shelf Science*, 49(2), 281–294. doi: <http://dx.doi.org/10.1006/ecss.1999.0512>
- Turner, B. L. (2004). Organic phosphorus transfer from terrestrial to aquatic environments *Organic Phosphorus in the Environment* (pp. 269–294).
- Udo, J., & Bakker, M. (2009). Sobek model Land van Maas en Waal (in Dutch). HKV Consultants, Lelystad, the Netherlands.
- Ulén, B. (2004). Size and settling velocities of phosphorus-containing particles in water from agricultural drains. *Water, Air, and Soil Pollution*, 157(1–4), 331–343. doi: 10.1023/B:WATE.0000038906.18517.e2
- Valentine, K., Mariotti, G., & Fagherazzi, S. (2014). Repeated erosion of cohesive sediments with biofilms. *Advances in Geosciences*, 39, 9–14. doi: 10.5194/adgeo-39-9-2014
- Van Beek, C. G. E. M., Breedveld, R. J. M., Juhász-Holterman, M., Oosterhof, A., & Stuyfzand, P. J. (2009). Cause and prevention of well bore clogging by particles. *Hydrogeology Journal*, 17(8), 1877–1886.
- Van Boekel, E., Bogaart, P., van Gerven, L., van Hattum, T., Kselik, R., Massop, H., . . . van der Bolt, F. (2013). Evaluatie landbouw en KRW Evaluatie meststoffenwet 2012: deelrapport ex post [Evaluation agriculture and WFD: Evaluation Manure Act 2012: section report ex-post] Alterra-rapport 2326. Alterra, Wageningen, the Netherlands.
- Van Boekel, E., Roelsma, J., Massop, H., Mulder, H., Jansen, P., Renaud, L., . . . Schipper, P. (2015). Achtergrondconcentraties in het oppervlaktewater van HHNK Hoofdrapport: analyse achtergrondconcentraties voor stikstof en fosfor op basis van water- en nutriëntenbalansen voor het beheergebied van HHNK [Analysis background concentrations of nitrogen and phosphorus based on water and nutrient balances for the area managed by HHNK] Alterra-rapport 2475. Alterra, Wageingen, the Netherlands.
- Van Boekel, E. M. P. M., Roelsma, J., Massop, H. T. L., Hendriks, R. F. A., Goedhart, P. W., & Jansen, P. C. (2012). Nitraatconcentraties in het drainwater in zeekelegebieden : oriënterend onderzoek naar de oorzaken van de verhoogde nitraatconcentraties (in Dutch) Alterra-rapport 2360. Alterra, Wageningen, the Netherlands.
- Van de Ven, G. P. (2004). Man-made lowlands, history of water management and land reclamation in the Netherlands. Uitgeverij Matrijs, Utrecht, the Netherlands.
- Van den Eertwegh, G. A. P. H. (2002). Water and Nutrient budgets at field and regional scale, travel times of drainage water and nutrient loads to surface water. PhD thesis, Wageningen University.
- Van den Roovaart, J., Meijers, E., Smit, R., Cleij, P., Van Gaalen, F., & Witteveen, S. (2012). Landelijke pilot KRW-Verkenner 2.0 Effecten van beleidsscenario's op de nutriëntenkwaliteit [National pilot WFD Explorer 2.0 Effects of policy scenarios on the nutrient quality] report no. 1205716-000-ZWS-0011. Deltares, Delft, the Netherlands
- Van der Grift, B., Behrends, T., Osté, L. A., Schot, P. P., Wassen, M. J., & Griffioen, J. (2016). Fe hydroxyphosphate precipitation and Fe(II) oxidation kinetics upon aeration of Fe(II) and phosphate-containing synthetic and natural solutions. *Geochimica et Cosmochimica Acta*, 186, 71–90. doi: 10.1016/j.gca.2016.04.035
- Van der Grift, B., Broers, H. P., Berendrecht, W., Rozemeijer, J., Osté, L., & Griffioen, J. (2016). High-frequency monitoring reveals nutrient sources and transport processes in an agriculture-dominated lowland water system. *Hydrology and Earth System Sciences*, 20(5), 1851–1868. doi: 10.5194/hess-20-1851-2016
- Van der Grift, B., Klein, J., De Boorder, N., & Rozemeijer, J. C. (2011). Grondwater aan de oppervlaktewaterkwaliteit in de Drentse Aa en Schuitenbeek [Groundwater contribution to surface water quality in the Drentse Aa and Schuitenbeek] Reeks Monitoring Stroomgebieden (Vol. 24, pp. 92). Deltares, Utrecht, the Netherlands.
- Van der Grift, B., Osté, L. A., Schot, P. P., Kratz, A., Van Popta, E. D. M., Wassen, M. J., & Griffioen, J. (2016). Particulate phosphorus speciation in ditches, channels and streams of agriculture-dominated lowland catchments: iron as phosphorus carrier. in prep.



- Van der Grift, B., Rozemeijer, J. C., Griffioen, J., & van der Velde, Y. (2014). Iron oxidation kinetics and phosphate immobilization along the flow-path from groundwater into surface water. *Hydrology and Earth System Sciences*, 18(11), 4687-4702. doi: 10.5194/hess-18-4687-2014
- Van der Linden, W., Berendrecht, W., Hendriksen, G., Veldhuizen, A., Massop, H., Heuven, A., & Zaadnoordijk, W. J. (2008). Groundwatermodelling Rivierenland; MORIA (In Dutch) Deltares/TNO rapport 2008-U-R0827/A. TNO/Deltares/Royal Haskoning /Tauw/Alterra, Utrecht, the Netherlands.
- Van der Salm, C., van den Toorn, A., Chardon, W. J., & Koopmans, G. F. (2012). Water and nutrient transport on a heavy clay soil in a fluvial plain in the Netherlands. *Journal of Environmental Quality*, 41(1), 229-241. doi: 10.2134/jeq2011.0292
- Van der Velde, Y., Rozemeijer, J. C., de Rooij, G. H., van Geer, F. C., & Broers, H. P. (2010). Field-Scale Measurements for Separation of Catchment Discharge into Flow Route Contributions. *Vadose Zone J.*, 9(1), 25-35. doi: doi:10.2136/vzj2008.0141
- Van der Velde, Y., Rozemeijer, J. C., De Rooij, G. H., Van Geer, F. C., Torfs, P. J. J. F., & De Louw, P. G. B. (2011). Improving catchment discharge predictions by inferring flow route contributions from a nested-scale monitoring and model setup. *Hydrology and Earth System Sciences*, 15(3), 913-930.
- Van der Velde, Y., Torfs, P. J. J. F., van der Zee, S. E. A. T. M., & Uijlenhoet, R. (2012). Quantifying catchment-scale mixing and its effect on time-varying travel time distributions. *Water Resources Research*, 48(6), n/a-n/a. doi: 10.1029/2011WR011310
- Van Duijvenbooden, W., Taat, J., & Gast, L. F. L. (1985). National groundwater quality monitoring network: final report of the implementation (in Dutch). report no. 840382001. National Institute for Public Health and the Environment (RIVM), Leidschendam, the Netherlands.
- Van Eck, G. T. M. (1982). Forms of phosphorus in particulate matter from the Hollands Diep/Haringvliet, The Netherlands. *Hydrobiologia*, 91-92(1), 665-681. doi: 10.1007/BF00940156
- Van Gaalen, F., Tiktak, A., Franken, R., Van Boekel, E. M. P. M., Van Puijenbroek, P. J. T. M., & Muilwijk, H. (2016). Water quality now and in the future, final report ex-ante evaluation of the Dutch package of measures for the Water Framework Directive (in Dutch) PBL-report (Vol. PBL-publicatienummer: 1727, pp. 58). Den Haag: PBL Netherlands Environmental Assessment Agency.
- Van Geen, A., Robertson, A. P., & Leckie, J. O. (1994). Complexation of carbonate species at the goethite surface: implications for adsorption of metal ions in natural waters. *Geochimica et Cosmochimica Acta*, 58, 2073-2086.
- Van Geest, G., & Noordhuis, R. (2014). Sturen op watervegetaties [Controlling water vegetaion] Deltares rapport 1208460-000-ZWS-0006. Deltares, Delft, the Netherlands.
- Van Genuchten, C. M., Gadgil, A. J., & Peña, J. (2014). Fe(III) Nucleation in the Presence of Bivalent Cations and Oxyanions Leads to Subnanoscale 7 Å Polymers. *Environmental Science & Technology*, 48(20), 11828-11836. doi: 10.1021/es503281a
- Van Gerven, L. P. A. (2016). The ecology of ditches; a modelling perspective. PhD thesis, Wageningen University.
- Van Grinsven, H. J. M., ten Berge, H. F. M., Dalgaard, T., Fraters, B., Durand, P., Hart, A., . . . Willems, W. J. (2012). Management, regulation and environmental impacts of nitrogen fertilization in northwestern Europe under the Nitrates Directive; a benchmark study. *Biogeosciences*, 9(12), 5143-5160. doi: 10.5194/bg-9-5143-2012
- Van Liere, L., Janse, J. H., & Arts, G. H. P. (2007). Setting critical nutrient values for ditches using the eutrophication model PCDitch. *Aquatic Ecology*, 41(3), 443-449. doi: 10.1007/s10452-005-2835-1
- Van Moorleghem, C., Six, L., Degryse, F., Smolders, E., & Merckx, R. (2011). Effect of Organic P Forms and P Present in Inorganic Colloids on the Determination of Dissolved P in Environmental Samples by the Diffusive Gradient in Thin Films Technique, Ion Chromatography, and Colorimetry. *Analytical Chemistry*, 83(13), 5317-5323.
- Van Popta, E. D. M. (2016). Particulate phosphorus speciation and phosphate release in streams and ditches of Dutch agricultural lowland catchments. Master thesis, Utrecht University.
- Van Prooijen, B. C., & Winterwerp, J. C. (2010). A stochastic formulation for erosion of cohesive sediments. *Journal of Geophysical Research: Oceans*, 115(C1), n/a-n/a. doi: 10.1029/2008JC005189
- Van Riemsdijk, W. H., van der Linden, A. M. A., & Boumans, L. J. M. (1984). Phosphate sorption by soils: III. the P diffusion-precipitation model tested for three acid sandy soils. *Soil Science Society of America Journal*, 48(3), 545-548.

- Van Rijn, L. C. (1984). Sediment transport, part I: bed load transport. *Journal of hydraulic engineering*, 110(10), 1431-1456.
- Van Rijn, L. C. (1993). *Principles of sediment transport in rivers, estuaries and coastal seas*. Aqua publications, Amsterdam, the Netherlands.
- Vanlierde, E. (2013). *Sediment concentrations, fluxes and source apportionment: methodology assessment and application in Nete and Demer tributary basins (river Scheldt basin, Belgium)*. PhD thesis, Ghent University.
- Vanlierde, E., De Schutter, J., Jacobs, P., & Mostaert, F. (2007). Estimating and modeling the annual contribution of authigenic sediment to the total suspended sediment load in the Kleine Nete Basin, Belgium. *Sedimentary Geology*, 202(1–2), 317-332. doi: 10.1016/j.sedgeo.2007.05.003
- Verdonschot, R. M., & Verdonschot, P. M. (2014). Shading effects of free-floating plants on drainage-ditch invertebrates. *Limnology*, 15(3), 225-235. doi: 10.1007/s10201-013-0416-x
- Viollier, E., Inglett, P. W., Hunter, K., Roychoudhury, A. N., & Van Cappellen, P. (2000). The ferrozine method revisited: Fe(II)/Fe(III) determination in natural waters. *Applied Geochemistry*, 15(6), 785-790.
- Visser, A., Broers, H. P., van der Grift, B., & Bierkens, M. F. P. (2007). Demonstrating trend reversal of groundwater quality in relation to time of recharge determined by 3H/3He. *Environmental Pollution*, 148(3), 797-807. doi: 10.1016/j.envpol.2007.01.027
- Voegelin, A., Kaegi, R., Frommer, J., Vantelon, D., & Hug, S. J. (2010). Effect of phosphate, silicate, and Ca on Fe(III)-precipitates formed in aerated Fe(II)- and As(III)-containing water studied by X-ray absorption spectroscopy. *Geochimica et Cosmochimica Acta*, 74(1), 164-186. doi: <http://dx.doi.org/10.1016/j.gca.2009.09.020>
- Voegelin, A., Senn, A. C., Kaegi, R., Hug, S. J., & Mangold, S. (2013). Dynamic Fe-precipitate formation induced by Fe(II) oxidation in aerated phosphate-containing water. *Geochimica et Cosmochimica Acta*, 117, 216-231.
- Vollrath, S., Behrends, T., & Van Cappellen, P. (2012). Oxygen Dependency of Neutrophilic Fe(II) Oxidation by *Leptothrix* Differs from Abiotic Reaction. *Geomicrobiology Journal*, 29(6), 550-560. doi: 10.1080/01490451.2011.594147
- Von Asmuth, J. R., Bierkens, M. F. P., & Maas, K. (2002). Transfer function-noise modeling in continuous time using predefined impulse response functions. *Water Resources Research*, 38(12), 23-21 - 23-12. doi: 10.1029/2001WR001136
- Von Gunten, U., & Schneider, W. (1991). Primary products of the oxygenation of iron(II) at an oxic—anoxic boundary: Nucleation, aggregation, and aging. *Journal of Colloid and Interface Science*, 145(1), 127-139. doi: [http://dx.doi.org/10.1016/0021-9797\(91\)90106-1](http://dx.doi.org/10.1016/0021-9797(91)90106-1)
- Wade, A. J., Palmer-Felgate, E. J., Halliday, S. J., Skeffington, R. A., Loewenthal, M., Jarvie, H. P., . . . Newman, J. R. (2012). Hydrochemical processes in lowland rivers: Insights from in situ, high-resolution monitoring. *Hydrology and Earth System Sciences*, 16(11), 4323-4342. doi: 10.5194/hess-16-4323-2012
- Walling, D. E. (2013). The evolution of sediment source fingerprinting investigations in fluvial systems. *Journal of Soils and Sediments*, 13(10), 1658–1675. doi: 10.1007/s11368-013-0767-2
- Walling, D. E., Collins, A. L., & Stroud, R. W. (2008). Tracing suspended sediment and particulate phosphorus sources in catchments. *Journal of Hydrology*, 350, 274-289.
- Wang, X., Li, W., Harrington, R., Liu, F., Parise, J. B., Feng, X., & Sparks, D. L. (2013). Effect of ferrihydrite crystallite size on phosphate adsorption reactivity. *Environmental Science and Technology*, 47(18), 10322-10331. doi: 10.1021/es401301z
- Wassen, M. J., Venterink, H. O., Lapshina, E. D., & Tanneberger, F. (2005). Endangered plants persist under phosphorus limitation. *Nature*, 437(7058), 547-550.
- Wellen, C., Kamran-Disfani, A.-R., & Arhonditsis, G. B. (2015). Evaluation of the Current State of Distributed Watershed Nutrient Water Quality Modeling. *Environmental Science & Technology*, 49(6), 3278-3290. doi: 10.1021/es5049557
- Wengrove, M. E., Foster, D. L., Kalnejais, L. H., Percuoco, V., & Lippmann, T. C. (2015). Field and laboratory observations of bed stress and associated nutrient release in a tidal estuary. *Estuarine, Coastal and Shelf Science*, 161, 11-24. doi: <http://dx.doi.org/10.1016/j.ecss.2015.04.005>
- Winterwerp, J. C., van Kesteren, W. G. M., van Prooijen, B., & Jacobs, W. (2012). A conceptual framework for shear flow-induced erosion of soft cohesive sediment beds. *Journal of Geophysical Research: Oceans*, 117(C10), C10020. doi: 10.1029/2012JC008072

- Withers, P. J. A., & Haygarth, P. M. (2007). Agriculture, phosphorus and eutrophication: a European perspective. *Soil Use and Management*, 23, 1-4. doi: 10.1111/j.1475-2743.2007.00116.x
- Withers, P. J. A., & Jarvie, H. P. (2008). Delivery and cycling of phosphorus in rivers: A review. *Science of The Total Environment*, 400, 379-395.
- Withers, P. J. A., Jarvie, H. P., Hodgkinson, R. A., Palmer-Felgate, E. J., Bates, A., Neal, M., . . . Wickham, H. D. (2009). Characterization of phosphorus sources in rural watersheds. *Journal of Environmental Quality*, 38(5), 1998-2011. doi: 10.2134/jeq2008.0096
- Withers, P. J. A., Ulén, B., Stamm, C., & Bechmann, M. (2003). Incidental phosphorus losses – are they significant and can they be predicted? *Journal of Plant Nutrition and Soil Science*, 166(4), 459-468. doi: 10.1002/jpln.200321165
- Woestenburg, M., & Van Tol-Leenders, D. (2011). *Sturen op schoon water; eindrapport project Monitoring Stroomgebieden* [Aiming for clean water. Final report project Monitoring Catchments]. Alterra / Deltares, Wageningen, the Netherlands.
- Wolf, J., Beusen, A. H. W., Groenendijk, P., Kroon, T., Rötter, R., & van Zeijts, H. (2003). The integrated modeling system STONE for calculating nutrient emissions from agriculture in the Netherlands. *Environmental Modelling & Software*, 18(7), 597-617. doi: [http://dx.doi.org/10.1016/S1364-8152\(03\)00036-7](http://dx.doi.org/10.1016/S1364-8152(03)00036-7)
- Wolthoorn, A., Temminghoff, E. J. M., Weng, L., & Van Riemsdijk, W. H. (2004). Colloid formation in groundwater: Effect of phosphate, manganese, silicate and dissolved organic matter on the dynamic heterogeneous oxidation of ferrous iron. *Applied Geochemistry*, 19(4), 611-622.
- Worrall, F., Swank, W. T., & Burt, T. P. (2003). Changes in stream nitrate concentrations due to land management practices, ecological succession, and climate: Developing a systems approach to integrated catchment response. *Water Resources Research*, 39(7), HWC11-HWC114.
- Worsfold, P., McKelvie, I., & Monbet, P. (2016). Determination of phosphorus in natural waters: A historical review. *Analytica Chimica Acta*, 918, 8-20. doi: <http://dx.doi.org/10.1016/j.aca.2016.02.047>
- Worsfold, P. J., Gimbert, L. J., Mankasingh, U., Omaka, O. N., Hanrahan, G., Gardolinski, P. C. F. C., . . . McKelvie, I. D. (2005). Sampling, sample treatment and quality assurance issues for the determination of phosphorus species in natural waters and soils. *Talanta*, 66(2), 273-293.
- Zak, D., Kleeberg, A., & Hupfer, M. (2006). Sulphate-mediated phosphorus mobilization in riverine sediments at increasing sulphate concentration, River Spree, NE Germany. *Biogeochemistry*, 80(2), 109-119.



# Summary

The release of phosphorus (P) to surface water from heavily fertilised agricultural fields is of major importance for surface water quality. The research reported in this thesis examined the role of geochemical and hydrodynamic processes controlling P speciation and transport in lowland catchments in the Netherlands. A better insight into these mechanisms contributes to the improvement of our understanding of P retention in watercourses and this, hopefully, will support water quality management. The research was based on a combination of laboratory and field experiments, field monitoring studies, and surveys in catchments. The next sections give a summary of the results for the following four research objective:

- how transformation processes during exfiltration of Fe(II)-bearing anoxic groundwater affect the immobilisation of dissolved P (chapters 2 and 3).
- the chemical speciation of particulate P in surface water of groundwater-fed lowland catchments (chapter 4).
- the P sources and transport processes in an agriculture-dominated lowland water system (chapter 5).
- the erodibility of soft sediments present in ditches and channels in lowland catchments and how this affects associated P resuspension (chapter 6).

The last section gives a summary of the implications of this research.

## **Transformation processes of dissolved phosphate during exfiltration of anoxic Fe(II)-bearing groundwater**

Chapter 2 presents a study of the removal of P from shallow groundwater that flows into surface water, as caused by the oxidation of naturally occurring dissolved Fe(II). The results of the experimental field set-up showed that the formation of Fe precipitates upon oxygenation of anaerobic Fe-bearing groundwater is a key process affecting the P speciation in surface waters in lowland catchments. We found that Fe oxidation rates are much slower in winter than in summer, but that removal of P by oxidising Fe(II) was highly efficient in both seasons, resulting in low dissolved P concentrations in the surface water throughout the year. More explicitly, we observed rapid immobilisation of dissolved P during the initial stage of the Fe(II) oxidation process, which results in P-depleted water before Fe(II) is completely oxidised. This observation cannot be explained by surface complexation of  $\text{PO}_4$  to freshly formed Fe oxyhydroxides but indicates that Fe(III) phosphate precipitates are formed preferentially.

Chapter 3 focuses in detail on the formation of P-rich Fe(III) precipitates during oxidation of Fe(II). In a series of aeration experiments with anoxic synthetic water and natural groundwater, we explored the relationship between solution composition, reaction kinetics and the characteristics of the produced Fe(III) precipitates. The aeration experiments with Fe(II)-containing solutions demonstrated that dissolved  $\text{PO}_4$  can be effectively immobilised in the form of a homogeneous Fe hydroxyphosphate. In the presence of dissolved  $\text{PO}_4$ , oxidation of Fe(II) led to the formation of Fe hydroxyphosphates whose molar P/Fe ratio remained virtually constant throughout the reaction

until  $\text{PO}_4$  has been depleted. However, the P/Fe ratio of the Fe hydroxyphosphate precipitates varied, depending on the initial aqueous P/Fe ratio and the pH value. The increase of initial aqueous P/Fe ratios from 0.12 to 0.9 resulted in an increase of the precipitate P/Fe ratio from 0.38 to 0.61. Experiments conducted at pH 6.4 resulted in precipitates with P/Fe ratios slightly lower than those forming at pH 6.1. After depletion of  $\text{PO}_4$ , the continued Fe(II) oxidation resulted in formation of Fe oxyhydroxides.

Fe(II) oxidation was generally slower in the presence of  $\text{PO}_4$  than in the absence of  $\text{PO}_4$ , but the decrease of the  $\text{PO}_4$  concentration during Fe(II) oxidation due to the formation of Fe hydroxyphosphates retarded the reaction rate even more. The progress of the Fe(II) oxidation reaction could be described using a pseudo-second-order rate law with first-order dependencies on  $\text{PO}_4$  and Fe(II) concentrations. After  $\text{PO}_4$  depletion, the Fe(II) oxidation rates increased again and the kinetics followed a pseudo-first-order rate law.

The aeration experiments with natural groundwater showed no principal differences in Fe(II) oxidation kinetics and in  $\text{PO}_4$  immobilisation dynamics compared with the results found for synthetic solutions with corresponding P/Fe ratio, pH and oxygen pressure. Phosphate sequestration is efficient as long as the P/Fe ratio of the groundwater that feeds the surface water is below 0.6. However, aeration of groundwater with relatively high DOC concentrations and a low salinity leads to stable P-rich Fe colloids that stay in the water phase longer.

### **Chemical speciation of particulate P in surface water of groundwater-fed lowland catchments**

Chapter 4 describes the results of a field survey on P speciation in ditches, channels and streams draining six agriculture-dominated lowland catchments in the Netherlands. The particulate P concentration was strongly dominant over the dissolved P concentration: on average, it accounted for 83% of the total P (TP) concentration. The suspended particulate matter (SPM) could be characterised as P-rich. The average value of  $8.8 \text{ mg g}^{-1}$  was about 2–10 times higher than the P contents of SPM reported in international studies. A sequential chemical extraction method was applied on SPM samples ( $n = 96$ ) to quantify different forms of particulate P under various environmental conditions. Iron-bound P was the most important particulate P fraction in the SPM samples (range 38–95%), followed by organic P (range 2–38%). Exchangeable P and calcium-bound P were less significant particulate P pools. Iron-bound P dominated the particulate P speciation in the entire range of watercourses, from headwater ditches to catchment outlets, and in samples taken during winter months as well as in samples taken during summer months. Furthermore, the PP speciation did not change markedly while flow conditions were being altered from low to high discharge. The dominance of the Fe-P pool denotes the presence of Fe(III) precipitates in SPM that originate from exfiltration of anoxic Fe-bearing groundwater. These authigenic Fe(III) precipitates are a main fraction of the total SPM concentration (range 4–67%). The results of this field survey confirmed the results from the field and lab experiments described in chapters 2 and 3, namely that precipitation of authigenic Fe(III) at the groundwater–surface water interface results in a rapid transformation of dissolved P to particulate P. Iron-rich particles are thus a major carrier phase of P in groundwater-fed lowland catchments.

### **Phosphate transport processes in an agriculture-dominated lowland water system**

Chapter 5 focuses on the hydrodynamic controls on P transport in a polder area. This chapter is based on one year of high-frequency water quality and turbidity measurements near a pumping station. Seasonal trends and short-scale temporal dynamics in concentrations indicated that the  $\text{NO}_3$  concentration at the pumping station originated from N loss from agricultural land. This, however, could not be concluded for total P (TP). Rainfall events that caused peaks in  $\text{NO}_3$  concentrations did not result in TP concentration peaks. The rainfall-induced and  $\text{NO}_3$ -enriched quick interflow is likely also enriched in TP, but then retention of TP due to sedimentation of particulate P in the surface water network resulted in the absence of TP concentration peaks at the pumping station. The TP concentration and turbidity almost doubled during operation of the pumping station, which indicates resuspension of particulate P from channel bed sediments induced by changes in water flow due to pumping. However, these changes in concentrations are considerably smaller than the changes reported for natural catchments, where resuspension of particulate P during high discharge events is a key transport mechanism. The TP export load from the polder that was caused by pumping amounted to 21 % of the annual TP load, whereas for natural catchments up to 80% of the annual fluxes were attributed to short periods of peak flow. Our observations suggest that the P retention potential of polder water systems is enhanced compared with that of natural catchments, because the artificial pumping regime prevents high discharge flow and, therefore, limits resuspension of particulate P.

### **Erodibility of soft sediments as present in drainage ditches and channels in lowland catchments and associated P release**

Chapter 6 presents a study of the erodibility of soft, drainage ditch sediments, carried out to gain a better understanding of the hydrodynamic controls on P transport processes in polder catchments. We used a device to quantify the erosion rate and P entrainment of the water column as a function of increasing bed shear stresses. Experiments with undisturbed sediment cores from field ditches and secondary channels in two polder catchments in the Netherlands revealed that the critical shear stress for erosion varied between 0.1 and 0.28 Pa. At bed shear stresses above the critical shear stress, the sediment erosion rate and P release were almost linearly related to the bed shear stress. By using a regional hydrodynamic model of a polder, we additionally showed that bed shear stresses above 0.1 Pa rarely occur in watercourses that drain the area. This implies that erosion of bed sediment is not a major process controlling P transport in polder catchments. Limited erosion of easily resuspendable material was, however, observed at bed shear stresses below the critical shear stress. This floc erosion may contribute to P transport in polder catchments, especially in watercourses near pumping stations, where flow velocities are relatively high.

### **Implications**

This study showed that the mobility and ecological impact of P in surface waters in lowland catchments or polders like those in the Netherlands are strongly controlled by the exfiltration of anoxic groundwater containing ferrous iron. Chemical precipitates derived from groundwater-associated Fe(II) seeping into the overlying surface water contribute to the immobilisation of

dissolved phosphate and, therefore, reduce its bioavailability. After the transformation of dissolved P to iron-bound particulate P, the transport of P in catchments or polders is controlled by sedimentation and erosion of suspended sediments. Hydrodynamic resuspension of phosphorus (P) stored in bed sediments of watercourses is commonly considered to be the main transport mechanism in lowland catchments. This study revealed contrasting insights. The water flow in surface watercourses in large parts of the Netherlands is such that flow-induced bed shear stress in watercourses seldom exceeds the critical shear stress for erosion. This is due to a dense network of drainage ditches and water flow that is controlled by weirs and pumping stations. This implies that erosion of bed sediment is generally not a key process controlling P transport in a polder catchment. A polder can thus be considered as a comprehensive peak flow control system that mitigates P export loads from agriculture.

Without the capacity of watercourses in the Netherlands to retain P loads, the eutrophication problems would likely be more severe, given the intensity of the agricultural sector and size of the country's manure surplus. However, sedimentation of SPM with high P contents results in a continuous build-up of a pool of 'legacy P' in the bed sediments of headwater ditches and in more surface water bodies further downstream, such as inland lakes or even estuaries or coastal areas that receive export loads from agricultural areas. This pool of 'legacy P' may have negative effects on water quality at longer timescales and this may retard the improvement of water quality in the future, even when reduction of P loads has been accomplished. Furthermore, we have to realise that the sequence of immobilisation, storage and remobilisation processes makes it difficult to link agricultural practice to P concentrations in the surface water. Thus, when assessing measures to reduce P loads from agriculture we should be aware of the long-term in-stream mechanisms controlling P concentrations in surface waters. A proper assessment of the effects of measures requires models that properly address these key mechanisms, in combination with detailed and long-term field studies and monitoring programmes at different spatial scales from field to catchment outlet. Knowledge about the mechanisms controlling P retention also provides opportunities for developing and implementing specific measures to retain and recycle P in catchments.



# Samenvatting

Het verbeteren van de waterkwaliteit is vooral wat betreft de concentraties van nutriënten een van de belangrijkste uitdagingen waarmee Nederland wordt geconfronteerd bij de uitvoering van het milieubeleid en de milieuwetgeving van de EU. Toevoer van een overmaat nutriënten, ook wel aangeduid als eutrofiëring, leidt tot onwenselijk effecten in oppervlaktewater zoals afname van de biodiversiteit, zuurstofloosheid en algenbloei en moet daarom worden teruggedrongen. Fosfor is één van deze nutriënten die problemen voor waterkwaliteit veroorzaken. In het verleden zijn grote stappen gemaakt om de fosfaatbelasting van het oppervlaktewater te verminderen. Dit is het gevolg van enerzijds verbeterde zuivering van riool- en afvalwater en invoer van fosfaatvrije wasmiddelen in Nederland en omliggende landen en anderzijds het mestbeleid, dat zich richt op vermindering van mestgebruik op landbouwgronden. Hierdoor is de waterkwaliteit op veel plekken verbeterd. Ondanks deze inspanningen blijkt echter dat in 2015 slechts 45% van de regionale oppervlaktewaterlichamen voldeed aan de fosfornorm voor een 'goede ecologische toestand'. Voorspellingen voor 2027 schatten dit percentage op 50%. Deze geringe toename van het percentage oppervlaktewaterlichamen in een 'goede ecologische toestand' wordt vooral toegeschreven aan verdere reductie van puntbronnen zoals verbeteringen in waterzuiveringen. De landbouwsector, die gekenmerkt wordt door grote overschotten van fosfor door import van ruwvoer, is momenteel de grootste bron in de nationale fosforbalans. Diffuse P emissies vanuit de bodem in het landelijk gebied omvatten nu ongeveer twee derde van de totale belasting van het regionale oppervlaktewater.

De belasting van regionale oppervlaktewaterlichamen door 'landbouw' fosfor vindt plaats door uit- afspoeling van fosfor vanuit de bodem naar perceelsloten gevolgd door transport van fosfor in het afwateringstelsel van sloten, vaarten en beken in stroomgebieden. Om betere schattingen te maken van de invloed van de landbouw op de waterkwaliteit, inclusief de effectiviteit van maatregelen voor verbetering van de waterkwaliteit, is het daarom van belang om beter inzicht te krijgen in de processen die het transport van P in sloten, vaarten en beken bepalen. Tijdens transport vinden er allerlei processen plaats, waardoor een deel van het P, al dan niet tijdelijk, wordt omgezet of vastgelegd in biomassa of het sediment. Het totaal van deze (tijdelijke) vastleggingsprocessen wordt aangeduid met de term retentie. Dit proefschrift richt zich op verbetering van het inzicht in deze processen.

Het onderzoek in dit proefschrift naar geochemische en hydrodynamische fosforretentie mechanismes in laagland stroomgebieden heeft het inzicht opgeleverd dat het transport en de biobeschikbaarheid van fosfaat in het oppervlaktewater in Nederland op grote schaal bepaald wordt door kwel van grondwater. Kwellend grondwater in Nederland is nagenoeg altijd anaeroob en meestal ook ijzerhoudend. Het ijzer in dit grondwater is opgelost gereduceerd ijzer en bij contact met zuurstof (in oppervlaktewater of slootbodem) wordt dit geoxideerd waarbij ijzerneerslagen worden gevormd. Tot nu toe werd verondersteld dat sorptie van fosfaat aan het oppervlak van Fe-hydroxyden het mechanisme is voor de interactie tussen fosfaat en ijzer in oppervlaktewater. Laboratorium experimenten met synthetisch en natuurlijk grondwater hebben aangetoond dat

als er tijdens deze chemische reactie opgelost fosfaat aanwezig is, dit als eerste wordt vastgelegd door de vorming van Fe-hydroxyfosfaten. Pas wanneer het opgeloste fosfaat 'op' is, ontstaan er Fe-hydroxyden. Fe-hydroxyfosfaten zijn amorfe vaste fasen met een molaire ijzer/fosfaat ratio van ongeveer twee, wat betekent dat de ijzerconcentratie slechts twee keer hoger hoeft te zijn dan de fosfaatconcentratie om al het opgeloste fosfaat vast te leggen. Vastlegging van fosfor in een vaste fase betekent verder dat het stevig is gebonden. De in dit proefschrift gevonden chemische reactie met neerslag van Fe-hydroxyfosfaten is fundamenteel anders dan sorptie van fosfaat aan Fe-hydroxyden. In vergelijking met sorptie van fosfaat aan Fe-hydroxydes wordt er per mol ijzer veel meer fosfaat gebonden en is dit fosfaat ook nog steviger gebonden. De snelheid van deze chemische reactie is hoog en afhankelijk van temperatuur, pH en beschikbaarheid van zuurstof. Normaal gesproken vindt de reactie plaats binnen minuten tot uren en in de winter hooguit enkele dagen. Het is dus een zeer effectief (en natuurlijk) fosfaat-immobilisatiemechanisme.

Een uitgebreide veldcampagne in zes landbouw-gedomineerde stroomgebieden in Nederland heeft vervolgens aangetoond dat, als gevolg van het hierboven genoemde proces, de opgeloste 'ortho-P' concentratie meestal laag is en gemiddeld genomen meer dan 60% van de totaal-fosfaatconcentratie in oppervlaktewater uit particulier ijzer-gebonden P bestaat. Dit ijzer-gebonden P blijkt de dominante fosfaatverbinding te zijn in het gehele afwateringsstelsel vanaf perceelsslotten tot het uitstroompunt zowel gedurende de winter als de zomer. Dit wordt op afstand gevolgd door organisch P en uitwisselbaar P. Het ijzer-gebonden fosfaat is nauwelijks biobeschikbaar zolang de condities oxidisch blijven en zal, als de deeltjes groot genoeg zijn, sedimenteren in sloten en vaarten.

Experimenteel onderzoek met ongestoorde waterbodempollen uit sloten in twee polders heeft vervolgens aangetoond dat het transport van particulier P als gevolg van opwerveling vanuit waterbodems door verhoogde stroomsnelheden gering is. Het waterpeil en daarmee de stroomsnelheden van water in sloten en vaarten in Nederland wordt veelal geregeld door stuwen en gemalen. De maximale stroomsnelheid van het water in sloten en vaarten is vaak niet hoog genoeg om de kritische schuifspanning voor erosie van een waterbodempol te overschrijden. In polders is alleen dicht bij het gemaal de stroomsnelheid hoog genoeg om opwerveling te veroorzaken. Tijdens bemaling kan de totaal-P concentratie als gevolg van opwerveling ongeveer twee keer zo groot worden. Dit is veel minder dan de toename in concentratie die tijdens hoge afvoeren in vrij afstromende gebieden is gemeten. Hier worden namelijk concentratietoenames van een factor 100 of meer gemeten. Polders met ijzerhoudend grondwater hebben dus een hoge capaciteit om fosfaat te bergen. Dit bleek ook uit continue metingen van nitraat en totaal-P bij een gemaal in Flevoland. Natte periodes die in de winter tot afvoer via drainagebuizen leiden veroorzaken 5 dagen later een piek in de nitraatconcentratie bij het gemaal. De totaal-P concentratie tijdens deze nitraatpiek was echter meestal lager dan de fosfaatconcentratie voorafgaand aan de neerslag. Het P dat tijdens natte periodes uitspoelt vanuit de bodem naar het oppervlaktewater komt dus niet direct na een regenperiode bij het uitstroompunt van de polder.

Gemalen zijn ook traditioneel een plek om de waterkwaliteit te monitoren. De toename van de totaal-P concentratie tijdens bemaling is dan wel een punt van aandacht. Steeds meer gemalen draaien volautomatisch, voornamelijk tijdens de nachtelijke uren, terwijl de waterkwaliteit nog

steeds vooral overdag wordt gemeten. Dit kan een aanzienlijke vertekening van de werkelijkheid opleveren wat een effect heeft op gerapporteerde P-vrachten en trends in waterkwaliteit.

De immobilisatie van opgelost P met ijzer uit grondwater en sedimentatie van ijzer-gebonden P blijken een dominante rol te spelen in het transport en de (bio)beschikbaarheid van P in Nederlandse stroomgebieden. Na sedimentatie van ijzer-gebonden P in waterbodems is het mogelijk dat (een deel van) het P weer vrijkomt als gevolg van biogeochemische omzettingsprocessen. Dit speelt met name in de zomer wanneer er door zuurstoftekort gereduceerde omstandigheden in de waterkolom en top van de waterbodem kunnen ontstaan. Meestal is de waterafvoer in de zomer ook gering waardoor het transport van opgelost P, dat afkomstig is van remobilisatie vanuit de waterbodem, naar stroomafwaarts gelegen oppervlaktewaterlichamen mee kan vallen.

Dit proefschrift toont aan dat sloten effectief zijn in het vasthouden van P in landbouwgebieden, zeker wanneer deze gevoed worden met ijzerhoudend grondwater. Dit inzicht wordt ondersteund door het feit dat er in het buitenland wordt geëxperimenteerd met het graven en optimaliseren van sloten als maatregel om P in stroomgebieden te bergen. Hierdoor kunnen we stellen dat, ondanks de zeer intensieve landbouwsector en hoge mestoverschotten, de eutrofiëringsproblemen als gevolg van landbouwemissies relatief meevallen. Anders gezegd: Nederland heeft in feite het geluk dat het watersysteem goed in staat is om opgelost fosfaat te immobiliseren en in sloten te bergen. Als dit niet zo was, zouden de eutrofiëringsproblemen waarschijnlijk veel groter zijn dan ze nu zijn.



# List of Publications

## This thesis

- Van der Grift, B., Rozemeijer, J.C., Griffioen, J., van der Velde, Y., 2014. Iron oxidation kinetics and phosphate immobilization along the flow-path from groundwater into surface water. *Hydrol. Earth Syst. Sci.* 18, 4687-4702.
- Van der Grift, B., Broers, H.P., Berendrecht, W., Rozemeijer, J., Osté, L., Griffioen, J., 2016. High-frequency monitoring reveals nutrient sources and transport processes in an agriculture-dominated lowland water system. *Hydrol. Earth Syst. Sci.* 20, 1851-1868.
- Vandergrift, B., Behrends, T., Osté, L.A., Schot, P.P., Wassen, M.J., Griffioen, J., 2016. Fe hydroxyphosphate precipitation and Fe(II) oxidation kinetics upon aeration of Fe(II) and phosphate-containing synthetic and natural solutions. *Geochimica et Cosmochimica Acta* 186, 71-90.
- Van der Grift, B., Osté, L.A., Schot, P.P., Kratz, A., Van Popta, E.D.M., Wassen, M.J., Griffioen, J., 2017. Particulate phosphorus speciation in ditches, channels and streams of agriculture-dominated lowland catchments: iron as phosphorus carrier. Under review at *Water Research*.

## Related to this thesis

- Baken, S., Moens, C., van der Grift, B., Smolders, E., 2016. Phosphate binding by natural iron-rich colloids in streams. *Water Research* 98, 326-333.
- Rozemeijer, J.C., Klein, J., Broers, H.P., van Tol-Leenders, T.P., van der Grift, B., 2014. Water quality status and trends in agriculture-dominated headwaters; a national monitoring network for assessing the effectiveness of national and European manure legislation in The Netherlands. *Environmental Monitoring and Assessment* 186, 8981-8995.

## Others

- René R. Wijngaard, R.R., Van der Perk, M., Van der Grift, B., De Nijs, T. C. M., Bierkens, M. F. P. 2017 The impact of climate change on metal transport in a lowland catchment. *Water, Air, & Soil Pollution* 228:107.
- Joris, I., Bronders, J., van der Grift, B., Seuntjens, P., 2014. Model-based scenario analysis of the impact of remediation measures on metal leaching from soils contaminated by historic smelter emissions. *Journal of Environmental Quality* 43, 859-868.
- Zhang, Y.C., Prommer, H., Broers, H.P., Slomp, C.P., Greskowiak, J., Van Der Grift, B., Van Cappellen, P., 2013. Model-based integration and analysis of biogeochemical and isotopic dynamics in a nitrate-polluted pyritic aquifer. *Environmental Science and Technology* 47, 10415-10422.
- Bonten, L.T.C., Kroes, J.G., Groenendijk, P., Van Der Grift, B., 2012. Modeling diffusive Cd and Zn contaminant emissions from soils to surface waters. *Journal of Contaminant Hydrology* 138-139, 113-122.
- Visser, A., Broers, H.P., Van Der Grift, B., Bierkens, M.F.P., 2009. Demonstrating trend reversal of groundwater quality in relation to time of recharge determined by  $^3\text{H}/^3\text{He}$ , *Nederlandse Geografische Studies*, pp. 31-46.

- Visser, A., Dubus, I., Broers, H.P., Brouyère, S., Korcz, M., Heerdink, R., Van Der Grift, B., Orban, P., Goderniaux, P., Batlle-Aguilar, J., Surdyk, N., Amraoui, N., Job, H., Pinault, J.L., Bierkens, M., 2009. Comparison of methods for the detection and extrapolation of trends in groundwater quality, *Nederlandse Geografische Studies*, pp. 71-89.
- Gerritse, J., van der Grift, B., Langenhoff, A., 2009. Contaminant Behaviour of Micro-Organics in Groundwater, *Groundwater Monitoring*, pp. 111-143.
- Van der Grift, B., Griffioen, J., 2008. Modelling assessment of regional groundwater contamination due to historic smelter emissions of heavy metals. *Journal of Contaminant Hydrology* 96, 48-68.
- Van den Brink, C., Zaadnoordijk, W.J., van der Grift, B., de Ruiter, P.C., Griffioen, J., 2008. Using a groundwater quality negotiation support system to change land-use management near a drinking-water abstraction in the Netherlands. *Journal of Hydrology* 350, 339-356.
- Fest, E.P.M.J., Temminghoff, E.J.M., Griffioen, J., Van Der Grift, B., Van Riemsdijk, W.H., 2007. Groundwater chemistry of Al under Dutch sandy soils: Effects of land use and depth. *Applied Geochemistry* 22, 1427-1438.
- Visser, A., Broers, H.P., van der Grift, B., Bierkens, M.F.P., 2007. Demonstrating trend reversal of groundwater quality in relation to time of recharge determined by  $3\text{H}/3\text{He}$ . *Environmental Pollution* 148, 797-807.
- Kolditz, O., Du, Y., Bürger, C., Delfs, J., Kuntz, D., Beinhorn, M., Hess, M., Wang, W., van der Grift, B., te Stroet, C., 2007. Development of a regional hydrologic soil model and application to the Beerze-Reusel drainage basin. *Environmental Pollution* 148, 855-866.
- Wildenborg, A.F.B., Leijnse, A.L., Kreft, E., Nepveu, M.N., Obdam, A.N.M., Orlic, B., Wipfler, E.L., van der Grift, B., van Kesteren, W., Gaus, I., Czernichowski-Lauriol, I., Torfs, P., Wójcik, R., 2005. Risk Assessment Methodology for CO<sub>2</sub> Storage: The Scenario Approach, *Carbon Dioxide Capture for Storage in Deep Geologic Formations*, pp. 1293-1316.
- Broers, H.P., Van Der Grift, B., 2004. Regional monitoring of temporal changes in groundwater quality. *Journal of Hydrology* 296, 192-220.

# Dankwoord

Het boekje is af. Er is een mijlpaal bereikt en die heb ik kunnen bereiken door de ondersteuning van velen. Graag wil ik iedereen bedanken die mij de afgelopen jaren direct of indirect heeft geholpen. Maar hoe is het begonnen?

Na bijna 15 jaar werken aan diverse projecten op het gebied van waterkwaliteit bij TNO en Deltares kreeg ik steeds meer het gevoel dat 'leren' synoniem werd aan het ontwikkelen van competenties. Er gingen dagen of misschien zelf weken voorbij zonder iets inhoudelijks nieuws te hebben ontdekt. Hierdoor kreeg ik sterk de behoefte om nieuwe kennis op te doen. Hoe kan je daar beter invulling aan geven dan starten met een promotieonderzoek? De jaren hiervoor had ik samen met collega's van Alterra en Deltares gewerkt aan het project 'Monitoring Stroomgebieden'. Een groot onderzoeksproject om het effect van het mestbeleid op de kwaliteit van het oppervlaktewater beter te begrijpen. Wat we toen nog niet goed in beeld hadden, en wat tevens mijn nieuwsgierigheid aanwakkerde, waren de processen die het transport van fosfaat in het oppervlaktewater bepalen.

In dezelfde periode kreeg Jasper (Griffioen) een aanstelling als buitengewoon hoogleraar Waterkwaliteitsbeheer aan de Universiteit Utrecht. Vanuit Deltares kreeg hij een 'bruidsschat' mee in de vorm van een aio. Het onderwerp voor de aio was, mede ingegeven door de bevindingen uit het project 'Monitoring Stroomgebieden' snel gevonden: fosfaatretentiemechanismes in oppervlaktewater. Bestaat toeval of niet? Ik heb geen idee, maar de lijntjes van mijn eigen ambities en het nieuwe aio-project kwamen snel bij elkaar.

Het was ontzettend fijn om te merken dat mijn promotoren en copromotoren er voor mij waren in die vier jaar waarin ik aan het onderzoek heb gewerkt. Ik begin met Jasper, mijn promotor en tevens al bijna 20 jaar mijn (onofficiële) mentor: bij jou kwam ik eind 1997 terecht om te werken aan een project om de mogelijkheden voor geochemische isolatie van een gipsstort van D.S.M. te onderzoeken. Achteraf gezien is dit nog steeds een van de leukste projecten die ik voor TNO/Deltares uit heb mogen voeren. Ik ben blij dat ik met jou mocht samenwerken en trots dat ik jouw eerste promovendus als hoogleraar mag zijn! Ik heb ontzettend veel van je geleerd en heb veel bewondering voor je scherpzinnige analyses, bevologenheid en de snelheid waarmee je mijn concepten altijd van commentaar voorziet. Ook de activiteiten die we buiten het werk hebben ondernomen heb ik altijd zeer gewaardeerd. De happy-tappies, concerten (waarvan Beth Hart, Poppa Chubby en Thirty Seconds to Mars indruk hebben gemaakt) en korte vakanties gekoppeld aan buitenlandse congressen zijn hier mooie voorbeelden van. Ik hoop dan ook dat we zowel binnen als buiten het werk samen kunnen blijven optrekken.

Martin daagde mij uit om het onderzoek te beginnen met het opstellen van hypothesen en hier eens goed over na te denken. Dit was ik vanuit mijn TNO/Deltares achtergrond eigenlijk niet gewend, daar hebben we een onderzoeksvraag en dan beginnen we gewoon. Dank voor alle interessante discussies. Het gemak waarmee jij structuur weet aan te brengen is bewonderenswaardig.

Ik wil Leonard bedanken voor zijn inzet om dit promotieonderzoek te realiseren en zijn ondersteuning tijdens dit project. Je had altijd tijd om met een bakkie koffie bij te praten en stimuleerde mij om processen te onderzoeken die buiten mijn eigen kennisveld lagen.

Paul wil ik bedanken voor de fijne samenwerking in de afgelopen jaren. Je deur stond altijd open voor overleg, je bleef doorvragen als ik het spoor wat bijster was totdat ik weer op de rit zat en je was altijd zeer geïnteresseerd in mijn resultaten.

Geachte leden van de beoordelingscommissie, prof. dr. J.B.M. Middelburg, prof. dr. ir. O. Oenema, prof. dr. ir. J.C. Winterwerp, prof. dr. P.C. de Rooter en prof. dr. E. Smolders, hartelijk dank voor het beoordelen van mijn manuscript.

Ook wil ik graag mijn Nederlandse mede-auteurs bedanken:

Ype van der Velde, bedankt voor de inspirerende discussies over de kleur van slootwater, jouw hulp bij voor mij (te) ingewikkelde wiskunde en dat je op het idee kwam dat ik op de VU het vak 'Water Quality' kon doceren. Dit was een erg leuke en leerzame ervaring.

Joachim Rozemeijer, bedankt dat je me ervan overtuigde dat de Hupsel-data ook erg interessant was om fosfaat processen op het grensvlak tussen grond- en oppervlaktewater te bestuderen en dat je me stimuleerde hoog-frequent te gaan meten.

Thilo Behrends, bedankt voor de fijne samenwerking bij hoofdstuk 3, het beschikbaar stellen van jouw pH-stat opstelling en de dubbelcheck op mijn integraties van hogere orde differentiaalvergelijkingen.

Wilbert Berendrecht, bedankt voor de hulp bij de tijdreeksanalyse in hoofdstuk 4 en de uitleg van de formules. Op een gegeven moment ging ik zelfs de statistiek hierachter een beetje snappen.

Hans Peter Broers, bedankt voor je bijdrage aan hoofdstuk 5. Het is altijd geweldig om met jou samen te kunnen werken!

Miguel de Lucas Pardo, many thanks for your support with the erosion experiments in chapter 6.

Veel dank ben ik verschuldigd aan de organisatie Deltares en in het bijzonder aan Gerard Blom, die het mogelijk maakte om het promotieonderzoek vanuit mijn aanstelling bij Deltares uit te voeren. Dit heb ik altijd als een groot voorrecht ervaren. In dit kader wil ik ook Hilde Passier bedanken, mijn afdelingshoofd. Dat we elkaar al een tijd kennen blijkt uit het feite dat je vertelde dat je mijn ambitie om te willen promoveren aan had zien komen. Verder wil ik mijn collega's bij van de afdeling Subsurface and Groundwater Quality bij Deltares bedanken voor de goede sfeer op de werkvloer, de koffieverhalen, de interesse in mijn onderzoek en de spannende foto's van vergaderzaaltjes (all-over-the-world) die via de App met elkaar worden gedeeld.

Bedankt ook alle collega's van Deltares die meegeholpen hebben bij mijn onderzoek: Piet Peereboom, André Cinjee, Mike van der Werf, Rob van Galen, Erik van Vilsteren, Thijs van Kessel, Erwin Meijers. Ditzelfde geldt ook voor de technische staf van de Universiteit Utrecht: Dineke van de Meent, Helen de Waard, Ton Zalm, Coen Mulder en Thom Claessen.

Een aantal studenten heeft me de afgelopen jaren geholpen bij het uitvoeren van het onderzoek en het verzamelen van meetgegevens. Deirdre Clarck, Arjen Kratz en Emma van Popta: bedankt voor jullie hulp, de velddagen onder soms barre omstandigheden en de kans om jullie te begeleiden.

De mannen van het gemaal 'De Blocq van Kuffeler' bij Almere en dan vooral Fred de Visser: bedankt voor jullie gastvrijheid, de hulp bij het in bedrijf houden van de continue meetopstelling voor waterkwaliteit, de kopjes koffie en het feit dat jullie geen half werk leveren wanneer er een 'bordes' moet worden gemaakt om waterkwaliteit sensoren aan op te hangen. In dit kader wil ik ook



Michiel Oudendijk van het Waterschap Zuiderzeeland bedanken, die dit project bij 'De Blocq van Kuffeler' mogelijk maakte.

Waar zouden we zijn zonder vrienden of familie? Ik in ieder geval nergens. Daarom wil ik ook jullie ook bedanken.

De mannen van de WTC Werkhoven. Een mooi clubje om mee te fietsen en na afloop een biertje mee te drinken. Maar waar moet ik jullie eigenlijk voor bedanken? In ieder geval niet dat ik eens bemoedigend wordt toegesproken als ik weer eens slechte benen heb. Voor de koershardheid zullen we dan maar zeggen....

Mijn vrienden van de *S.U.R.F.* (Sware Utrechtse Roei Fereniging): Cees en Hans (fijn dat jullie mijn paranimfen wilden zijn), Gideon, Dirk, Ronald, Erwin, Frank, Franck. Super dat we elkaar al zo'n tijd en inmiddels ook door en door kennen. Onze band, die ontstaan is in een roeiboort op een Utrechts kanaal in de herfst van 1991, zal voor altijd blijven bestaan. Bedankt voor jullie vriendschap! Wanneer gaan we nu eens met z'n allen op Wildcamp?

Mijn familie, een erg fijn nest. Helaas heeft mijn moeder dit proefschrift en andere belangrijke gebeurtenissen in het leven van Annemiek en mij niet mee kunnen maken. Je mag best trots zijn op je kinderen, die alle twee heel goed terecht zijn gekomen. Papa, bedankt dat je altijd voor me klaarstaat en me altijd hebt gesteund in de keuzes die ik heb gemaakt. Lieve Annemiek, ik vind het heel fijn dat jij mijn zus bent. Lieve tante Klasien, bedankt voor alles wat je voor mij, Anke en de kindjes hebt gedaan, je was een super super tante! Loes, dank voor al je goede zorgen. Ik ben blij dat de kindjes zo op je gesteld zijn. En ook mijn schoonouders, bedankt voor alle heerlijke verse groentes die nodig zijn om lichaam en geest fit te houden en voor de fijne opvang van de kindjes als ik aan het werk of op reis was.

En dan het thuisfront, jullie zijn het allerbelangrijkste in mijn leven.

Lieve Merlijn en Resa. Onderzoek doen, is op zoek gaan naar iets dat je nog niet weet in de hoop dat dit iets waardevols oplevert. Eigenlijk wat jullie ook dagelijks doen: de wereld om je heen steeds verder ontdekken en deze ook nog eens een beetje mooier maken. Ik ben heel blij dat ik jullie daarbij mag helpen. En wat ben ik trots op wat jullie allemaal al ontdekt hebben!

Lieve, lieve Anke, wat ben ik toch blij met jou! We hebben al heel veel mooie dingen samen mogen meemaken de afgelopen 21 jaar en wat heb ik veel van je geleerd. Heel veel dank voor je liefde, steun en geduld de afgelopen jaren. Ik heb zin in heel veel fijne dingen met ons samen. Ik ben klaar!



# Curriculum Vitae

Bas van der Grift is geboren op 16 juni 1972 in Benthuisen. Daar is hij tot zijn 19-de jaar blijven wonen. In 1991 behaalde hij zijn VWO diploma op het Erasmus college te Zoetermeer. Daarna is hij begonnen met de studie Scheikunde aan de Universiteit Utrecht. Na het behalen van zijn propedeuse is hij in 1992 overgestapt naar de toenmalige bovenbouwstudie Geochemie aan dezelfde universiteit. In 1997 haalde hij zijn doctoraal diploma. Bas heeft zijn gecombineerde stage en afstudeeronderzoek gedaan bij het toenmalige KIWA Onderzoek & Advies in Nieuwegein. Het onderwerp van zijn scriptie was de toename van de hardheid van grondwater dat wordt gebruikt voor drinkwaterproductie.

Bas begon zijn loopbaan in 1997 als projectmedewerker bij KIWA Onderzoek & Advies waar hij werkte aan indicatoren voor monitoring van grensoverschrijdende grondwaterlichamen. Op 1 januari 1998 begon hij als hydrogeochemicus bij het Nederlands Instituut voor Toegepaste Geowetenschappen TNO. In 2008 ging hij met zijn TNO collega's over naar Deltares. Bij TNO en later Deltares werkte hij hier aan een breed scala projecten rondom het thema waterkwaliteit. Zijn werk aan de zware metalen verontreiniging in de Belgische en Nederlandse Kempen is gedurende een langere periode een rode draad door zijn loopbaan geweest. In 2012 begon hij met zijn promotieonderzoek naar fosfaat in oppervlaktewater aan de Faculteit Geowetenschappen van de Universiteit Utrecht. Het boek dat voor u ligt getuigt hiervan. Na afronding van zijn promotieonderzoek keerde hij terug naar zijn werk bij de unit Bodem en Grondwater Systemen van Deltares in Utrecht. Bas woont in Werkhoven met zijn vrouw Anke, zoon Merlijn en dochter Resa.



